Aspects of Amplitudes, Gravity & Complexity

Nathan Moynihan

February, 2019

NMOYNIHAN.COM

A thesis submitted for the degree of Doctor of Philosophy in Applied Mathematics, Department of Mathematics and Applied Mathematics, University of Cape Town.

"Believe those who are seeking the truth; doubt those who find it."

– André Gide, *So Be It: Or The Chips Are Down*

Current Edition, February 2019

Abstract

In this thesis, we explore two aspects of modern theoretical physics: scattering amplitudes in gravitational theories and entanglement entropy & complexity in quantum field theory.

In part one, we utilise modern scattering amplitude techniques to efficiently calculate the deflection angle of both light and gravity due to the presence of a massive body. We find this to be in complete agreement with the prediction by General relativity. We then construct the scattering amplitudes of massive gravitons to probe the so-called van Dam-Veltman-Zakharov (vDVZ) discontinuity in a purely on-shell manner, which we again find to be in agreement with the usual result. Additionally, we provide a clear physical picture as to the source of the discontinuity that is often obscured by the usual formulation.

In part two, we compare three different measures of complexity for a free bosonic QFT: circuit complexity, Fubini-Study complexity, and complexity from the covariance matrix. We show that circuit complexity is the most sensitive of the three, being the only measure able to distinguish between particular physically distinct time-evolved states.

Finally, we compute the entanglement entropy, entanglement spectrum, and complexity for various phases of a topological insulator (described in this case by the Su-Schrieffer-Heeger (SSH) model), showing which physical features of the system each quantity captures as it transitions between conformal, topological and massive phases. We show that under certain circumstances, the complexity saturates *later* than the entanglement entropy, which contradicts the expectation from back hole interiors and AdS/CFT.

Acknowledgements

First and foremost, I must express my gratitude to my advisor Jeff Murugan, whose enthusiasm for physics, mathematics and apple products continues to deeply shape my thinking. I have benefited enormously from his patient guidance and broad knowledge of physics, and especially his encouragement to travel, attend conferences and collaborate extensively.

I am extremely grateful to Amanda Weltman for her counsel, deep knowledge of physics and uplifting comments, and especially for creating a wonderfully stimulating research environment that fosters collaboration & discussion.

My research has been strongly influenced by Jonathan Shock, whose door was always open and whose insights – into physics or otherwise – were always meaningful. Jonathan's awe-inspiring knowledge of Mathematica has been the saviour of many a calculation, and I am lucky to have learned so much from him. I also owe a particularly special thanks to Shajid Haque for helping me in countless ways during the course of my PhD, and for his thoughtful advice, mentorship and wisdom.

I am both exceptionally grateful and deeply sorry to my comrade-in-arms Daan Burger; grateful for all the beers we shared and frank discussions we had, and deeply sorry for distracting him constantly with frank discussions and beer invitations. I have enjoyed many pleasant conversations with Alastair, Alvaro, Christhiam, Emma, George, Guilherme, Hume, Isobel, Jake, Jean-Gabriel, Julian, Michael, Renato, Ru, Thando, Tony, Will Emond and Will Horowitz at the University of Cape Town, thank you for making my stay in South Africa so enjoyable. I am particularly thankful to my friends Raúl & Estela, not only for the countless stimulating discussions of physics but for the fond memories I have of exploring South Africa & Canada together.

I am indebted to all of my collaborators: Tibra Ali, Arpan Bhattacharyya, Raúl Carballo-Rubio, Saurya Das, Francesco Di Filippo, Eugene Kim, Tatsuma Nishioka & Bret Underwood, and to the Hospitality provided by the Perimeter Institute – and Tibra in particular – where part of the research for this thesis was conducted.

It is a pleasure to thank my long suffering girlfriend Caroline for her love and encouragement over the years. I owe a very special thanks to David & Catherine Reid for their support, incredible family holidays exploring Africa and continuous encouragement. To my family, and especially my mother Olivia, thank you for always being there and for pushing me to chase my dreams, whatever the cost.

Declaration

The content of this thesis is partially based on collaborations with a number of individuals: Tibra Ali (Perimeter Institute for Theoretical Physics), Arpan Bhattacharyya (Yukawa Institute for Theoretical Physics), Daniel Burger (University of Cape Town), Raúl Carballo-Rubio (SISSA, International School for Advanced Studies), S. Shajidul Haque and Eugene Kim (University of Windsor) and Jeff Murugan and Amanda Weltman (University of Cape Town).

The list below identifies section of this thesis which are partially based on the listed publications or preprints, with the works [1, 2] being completed during the course of the PhD but not contributing to this thesis.

Chapter 5: D. J. Burger, R. Carballo-Rubio, N. Moynihan, J. Murugan and A. Weltman, *Amplitudes for Astrophysicists: Known Knowns*, *Gen. Rel. Grav.* (2017) , [arXiv:1704.05067]

Chapter 6: N. Moynihan and J. Murugan, *Comments on scattering in massive gravity, vDVZ and BCFW*, *Class. Quant. Grav.* **35** (2017) 155005, [arXiv:1711.03956]

Chapter 10: T. Ali, A. Bhattacharyya, S. Shajidul Haque, E. H. Kim and N. Moynihan, *Time Evolution of Complexity: A Critique of Three Methods*, arXiv:1810.02734

Chapter 11: T. Ali, A. Bhattacharyya, S. Shajidul Haque, E. H. Kim and N. Moynihan, *Post-Quench Evolution of Distance and Uncertainty in a Topological System: Complexity, Entanglement and Revivals*, arXiv:1811.05985

I hereby declare that this thesis has not been submitted, either in the same or different form, to this or any other university for a degree and that it represents my own work.

Signed by candidate

Nathaniel Timothy Babakar Seck Moynihan Date

Contents

1 Introduction 1

I Scattering Amplitudes 2

2 Introduction to Part I 3

3 Amplitudes Review 5
- 3.0.1 What are scattering amplitudes? 5
- 3.0.2 Classical scattering 5
- 3.0.3 Scattering Amplitudes 6
- 3.0.4 Asymptotic States and The S Matrix 7
- 3.0.5 Unitarity 10
- 3.0.6 Gauge Theories 13

4 Modern Amplitude Techniques 17

4.1 The Spinor Helicity Formalism 17
- 4.1.1 Square and angle bra-ket notation 18
- 4.1.2 Little group scaling 22
- 4.1.3 Massive Particle Amplitudes 25
- 4.1.4 High energy limit 28

4.2 Recursion Relations 28
- 4.2.1 Complex shifts and poles 28
- 4.2.2 The residue theorem and BCFW recursion 31
- 4.2.3 Showing shift-validity 33
- 4.2.4 BCFW with massive particles 35

4.3 Loops 36
- 4.3.1 Loop Amplitude Representations 37
- 4.3.2 One-loop amplitudes from unitarity cuts 39

5 Deflection by Gravitation: a Modern Perspective 42

5.1 Light Bending by Gravity 42

5.2 Gravitational Wave Bending by Gravity 51

6 THE vDVZ DISCONTINUITY: A MODERN AMPLITUDE PERSPECTIVE **55**
6.0.1 Calculation of 3-point amplitudes . . . 58
6.1 Four-point functions from BCFW . . . 61
6.1.1 Photon-Scalar Amplitude . . . 61
6.1.2 Scalar-Scalar Amplitude . . . 63
7 CONCLUSION TO PART I **67**

II Entanglement Entropy & Complexity 68

8 INTRODUCTION TO PART II **69**
9 ENTANGLEMENT ENTROPY & COMPLEXITY REVIEW **71**
9.1 Entanglement Entropy in Quantum Mechanics . . . 71
9.1.1 Quantum States & Bi-partite Entanglment . . . 71
9.1.2 Rényi Entropy . . . 74
9.1.3 2 State Example . . . 75
9.1.4 Properties of Entanglement Entropy . . . 76
9.1.5 Relative & Average Entropy . . . 77
9.1.6 Purifications . . . 79
9.2 Entanglement Entropy in Quantum Field Theory . . . 80
9.2.1 Density Operators as Path Integrals . . . 80
9.2.2 The Replica Trick . . . 81
9.2.3 Twist Fields . . . 85
9.2.4 Geometric Entanglement Entropy . . . 89
9.2.5 Spherical Entangling Surfaces in D dimensions . . . 91
9.2.6 Example: Entanglement Entropy of a (1+1)-d CFT . . . 93
9.2.7 The Entanglement Spectrum & Correlation Matrices . . . 94
9.3 Quantum Circuits and Complexity . . . 96
9.4 Complexity in Quantum Field Theory . . . 99
9.4.1 Fidelity as a measure of state distinguishability . . . 99
9.4.2 Circuit Complexity á la Nielsen . . . 102
9.4.3 Fubini-Study Complexity . . . 108
9.4.4 Covariance Matrix Complexity . . . 112
10 TIME EVOLUTION OF COMPLEXITY: A CRITIQUE OF THREE METHODS **117**
10.1 The Model and Quench Protocol . . . 118
10.2 Quench Complexity á la Nielsen . . . 120

10.3 Quench Complexity from Fubini-Study 122
10.4 Quench Complexity from the Covariance Matrix 124
10.5 A Complexity Comparison: The Loschmidt Echo vs the Fidelity 126
10.5.1 LE vs F: Nielsen Complexity 127
10.5.2 LE vs F: Fubini-Study Complexity 129
10.5.3 LE vs F: Covariance Matrix Complexity 131
10.6 A general statement on complexity 132

11 Complexity in a Topological System **134**
11.1 The Su-Schrieffer-Heeger Model 134
11.2 Complexity in the SSH model 137
11.3 Entanglement Entropy, Spectrum and Complexity 140

12 Conclusion to Part II **I**

III Appendix **II**

A Passarino-Veltman Integral Reduction **III**

B Bogoliubov Transformations, SU(1,1) and SP(2N, $\mathbb{R}$) **VI**

Index **XI**

Bibliography **XIII**

I

Introduction

"It may seem difficult at first, but everything is difficult at first."

– Miyamoto Musashi, The Book of Five Rings

In this thesis, we will explore two apparently distinct areas of contemporary physics: scattering amplitudes and quantum complexity. Both of these can be defined in the context of quantum mechanics and quantum field theory, and there is tantalising circumstantial evidence that both may ultimately be essential to our understanding of quantum gravity.

Quantum field theory can be thought of as a natural consequence of the composition of three elements: quantum mechanics, Lorentz invariance and the cluster decomposition theorem [7]. Roughly speaking, the cluster decomposition theorem demands that the S-matrix is local, meaning that it doesn't depend on information about distant regions of the universe[1]. It seems natural then to formulate theories using local Lagrangians, which ensures that locality is manifest every step of the way. However, this is not a priori a requirement, and in fact discards the possibility that locality may be emergent and not fundamental.

Relaxing the requirement that locality is manifest at every step has lead to some impressive advances for both scattering amplitudes and (holographic) complexity, which in turn has resulted a flurry of intense activity in both fields over the last few years.

Throwing classical intuition out of a non-local window has some surprising benefits, allowing both scattering amplitudes, entanglement entropy and complexity to be described geometrically, revealing a deep structure that was previously obscured. It is precisely this structure that we shall exploit in this thesis, using it to calculate interesting quantities in both gravitational and quantum field theories.

[1] Entanglement is allowed under the cluster decomposition theorem, since it can't affect the probabilities of measuring any particular outcome, i.e. the scattering amplitudes

Part I

Scattering Amplitudes

II

Introduction to Part I

> *"On Mondays, Wednesdays, and Fridays we use the wave theory; on Tuesdays, Thursdays, and Saturdays we think in streams of flying energy quanta or corpuscles."*
>
> – William Henry Bragg; quoted in Dictionary of Scientific Quotations

Quantum field theory (QFT) seeks to provide a qualitative explanation of fundamental physics by describing the world as a set of interacting fields. However, what we can actually measure are particles, which as any field theorist will tell you are nothing more than the excitations of some particular quantised classical field. We distinguish these fields via Wigner's classification [8, 9], which tells us that quantum fields are classified according to their spin (and additionally their mass), conveniently deducible from irreducible representations of the Poincaré group. It is this feature of quantum field theory that has led to something of a revolution in the calculation of scattering amplitudes over the last two decades.

The traditional Feynman diagram approach to computing amplitudes from a path integral makes the intuitive notions of locality and unitarity manifest at each step of a calculation. This comes at a hefty price, however, in the form of both gauge and field redefinition redundancies. These redundancies have historically been useful tools in their own right, but from a computational perspective, they introduce a lot of unwelcome complexity that the final answer typically does not share [10–13]. Additionally, choosing these specific quantities to be manifest often leads to the obfuscation of interesting symmetries that may exist, and indeed many have since been discovered or conjectured [14–17].

The modern scattering amplitude program, initiated by an observation made by Parke and Taylor in the 1980s [10], favours a different approach to computing amplitudes by demanding that locality and unitarity are manifest in the final result, but not necessarily at every intermediate step. One key goal of the program is to construct amplitudes directly from physical principles without the self-indulgent requirement of classical intuition.

The main philosophy is that the S-matrix should be constructible from an ansatz, specifically one that can be fixed from physical principles alone. Rather than

considering Feynman diagrams, we consider pure functions of the physical data only and demand that they satisfy the physical requirements: locality, in the form of poles that come from local interactions (i.e. from propagators and none from, say, delta functions [7]) and unitarity in the form of factorization around those poles. Combining these requirements with the standard tools of dimensional analysis and Lorentz invariance, we will see that we can get a very long way indeed.

III

Amplitudes Review

"Nobody ever reads a paper in which someone has done an experiment involving photons with a footnote that says 'this experiment was done using the Coulomb gauge'."

– Sidney Coleman

3.0.1 What are scattering amplitudes?

Scattering amplitudes are the main quantity of interest in perturbative Quantum Field Theory (QFT). In its initial formulation, the scattering amplitude was simply the answer to a particular question: given some interaction (a "scattering event"), what is the probability of a certain outcome? However, it has since been realised that scattering amplitudes themselves contain a much richer structure, and may well be able to answer a lot more than the question that brought them into being. Before surveying the landscape and diving head-first into the jargon of scattering amplitudes in QFT, lets take a moment to look at classical scattering.

3.0.2 Classical scattering

We will consider an idealised scattering experiment, where we have some precise beam of particles with known momentum $\vec{p}$ fired into a potential $V(r)$ localized around a scattering centre S. The particles originate at asymptotic infinity ($\vec{r} \to -\infty$) and are later measured at asymptotic infinity ($\vec{r} \to +\infty$). The particles scatter off at some angle θ, with the distance b known as the *impact parameter*, the distance from the scattering centre to the path the incident beam would have taken if it were not for the potential. The scattering angle θ depends on the impact parameter and can be determined by noting that the number of particles scattered per unit time through $\theta + d\theta$ is equal to the number of incident particles through $b + db$ (see fig. 3.1).

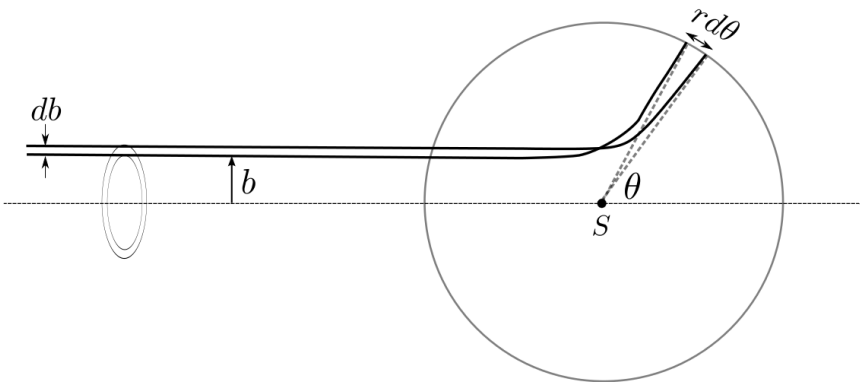

Figure 3.1: Classical Scattering

Let's consider an incident flux of particles j, through an imaginary surface of area πb^2, all eventually scattered off a target into the solid angle Ω. The detector on the other side of the target registers N particle detections per unit time at some solid angle Ω. Infinitesimally, we find

$$N d\Omega = 2\pi N \sin\theta d\theta = 2\pi j b db, \tag{3.0.1}$$

which is to say we have assumed that the number of particles scattered per unit time through θ and $\theta + d\theta$ is *equal* to the number of incident particles per unit time through b and $b + db$. This allows us to define the **differential cross section**

$$\frac{d\sigma}{d\Omega} \equiv \frac{N}{j} = \frac{b}{\sin\theta}\left|\frac{db}{d\theta}\right|. \tag{3.0.2}$$

The differential cross section is a ratio between the area $d\sigma$ that the particle passes through on its way to the target, and the angle $d\Omega$ that it passes through afterwards. For this reason, it has units of area.

Knowing the differential cross section allows you to calculate scattering angles, i.e. the likely angle that a particular projectile might have scattered from a potential $V(r)$. Typically, you will derive a formula relating the scattering angle θ and the impact parameter b, both measurable quantities.

We won't delve into classical scattering any more here, since it's not too relevant for what's coming next, but we will keep the idea in mind for future sections.

3.0.3 Scattering Amplitudes

In quantum mechanics, we will consider plane waves scattering off some target in exactly the same way as we did in fig. 3.1. However, we now have to deal with

probabilities, since that's the only relevant information we can obtain from some given wave function.

Considering a plane wave scattering from a target, we can approximate the outgoing wave as spherical. A plane wave traveling in the positive z direction has wavefunction $\psi(z) = Ae^{ikz}$, where $k = \sqrt{2mE}$ and A is the amplitude. Assuming a simple potential that is proportional to $1/r$, the outgoing spherical wave must fall off in the same manner, meaning that if we include our scattering object in the system, we have a wavefunction of the form

$$\psi(r, \theta, \phi) = A\left(e^{ikz} + f(\theta, \phi)\frac{e^{ikr}}{r}\right), \tag{3.0.3}$$

where $f(\theta, \phi)$ is the scattering amplitude.

It should be clear from this expression that if there is no scattering, then $f(\theta, \phi) = 0$ and the plane wave continues on its original trajectory. Any non-trivial scattering is then completely encapsulated by the function $f(\theta, \phi)$.

Consider plane waves travelling in the $+z$ direction at a speed v, towards a target. The probability that they will pass through an area $d\sigma$ in time dt is given by

$$dP_{in} = |\psi_{plane}|^2 dV = |A|^2 v\ dt\ d\sigma. \tag{3.0.4}$$

Similarly, the probability of finding it having scattered at an angle θ, i.e. in an area $v\ dtr^2\ d\Omega$ is given by

$$dP_{out} = |\psi_{spherical}|^2 dV = \frac{|Af|^2}{r^2} v\ dtr^2\ d\Omega. \tag{3.0.5}$$

Making the *assumption* that the probabilities for each event are the same, i.e. $dP_{in} = dP_{out}$, then we find that

$$\frac{d\sigma}{d\Omega} = |f(\theta, \phi)|^2, \tag{3.0.6}$$

meaning the scattering amplitude is nothing but the square root of the differential cross section. Scattering amplitudes are exactly what we can compute in quantum field theories and it is something that can be reliably measured by experiment.

3.0.4 Asymptotic States and The S Matrix

Consider a scattering event between two particles, in a theory with arbitrarily complicated interactions. After an interaction takes place, we know that each

particle will eventually behave like a free particle, assuming that the potential of each particle falls off quickly as we approach infinity, i.e. $V(r) \to 0$ as $r \to \infty$.

If we only care about the interaction (and not what happened before or afterwards), we might as well take $r = \infty$, which is to say that the particles originated at past infinity and evolved to future infinity with some complicated interaction in between. When we say *infinity* here, we really mean the boundary of 4D Minkowski space[1], best imagined via the Penrose diagram given in figure 3.2.

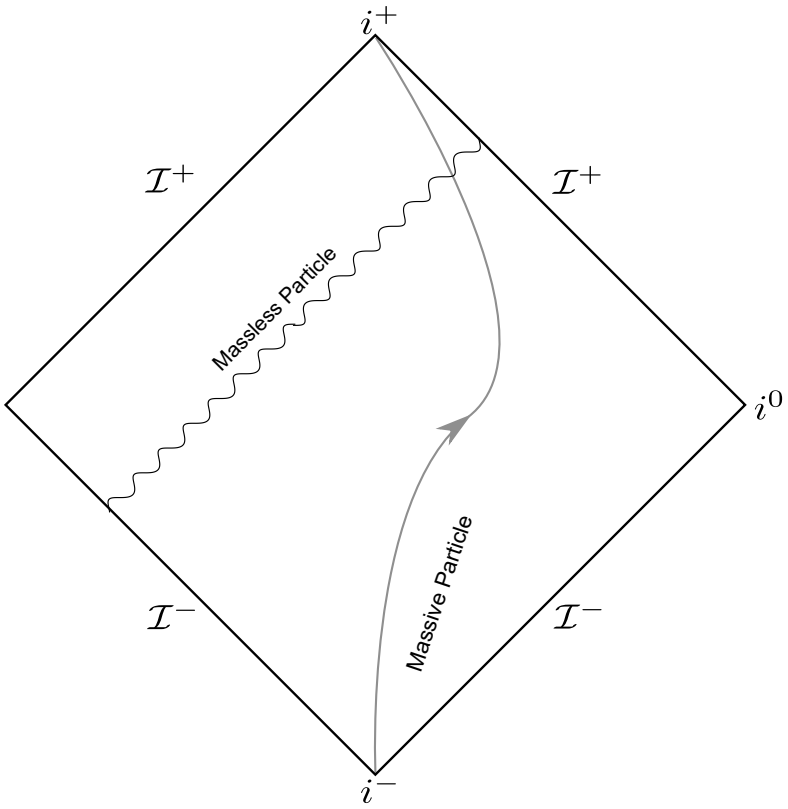

Figure 3.2: Penrose Diagram for Minkowski Spacetime

States that live at this boundary are called **asymptotic states**, and we say that initial states live in the infinite past at $\mathcal{I}^-$ while final states live in the infinite future at $\mathcal{I}^+$. Our particle emitters and detectors therefore live on $\mathcal{I}^-$ and $\mathcal{I}^+$ respectively, and particle experimenters only ever have to deal with free theories.

In a QFT, multi-particle states are created out of the vacuum via the creation operator $a^\dagger_{\vec{P}_1}(t)$, which creates a particle with momentum $\vec{P}_1$ at a time t. An n

[1]That said, we can define analogues of the S matrix and asymptotic states for other (often asymptotically flat) spacetimes.

particle state is given by

$$|P_1, P_2, ..., P_n\rangle = a^\dagger_{P_1} a^\dagger_{P_1} ... a^\dagger_{P_n} |0\rangle \,. \tag{3.0.7}$$

We can then define asymptotic states that live on $\mathcal{I}^\pm$ as

$$|\pm; P_1, P_2, ..., P_n\rangle = a^\dagger_{P_1}(\pm\infty) a^\dagger_{P_1}(\pm\infty) ... a^\dagger_{P_n}(\pm\infty) |0\rangle \,, \tag{3.0.8}$$

and choosing $-$ is an in free state and $+$ an out free state.

Since we are only considering a free theory, we can use what we know about free theories: they evolve via the unitary time evolution operator $U = e^{iHt}$. When we evaluate this operator in the limit of $t = \pm\infty$, we give it a new name – the **S matrix** (S for scattering), defined as

$$S_{fi} \equiv {}_{free}\langle\psi_f|\psi_i\rangle_{free} = \lim_{t_i \to -\infty} \lim_{t_f \to +\infty} \langle\psi_f|e^{-iH(t_i - t_f)}|\psi_i\rangle \tag{3.0.9}$$

$$= \langle\psi_f|S|\psi_i\rangle \,. \tag{3.0.10}$$

Formally, in flat space, the S-matrix is an operator that acts on irreducible unitary representations of the Poincaré group, and if you know its elements, you know everything about the scattering event. Most importantly, we say that the S matrix maps asymptotic in states to asymptotic out states, schematically

$$|\psi_f\rangle = S\,|\psi_i\rangle \,. \tag{3.0.11}$$

In a quantum field theory, asymptotic states live in a Fock space $\mathcal{F}^\pm$ defined on $\mathcal{I}^\pm$.

The S matrix has some noteworthy properties, for example the vacuum states $|0\rangle$ and one particle states $|\varphi\rangle$ are invariant under the S matrix

$$S\,|0\rangle = |0\rangle \,, \qquad \langle\varphi_{in}|S|\varphi_{in}\rangle = \langle\varphi_{out}|\varphi_{in}\rangle = \langle\varphi_{in}|\varphi_{in}\rangle = 1. \tag{3.0.12}$$

Since the S matrix must also describe the case where nothing is scattered (S is then a unit matrix), we normally define the transition matrix

$$S_{fi} = \delta_{fi} + iT_{fi}. \tag{3.0.13}$$

The S matrix ought to be translation invariant, meaning we require that its behaviour under translation operators is

$$\langle\psi_f|S|\psi_i\rangle = \langle\psi_f|e^{-ip_f\cdot x} S e^{-ip_i\cdot x}|\psi_i\rangle = e^{-i(p_f - p_i)\cdot x}\,\langle\psi_f|S|\psi_i\rangle \,. \tag{3.0.14}$$

This is only true if momentum conservation holds, therefore scattering amplitudes $\mathcal{A}$ are *defined* as matrix elements of T with an overall momentum-conserving delta function stripped out

$$\langle\psi_f|S-\delta|\psi_i\rangle = i\langle\psi_f|T|\psi_i\rangle = i(2\pi)^D\delta^D(P_i-P_f)\mathcal{A}(p_1,...,p_m;q_1,...,q_n), \tag{3.0.15}$$

where the $\mathcal{A}$ represents the scattering amplitude for a $m \longrightarrow n$ scattering event and D is the dimension of spacetime.

It will be useful later on to know the mass-dimension of the scattering amplitude $\mathcal{A}$, so we shall derive it here.

One particle states are normalised as

$$\langle p', x'|p, x\rangle = (2\pi)^{D-1}2E \times \delta^{(D-1)}(\vec{p}-\vec{p}')\delta_{xx'}, \tag{3.0.16}$$

and from eq. 3.0.15 we note that

$$[\mathcal{A}_N] = [T_{fi}] - [\delta^{(D)}(P_i - P_f)]. \tag{3.0.17}$$

Given the normalisation in eq. 3.0.16, and the fact that $[\delta^{(J)}(f)] = [f]^{-J}$, we can see that an $N = n + m$ particle matrix must have dimension

$$[T_{fi}] = \frac{N}{2}(2-D), \tag{3.0.18}$$

where $[|p, x\rangle] = \frac{2-D}{2}$. Then, we find that a scattering amplitude with N external legs has mass dimension

$$[\mathcal{A}_N] = \frac{N}{2}(2-D) + D. \tag{3.0.19}$$

In four dimensions, this is then

$$[\mathcal{A}_N] = 4 - N. \tag{3.0.20}$$

3.0.5 Unitarity

Since we defined the S matrix as the limit of a unitary transformation, we should of course expect it to be unitary. It turns out that the unitary nature of the S matrix places interesting constraints on generic amplitudes.

Unitarity means that

$$1 = SS^\dagger = S^\dagger S \qquad \Longrightarrow \qquad T - T^\dagger = iTT^\dagger. \tag{3.0.21}$$

Writing the transition operator in this way, we find that we can write

$$\langle f|T - T^\dagger|i\rangle = \langle f|T|i\rangle - \langle f|T^\dagger|i\rangle \equiv T_{fi} - T^*_{if}. \tag{3.0.22}$$

We can insert a complete set of states, to find that

$$i\,\langle f|TT^\dagger|i\rangle = i\sum_q \int dq\ \ \langle f|T|q\rangle\,\langle q|T^\dagger|i\rangle \equiv \int dq T_{fq}T^*_{iq}. \tag{3.0.23}$$

We can use this relation along with the definition of a scattering amplitude to derive a result known as the **generalised optical theorem**

$$\mathcal{A}_{fi} - \mathcal{A}^*_{if} = i\int d\mu \mathcal{A}_{f\mu}\mathcal{A}^*_{i\mu}, \tag{3.0.24}$$

where $\int d\mu \ \equiv (2\pi)^4 \sum_\mu \int d\mu \delta^4(\sum p)$ and the summation and integration is over all final states, helicities and integrals over intermediate on-shell states.

This equation *must* be satisfied by any on-shell amplitudes in order for the theory to be unitary and for probability conserved.

Taking $i = f$, we obtain the **optical theorem**

$$\Im(\mathcal{A}_{ii}) = \frac{1}{2}\int d\mu\ |\mathcal{A}_{i\mu}|^2. \tag{3.0.25}$$

This relates the imaginary part of the scattering amplitude to its square modulus, meaning the imaginary part must be related to the cross section we discussed earlier.

More importantly, it relates orders in perturbation theory: at order λ^2 in the coupling, we see that we must have at least *some* agreement between both loop and square of tree level amplitudes, meaning that in principle we can determine the imaginary part of loop amplitudes using trees. We can see this by expanding T in the coupling constant

$$T = \lambda T^{\text{tree}} + \lambda^2 T^{\text{1-loop}} + \lambda^3 T^{\text{2-loop}} + \cdots. \tag{3.0.26}$$

Plugging this into eq. 3.0.21 and comparing orders of coupling constant, we see that we must have

$$T^{\text{tree}} = T^{\text{tree}\dagger}, \qquad -i(T^{\text{1-loop}} - T^{\text{1-loop}\dagger}) = (T^{\text{tree}})^2. \tag{3.0.27}$$

An important consequence of this is that if second order trees exist *so must second order loops*: a classical field theory *without* loops violates the optical theorem and therefore violates unitarity.

Within amplitudes, imaginary terms are found in the internal propagators. We can write the imaginary part of the free massive scalar propagator as

$$\Im\left(\frac{1}{p^2+m^2+i\epsilon}\right)=\frac{1}{2i}\left(\frac{1}{p^2+m^2+i\epsilon}-\frac{1}{p^2+m^2-i\epsilon}\right)=\frac{-\epsilon}{(p^2+m^2)^2+\epsilon^2}. \quad (3.0.28)$$

This vanishes for $\epsilon \longrightarrow 0$, however not in the case of the propagator being on shell where $p^2=-m^2$. Integrating this equation wrt p implies that the imaginary part must go like

$$\Im\left(\frac{1}{p^2+m^2+i\epsilon}\right)=-\pi\delta(p^2+m^2). \quad (3.0.29)$$

This is interesting because it says that the propagator is real unless it goes on-shell. Additionally, this also means that the imaginary part of loop amplitudes correspond to internal lines going on shell.

Using the same trick as before, we can see that the propagator in eq, 3.0.28 actually decomposes into two distinct objects: one representing the positive energy flow and one negative - essentially describing the propagation of a particle either from x to y or from y to x. We can see this by writing the propagator in the form

$$D_F(p)=\frac{i}{p^2+m^2+i\epsilon}=\frac{i}{2E_p}\left(\frac{1}{p_0+E_p+i\epsilon}-\frac{1}{p_0-E_p-i\epsilon}\right). \quad (3.0.30)$$

We only want to consider positive energy contributions to the propagator, due to an argument from causality (see [18] for an elegant derivation from the largest time equation), and thus we find that we need to replace our propagator with

$$\frac{i}{p^2+m^2+i\epsilon}\longrightarrow 2\pi i\theta(p^0)\delta(p^2+m^2). \quad (3.0.31)$$

As a direct result of unitarity, we can therefore replace an internal line with a delta function (bring it on-shell), and split it into a product of tree amplitudes - these are known as *cut conditions* or *Cutkosky's rule*. In equation form, this is

$$2\Im\left(\mathcal{A}_{fi}^{\text{1-loop}}\right)=-i\text{Disc}_s\left(\mathcal{A}_{fi}^{\text{1-loop}}\right)=\int d\mu\ \mathcal{A}_{f\mu}^{\text{tree}}\mathcal{A}_{\mu i}^{\text{tree}}, \quad (3.0.32)$$

and we define the *discontinuity* of a function as

$$\text{Disc}_s\left(F(s)\right)\equiv\lim_{\epsilon\longrightarrow 0}\left[F(s\pm i\epsilon)-F(s\mp i\epsilon)\right]. \quad (3.0.33)$$

By making the two above equal, we are assuming that A_{fi} is positive and satisfies the Schwarz reflection principle, meaning that the discontinuity is localized to the imaginary piece of A_{fi} only. The discontinuity of a function gives the value of the discontinuity of F as the variable s crosses a branch cut located on the real axis, i.e.

we move from one Riemann sheet to another and evaluate the function at points nearby the cut on either side. Essentially, discontinuities can be thought of as the residues of a given amplitude when integrating over two complex propagators as they go on-shell on the complex plane. If there is no branch cut, or if F is independent of s, then the $\text{Disc}_s F = 0$. Discontinuities of this type occur exactly when we put the propagator on-shell [19, 20]. We will see later on that this is very useful for computing loop integrals.

3.0.6 Gauge Theories

We will now review the properties of gauge theories in order to introduce some important concepts.

The Lagrangian for a Yang-Mills gauge theory is

$$\mathcal{L} = -\frac{1}{4}\text{Tr}\left(F_{\mu\nu}F^{\mu\nu}\right), \tag{3.0.34}$$

where $F^a_{\mu\nu} = \partial_\mu A^a_\nu - \partial_\nu A^a_\mu - ig[A_\mu, A_\nu]^a$ and $A_\mu \equiv A^a_\mu T^a$.

A_μ is a matrix valued gauge field, with gauge group $G = SU(N)$, meaning we have N different colours in our theory. The indices μ, ν are spacetime indices, while the index a labels the adjoint representation of $SU(N)$, which has $N^2 - 1$ generators, thus $a = 1, 2, ...N^2 - 1$.

We choose the generators of $SU(N)$ to be normalised such that $\text{Tr}\left(T^a T^b\right) = \delta^{ab}$ and $[T^a, T^b] = if^{abc}T^c$, where the trace is over the fundamental representation. Given these two equations, we define the structure constants via

$$if^{abc} = \text{Tr}\left([T^a, T^b]T^c\right), \tag{3.0.35}$$

and in order to read off the Feynman rules, we are forced to choose and fix a gauge. The path integral for our theory is

$$Z = \int \mathcal{D}A^a_\mu(x) \exp\left(-\frac{i}{4}\int d^4x \ \text{Tr}\left(F_{\mu\nu}F^{\mu\nu}\right)\right), \tag{3.0.36}$$

which is over all field configurations - including those related by gauge transformations. As Sidney Coleman one said, no one has ever read a paper with the footnote 'in this experiment we used the Feynman gauge', so we had better make sure our gauge redundancy is removed if we want sensible results - in other words, we had better fix a gauge. The standard way to do this is via the Fadeev-Popov method, meaning we add a term to the action to eat up the gauge freedom to ensure our path integral does not over count field configurations.

The gauge we will choose is the Gervais-Neveu gauge, which after adding the gauge-fixing term Lagrangian, results in

$$\mathcal{L}_{GF} = \mathrm{Tr}\left(-\frac{1}{2}\partial^\mu A^\nu \partial_\mu A_\nu - i\sqrt{2}g\partial^\mu A^\nu A_\nu A_\mu + \frac{1}{4}g^2 A^\mu A^\nu A_\mu A_\nu\right). \tag{3.0.37}$$

This gauge choice is particularly useful for a number of reasons. Firstly, it doesn't introduce any unphysical degrees of freedom ("ghosts"), and secondly, it greatly simplifies computing tree-level amplitudes. As an interesting aside, we find that in this particular gauge the off-shell three-gluon vertex *double copies* to the three-graviton vertex, meaning that we can write it as [21]

$$V_{graviton}^{\mu_1\nu_1,\mu_2\nu_2,\mu_3\nu_3} \sim V_{gluon}^{\mu_1\mu_2\mu_3} V_{gluon}^{\mu_1\mu_2\mu_3}. \tag{3.0.38}$$

Before actually writing down the Feynman rules of the theory, we will define some conventions so that in what follows we can in some sense ignore contributions from colour factors until *after* we have calculated an amplitude, by stripping away the colour information *by convention* [22–24].

Ignoring any kinematic contributions, 3-vertices are proportional to the structure constants

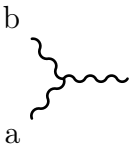

$$\propto f^{abc} = \mathrm{Tr}\left(T^a T^b T^c\right) - \mathrm{Tr}\left(T^a T^c T^b\right). \tag{3.0.39}$$

For $SU(N)$, there is a Jacobi relation of the form

$$[T^a,[T^b,T^c]] + [T^b,[T^c,T^a]] + [T^c,[T^a,T^b]] = 0 \tag{3.0.40}$$

Which then provides a relation for the structure constants[2]

$$f^{ab}{}_e f^{ecd} + f^{ad}{}_e f^{ebc} + f^{ac}{}_e f^{edb} = 0, \tag{3.0.41}$$

where the label e indicates the 'internal' colour that must be summed over.

We can now compile the products of traces into *single traces*, using the **completeness relation** of $SU(N)$. To derive this, we note that we can use the generators T^a, plus a unit matrix, as the basis for any hermitian matrix H, which can then be written

$$H = \alpha I + \beta_a T^a, \tag{3.0.42}$$

with α and β_a constants to be determined. We then take the trace of H, using the fact that $\mathrm{Tr}\left(T^a\right) = 0$, and then the trace of $T^a H$,

$$\mathrm{Tr}\left(H\right) = \alpha N, \qquad \mathrm{Tr}\left(T^a H\right) = \beta_a. \tag{3.0.43}$$

[2]Note that we will rediscover this equation in a particularly elegant way later in section 4.1.2

Plugging this in, we find

$$H^l_k = H^i_j \left[\frac{1}{N} \delta^j_i \delta^l_k + (T^a)^j_i (T^a)^l_k \right] = \delta^l_i \delta^j_k H^i_j. \tag{3.0.44}$$

Since this is valid for arbitrary H, we find the Fierz identity

$$(T^a)_i{}^j (T^a)_k{}^l = \delta_i{}^l \delta_k{}^j - \frac{1}{N} \delta_i{}^j \delta_k{}^l, \tag{3.0.45}$$

and the general definition of the trace

$$\mathrm{Tr}\left(T^{a_1} T^{a_2} \cdots T^{a_n}\right) = (T^{a_1})^i_{j_1} (T^{a_2})^{j_1}_{j_2} (T^{a_3})^{j_2}_{j_3} \cdots (T^{a_n})^{j_{n-1}}_i. \tag{3.0.46}$$

Taking the large N limit, we find[3],

$$\mathrm{Tr}\left(T^{a_1} T^{a_2} \cdots T^c\right) \mathrm{Tr}\left(T^c T^{b_1} T^{b_2} \cdots\right) = \mathrm{Tr}\left(T^{a_1} T^{a_2} \cdots T^{b_1} T^{b_2} \cdots\right). \tag{3.0.47}$$

As an example, consider the s channel 4-pt, which yields, eventually

$$f^{a_1 a_2 b} f^{b a_3 a_4} \propto \mathrm{Tr}\left([T^{a_1}, T^{a_2}] T^b\right) \mathrm{Tr}\left([T^{a_3}, T^{a_4}] T^b\right) \tag{3.0.48}$$

$$= \mathrm{Tr}\left([T^{a_1}, T^{a_2}][T^{a_3}, T^{a_4}]\right) + \mathcal{O}(\frac{1}{N}), \tag{3.0.49}$$

with the u, t channels found by permutation. For n objects inside any given single trace, there can be only $(n-1)!$ unique traces (the minus one coming from the fact that the trace is cyclic). We can use this object as a basis, the so called **colour ordered basis**. We do this be expressing the full amplitude in terms of **partial amplitudes** multiplied by single trace colour factors. As an added bonus, all our partial amplitudes will be gauge invariant.

This boils down to is the following equation

$$\mathcal{A}^{full,tree}_n = g^{n-2} \sum_{\text{perms } \sigma} A_n[1\sigma(2...n)] \mathrm{Tr}\left(T^{a_1} T^{\sigma(a_2 \cdots} T^{a_n)}\right), \tag{3.0.50}$$

and A_n is the gauge invariant partial amplitude or colour ordered amplitude.

For example for a 4-gluon amplitude, this would read:

$$\mathcal{A}_4 = g^2 (A_4[1234] \mathrm{Tr}\left(T^{a_1} T^{a_2} T^{a_3} T^{a_4}\right) + \text{perms of } (234)). \tag{3.0.51}$$

However, we said that the colour ordered basis has $(n-1)!$ elements, which seems to be over-complete. This is indeed true, and in fact not all the elements are unique, since the partial amplitudes A_n satisfy a number of relations

[3] The fact that single traces factorise is important for the consistency of tree level amplitudes, however you might complain that it appears to be spoiled by the $1/N$ term in this case. It turns out, however, that the $1/N$ piece always vanishes for tree level amplitudes in Yang-Mills, due to a dual Ward identity or $U(1)$ decoupling identity in eq. 3.0.52.

- They are **cyclic**: $A_n[12\cdots n] = A_n[2\cdots n1]$.
- They are **reflection invariant** (up to a sign)

$$A_n[12\cdots n] = (-1)^n A_n[n\cdots 21].$$

- They satisfy the **U(1) decoupling identity**

$$A_n[123\cdots n] + A_n[213\cdots n] + A_n[231\cdots n] + \cdots + A_n[23\cdots 1n] = . \quad (3.0.52)$$

- They *only* depend on kinematics

The first two properties follow directly from the properties of the trace.

To derive the U(1) decoupling identity, we decide to exchange one of the legs in our amplitude for a photon (from $U(1)$) rather than a gluon. We do this because the partial amplitudes for photons and gluons are the same, but their generators are not. We also know that photons don't couple to gluons, so by replacing just one leg, we know that the total amplitude must equal zero.

Technically, this amounts to setting one of the generators (T^{a_2} in our example) to the identity I, to get

$$\mathcal{A}_n = g^{n-2} \sum_{\text{perms } \sigma} A_n[1\sigma(2...n)] \text{ Tr}\left(T^{a_1} T^{\sigma(a_2\cdots} T^{a_n)}\right)\Big|_{T^{a_2}\longrightarrow I} = 0. \quad (3.0.53)$$

For example the 4pts

$$\mathcal{A}_4 = g^2\Big[A_4[1234]\text{Tr}\left(T^{a_1}T^{a_3}T^{a_4} + T^{a_1}T^{a_4}T^{a_3}\right) + A_4[1324]\text{Tr}\left(T^{a_1}T^{a_3}T^{a_4} + T^{a_1}T^{a_4}T^{a_3}\right) + \quad (3.0.54)$$

$$A_4[1342]\text{Tr}\left(T^{a_1}T^{a_3}T^{a_4} + T^{a_1}T^{a_4}T^{a_3}\right)\Big] \quad (3.0.55)$$

$$= g^2\text{Tr}\left(T^{a_1}T^{a_3}T^{a_4} + T^{a_1}T^{a_4}T^{a_3}\right)\left(A_4[1234] + A_4[1324] + A_4[1342]\right) = 0. \quad (3.0.56)$$

Having discussed the structure of pure Yang Mills amplitudes - at least at tree level - lets see how to bootstrap[4] them using modern techniques.

[4]The concept of bootstrapping refers to the idea that we can simply construct objects using only physical symmetries and not by overly involved calculation.

IV

Modern Amplitude Techniques

"The most merciful thing in the world, I think, is the inability of the human mind to correlate all its contents."

– H. P. Lovecraft, *The Call of Cthulhu*

In this chapter we will introduce some modern techniques for calculating scattering amplitudes, before moving

4.1 The Spinor Helicity Formalism

This section closely follows the treatment found in [25], [26] and [27], and which we refer the interested reader for further details.

We begin in four spacetime dimensions with the familiar Lorentz group of rotations and boosts, that can be mapped to the group of 2×2 matrices with complex entries and unit determinant, prescribed by the relationship

$$SO(1,3) \simeq SL(2,\mathbb{C}). \tag{4.1.1}$$

This innocuous observation allows us to decompose any Lorentz four vector, P^μ, into a **bi-spinor**, a 2×2 matrix with two indices from $SL(2,\mathbb{C})$, *i.e.*

$$P^\mu \in SO(1,3) \;\longrightarrow\; P_{a\dot{b}} = P_\mu (\sigma^\mu)_{a\dot{b}} \in SL(2,\mathbb{C}). \tag{4.1.2}$$

This mapping is defined through the set of matrices $(\sigma^\mu)_{a\dot{b}}$, which consists of the identity $\mathbf{1}_{a\dot{b}}$ and the usual Pauli matrices of quantum mechanics,

$$(\sigma^\mu)_{a\dot{b}} = (\mathbf{1}, \sigma^i)_{a\dot{b}}. \tag{4.1.3}$$

Notice that since the Lorentz indices in (4.1.2) are summed over, we have effectively traded *one* spacetime index for *two* matrix indices with the undotted index corresponds to the row label and the dotted one to the column label. In this language, the invariant square $P_\mu P^\mu$ of the vector P^μ is given by the determinant

of the bi-spinor $P_{a\dot{b}}$. For null vectors, this means that the 2×2 matrix $P_{a\dot{b}}$ can be written as the product of two-component spinors since,

$$\det(P_{a\dot{b}}) = 0 \iff P_{a\dot{b}} = -\lambda_a \tilde{\lambda}_{\dot{b}}. \tag{4.1.4}$$

These objects are complex columns known as **Weyl spinors**, and they will provide the basic building blocks for what follows. They will obviously depend on the real vector P^μ, and have components:

$$\lambda_a = \begin{pmatrix} \sqrt{P^0 + P^3} \\ \frac{P^1 + iP^2}{\sqrt{P^0 + P^3}} \end{pmatrix}, \qquad \tilde{\lambda}_{\dot{a}} = \begin{pmatrix} \sqrt{P^0 + P^3} \\ \frac{P^1 - iP^2}{\sqrt{P^0 + P^3}} \end{pmatrix}. \tag{4.1.5}$$

Notice that for a real vector, these associated spinors are complex conjugates of one another. This is no longer the case if the components of P^μ are complex. Instead of using Eq. (4.1.2), the mapping between Lorentz vectors and bi-spinors may alternatively be defined through

$$P^{\dot{a}b} \equiv P_\mu (\bar{\sigma}^\mu)^{\dot{a}b}, \tag{4.1.6}$$

where now

$$(\bar{\sigma}^\mu)^{\dot{a}b} = (\mathbf{1}, -\sigma^i)^{\dot{a}b}. \tag{4.1.7}$$

Technically speaking, this furnishes another representation of the bi-spinors. However, these two representations can be linked with the completely antisymmetric Levi-Civita symbols ϵ^{ab} and ϵ_{ab} defined as $\epsilon^{12} = -\epsilon^{21} = \epsilon_{21} = -\epsilon_{12} = 1$, with all the other components zero. Specifically since,

$$(\bar{\sigma}^\mu)^{\dot{a}b} = \epsilon^{bc} \epsilon^{\dot{a}\dot{d}} (\sigma^\mu)_{c\dot{d}}\,. \tag{4.1.8}$$

it follows that the bi-spinors $P_{a\dot{b}}$ and $P^{\dot{a}b}$ are not independent quantities. Raising and lowering spinor indices is also naturally defined for Weyl spinors so that, if $P^{\dot{a}b} = -\tilde{\lambda}^{\dot{a}} \lambda^b$,

$$\lambda_a = \epsilon_{ab} \lambda^b, \qquad \tilde{\lambda}_{\dot{a}} = \epsilon_{\dot{a}\dot{b}} \tilde{\lambda}^{\dot{b}}. \tag{4.1.9}$$

4.1.1 Square and angle bra-ket notation

To circumvent a proliferation of unwieldy dotted and undotted indices, we will now introduce a simple and intuitive modern notation for our two-component spinors. Let's consider the Lorentz 4-momentum p^μ for definiteness sake and carry out the split into Weyl spinors above. then associated to this vector, we will have the spinors[1]

[1] We find the following mnemonics helpful: (bra)ket $\leftrightarrow$ (anti-) spinor and (square) angle $\leftrightarrow$ (positive) negative helicity.

- $\lambda_a = |p]_a \equiv |p]$ A positive helicity spinor
- $\tilde{\lambda}^{\dot{a}} = |p\rangle^{\dot{a}} \equiv |p\rangle$ A negative helicity spinor
- $\lambda^a = [p|^a \equiv [p|$ A positive helicity anti-spinor
- $\tilde{\lambda}_{\dot{a}} = \langle p|_{\dot{a}} \equiv \langle p|$ A negative helicity anti-spinor

All of the angle and square spinors commute with one another, and the operations of raising and lowering indices defined in Eq. (4.1.9) now take the form,

$$[p|^a = \epsilon^{ab}|p]_b \qquad |p\rangle^{\dot{a}} = \epsilon^{\dot{a}\dot{b}}\langle p|_{\dot{b}} \,. \tag{4.1.10}$$

In words, the Levi-Civita symbol converts a spinor into an anti-spinor while preserving its helicity. Moreover, for real momenta p^μ, complex conjugation changes spinors into anti-spinors and flips their helicities since, as can be checked explicitly,

$$[p|^a = (|p\rangle^{\dot{a}})^*, \qquad \langle p|_{\dot{a}} = (|p]_a)^*. \tag{4.1.11}$$

The four-momentum of some particle in our new notation is again the product of two spinors of opposite helicity,

$$p_{a\dot{b}} = -|p]_a\,\langle p|_{\dot{b}}\,, \qquad p^{\dot{a}b} = -|p\rangle^{\dot{a}}\,[p|^b\,. \tag{4.1.12}$$

Using the explicit expression for the momentum spinors, it is interesting to note that acting on either of them with the original bispinor $p_{a\dot{b}}$ gives us zero; for instance,

$$p_{a\dot{b}}\,|p\rangle^{\dot{b}} = p_{a\dot{b}}\epsilon^{\dot{b}\dot{c}}\,\langle p|_{\dot{c}} \tag{4.1.13}$$

$$= \sqrt{2E}\begin{pmatrix} -\sin^2(\theta/2) & \sin(\theta/2)\cos(\theta/2)\,e^{-i\varphi} \\ \sin(\theta/2)\cos(\theta/2)e^{i\varphi} & -\cos^2(\theta/2) \end{pmatrix}\begin{pmatrix} 0 & 1 \\ -1 & 0 \end{pmatrix}\begin{pmatrix} \sin(\theta/2) \\ -\cos(\theta/2)\,e^{-i\varphi} \end{pmatrix} \tag{4.1.14}$$

$$= \begin{pmatrix} -\sin^2(\theta/2)\cos(\theta/2)\,e^{-i\varphi} + \sin^2(\theta/2)\cos(\theta/2)\,e^{-i\varphi} \\ \cos^2(\theta/2)\sin(\theta/2) - \cos^2(\theta/2)\sin(\theta/2) \end{pmatrix}$$

$$= 0. \tag{4.1.15}$$

This is one form of the massless **Weyl equation**, which is the two-component spinor equivalent of the massless Dirac equation. This equation is satisfied by all the momentum spinors introduced above, and will be extremely useful in order to deal with scattering amplitudes. To conclude this example, we will summarise the form of the Weyl equation for the different momentum spinors,

$$p_{a\dot{b}}\,|p\rangle^{\dot{b}} = 0, \qquad \langle p|_{\dot{a}}\,p_{\dot{a}b} = 0, \qquad [p|^a p_{a\dot{b}} = 0, \qquad p^{\dot{a}b}[p|_b = 0. \tag{4.1.16}$$

Continuing on with our discussion of the bra-ket notation, it is worth highlighting several other relevant properties of spinors that are captured by this notation. The first of these is the angle spinor bra-ket and square spinor bra-ket which, for two lightlike vectors p^μ and q^μ, are defined as

$$\langle pq\rangle \;=\; \langle p|_{\dot a}\;|q\rangle^{\dot a} = -\,\langle qp\,\rangle\,, \qquad\qquad [p\,q] \;=\; [p|^a\,|q]_a = -[q\,p]\,. \tag{4.1.17}$$

The antisymmetry of the bra-kets follows from the Levi-Civita symbols that are used to raise and lower spinor indices. For the same reason, all other combinations of bra-kets *e.g.* $\langle pq]$ vanish. These new **spinor-helicity variables** satisfy a number of remarkable identities, many of which have been enumerated in detail in, for example, appendix A of [25]. While we will not recount all of them here, it will be useful for our purposes to elaborate on one or two. The first of these is that two null vectors p^μ and q^μ satisfy

$$(p+q)^2 = 2p\cdot q = \langle pq\rangle\,[pq]\,. \tag{4.1.18}$$

The second is the re-formulation of momentum conservation in spinor-helicity variables. If all the external particles (corresponding to external lines in the Feynman diagram) are massless, then starting from momentum conservation $\sum_i p_i = 0$ and multiplying both sides from the left and right with $\langle q|$ and $|k]$ respectively gives

$$\begin{aligned}
0 &= \langle q|\sum_{i=1}^{n} p_i|k] \\
&= \sum_{i=1}^{n}\langle q|p_i|k] \\
&= \sum_{i=1}^{n}\langle q|_{\dot a}\,p_i^{\dot a b}\,|k]_b \\
&= \sum_{i=1}^{n}\langle q|_{\dot a}\,(-\,|p_i\rangle^{\dot a}\,[p_i|^b)\,|k]_b \\
&= -\sum_{i=1}^{n}\langle qi\rangle\,[ik].
\end{aligned} \tag{4.1.19}$$

In the last equality, we have introduced the shorthand notation which replaces the internal momenta p_i with i, so that $p_i = -\,|i\rangle\,[i|$. This notation will be used frequently in what follows. Eq. (4.1.19) leads to a new definition of momentum conservation, valid for *any* q and k,

$$\sum_{i=1}^{n}\langle qi\rangle\,[ik] = 0. \tag{4.1.20}$$

The final quantity that requires introduction is the **polarization vector**, since we are going to be dealing with massless particles that have spin. According to Wigner, particles with spin s are represented by tensors with s Lorentz indices [8]. Wigner showed that if $s > 0$, each particle has $2s + 1$ degrees of freedom on shell: we call these polarization states. Polarization states are described by vectors with s indices, which you might think leads to $D = 4$ different polarizations, however only three polarizations are independent.

For massless particles, requiring gauge invariance knocks out another, and we end up with two polarizations in the end. What this boils down to is that massless spin-1 particles have polarization vectors ϵ_μ^λ have to satisfy

$$\epsilon_i^\lambda \cdot P_i = 0, \qquad \epsilon_i^\lambda \cdot \epsilon_i^\lambda = 0, \qquad \epsilon_i^{\lambda *} = \epsilon_i^{-\lambda}, \qquad \epsilon_i^\lambda \cdot \epsilon_i^{-\lambda'} = -\delta^{\lambda\lambda'} \tag{4.1.21}$$

Where $\epsilon_{i,\mu}^\lambda \equiv \epsilon(P_i, \lambda)_\mu$ and λ is the helicity of the particle.

Following the conventions laid out in [25], we find that a convenient choice of polarization vectors is

$$\epsilon_{p,\mu}^+ = -\frac{\langle q|\,\gamma_\mu|p]}{\sqrt{2}\,\langle qp\rangle}, \qquad \epsilon_{p,\mu}^- = -\frac{\langle p|\,\gamma^\mu|q]}{\sqrt{2}[qp]}\,, \tag{4.1.22}$$

respectively.

For massive spin-1 objects, there is one extra polarization - since including a mass breaks gauge invariance. This additional polarization is a *scalar* mode, corresponding to $\lambda = 0$. We will return to the case of massive polarization modes later in this thesis.

Let's unpack the massless case objects. The γ-matrices satisfy the anticommutation relations $\{\gamma^\mu, \gamma^\nu\} = -2\eta^{\mu\nu}$ and can be realized in terms of the Pauli matrices as

$$\gamma^\mu = \begin{pmatrix} 0 & (\sigma^\mu)_{a\dot{b}} \\ (\bar{\sigma}^\mu)^{\dot{a}b} & 0 \end{pmatrix}. \tag{4.1.23}$$

The polarization vector is a function of the momentum p and an arbitrary reference momentum q, which is an *auxiliary* variable in that it does not correspond to any physical quantity. Its presence reflects a gauge freedom in the formalism; we are free to shift the polarization vectors by an arbitrary constant multiple of the momentum p without changing the on-shell amplitude[2], A_n. We can freely choose q to be whatever we like, however it is often useful to make q equal to one of the external momenta p_i when actually trying to calculate amplitudes. It is important

[2]Technically, this is encoded in the **Ward identity**, $p_\mu A_n^\mu = 0$.

that the final form of the amplitude *does not* depend on this choice of momentum, however. In practice, the choice does tend to matter and making clever choices can often immensely simplify calculations.

At tree level (*i.e.* without quantum corrections), there are only two ingredients that are needed in order to calculate anything we might want: 3-point amplitudes, which represent interactions of three particles, and 2-point functions (Green's functions or propagators), which represent a single particle propagating between two spacetime points.

To derive the n-point amplitudes that encode the scattering of n particles we would need to start from the action of the theory and derive the Feynman rules. For many theories like Einstein gravity, these often result in a hideous mess of many terms and a plethora of indices, even though the on-shell final expression is often ludicrously simple by comparison (for example, the 3pt vertex in general relativity contains 171 terms, many of which cancel to give a beautifully simple result). The origin of this complication is the requirement that locality and unitarity as manifest as possible in the calculation (introducing the notion of virtual particles), the price of which is often the introduction of unphysical (gauge) redundancies and the obfuscation of often useful symmetries. An alternative and much simpler approach is to use the symmetries of the problem, along with some physical principles, to constrain the possible final answers without a virtual particle ever being seen. The key demands that we will make of any well behaved amplitude is that the final answer is local (no poles other than $1/p^2$), that it is Lorentz invariant and that it has the correct mass dimensions. As we will see, these principles alone will take us extremely far.

4.1.2 Little group scaling

The requirement that amplitudes be Lorentz invariant means that they ought to come packaged as Lorentz scalars, typically functions only of the Mandelstam invariants. In addition to this, amplitudes with spin also need to be entirely covariant under the **little group**, a subgroup of some group that leaves a particular state invariant. Specifically, if the group G acts on a space M in which $m \in M$ is some fixed element and $H \subset G$ is a subgroup that acts on m leaving it invariant then H is called a little group of G.

For our purposes, the group of interest will be the Poincaré group of spatial rotations, boosts and spacetime translations in four dimensions. This group acts on the space of 4-vectors x^μ. If x^μ is a timelike vector then the little group is the $SO(3) \simeq SU(2)$ subgroup of the Poincaré group in the 3-space orthogonal to x^μ.

On the other hand, if x^μ is spacelike or null, the little group will be $SO(2,1)$ or $SO(2) \simeq U(1)$ respectively.

In introducing the spinor helicity formalism, we used the central notion of a null vector being represented as a momentum bi-spinor, $p_{a\dot{b}} = -|p]_a \langle p|_{\dot{b}}$. For real momenta, if we take t to be a complex phase then it is clear that scaling the individual spinors

$$|p\rangle \to t\,|p\rangle\,, \qquad\qquad |p] \to t^{-1}|p], \tag{4.1.24}$$

keeps the momentum bi-spinor invariant. For complex momenta, any complex number t will do as the little group scale factor. Physically, only external momenta scale under the little group; vertices and internal lines do not.

Individual spinors have helicity $h = \pm\frac{1}{2}$, and so they scale as t^{-2h} under a little group scaling. Additionally, spin 1 bosons also scale as t^{-2h} (you can convince yourself of this by scaling the polarisation vectors), meaning that under a little group transformation, any amplitude transforms as

$$A[1,2,3...] \overset{\lambda_i \to t\lambda_i}{\longrightarrow} t^{-2h_i} A[1,2,3...] \tag{4.1.25}$$

Under any little group transformation of particle i.

Suppose we have two incoming massless particles with momenta p_1 and p_2 that interact to produce a single massless particle with momentum p_3. To state clearly the following argument we will briefly permit these momenta to be complex (more details about complex extensions will be given in section 4.2.1). Energy-momentum conservation demands that $p_1 + p_2 + p_3 = 0$, and that $(p_1 + p_2)^2 = p_3^2 = 0$. In spinor helicity notation, this means that $\langle 12\rangle\,[12] = 0$. Since the momenta p_1 and p_2 are complex, the quantities $\langle 12\rangle$ and $[12]$ are independent. Let's suppose further that $[12]$ is zero in order to make the product zero. In that case, we must also have $\langle 12\rangle\,[23] = \langle 1|\,(p_1 + p_3)\,|3\rangle = 0$, so $[23] = 0$ and similarly for $[13]$. We see then that all square brackets are vanish if even one of them is zero. We could well have taken $\langle 12\rangle = 0$ instead, but we would have simply found the same thing; all angle brackets vanish and our amplitude only depends on square brackets.

In short, this means that 3-point functions of massless particles with *complex* momenta can *only* depend on either angle brackets or square brackets, but not both.

A corollary of this result is that 3-point amplitudes for massless particles with *real* momenta must actually vanish on-shell in 4 dimensions. Indeed, Eq. $\langle 12\rangle\,[12] = 0$ implies that both $\langle 12\rangle$ and $[12]$ have to be identically zero, and something similar can be shown to occur with the remaining brackets. That we have chosen complex momenta to construct non-vanishing 3-point functions may seem daft at the

moment, but it will become clear in the next section. Let us also mention that there are, in principle, many ways to construct non-vanishing 3-point functions by relaxing the on-shell constraints, *i.e.* instead of continuing the external momenta from real to complex values, we could well consider relaxing momentum conservation instead.

Now, here's the kicker: all massless 3-particle amplitudes are completely fixed by little group scaling. The reasoning is as simple as solving three algebraic equations which can be found in [25]. We will content ourselves to quote the result. The amplitudes for three massless particles with momenta and helicity (p_i, h_i) (for $i = 1, 2, 3$) are given by

$$A_3(1^{h_1}2^{h_2}3^{h_3}) = C \begin{cases} \langle 12\rangle^{h_3-h_1-h_2}\langle 13\rangle^{h_2-h_1-h_3}\langle 23\rangle^{h_1-h_2-h_3} \\ [12]^{h_1+h_2-h_3}[13]^{h_1+h_3-h_2}[23]^{h_2+h_3-h_1} \end{cases} \tag{4.1.26}$$

Since we are now working with complex momenta, we had better ensure that when making our momenta real our amplitude smoothly goes to zero. This means that we had better be able to take $\langle ij\rangle \longrightarrow \epsilon$ and $[ij] \longrightarrow \epsilon$ smoothly. We find that

$$A_3(1^{h_1}2^{h_2}3^{h_3}) = C \begin{cases} \langle 12\rangle^{h_3-h_1-h_2}\langle 13\rangle^{h_2-h_1-h_3}\langle 23\rangle^{h_1-h_2-h_3} \longrightarrow \epsilon^{-(h_1+h_2+h_3)} \\ [12]^{h_1+h_2-h_3}[13]^{h_1+h_3-h_2}[23]^{h_2+h_3-h_1} \longrightarrow \epsilon^{h_1+h_2+h_3} \end{cases} \tag{4.1.27}$$

Which means we choose the angle brackets when $h_1 + h_2 + h_3 < 0$ and the square brackets otherwise.

The constants in the above expressions are usually fixed by expanding the Lagrangian for the theory and identifying the coupling constants in the appropriate interaction term. If we know the couplings, or rather if we know their dimensions, then we can utilise an important fact about scattering amplitudes that we derived in eq. 3.0.20, which restated in words is

> **An n-particle amplitude in $d = 4$ must have mass-dimension $4 - n$.**

Surprisingly, this means that massless three point amplitudes are entirely fixed by little group scaling and dimensional analysis, up to a constant C.

Coupling Constants

Given the rule above, we know that three point amplitudes mass have mass dimension 1, which means that we can also determine the mass dimension of the coupling C as well. However, the properties of the coupling is in turn determined by other physical principles as well, and is a function of the choice of particles

and their helicities. We will label the coupling C_{abc}, where a, c, b labels the particle type. For example, integer spin-s particles have only four possible amplitudes

$$A_3(1_a^-, 2_b^-, 3_c^+) = C_{abc}\left(\frac{\langle 12\rangle^3}{\langle 23\rangle\langle 31\rangle}\right)^s \qquad A_3(1_a^+, 2_b^+, 3_c^-) = C_{abc}\left(\frac{[12]^3}{[23][31]}\right)^s \tag{4.1.28}$$

$$\tag{4.1.29}$$

and

$$A_3(1_a^-, 2_b^-, 3_c^-) = \overline{C}_{abc}\left(\langle 12\rangle\langle 23\rangle\langle 31\rangle\right)^s, \qquad A_3(1_a^+, 2_b^+, 3_c^+) = \overline{C}_{abc}\left([12][23][31]\right)^s \tag{4.1.30}$$

Assuming that the coupling is real and that the first two amplitudes are related by complex conjugation fixes the two couplings to be the same in each pair. We also see immediately by dimensional analysis that $[C_{abc}] = m^{1-|\sum_i h_i|}$, meaning a minimal coupling of dimension 0 for spin-1 particles and -1 for spin-2.

If we take $s = 1$ for the moment, we see immediately that C_{abc} has to be anti-symmetric in its indices, since the amplitude must be be equal under boson exchange. Since the amplitude picks up a minus sign, the coupling had better cancel it. It was shown in [28] that by considering the fact that four particle amplitudes must factorise into three particle amplitudes on-shell, the coupling constants must satisfy a Jacobi-relation

$$\sum_I C_{abI}C_{Icd} + C_{adI}C_{Icb} + C_{acI}C_{Idb} = 0 \tag{4.1.31}$$

This means that interacting spin-1 particles must be described by not only kinematical data, but by data coming from the adjoint representation of some group: spin-1 particles must be described by a Yang-Mills theory.

For spin-2, the couplings need to be symmetric in all its indices since the amplitude piece remains positive under boson exchange. By constructing the four-point amplitudes in $\mathcal{N} = 1$ supergravity, it is shown in [28] that all couplings between spin-2 and spin ≥ 1 must be identical, a result that is very nearly the equivalence principle, which we will return to later in this thesis.

4.1.3 Massive Particle Amplitudes

So far, we have discussed spinor representations of massless particles, but we can also represent massive particles in a similar way. Before we delve into spinors, let's just think about regular massive momenta. For a particle with massive momentum

P^μ, where we now have $P^2 = m^2$, we can decompose it into two *massless* momentum vectors via [29]

$$P_\mu = k_\mu + \frac{P^2}{2q \cdot k} q_\mu \,, \tag{4.1.32}$$

where P is a massive vector and k and q are lightlike vectors. While k_μ is a unique lightlike vector, q_μ can be freely chosen provided $q \cdot k \neq 0$ and $q \cdot P \neq 0$. In effect, this gives a representation of massive vectors as massless ones, which can then be represented by spinors. Schematically we can write this as

$$P_{massive} = \lambda\tilde{\lambda} + \alpha\eta\tilde{\eta} \,. \tag{4.1.33}$$

It will prove more convenient, however, to follow the methods presented in [30]. In this formalism we would instead demand a decomposition

$$P_{\alpha\dot{\alpha}} = \lambda^I_\alpha \tilde{\lambda}_{\dot{\alpha} I} \,. \tag{4.1.34}$$

Here $I = 1, 2$ is an $SL(2)$ index that transforms under the $SU(2)$ subgroup for real, Lorentzian momenta as

$$\lambda^I_\alpha \longrightarrow W^I_J \lambda^J_\alpha \,. \tag{4.1.35}$$

Where the I, J indices are raised and lowered with ϵ^{IJ}. In this new language, the equivalent of the Dirac equation reads

$$P_{\alpha\dot{\alpha}}\lambda^{\alpha I} = -m\tilde{\lambda}^I_{\dot{\alpha}}, \qquad P_{\alpha\dot{\alpha}}\tilde{\lambda}^{\dot{\alpha} I} = m\lambda^I_\alpha \,. \tag{4.1.36}$$

Conversion between dotted and undotted indices can, if desired, be facilitated by the operator

$$(J_i)^\alpha_{\ \dot{\alpha}} = \frac{(P_i)^\alpha_{\ \dot{\alpha}}}{m} \,. \tag{4.1.37}$$

Key to this formulation of the problem is Wigner's "little group" that governs the kinematics of particle scattering. For massless particles, the kinematical on-shell constraints are trivialized through the introduction of little group-adapted vaiables like spinor-helicity, twistor or momentum-twistor variables. This is turn allows for one to side-step quantum fields and all their subtlties and work directly with the concept of a particle. Since the little group for massive particles is $SU(2)$, amplitudes must be constructed by working with objects that transform appropriately under $SU(2)$. Specifically, these are symmetric tensors with $2S$ indices, where S is the magnitude of the total spin of the particle. In what follows, we will choose to express these amplutudes in a purely chiral basis, meaning that the constructed objects are indexed by $\alpha_1\alpha_2\cdots\alpha_{2S}$, using the operator we just defined.

Summarising the results of [30], a general strategy for constructing 3-point amplitudes is as follows:

- For each massless leg, assign a helicity h_i.
- For each massive leg of spin S, assign 2S spinor indices, $\alpha_1\alpha_2\cdots\alpha_{2S}$
- Using physical variables with spinor indices ($\lambda_\alpha, P_{\alpha\dot{\alpha}}$ etc) and the conversion operator defined above, construct a basis of $SL(2)$
- Write down every possible unique, maximally symmetric object with $2S$ indices in the newly constructed basis to get the **stripped amplitude**

$$M_{\{\alpha_1\alpha_2\cdots\alpha_{2S_1}\},\{\beta_1\beta_2\cdots\beta_{2S_2}\},\{\gamma_1\gamma_2\cdots\gamma_{2S_3}\}}.$$

- Contract each massive leg i with $2S$ massive spinors λ_i^I to find the final amplitude, which should now be labelled with helicities h and $SL(2)$ indices $I, J, K....$

$$\begin{aligned} M^{I_1 I_2\cdots I_{2S},h_i,h_j\cdots} = (\lambda_1)^{I_1\alpha_1}\cdots(\lambda_1)^{I_{2S_1}\alpha_{2S_1}}\cdots(\lambda_3)^{J_1\gamma_1}\cdots(\lambda_1)^{J_{2S_3}\gamma_{2S_3}} \\ \times M_{\{\alpha_1\alpha_2\cdots\alpha_{2S_1}\},\{\beta_1\beta_2\cdots\beta_{2S_2}\},\{\gamma_1\gamma_2\cdots\gamma_{2S_3}\}}. \end{aligned} \tag{4.1.38}$$

In order to determine the amplitude for any one particular helicity configuration then, we simply project it out by contracting this stripped amplitude with the appropriate combination of chiral spinors and select the appropriate $SL(2)$ indices. This is essentially because the massive spinors can be expresses in a basis that is aligned and anti-aligned with the direction of the spinor, *i.e.*

$$\lambda^I = \lambda\zeta^{-I} + \eta\zeta^{+I}, \tag{4.1.39}$$

with $\zeta^{+I} = \begin{pmatrix}1\\0\end{pmatrix}$ and $\zeta^{-I} = \begin{pmatrix}0\\1\end{pmatrix}$.
In this basis, the negative and positive helicity components are selected by $I = 1$ and $I = 2$ respectively.

For a massive particle with momentum P_k, we can choose the convention that $\langle k\eta_k\rangle [k\eta_k] = m_k^2$ and therefore that $[k\eta_k] = \langle k\eta_k\rangle = m_k$. For massless particles, contractions of like spinors are zero, $[ii] = \langle ii\rangle = 0$, but for massive particles (using **bold** notation) this is no longer true

$$[\mathbf{k}_I\mathbf{k}_J] = \langle\mathbf{k}_I\mathbf{k}_J\rangle = \begin{cases} m & I > J \\ -m & I < J \\ 0 & I = J \end{cases} \tag{4.1.40}$$

We also note the useful identity $\langle i|\, P_k P_k\, |j\rangle = -\langle j|\, P_k P_k\, |i\rangle = m_k^2\, \langle ij\rangle$, which can easily be proved using the Schouten identity.

4.1.4 High energy limit

In what follows, we will need to take the high energy limit of particular massive amplitudes. Naively, it would seem like this should be implemented by sending $\eta \longrightarrow 0$ in eq. 4.1.33. This is, however, too naive. In general such amplitudes contain terms of the form $\frac{\langle \eta i \rangle}{m}$ and so in the limit $\eta, m \longrightarrow 0$, are indeterminate. To circumvent this, a more sensible alternative is presented in [30], where

$$|\eta\rangle \longrightarrow m\,|\bar{\eta}\rangle\,, \qquad |\eta] \longrightarrow m|\bar{\eta}]\,, \tag{4.1.41}$$

and, should either case arise explicitly, $\langle \lambda \bar{\eta} \rangle$ and $[\lambda \bar{\eta}]$ are set to unity, before taking the $m \longrightarrow 0$ limit.

4.2 Recursion Relations

4.2.1 Complex shifts and poles

An arbitrary n-point scattering amplitude is a function of the (real) external momenta of the interacting particles. Typically, amplitudes contain the following momentum dependence in the denominator, coming from the propagators representing virtual particles

$$\frac{1}{P^2_{abc\cdots}} = \frac{1}{(p_a + p_b + p_c + \cdots)^2}. \tag{4.2.1}$$

Here $a, b, c, ...$ are indices labelling different external momenta. In the cases we will consider explicitly, only two momenta will enter in this kind of expressions, so for simplicity we will just consider internal momenta of the form P_{ab} (in any case there is no difference in the following treatment, so this is just a notational issue).

The reason we focus our attention on this feature is that an amplitude containing a dependence like Eq. (4.2.1) would become singular if we enforce the internal momentum P_{ab} of the corresponding virtual particle to be on-shell, namely $P^2_{ab} = 0$. In the standard approach to quantum field theory, virtual particles are off-shell; putting the virtual particles on-shell would imply constraints on the external particles. Let us consider an amplitude with propagator contribution $q = P_{12}$, which becomes on-shell only if $p_1 \cdot p_2 = 0$, namely if the incoming and outgoing photons are orthogonal. For other values of the angle between the two photons, the momentum of the virtual particle cannot be on-shell.

However, there is a way to enforce the on-shell nature of the internal momentum P_{ab}, at the price of considering complex momenta. The complex extension of

the momenta of the virtual particle is denoted by $\hat{P}_{ab}$ in order to highlight the difference with real momenta P_{ab}. In order to be more explicit, let us also write $\hat{P}_{ab} = P_{ab} + \Delta P_{ab}$, and demand that this quantity goes on-shell precisely due to this complex extension. Due to the additional freedom associated with the introduction of the complex piece ΔP_{ab}, it is possible to do so without imposing constraints on the real momenta of external particles, but rather by fixing the value of the complex part of the internal momenta. In other words, ΔP_{ab} is fixed in order to guarantee that $\hat{P}_{ab}$ is on-shell. Provided the scattering amplitudes are analytic functions, this procedure turns the scattering amplitude into a meromorphic function - analytic everywhere except at some isolated poles, namely the places in which the complex momentum $\hat{P}_{ab}$ goes on-shell. Even if this is hardly apparent at this point of the discussion, as discussed below this permits us to exploit the powerful methods of complex analysis in order to obtain n-point amplitudes in an efficient way.

There are in principle many ways of extending the real external momenta to complex quantities. We will deal explicitly with complex extensions of the momenta of two given particles, i and j, being $\hat{p}_i$ and $\hat{p}_j$ the corresponding complex momenta. The particular complex extension described below is chosen so as to guarantee certain properties: (i) conservation of all the external momenta, (ii) that both $\hat{p}_i$ and $\hat{p}_j$ are null vectors, and (iii) that the complex poles associated with propagators are simple poles. These are satisfied by the complex shift

$$\hat{p}_i = p_i + z\eta, \qquad \hat{p}_j = p_j - z\eta, \tag{4.2.2}$$

where $z \in \mathbb{C}$ and the vector η has to satisfy certain conditions, namely $\eta \cdot p_i = \eta \cdot p_j = \eta^2 = 0$. Both conditions (i) and (ii) above guarantee that we can deal with scattering amplitudes of the shifted momenta in the same way as scattering amplitudes of real momenta; we will elaborate later in this section on the meaning of (iii). Hence under this shift, we extend the amplitude A_n to a function $\hat{A}_n(z)$ with non-trivial dependence on the complex variable z.

The simplest scenario is that in which both particles i and j are massless particles (dealing with massive particles is explained in section 4.2.4). Then, we can write both orthogonality conditions as

$$\eta \cdot p_i = \frac{1}{2} \langle \eta i \rangle [\eta i] = 0, \qquad \eta \cdot p_j = \frac{1}{2} \langle \eta j \rangle [\eta j] = 0. \tag{4.2.3}$$

As two spinors are orthogonal if and only if they are proportional, there are two solutions to the equations above. Fixing the arbitrary proportionality constants to unity, one such solution to this system of equations is

$$|\eta] = |j], \qquad |\eta\rangle = |i\rangle \,. \tag{4.2.4}$$

The only other solution is physically equivalent under the exchange of particles i and j and multiplication of the complex variable z by a (-1) factor.

Decomposing all the elements in Eq. (4.2.2) in terms of spinors, and using Eq. (4.2.4), the complex shift above is given in spinor-helicity notation by

$$|\hat{i}] = |i] + z|j], \qquad |\hat{j}] = |j], \qquad |\hat{i}\rangle = |i\rangle\,, \qquad |\hat{j}\rangle = |j\rangle - z\,|i\rangle\,. \tag{4.2.5}$$

This is called a $[i,j\rangle$-shift. Note that for complex momenta, angle and square brackets are no longer related by complex conjugation, but rather are independent quantities. It is important to keep in mind this feature in order to properly understand the equation above. Indeed, it is the complex nature of the extension of external momenta which permits to write the shift (4.2.2) in such a simple way in terms of spinor-helicity variables.

Now let us come back to the discussion about the shifted internal momenta $\hat{P}_{ab}$. If we choose the particles a and b to be the particles i and j, from Eq. (4.2.2) is easy to see that $\hat{P}_{ab} = P_{ab}$ and the internal momentum is not shifted. Hence let us consider $a = i$ and $b \neq j$. Then, using the equations above,

$$\hat{P}_{ib}^2 = (p_i + p_b + z\eta)^2 = P_{ib}^2 + 2z\, P_{ib}\cdot\eta = 0. \tag{4.2.6}$$

As stated above, it is now straightforward to see that we can choose the complex part of the shifted momenta, or in other words the value of z, in order to ensure the on-shell nature of $\hat{P}_{ib}$. This value is given by

$$z_{ib} \equiv z|_{\hat{P}_{ib}^2=0} = \frac{-P_{ib}^2}{2P_{ib}\cdot\eta}. \tag{4.2.7}$$

Most importantly, the shifted n-point amplitude $\hat{A}_n(z)$ obtained shifting the momenta of particles i and j presents a simple pole at $z = z_{ib}$; namely, a singularity that behaves as $(z - z_{ib})^{-1}$:

$$\frac{1}{\hat{P}_{ib}^2} = \frac{1}{P_{ib}^2 + 2z\, P_{ib}\cdot\eta} = \frac{1}{2P_{ib}\cdot\eta}\frac{1}{z - z_{ib}} = -\frac{z_{ib}}{P_{ib}^2}\frac{1}{z - z_{ib}}. \tag{4.2.8}$$

The most relevant quantity associated to each pole of a given complex function is its residue, which is the finite value obtained when removing the singularity of the function by a suitable multiplicative factor. The residue of the complexified n-point amplitude can be evaluated using the standard definition of the residue of a simple pole:

$$\mathrm{Res}_{z=z_{ib}}\hat{A}_n(z) = \lim_{z\to z_{ib}}(z - z_{ib})\hat{A}_n(z). \tag{4.2.9}$$

The rules that permit the evaluation of the residue in a simple way will be discussed in the next section.

In order to illustrate the relevance of poles for the evaluation of the physical n-point amplitude A_n, let us consider the slightly modified complex function $f(z) = \hat{A}_n(z)/z$

instead of $\hat{A}_n(z)$. For general external momenta the other poles of the function, of the form given in Eq. (4.2.7), are away from $z = 0$. Hence $\hat{A}_n(z)/z$ has a single pole at $z = 0$, being the corresponding residue

$$\text{Res}_{z=0} f(z) = \lim_{z\to 0} z f(z) = \hat{A}_n(0) = A_n. \tag{4.2.10}$$

This equation is not particularly useful by itself, as it just relates two different quantities, the n- point amplitude A_n and its complex extension $\hat{A}_n(z)$, none of which are known in advance, but will need to be obtained. However, as we discuss in the next section, Cauchy's residue theorem permit to combine Eqs. (4.2.9) and (4.2.10) in a way which, together with the simple rules that permit to evaluate the residue in Eq. (4.2.9), leads to a useful expression for A_n that can be applied in a variety of situations.

4.2.2 The residue theorem and BCFW recursion

The poles of the complex function $f(z) = \hat{A}_n(z)/z$ described above can be related using Cauchy's residue theorem. This is one of the basics theorems in complex analysis which applies to meromorphic functions, namely complex functions which are differentiable (in the complex sense) everywhere but at its poles. Cauchy's residue theorem states that the integral of a complex function along a given closed curve that does not meet any of its poles equals the residues enclosed by the curve, up to a $2\pi i$ factor.

Let us consider a closed curve γ which encloses all the poles of the function $f(z)$; for instance, a circle with radius $R \to \infty$. Then Cauchy's residue theorem implies that

$$B_n = \frac{1}{2\pi i} \oint_\gamma dz\, f(z) = \text{Res}_{z=0} \frac{\hat{A}_n(z)}{z} + \sum_{z_{ib}} \text{Res}_{z=z_{ib}} \frac{\hat{A}_n(z)}{z}, \tag{4.2.11}$$

where we have defined the "boundary term" B_n as the integral over the curve γ (the reason behind this notation will become clear in the next section).

What should now be obvious given our previous discussion is that the residue at $z = 0$ yields back A_n, which now permits us to write the physical n-point amplitude as

$$A_n = -\sum_{z_{ib}} \text{Res}_{z=z_{ib}} \frac{\hat{A}_n(z)}{z} + B_n. \tag{4.2.12}$$

Admittedly, this equation may not seem specially useful in its current version. A first simplification stems from the fact that the boundary term vanishes in a large number of situations if the particles i and j being shifted are adequately chosen.

We will discuss this in the next section; for the moment, let us put $B_n = 0$ in the previous equation.

Then the n-point amplitude A_n is determined entirely by the residues of $\hat{A}_n(z)/z$ at the $z = z_{ib}$ poles. The second simplification arises from the fact that each of these residues can be written as a product of on-shell lower-point amplitudes evaluated with complex momenta. In order to understand this feature, let us recall that the residue for a given pole $z = z_{ib}$ comes from a Feynman diagram with two particles i and $b \neq j$ on one side of the propagator. The momentum flowing in the propagator, $\hat{P}_{ib} = \hat{p}_i + p_b$, becomes on-shell at the pole $z = z_{ib}$. When the momentum flowing in the propagator becomes on-shell, the amplitude represented by this complex Feynman diagram factorizes, so that

$$\text{Res}_{z=z_{ib}} \frac{\hat{A}_n(z)}{z} = -iA_L(z_{ib}) \frac{1}{P_{ib}^2} A_R(z_{ib}). \tag{4.2.13}$$

Here $A_L(z_{ib})$ is the on-shell amplitude for the particles i, $b \neq j$ and the one in the propagator, and $A_R(z_{ib})$ the on-shell amplitude for the particle in the propagator and the remaining particles in the n-point amplitude.

It is not our aim to prove this factorization property here, but we can illustrate that it is reasonable using a fairly general example. Let us consider an n-particle interaction mediated by a virtual fermion with spin 1/2, with arbitrary external particles. Then any non-zero complex amplitude associated with a given shifted Feynman diagram would have the structure

$$g(z) = -i \frac{\langle \hat{X} | \hat{P}_{ib} | \hat{Y}]}{\hat{P}_{ib}^2}. \tag{4.2.14}$$

Here $|\hat{X}\rangle$ and $|\hat{Y}]$ depend on the particular kinds of external particles being considered (note that these spinors are shifted). Taking into account that the pole in $z = z_{ib}$ appears due to the denominator, due to Eq. (4.2.8), it is straightforward to check that the residue of the quantity above divided by z is given by

$$\text{Res}_{z=z_{ib}} \frac{g(z)}{z} = \frac{i}{P_{ib}^2} \langle \hat{X} | \hat{P}_{ib} | \hat{Y}] = -i \langle \hat{X} \hat{P}_{ib} \rangle \frac{1}{P_{ib}^2} [\hat{P}_{ib} \hat{Y}]. \tag{4.2.15}$$

In the last equation we have exploited the property that, when $\hat{P}_{ib}$ is on-shell, it can be written in terms of spinors as $\hat{P}_{ib} = -|\hat{P}_{ib}\rangle[\hat{P}_{ib}| - |\hat{P}_{ib}]\langle\hat{P}_{ib}|$. But Eq. (4.2.15) displays the structure of Eq. (4.2.13): $\langle \hat{X} \hat{P}_{ib} \rangle$ is the on-shell amplitude for the particles to the left of the propagator and the spin-1/2 fermion, while $[\hat{P}_{ib} \hat{Y}]$ is the corresponding quantity for the particles on the other side of the propagator. These on-shell amplitudes necessarily involve less than n particles, and are evaluated in the particular values of the complex momenta determined by the condition $z = z_{ib}$.

Remarkably, this factorization property holds in general. Hence we can write each residue in the left-hand side of Eq. (4.2.12) as in Eq. (4.2.13), so that the A_n amplitude is given by

$$A_n = i \sum_{z_{ib}} \sum_{h} A_L(z_{ib}) \frac{1}{P_{ib}^2} A_R(z_{ib}). \tag{4.2.16}$$

This equation contains an additional sum over h, the index corresponding to the helicity of the internal particle. In the example given above with an internal spin-1/2 fermion this sum was implicit, through the use of the relation $\hat{P}_{ib} = -|\hat{P}_{ib}\rangle[\hat{P}_{ib}| - |\hat{P}_{ib}]\langle\hat{P}_{ib}|$, though one of the contributions were identically zero.

Eq. (4.2.16) condenses the content of the celebrated BCFW recursion relations [31–33]. In general, this equation implies that a given n-point amplitude can be written as a sum of products of lower-point amplitudes, where the sum has to be taken on arrangements of external particles that guarantee that the internal momenta are shifted, as well as on the helicity of internal particles. Knowing what we do about little group scaling and 3-point kinematics, we can now break down any complicated amplitude of n particles into products of 3-point amplitudes which are themselves easily calculated.

As an example at this stage, lets consider the colour-ordered gluon 4-pt, with two particles of negative helicity and two of positive. We will do an $[1,2\rangle$ shift, meaning we have

$$A_4[1^-,2^-,3^+,4^+] = \sum_{h=\pm} A_3[\hat{1}^-,\hat{P}^h,4^+,] \frac{1}{P^2} A_3[-\hat{P}^{-h},\hat{2}^-,3^+] \tag{4.2.17}$$

$$= A_3[\hat{1}^-,\hat{P}^-,4^+,] \frac{1}{P^2} A_3[-\hat{P}^+,\hat{2}^-,3^+] \tag{4.2.18}$$

$$= C^2 \frac{\langle 1\hat{P}\rangle^3}{\langle\hat{P}4\rangle\langle 41\rangle} \frac{1}{\langle\hat{2}3\rangle[23]} \frac{[\hat{P}3]^3}{[23][3P]} \tag{4.2.19}$$

After some algebra and simplifications, we find that this simplifies to

$$A_4[1^-,2^-,3^+,4^+] = C^2 \frac{\langle 12\rangle^4}{\langle 12\rangle\langle 23\rangle\langle 34\rangle\langle 41\rangle} \tag{4.2.20}$$

We will thoroughly illustrate this concept further in examples associated with particular processes of astrophysical significance.

4.2.3 Showing shift-validity

The simplicity of the recursion relations in Eq. (4.2.16) above rests on the assumption that the boundary term vanishes, $B_n = 0$. Using the definition of

this quantity in Eq. (4.2.11), namely

$$B_n = \frac{1}{2\pi i} \oint_\gamma dz\, f(z), \tag{4.2.21}$$

and considering a contour that goes to infinity, this is equivalent to $\lim_{|z|\to\infty} zf(z) = 0$. In terms of the complex amplitude $\hat{A}_n(z)$, this condition translates into

$$\lim_{|z|\to\infty} \hat{A}(z) = 0. \tag{4.2.22}$$

Hence in order to ensure that usage of the recursion relations is justified, it is necessary to ensure that the complex extension of the n-point amplitude that we want to evaluate decays to zero in the limit of complex infinity. Not every imaginable shift choosing arbitrary particles i and j would verify this constraint; the combinations of shifted particles that satisfy this condition are known as "valid" shifts.

There is no general rule to follow in order to show that a given shift is valid, but different situations require different approaches. The general strategy is to show that Eq. (4.2.22) is satisfied by looking for a bound on the leading behavior of $\hat{A}(z)$ at complex infinity, namely $|\hat{A}(z)| \leq k|z|^{-\alpha}$ for some real constant k and positive real exponent $\alpha > 0$.

The simplest bound that can be obtained follows from the behavior of all individual Feynman diagrams that contribute to a given amplitude. The evaluation of a given n-point amplitude using on-shell recursion relations represents a more effective determination of all the contributions to a given process coming from different Feynman diagrams. However, at the end of the day the results of both evaluations have to be the same. In particular, the leading behavior with z of complex n-point amplitude $\hat{A}(z)$ has to be the same as the leading behavior of the sum of all individual Feynman diagrams contributing to the complex amplitude. Hence an upper bound to the asymptotic behavior of $\hat{A}(z)$ at complex infinity can be obtained as the leading contribution from the dominant individual Feynman diagram at large $|z|$. This is an upper bound due to the fact that when summing all the contributions coming from the different Feynman diagrams, cancellations of the apparent leading term in z can take place.

What makes this bound useful is that it is straightforward to compute. Feynman diagrams are a product of different elements: external legs, interaction vertices, and propagators. It is not difficult to obtain the leading behavior with z of each of these elements, and then take their product in order to obtain the leading behavior with z for a given Feynman diagram. For instance, let us consider an $[i, j\rangle$-shift where the helicities of the shifted particles are $(h_i, h_j) = (-1, +1)$. Due to

Eq. (4.2.8), the internal propagator $1/\hat{P}_{ib}^2$ behaves as z^{-1}. Individual polarization vectors are given in Eq. (4.1.22) and, for the chosen shift, also lead to a z^{-1} dependence; for instance,

$$\epsilon_+^\mu(\hat{p}_j;q) = -\frac{\langle q|\,\gamma^\mu|j]}{\sqrt{2}\,\langle q\hat{j}\rangle}. \tag{4.2.23}$$

Note that, for the same helicities of external particles, the alternative $[j,i\rangle$-shift leads to a leading behavior linear in z instead. Hence it is important to choose properly the shift in order to use this method to show its validity. Lastly, the behavior of interaction vertices depends on the particular theory being considered. With all these ingredients, it is possible to extract the leading behavior with z of individual Feynman diagrams, hence obtaining a bound to the asymptotic behavior of a given (complex) n-point amplitude $\hat{A}_n(z)$. This method works in a large number of situations, provided a wise choice of shift is made. This will be illustrated through the examples presented in the main body of the paper. However, it may occur that this bound is not tight enough to show that at least one shift for a given n-point amplitude is valid. In these situations, the only systematic way to proceed is to consider shifts of more than two particles, which may improve the leading behavior with z of individual Feynman diagrams [33,34]. If this does not work there is no general rule to apply, though it is customary to refine the bounds coming from the leading behavior of individual Feynman diagrams by checking for potential cancellations of the apparent leading terms in z.

4.2.4 BCFW with massive particles

The BCFW relations for two shifted particles can be easily extended to include a massive particle (shifting two massive particles forbids solving explicitly for the shift in terms of spinor-helicity variables [35, 36]). As in the massless case, we introduce a null vector η^μ and consider the shift of the external momenta

$$\hat{p}_i = p_i + z\eta, \qquad \hat{p}_j = p_j - z\eta. \tag{4.2.24}$$

However, let us now assume that the particle j is massive. This makes the determination of η^μ slightly different, as the orthogonality relation $\eta\cdot p_j$ now takes a different form. Since η^μ is still null, we can decompose $\eta^{\dot{a}b}$ as

$$\eta^{\dot{a}b} = -|\eta\rangle^{\dot{a}}[\eta|^b. \tag{4.2.25}$$

This null vector has to be orthogonal to p_i and p_j. The first of these conditions is the same as in the purely massless case, namely the first condition in Eq. (4.2.3):

$$\eta\cdot p_i = \frac{1}{2}\langle\eta i\rangle[\eta i] = 0. \tag{4.2.26}$$

This requires either $|\eta\rangle^{\dot{a}} = |i\rangle^{\dot{a}}$ or $[\eta|^b = [i|^b$. Let us consider explicitly the first solution, that corresponds to the analogue of the $[i,j\rangle$-shift (the discussion in the alternative case is completely parallel).

On the other hand, the second orthogonality condition is now written as

$$\eta \cdot p_j = \frac{1}{2}[\eta|^b (p_j)_{b\dot{a}} |\eta\rangle^{\dot{a}} = \frac{1}{2}[\eta|^b (p_j)_{b\dot{a}} |i\rangle^{\dot{a}} = 0. \tag{4.2.27}$$

If the particle j was massless, we could use the decomposition of p_j in terms of spinors to obtain the second orthogonality condition in Eq. (4.2.3). In any case, for j massive it is still possible to solve explicitly Eq. (4.2.27) as

$$[\eta|^b = \epsilon^{bc} (p_j)_{c\dot{a}} |i\rangle^{\dot{a}}. \tag{4.2.28}$$

In summary, the equivalent of Eq. (4.2.5) is now given by

$$|\hat{i}] = |i] + z p_j |i\rangle, \qquad |\hat{i}\rangle = |i\rangle, \qquad \hat{p}_j^{\dot{a}b} = p_j^{\dot{a}b} - z |i\rangle^{\dot{a}} \epsilon^{bc} (p_j)_{c\dot{b}} |i\rangle^{\dot{b}}. \tag{4.2.29}$$

The rest of the discussion is parallel to the massless case, but taking into account that for internal particles with mass m_{ib}, poles arise for the values $z = z_{ib}$ that make $\hat{P}_{ib}^2 = -m_{ib}^2$. The equivalent of Eq. (4.2.16) is now given by

$$A_n = i \sum_{z_{ib}} \sum_h A_L(z_{ib}) \frac{1}{P_{ib}^2 + m_{ib}^2} A_R(z_{ib}), \tag{4.2.30}$$

where m_{ib} is the mass of the internal particle for the partition in which the particles labelled by i and b are on the same side of the propagator.

4.3 Loops

So far, we have only dealt with tree-level amplitudes, however we must also consider internal lines that form closed loops. This, too, has a modern formulation using the same basic principles of the amplitudes program. We will restrict ourselves to discussing the efficient calculation of one-loop amplitudes, although by now many sophisticated techniques to compute higher loop contributions in many theories.

We will discuss the method of generalised unitarity [37–41], a technique to build loops from trees using unitarity, as presented in section 3.0.5.

4.3.1 Loop Amplitude Representations

For a generic QFT, amplitudes of n external particles and L internal loops take the general form[3]

$$A^{(L)}_{n,j}[\mathcal{N}] = \underbrace{\sum_{\text{Diags}} \int \prod_{l=1}^{L} \frac{d^D k}{(2\pi)^D}}_{\text{Loop Integral}} \times \underbrace{\frac{\mathcal{N}(p,k,\epsilon)}{\prod_j D_j(p^2,k^2,m^2)}}_{\text{Loop Integrand}}. \tag{4.3.1}$$

The loop integral is performed over all *internal* momenta k, and it is this that is the source of most divergences in quantum field theory. The loop integrand, by contrast, is just some rational function of momenta, both internal and external, and polarization vectors (tensors). We can always rewrite this loop amplitude using Feynman parameterisation

$$\frac{1}{D_1 D_2 D_3 \cdots D_s} = \int_0^1 da_1 da_2 \cdots da_s \frac{(s-1)!\delta(1-\sum a_i)}{(a_1 D_1 + a_2 D_2 + \cdots + a_s D_s)^s} \tag{4.3.2}$$

$$= \frac{1}{(2\pi)^D} \int_0^1 \frac{d\eta}{(a_1 D_1 + a_2 D_2 + \cdots + a_s D_s)^s} \tag{4.3.3}$$

$$= \frac{1}{(2\pi)^D} \int_0^1 \frac{d\eta}{\mathcal{D}^s}. \tag{4.3.4}$$

Writing it in this way, we note that $\mathcal{D}$ is a second order polynomial in the loop momenta k. We can eliminate any terms that are linear in k by a change of variables, namely $k' = k + \delta$, where δ is some constant function of the external momentum.

Considering a one loop amplitude, we can now write it as

$$A_n = \int \frac{d^D k' d\eta}{(2\pi)^D} \frac{\mathcal{N}(p,k',\epsilon)}{(k'^2 - \Delta(m,p))^s}, \tag{4.3.5}$$

where Δ could be a function of external momenta, feynman parameters and particle mass, and is independant of loop momenta. It is clear then, that for any scalar integral, we can write it in the form

$$A_n = \int \frac{d^D k d\eta}{(2\pi)^D} \frac{1}{(k^2 - \Delta(m,p))^s}. \tag{4.3.6}$$

For $s = 1, 2$ and $D = 4$, it's obvious that these integrals diverge by simple power counting - either quadratically or logarithmically. We need to regulate these (UV or IR) divergences, and we choose to do so via dimensional regularisation [42],

[3] We omit factors of $i\epsilon$ and trust that the reader can imagine when these might be needed.

i.e. we choose $D = 4 - 2\epsilon$. Although there are many regularisation schemes to choose from, each with their own merits and drawbacks, we select dimensional regularisation due to the fact that it doesn't spoil S-matrix unitarity, since it preserves the ward identities by ensuring translation invariance of the amplitudes.

After a Wick rotation where $k_0 \longrightarrow ik_{0E}$, we can write a one-loop scalar integral as

$$I(s, \Delta) = \int \frac{d^D k_E}{(k_E^2 + \Delta)^s}, \tag{4.3.7}$$

and we will omit the parameter integration for the time being. It is convenient to write the propagator using the Schwinger proper time representation

$$\frac{1}{(k_E^2 + \Delta)^s} = \frac{1}{\Gamma(s)} \int_0^\infty d\tau \ \tau^{s-1} e^{-\tau(k_E^2 + \Delta)}, \tag{4.3.8}$$

where $\Gamma(z)$ is the Gamma function, with simple poles at $z = 0, -1, -2, ...$ and obeying $z\Gamma(z) = \Gamma(z + 1)$ for z a complex number. Computing I then becomes

$$I(s, \Delta) = \int d^D k_E \frac{1}{\Gamma(s)} \int_0^\infty d\tau \ \tau^{s-1} e^{-\tau(k_E^2 + \Delta)} \tag{4.3.9}$$

$$= \frac{\pi^{D/2}}{\Gamma(s)} \int d\tau \ \tau^{s-1-D/2} e^{-\tau\Delta} \tag{4.3.10}$$

$$= \frac{\pi^{D/2}}{\Gamma(s)} \Delta^{D/2-s} \Gamma(s - D/2). \tag{4.3.11}$$

Knowing the pole structure of the Gamma function, we see that these integrals are divergent exactly when $s - D/2 = 0, -1, -2....$ To be able to control this divergence, and analyse it properly, we take $D \longrightarrow 4 - 2\epsilon$ to find

$$I(s, \Delta) = \frac{\pi^{2-\epsilon}}{\Gamma(s)} \Delta^{2-s-\epsilon} \Gamma(s - 2 + \epsilon). \tag{4.3.12}$$

Considering the tadpole diagram where $s = 1$ (two external legs, one propagator) and $\Delta = m^2$, we find

$$I(1, m^2) = \pi^2 (m^2)^{1-\epsilon} \Gamma(\epsilon - 1). \tag{4.3.13}$$

We notice something interesting: in dimensional regularization, the tadpole diagram vanishes for massless particles.

Let's consider the bubble diagram with $s = 2$. We will consider particles with the same mass m and write the propagators in Feynman paraterisation as

$$\int \frac{d^D k}{(k^2 - m^2)[(k + p)^2 - m^2]} = \int \int_0^1 \frac{d^D k da}{[(k + ap)^2 + a(1 - a)p^2]^2}. \tag{4.3.14}$$

We are free to change variables via a shift to $k' = k + ap$, meaning we find $\Delta = m^2 - a(1-a)p^2$ and

$$\int \frac{d^D k}{(k^2 - m^2)[(k+p)^2 - m^2]} = \int_0^1 I[2, m^2 - a(1-a)p^2]da \tag{4.3.15}$$

$$= \pi^{2-\epsilon}\Gamma(\epsilon)\int_0^1 \frac{1}{(m^2 - a(1-a)p^2)^\epsilon}da. \tag{4.3.16}$$

The remaining integrand has two branch cut singularities along the positive and negative real axis for $p^2 > 2m^2$

$$a_\pm = \frac{1}{2}\left(1 \pm \sqrt{1 - \frac{4m^2}{p^2}}\right) \tag{4.3.17}$$

If we were to allow complex values of momentum, then we can turn this into a contour integral and use the Cauchy principal value to compute the discontinuity across the branch cut, giving us the amplitude up to an analytic piece. However, we saw in section 3.0.5 that the value of this discontinuity is given by putting the propagator on shell and using Cutkosky's rules, which we derived in eq 3.0.32. This means that instead of computing the loop directly, we can can simply cut two of the propagators in the loop and compute two tree amplitudes.

4.3.2 One-loop amplitudes from unitarity cuts

As discussed in detail in appendix A, any n-point one-loop integral with arbitrary tensorial structure in the numerator can be written as a linear combination of scalar boxes, bubbles, triangles, and tadpoles, along with a rational piece

$$\mathcal{I}_n = \sum_{j_4} c_4 I_4^{(j4)} + \sum_{j_3} c_3 I_3^{(j3)} + \sum_{j_2} c_2 I_2^{(j2)} + \sum_{j_1} c_1 I_1^{(j1)} + \mathcal{R} + \mathcal{O}(\epsilon), \tag{4.3.18}$$

with $I_n^{(j} = \int d\eta\ I(n, \Delta)$, j refers to the various distributions of the different n legs and $\mathcal{R}$ is a rational function of mandelstam variables left over from dimensional regularisation. The coefficients c_j are also rational functions of mandelstam variables.

The logic of this approach is to try and determine the c_i coefficients by comparing the discontinuity of the loop diagram on one side with the discontinuity of the on-shell cut amplitudes on the other, according to the prescription given to us by Cutkosky in eq. 3.0.32. It is important to first discuss the drawbacks of this method. For starters, we can only calculate contributions that actually have discontinuities: the rational term $\mathcal{R}$ and the tadpole diagrams have no such

discontinuities and therefore this method is blind to their existence. Thankfully, we showed that using dimensional regularization the tadpole is absent, and it can be shown for some theories (especially supersymmetric theories) that the rational term is also often absent. The fundamental equation we will consider is

$$\begin{aligned}\text{Disc}_c\left(\mathcal{A}_{fi}^{\text{1-loop}}\right) &= i\int d\mu\ \mathcal{A}_{f\mu}^{\text{tree}}\mathcal{A}_{\mu i}^{\text{tree}} \\ &= \sum_{j_4} c_4 \text{Disc}_c I_4^{(j4)} + \sum_{j_3} c_3 \text{Disc}_c I_3^{(j3)} + \sum_{j_2} c_2 \text{Disc}_c I_2^{(j2)}, \end{aligned} \tag{4.3.19}$$

where Disc_c means we are considering the discontinuity that arises from cutting channel c, where the propagators corresponding to channel c are put on-shell.

The idea is then to isolate specific coefficients by making tactical choices about which channels to cut. The best way to see how this works is by example, and we will choose to calculate the first loop correction to the four-gluon amplitude we computed in section 4.2.2, namely $A_4[1^-, 2^-, 3^+, 4^+]$.

First, we know that we can express the amplitude as

$$A_4^{(1)}[1^-, 2^-, 3^+, 4^+] = c_4 I_4 + \sum_{j_3} c_3 I_3^{(j3)} + \sum_{j_2} c_2 I_2^{(j2)} + \mathcal{R} + \mathcal{O}(\epsilon). \tag{4.3.20}$$

We now choose compute the s-channel cut (discontinuity) of this amplitude

$$\begin{aligned}\text{Disc}_s A_4^{(1)}[1^-, 2^-, 3^+, 4^+] &= -\sum_{h_i=\pm}\int d\mu\ A[1^-, 2^-, k_1^{h_1}, k_2^{h_2}]A[3^+, 4^+, -k_2^{-h_2}, -k_1^{-h_1}] \\ &= -\int d\mu\ A[1^-, 2^-, k_1^+, k_2^+]A[3^+, 4^+, -k_2^-, -k_1^-] \\ &= c_4 \text{Disc}_s I_4 + \sum_{j_3} c_3 \text{Disc}_s I_3^{(j3)} + \sum_{j_2} c_2 \text{Disc}_s I_2^{(j2)}, \end{aligned} \tag{4.3.21}$$

and we can reuse our result from eq. 4.2.20 to find that this becomes

$$-\int d\mu\ A[1^-, 2^-, k_1^+, k_2^+]A[3^+, 4^+, -k_2^-, -k_1^-] = \tag{4.3.22}$$

$$= -\int d\mu \frac{\langle 12\rangle^4}{\langle 12\rangle\langle 2k_1\rangle\langle k_1k_2\rangle\langle k_21\rangle}\frac{\langle k_1k_2\rangle^4}{\langle k_1k_2\rangle\langle k_13\rangle\langle 34\rangle\langle 4k_2\rangle} \tag{4.3.23}$$

$$= \int d\mu \frac{\langle 12\rangle^4}{\langle 12\rangle\langle 23\rangle\langle 34\rangle\langle 41\rangle}\frac{\langle k_1k_2\rangle^2\langle 23\rangle\langle 41\rangle}{\langle k_13\rangle\langle 4k_2\rangle\langle 2k_1\rangle\langle k_21\rangle} \tag{4.3.24}$$

$$= A_4[1^-, 2^-, 3^+, 4^+]\int d\mu \frac{st}{\langle k_21\rangle[1k_2]\langle k_13\rangle[3k_1]}. \tag{4.3.25}$$

Here, we have simplified the integrand by multiplying by $1 = \frac{[3k_1][1k_2]}{[1k_2][3k_1]}$ and noting that $k_1 + k_2 = p_3 + p_4 = -p_1 - p_2$.

We can now compare integrands with the scalar integrals (both come with the same integral measures $d\mu$), and we find that $c_4 = A_4[1^-, 2^-, 3^+, 4^+]st$ with the other $c_{i<4}$ undetermined. Our answer for the s channel cut is then

$$A_4^{(1)}[1^-, 2^-, 3^+, 4^+] = stA_4[1^-, 2^-, 3^+, 4^+]I_4 + \text{triangles} + \text{bubbles} + \mathcal{R}. \tag{4.3.26}$$

Where the triangles and bubbles don't have discontinuities in the s channel. To compute the triangles and bubbles, one would now need to do the t channel cut in much the same way. However, computing the t channel cut depends on the theory of interest, specifically its particle content and amount of supersymmetry. For $\mathcal{N} = 4$ super Yang Mills for example, the triangles, bubbles and rational pieces all vanish. As theories with supersymmetry are beyond the scope of this thesis, we will not comment further on this derivation, however the interested reader may consult [25, 27, 43–48] for further details. Included in these accounts are useful generalisation of these methods, i.e. where one performs unphysical cuts not determined by unitarity, and yet obtains the same results in easier ways.

V

Deflection by Gravitation: a Modern Perspective

"A huge mountain might be scaled by strong men only after many centuries of failed attempts, but a few decades later grandmothers will be strolling up it for tea and then wandering back afterward to see where they left their glasses."

– Terry Pratchett, *Masquerade*

In this chapter, we apply the techniques outlined above to derive two classical result from General Relativity: the bending of both an electromagnetic and a gravitational wave around a massive object.

5.1 Light Bending by Gravity

The phenomenon of light bending around a massive body via Gravitation remains one of the greatest tests of General Relativity (GR) to date. While Newtonian gravity also predicts light bending by Gravitation, Einstein pointed out that this result was incorrect by a factor of 2, with the correct result being derived via GR in 1915.

In this section, we will derive this result directly from the amplitude formalism, without any notion of the Einstein-Hilbert action, diffeomorphism symmetry or bending space: only the postulate that gravity must act via spin two fields.

Evaluation of the scattering amplitude

We consider the gravitational force between a massive, spinless object (such as a non-rotating star) and a massless photon. Diagrammatically, this looks like

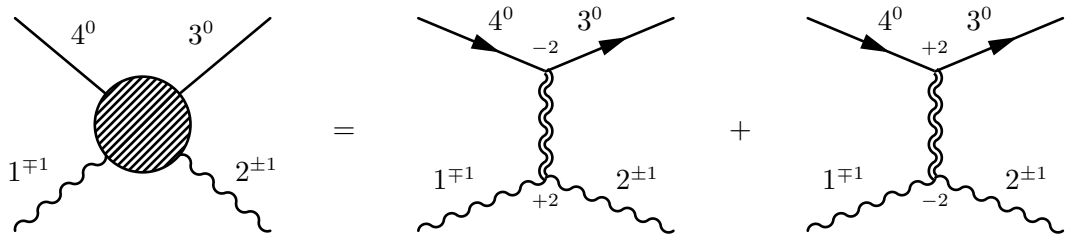

(5.1.1)

Notice that we are not explicitly including symmetrization with respect to identical particles. Following our conventions, we imagine this as particles 1 and 4 incoming, exchanging a graviton and then outgoing with momentum 2 and 3. Particles 3 and 4 are massive, with on-shell condition $p_3^2 = p_4^2 = -m^2$.

Following our discussion on the BCFW relations, the goal in this section is to evaluate the 4-point amplitude depicted in Fig. 6.1.7 from the knowledge of the relevant 3-point (sub-)amplitudes. Let us therefore start by calculating the two 3-point amplitudes associated with this diagram. The first one is given by:

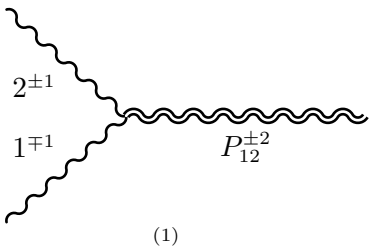

(5.1.2)

Recall that $P_{12} = p_1 + p_2$. Since this first diagram involves only massless particles, we can use little group scaling to calculate the associated 3-point amplitude.

From all the possible helicity choices, we can now show that in order to evaluate the light-bending angle it is only necessary to consider these in which h_1 and h_2 are different. Amplitudes such that $h_1 = h_2$ describe a change of helicity of the photon, due to its gravitational interaction with the massive scalar field. This process is not allowed in GR, as can be easily seen using dimensional analysis. We observe that the Ricci scalar R has mass dimension 2, since it contains two derivatives of the dimensionless field $h_{\mu\nu}$. The coupling constant κ must then have mass dimension -1, so that the total mass dimension of $2R/\kappa^2$ is 4 as required (to ensure that the action is dimensionless). The angle and square brackets have mass dimension 1, since each corresponds to some (possibly complex) momentum. As explained at the end of section 4.1.2, we require that any amplitude involving n external legs hass mass dimension $4 - n$ in 4 dimensions, thus we require that $[A] = 1$.

Let us consider for instance the helicity configuration $(h_1, h_2, h_3) = (-1, -1, +2)$.

Little group scaling tells us that the amplitude $A_3(1^{-1}2^{-2}P_{12}^{+2})$ is either given by

$$-\frac{\kappa}{2}\frac{\langle 12\rangle^4}{\langle 1P_{12}\rangle^2\langle 2P_{12}\rangle^2} \tag{5.1.3}$$

or

$$-\frac{\kappa}{2}\frac{[1P_{12}]^2[2P_{12}]^2}{[12]^4}. \tag{5.1.4}$$

It is straightforward to see that neither of these expressions have the correct dimensionality. This means that this helicity choice does not contribute to the scattering amplitude. A similar argument applies to the choices $(h_1, h_2, h_3) = (+1, +1, -2)$, $(+1, +1, +2)$ and $(-1, -1, -2)$.

These leave us with only two possibilities. For instance, for the choice $(h_1, h_2, h_3) = (+1, -1, -2)$, one has

$$A_3(1^{+1}2^{-1}P_{12}^{-2}) = -\frac{\kappa}{2}\frac{\langle 2P_{12}\rangle^4}{\langle 12\rangle^2}. \tag{5.1.5}$$

As discussed in section 4.1.2, arguments based in little group scaling leave freedom to consider either the square bracket version or the angle bracket version of a given 3-point amplitude. However, here is where dimensional analysis enters into play. The amplitude in Eq. (5.1.6) below satisfies this requirement, as it has dimension 1. On the other hand, the angle bracket version of $A(1^{-1}2^{+1}P_{12}^{+2})$, as determined by little group scaling, would be proportional to $\kappa\langle 12\rangle^2\langle 2P_{12}\rangle^4$, which clearly does not display the correct dimensions, and therefore can be discarded.

Making parallel arguments, the remaining choice of helicities, $(h_1, h_2, h_3) = (-1, +1, +2)$, leads to

$$A_3(1^{-1}2^{+1}P_{12}^{+2}) = -\frac{\kappa}{2}\frac{[2P_{12}]^4}{[12]^2}. \tag{5.1.6}$$

The next 3-point amplitude that we have to evaluate is diagrammatically represented by

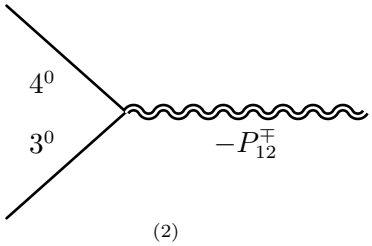

(5.1.7)

Note that we are exploiting the fact that, due to momentum conservation, $P_{12} = -p_3 - p_4$. To evaluate this diagram we cannot resort to little group scaling, as two of the legs are massive. Hence we have to use the relevant vertex, obtained as part of the Feynman rules of the theory:

$$V^{\mu\nu}(3^0 4^0) = \frac{-i\kappa}{2}\left[p_3^\mu p_4^\nu + p_3^\nu p_4^\mu - \eta^{\mu\nu}(p_3 \cdot p_4 - m^2)\right]. \tag{5.1.8}$$

We dot this with our chosen polarization vectors, in this case $\epsilon^{\pm}(-P_{12})_\mu \epsilon^{\pm}(-P_{12})_\nu$, to find the two possible 3-point amplitudes:

$$A_3((-P_{12})^{-2}3^0 4^0) = \frac{-i\kappa}{2}\left[2(p_3\cdot\epsilon^-)(p_4\cdot\epsilon^-)\right] = \frac{-i\kappa\,\langle P_{12}|\,p_3|q]\,\langle P_{12}|\,p_4|q]}{2[qP_{12}]^2}, \tag{5.1.9}$$

and

$$A_3((-P_{12})^{+2}3^0 4^0) = \frac{-i\kappa}{2}\left[2(p_3\cdot\epsilon^+)(p_4\cdot\epsilon^+)\right] = \frac{-i\kappa\,\langle q|\,p_3|P_{12}]\,\langle q|\,p_4|P_{12}]}{2\,\langle qP_{12}\rangle^2}. \tag{5.1.10}$$

In these equations, we have used $|-p\rangle = -|p\rangle$ and $|-p] = +|p]$ (see [25] for instance).

It is a good moment to introduce a particular manipulation involving spinors and momenta that will be used often below (most of the times, implicitly). Let us take for instance the piece $\langle P_{12}|p_4|q]$ in Eq. (5.1.9). Due to momentum conservation, $p_4 = P_{34} - p_3 = -P_{12} - p_3$, so that

$$\langle P_{12}|p_4|q] = -\langle P_{12}|P_{12}|q] - \langle P_{12}|p_3|q] = -\langle P_{12}|p_3|q]. \tag{5.1.11}$$

The term $\langle P_{12}|P_{12}|q]$ is identically zero using the relevant form of the Weyl equation in Eq. (4.1.16), as $\langle P_{12}|P_{12} = 0$. This permits to simplify the form of the 3-point amplitude (5.1.9). This is one of the manipulations that permits huge simplifications of scattering amplitudes.

Hence we have determined the relevant 3-point amplitudes to be used. In the following let us focus in the case $(h_1, h_2) = (+1, -1)$. The steps to be followed for the complementary case $(h_1, h_2) = (-1, +1)$ are identical but, most importantly, this other case can be obtained straightforwardly by exchanging the particles 1 and 2 in the final expression of $A_4(1^{+1}2^{-1}3^0 4^0)$. The next step is choosing the momentum that we wish to make complex, which we will take to be the adjacent momenta 2 and 3, that is, choosing one massive and one massless. In principle, the choice of shift is dictated by the requirement of being valid (in the sense defined in section 4.2.3). However, in this particular example it is not possible to show that any of the possible two-particle shifts is valid. For instance, for the choice we are going to follow below, namely a $[2,3\rangle$-shift, the leading behavior of individual Feynman diagrams is as follows. Each interaction vertex contributes a factor of z, since each numerator depends on at least one shifted momenta. The propagator contributes a factor of $1/z$, and the shifted polarization vector $\epsilon^\mu_-(p_2)$ will contribute a factor of $1/z$ (recall Eq. (4.1.22)). This means that in total, our z-dependence is actually z^0, which means in principle there could be a boundary contribution to this process. However, we can justify using this shift by implementing an "auxiliary" shift, as described in [35, 49]. We will not go through the details here as it involves introducing additional technical machinery, but we

have checked that using a three-particle shift as an auxiliary shift permits to show that the shift we are using is valid. In the example of the next section, we will show explicitly the validity of the corresponding two-particle shift.

To apply the $[2,3\rangle$-shift to this case we just have to particularize the general discussion in section 4.2.4 to $i = 2$ and $j = 3$ in the present discussion. Eq. (4.2.29) leads to

$$\begin{aligned}\hat{p}_2^{a\dot{b}} &= |2\rangle^a\,[\hat{2}|^{\dot{b}} = |2\rangle^a\,[2|^{\dot{b}} + z\,|2\rangle^a\,(\langle 2|\not{p}_3)^{\dot{b}},\\ \hat{p}_3^{a\dot{b}} &= p_3^{a\dot{b}} - z\,|2\rangle^a\,(\langle 2|\not{p}_3)^{\dot{b}}.\end{aligned} \tag{5.1.12}$$

For simplicity, we will mostly write these as

$$\hat{p}_2 = |2\rangle\,[2| + z\,|2\rangle\,[\eta|, \qquad \hat{p}_3 = p_3 - z\,|2\rangle\,[\eta|, \tag{5.1.13}$$

where

$$|\eta] = p_3|2\rangle. \tag{5.1.14}$$

For this choice of shifted particles, there is only one possible arrangements of the particles: $\hat{2}$ and 4 on one side (e.g., left) of the shifted propagator, and 1 and $\hat{3}$ on the other side (that is, on the right). The application of the recursion relations (4.2.16) lead therefore to

$$\begin{aligned}A_4(1^{+1}2^{-1}3^0 4^0) = &\frac{i}{P_{12}^2} A_3(1^{+1}\hat{2}^{-1}\hat{P}_{12}^{-2}) A_3((-\hat{P}_{12})^{+2}\hat{3}^0 4^0)\\ &+ \frac{i}{P_{12}^2} A_3(1^{+1}\hat{2}^{-1}\hat{P}_{12}^{+2}) A_3((-\hat{P}_{12})^{-2}\hat{3}^0 4^0),\end{aligned} \tag{5.1.15}$$

where shifted momenta are evaluated on $z = z_{12}$ that guarantees that the shifted momentum in the propagator, $\hat{P}_{12} = p_1 + \hat{p}_2$, is on-shell. Taking into account Eq. (4.1.18), this means that

$$\hat{P}_{12}^2 = 2p_1 \cdot \hat{p}_2 = \langle 12\rangle\,[1\hat{2}] = \langle 12\rangle\,([12] + z_{12}[1|p_3|2\rangle) = 0 \tag{5.1.16}$$

or, equivalently,

$$[1\hat{2}] = [12] + z_{12}[1|p_3|2\rangle = 0, \tag{5.1.17}$$

which permits to obtain

$$z_{12} = -\frac{[12]}{[1|p_3|2\rangle}. \tag{5.1.18}$$

Eqs. (5.1.15) and (5.1.18), together with the 3-point amplitudes evaluated just above, are all we need to obtain the 4-point amplitude. For this, the only necessary step is writing the 3-point amplitudes in terms of the shifted momenta. Let us

start with the first line of Eq. (5.1.15). This term contains the following 3-point amplitude:

$$A_3(1^{+1}\hat{2}^{-1}\hat{P}_{12}^{+2}) = -\frac{\kappa}{2}\frac{[1\hat{P}_{12}]^4}{[1\hat{2}]^2} = -\frac{\kappa}{2}\frac{[1\hat{2}]^2\,\langle 12\rangle^4}{\langle 1\hat{P}_{12}\rangle^4} = 0. \tag{5.1.19}$$

To write the second identity we have multiplied by $\langle 1\hat{P}_{12}\rangle^4/\langle 1\hat{P}_{12}\rangle^4$. That the quantity above vanishes follows then from Eq. (5.1.17). This means that the first term in Eq. (5.1.15) does not contribute to the amplitude.

Let us consider the only remaining contribution, namely the second line in Eq. (5.1.15). The two 3-point amplitudes involved are

$$A(1^{+1}\hat{2}^{-1}\hat{P}_{12}^{-2}) = -\frac{\kappa}{2}\frac{\langle 2\hat{P}_{12}\rangle^4}{\langle 12\rangle^2} \tag{5.1.20}$$

and

$$A((-\hat{P}_{12})^{+2}\hat{3}^0 4^0) = \frac{-i\kappa}{2}\frac{\langle q|\,\hat{p}_3|\hat{P}_{12}]\,\langle q|\,p_4|\hat{P}_{12}]}{\langle q\hat{P}_{12}\rangle^2} = \frac{i\kappa}{2}\frac{\langle q|\,p_4|\hat{P}_{12}]^2}{\langle q\hat{P}_{12}\rangle^2}, \tag{5.1.21}$$

where we have used $\hat{p}_3 = -p_4 - \hat{P}_{12}$.

Hence the full 4-point amplitude is given by

$$\begin{aligned} A_4(1^{+1}2^{-1}3^0 4^0) &= A(1^{+1}\hat{2}^{-1}\hat{P}_{12}^{-2})\frac{i}{P_{12}^2}A((-\hat{P}_{12})^{+2}\hat{3}^0 4^0) \\ &= \left(-\frac{\kappa}{2}\frac{\langle 2\hat{P}_{12}\rangle^4}{\langle 12\rangle^2}\right)\frac{i}{P_{12}^2}\left(\frac{i\kappa\,\langle q|\,p_4|\hat{P}_{12}]^2}{2\,\langle q\hat{P}_{12}\rangle^2}\right) \\ &= \frac{\kappa^2}{4}\frac{1}{P_{12}^2}\frac{\langle q|\,p_4|\hat{P}_{12}]^2\,\langle 2\hat{P}_{12}\rangle^4}{\langle 12\rangle^2\,\langle q\hat{P}_{12}\rangle^2}. \end{aligned} \tag{5.1.22}$$

This expression can be simplified using

$$\langle q|\,p_4|\hat{P}_{12}]\,\langle P_{12}2\rangle = -\,\langle q|\,p_4|1]\,\langle 12\rangle\,, \tag{5.1.23}$$

leading to the following closed form of the amplitude:

$$A_4(1^{+1}2^{-1}3^0 4^0) = \frac{\kappa^2}{4}\frac{\langle q|\,p_4|1]^2}{P_{12}^2}\frac{\langle 2\hat{P}_{12}\rangle^2}{\langle q\hat{P}_{12}\rangle^2}. \tag{5.1.24}$$

This expression is written in terms of the arbitrary reference bispinor $\langle q|$. To evaluate the cross-section, it is necessary to obtain the modulus (in the complex sense) of Eq. (5.1.24). It can be show explicitly that, in this step, the dependence in this arbitrary reference spinor drops off, which means that physical results do

not depende on this choice (physical results are gauge invariance). Hence, for the sake of simplicity, we can simplify the expression above if we take $\langle q| = \langle 2|$, which leads to the simpler expression

$$A_4(1^{+1}2^{-1}3^04^0) = \frac{\kappa^2}{4}\frac{\langle 2|\,p_4|1]^2}{P_{12}^2}. \tag{5.1.25}$$

Evaluation of the cross-section

Eq. (5.1.25) is not enough to extract the physics of scattering events. It is necessary to compute the modulus of this (generally complex) quantity, in order to obtain the cross-section. Also in this procedure, spinor-helicity variables will be transformed to momentum (or Mandelstam) variables in order to make easier the interpretation of the result.

First of all, using the rule $\langle 2|\,p_4|1]^\dagger = \langle 1|\,p_4|2]$, the modulus of $A_4(1^{+1}2^{-1}3^04^0)$ can be written as

$$|A_4(1^{+1}2^{-1}3^04^0)|^2 = \frac{\kappa^4}{16}\frac{(\langle 2|\,p_4|1]\,\langle 1|\,p_4|2])^2}{P_{12}^4}. \tag{5.1.26}$$

For the next step, it is instructive to make the spinor indices explicit, in order to show that the spinors in the numerator constitute the trace of four momentum vectors:

$$\begin{aligned}
&(\langle 2|\,p_4|1]\,\langle 1|\,p_4|2])^2 \\
&= (\langle 2|_{\dot a}\,(p_4)^{\dot a b}|1]_b\,\langle 1|_{\dot c}\,(p_4)^{\dot c d}|2]_d)^2 \\
&= ((p_4)^{\dot a b}|1]_b\,\langle 1|_{\dot c}\,(p_4)^{\dot c d}|2]_d\,\langle 2|_{\dot a})^2 \\
&= ((p_4)^{\dot a b}(p_1)_{b\dot c}(p_4)^{\dot c d}(p_2)_{d\dot a})^2.
\end{aligned} \tag{5.1.27}$$

Hence we recognise that the square object in the numerator of Eq. (5.1.26) is none other than a trace. Hence the modulus of the scattering amplitude can be written purely in terms of momentum vectors as

$$|A_4(1^{+1}2^{-1}3^04^0)|^2 = \frac{\kappa^4}{16}\frac{\left(\mathrm{Tr}_-\,(p_4p_1p_4p_2)\right)^2}{P_{12}^4}. \tag{5.1.28}$$

We have recognised this as the negative trace due to the ordering of indices, recalling that in the equation above, momenta are bispinors given by $p^{\dot a b} \equiv p_\mu(\bar\sigma^\mu)^{\dot a b}$. Dealing with this kind of expression is facilitated by the properties of the trace of Pauli matrices. These properties are well-known and can be found in many sources [50, 51]. For instance, in our case we can use

$$\mathrm{Tr}_-\,(\bar\sigma^\mu\sigma^\nu\bar\sigma^\rho\sigma^\lambda) = 2(\eta^{\mu\nu}\eta^{\rho\lambda} - \eta^{\mu\rho}\eta^{\nu\lambda} + \eta^{\mu\lambda}\eta^{\rho\nu} - i\epsilon^{\mu\nu\rho\lambda}). \tag{5.1.29}$$

When evaluating traces of slashed momenta, this becomes:

$$\begin{aligned}&\mathrm{Tr}_{\pm}\left(p_4 p_1 p_4 p_2\right)\\&= 2\left[(p_4\cdot p_1)(p_4\cdot p_2)-(p_4\cdot p_4)(p_1\cdot p_2)+(p_4\cdot p_2)(p_1\cdot p_4)\pm i\epsilon_{\mu\nu\rho\lambda}(p_4)^{\mu}(p_1)^{\nu}(p_4)^{\rho}(p_2)^{\lambda}\right].\end{aligned} \tag{5.1.30}$$

Since two of the momentum vectors are the same within the trace, the antisymmetric component of this is zero, namely $\epsilon_{\mu\nu\rho\lambda}(p_4)^{\mu}(p_1)^{\nu}(p_4)^{\rho}(p_2)^{\lambda}=0$, and we are left with the simpler result

$$\begin{aligned}|A_4(1^{+1}2^{-1}3^0 4^0)|^2 &= \frac{\kappa^4}{8}\frac{\left[(p_4\cdot p_1)(p_4\cdot p_2)-(p_4\cdot p_4)(p_1\cdot p_2)+(p_4\cdot p_2)(p_1\cdot p_4)\right]^2}{P_{12}^4}\\&= \frac{\kappa^4}{8}\frac{\left[2(p_1\cdot p_4)(p_2\cdot p_4)+m^2(p_1\cdot p_2)\right]^2}{(p_1+p_2)^4}.\end{aligned} \tag{5.1.31}$$

In the second equation we have used the on-shell condition $p_4=-m^2$ to simplify one of the three terms, and notice that the remaining two ones are indeed the same.

We can now write this in terms of Mandelstam invariants, defined as

$$\begin{aligned}s_{12}&=-(p_1+p_2)^2=-2p_1\cdot p_2,\\s_{13}&=-(p_1+p_3)^2=m^2-2p_1\cdot p_3,\\s_{14}&=-(p_1+p_4)^2=m^2-2p_1\cdot p_4.\end{aligned} \tag{5.1.32}$$

The second identities above can be used by just using the on-shell conditions on the different momenta (both massless and massive). These invariants satisfy

$$s_{12}+s_{13}+s_{14}=-2m^2. \tag{5.1.33}$$

In terms of Mandelstam variables, the modulus of the amplitude reads

$$|A_4(1^{+1}2^{-1}3^0 4^0)|^2=\frac{\kappa^4}{16}\frac{\left[s_{13}s_{14}+m^2(s_{12}+s_{13}+s_{14})+m^4\right]^2}{s_{12}^2}=\frac{\kappa^4}{16}\frac{\left(s_{13}s_{14}-m^4\right)^2}{s_{12}^2}. \tag{5.1.34}$$

We have used Eq. (5.1.33) to write the second identity above. This last expression of the modulus of the amplitude is manifestly invariant under the exchange of particles 3 and 4.

We are now interested in calculating the cross-section of this interaction. We choose again the centre of mass frame, in which the cross-section is given by the formula:

$$\frac{d\sigma}{d\Omega}=\frac{1}{64\pi^2 s_{14}}|A_4(1^{+1}2^{-1}3^0 4^0)|^2. \tag{5.1.35}$$

In the low energy limit, we imagine that the photon's energy as small compared with the scalar mass m. This leads to the following simplified expressions of the Mandelstam invariants:

$$\begin{aligned} s_{12} &\simeq \vec{P}^2 = 4E^2 \sin^2(\theta/2), \\ s_{13} &\simeq m^2 - 2mE - 4E^2 \sin^2(\theta/2), \\ s_{14} &\simeq (m+E)^2 \simeq m^2 + 2mE. \end{aligned} \tag{5.1.36}$$

Furthermore, if we take the scattering angle to be small, then $\sin(\theta/2) \simeq \theta/2$.

Under all the simplifications, we can write the cross-section in this limit as

$$\frac{d\sigma}{d\Omega} = \frac{1}{64\pi^2 s_{14}} |A_4(1^{+1}2^{-1}3^0 4^0)|^2 = \frac{\kappa^4}{16} \frac{\left[4m^2E^2 + 4m^2E^2\sin^2(\theta/2)\right]^2}{1024\pi^2 m^2 E^4 \sin^4(\theta/2)} \tag{5.1.37}$$

$$\simeq \frac{\kappa^4 m^2}{1024\pi^2} \left(\frac{\sin^2(\theta/2)+1}{\sin^2(\theta/2)}\right)^2 \simeq \frac{\kappa^4 m^2}{64\pi^2\theta^4}, \tag{5.1.38}$$

where we have used that $m + 2E \simeq m$ and $\sin^2(\theta/2) \ll 1$. We can now recall that $\kappa^2 = 32\pi G$ to find that:

$$\frac{d\sigma}{d\Omega} = \frac{16G^2m^2}{\theta^4}. \tag{5.1.39}$$

This result exactly matches the result obtained via Feynman diagrams. Hence we have finished our evaluation of the cross-section using on-shell methods.

To compare this with the more familiar result from general relativity, we need to relate the cross-section to the impact parameter b, the perpendicular offset of the incoming photons. Some elementary geometry shows that $\sigma = \pi b^2$, or, infinitesimally,

$$b\ db = -\frac{d\sigma}{d\Omega} \sin\theta d\theta. \tag{5.1.40}$$

The scattering angle can be found by integrating this equation, using eq. (3.0.2) in the small angle approximation

$$\int b\ db = \frac{b^2}{2} = -\int \frac{d\sigma}{d\Omega}\theta d\theta = \frac{8G^2m^2}{\theta^2}, \tag{5.1.41}$$

where the integration constant can be set to zero by comparing to the flat space ($m = 0$) case. Physically, we expect the maximum deflection angle θ_D when the photon just grazes the surface of the lens where $b = R_0$ and

$$\theta_{\rm D} = \frac{4Gm}{R_0}. \tag{5.1.42}$$

This is nothing but the classical result for the gravitational light-bending angle obtained in general relativity if we make the natural identification between the mass of the scalar m and the Schwarzschild mass M.

5.2 Gravitational Wave Bending by Gravity

In this section, we will show that calculating the same process for a gravitational wave, rather than electromagnetic, is really no more difficult. This is not the case in traditional Quantum Field Theory, where typically Feynman diagrams containing gravitons are orders of magnitude more difficult to compute.

Evaluation of the scattering amplitude

Instead of considering a light ray passing close to a massive object, we could instead imagine a gravitational wave. This corresponds to replacing the external photons with external gravitons. Using traditional quantum field theory methods (i.e. Feynman rules), the 3-graviton vertex is a nightmare inducing 6 index tensor dependant on the three momenta. Thankfully for us, we can happily just use little group scaling to derive the 3-point primitives trivially using Eq. (4.1.27).

The scattering amplitude that we want to obtain can be represented diagramatically by

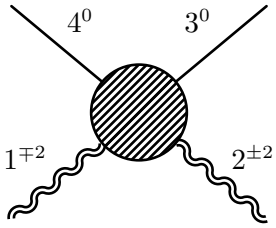

(5.2.1)

If expanded in terms of Feynman diagrams, this amplitude contains different processes allowed by the interactions in the Lagrangian. However, we can omit this step in the calculation using the BCFW recursion relations.

There is an important difference between this amplitude and the amplitude involving external photons. For the case of photon scattering, scattering amplitudes with helicity configuration $(h_1, h_2) = (\pm 1, \pm 1)$ for the two photons were identically zero. However, this is not true with gravitons, namely scattering amplitudes with helicity configuration $(h_1, h_2) = (\pm 2, \pm 2)$ do not vanish. In physical terms, this is due to the fact that a graviton can be absorbed by the scalar and be ejected at some later time, potentially with a different helicity (this process is not allowed for photons, at least for matter that is electrically neutral). However, the physical process we are interested in is the change of angle of a gravitational wave, the wavelength of which is much smaller than the distance to the source of the gravitational field (represente by the scalar field). In this process, the helicity of the wave cannot change. This is the reason why we focus in the following in helicity configurations $(h_1, h_2) = (\mp 2, \pm 2)$ for external gravitons, as the corresponding amplitudes contain the information about the physical process of interest. The

remaining amplitudes would be important to describe other processes, such as the interaction of gravitatonal waves and matter in the early universe, but discussing this phenomenon is out of the scope of this paper.

Hence let us focus on the helicity configuration $(h_1, h_2) = (-2, +2)$, namely we want to evaluate the scattering amplitude $A_4(1^{-2}2^{+2}3^04^0)$. The other helicity configuration can be obtained just by exchanging the two gravitons. The simplest shift we can imagine making is the one where we consider shifting only the two massless gravitons, with external momenta p_1 and p_2. In this case, it is possible to show using the leading behavior of Feynman diagrams that the shift $[1, 2\rangle$-shift is valid for the chosen helicity configuration. Note that we are shifting massless particles (contrary to what we did in the photon case), so the expression of the shift in terms of spinor-helicity variables is simple, and is given by Eq. (4.2.5) with $i = 1$ and $j = 2$, namely

$$|\hat{1}] = |1] + z|2], \qquad |\hat{2}\rangle = |2\rangle - z\,|1\rangle\,. \tag{5.2.2}$$

Counting the leading z-dependence from this Feynman diagram, we find that each vertex contributes a factor z, the propagator contributes z^{-1} and the contribution from the each product of polarization vectors is z^{-2}. This is sketched in the following figure:

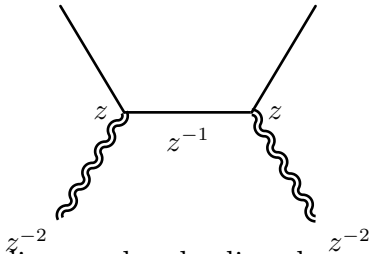

(5.2.3)

This means that the total diagram has leading dependence z^{-3}, to that the shift is valid as explained in section 4.2.3.

Note that for this shift there are only two possible arrangements of particles that lead to poles, and therefore will contribute to the scattering amplitude as evaluated using BCFW. These two contributions are represented diagrammatically by

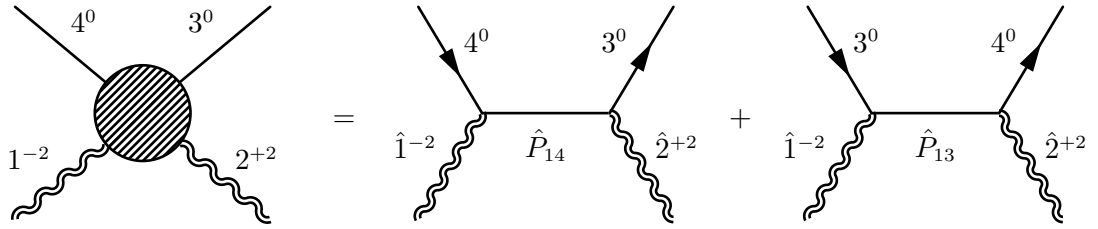

(5.2.4)

Let us calculate the contributions corresponding to these diagrams using Eq. (4.2.16):

$$A_4(1^{-2}2^{+2}3^04^0) = A_3(\hat{1}^{-2}4^0\hat{P}^0_{14})\frac{i}{P^2_{14}+m^2}A_3(\hat{2}^{+2}3^0(-\hat{P}_{14})^0) + A_3(\hat{1}^{-2}3^0\hat{P}^0_{13})\frac{i}{P^2_{13}+m^2}A_3(\hat{2}^{+2}4^0(-\hat{P}_{13})^0). \tag{5.2.5}$$

First of all, let us notice that the only 3-point amplitudes that we need involve two scalar particles and a graviton. These were evaluated in Eqs. (5.1.9) and (5.1.10). Hence now it is just a matter of using these expressions and simplifying the answer.

Let us consider the product of 3-point amplitudes in the first line of Eq. (5.2.5). This is given by

$$A_3(\hat{1}^{-2}4^0\hat{P}^0_{14})A_3(\hat{2}^{+2}3^0(-\hat{P}_{14})^0) = -\frac{\kappa^2}{4}\frac{\langle 1|p_4|q]^2\langle g|p_3|2]^2}{[q\hat{1}]^2\langle g\hat{2}\rangle^2}. \tag{5.2.6}$$

In this expressions, both $|q]$ and $|g\rangle$ can be fixed by choosing a particular gauge (physical results will be independent of this choice). The choice that leads to the simplest result is

$$|q] = |2], \qquad |g\rangle = |1\rangle, \tag{5.2.7}$$

which permits to write

$$A_3(\hat{1}^{-2}4^0\hat{P}^0_{14})A_3(\hat{2}^{+2}3^0(-\hat{P}_{14})^0) = -\frac{\kappa^2}{4}\frac{\langle 1|p_4|2]^2\langle 1|p_3|2]^2}{\langle 12\rangle^2[12]^2} = -\frac{\kappa^2}{4}\frac{\langle 1|p_4|2]^4}{\langle 12\rangle^2[12]^2}. \tag{5.2.8}$$

Following the same procedure with the second term in Eq. (5.2.5), we have

$$A_4(1^{-2}2^{+2}3^04^0) = -\frac{i\kappa^2}{4}\frac{\langle 1|\,p_4|2]^4}{\langle 12\rangle^2\,[12]^2}\left(\frac{1}{P^2_{13}+m^2}+\frac{1}{P^2_{14}+m^2}\right) \tag{5.2.9}$$

$$= -\frac{i\kappa^2}{4}\frac{\langle 1|\,p_4|2]^4}{\langle 12\rangle^2\,[12]^2}\left(\frac{1}{2p_1\cdot p_3}+\frac{1}{2p_1\cdot p_4}\right) \tag{5.2.10}$$

$$= -\frac{i\kappa^2}{4}\frac{\langle 1|\,p_4|2]^4}{\langle 12\rangle^2\,[12]^2}\left(\frac{-2p_1\cdot p_2}{4(p_1\cdot p_3)(p_1\cdot p_4)}\right) \tag{5.2.11}$$

$$= \frac{i\kappa^2}{16}\frac{\langle 1|\,p_4|2]^4}{\langle 12\rangle\,[12]}\left(\frac{1}{(p_2\cdot p_3)(p_2\cdot p_4)}\right). \tag{5.2.12}$$

Evaluation of the cross-section

As we have done in all the previous examples, we have to obtain the modulus of Eq. (5.2.12) in order to extract its physical implications. Proceeding as we did in the photon case and converting to Mandelstam variables, we find that

$$|A_4(1^{-2}2^{+2}3^04^0)|^2 = |A_4(1^{-1}2^{+1}3^04^0)|^2 f(s_{12},s_{13},s_{14})^2, \tag{5.2.13}$$

where we have defined the following function of the Mandelstam invariants:

$$f(s_{12}, s_{13}, s_{14}) = 1 - \frac{m^2 s_{12}}{(s_{13} + m^2)(s_{14} + m^2)}. \tag{5.2.14}$$

Eq. (5.2.13) implies that the cross-section for external gravitons is proportional to the cross-section for external photons, with proportionality factor given in Eq. (5.2.14). In general relativity, we expect that these two cross-sections should be the same in the geometric optics limit (in which both massless particles follow null geodesics).

Indeed, considering the same approximations as we in the photon case (small deflection angles and large gravitational mass), we find that the function $f(s,t,u)^2 \simeq 1$:

$$f(s_{12}, s_{13}, s_{14}) \simeq 1 - \frac{2mE \sin^2(\theta/2)}{2mE + 4E^2 \sin^2(\theta/2)} \simeq 1. \tag{5.2.15}$$

Again, in this approximation $E \ll m$ and $\sin^2(\theta/2) \ll 1$. Therefore, we can conclude that the cross-section, and hence the scattering angle, for gravitational and electromagnetic waves is the same in the geometric optics limit. This is in exact agreement with GR.

VI

The vDVZ Discontinuity: a Modern Amplitude Perspective

> *"There's a certain irrationality to any work in gravitation, so it's hard to explain why you do any of it."*
>
> – Richard Feynman, *Quantum theory of gravitation*, 1963

The idea that the graviton, the quantum of gravity, may have a small but non-vanishing mass is one that has been around since Fierz and Pauli's original work on massive spin-2 field theory. Phenomenologically, there is much appeal to a theory in which General Relativity is modified in this way at large distances, not the least of which is a possible explanation of the current acceleration of the Universe that does not invoke any dark energy. Unfortunately, massive gravity also suffers from a range of pathologies that, at least historically, have severely constrained its viability. These include the presence of the Boulware-Deser ghost and a discontinuity with General Relativity (GR) as the graviton mass is sent to zero. While we will have nothing to contribute to the discussion of ghosts, it will be the so-called vDVZ discontinuity [52, 53] that will form the basis for this chapter.

The inability of the massive theory to smoothly reduce to GR in the limit that the mass of the graviton is taken to zero famously manifests in a gravitational lensing angle only three quarters of the observed value. Physically, this is understood by observing that a massive spin-2 field propagated three additional degrees of freedom than its massless counterpart. These are repackaged as a vector and a scalar, and it is found that the scalar couples to the trace of the stress-energy tensor of any matter coupled to the massive gravity, providing an additional force. In order to reconcile this with the classical Newtonian potential, the gravitational coupling must be rescaled to three quarters its value in the Einstein theory. However, since the gravitational lensing of light is blind to the scalar (its stress energy tensor being traceless), this results in a proportionally smaller lensing angle than that computed in GR. In the interests of pedagogy, let's unpack the details of this argument.

Giving the graviton mass breaks the full diffeomorphism invariance of GR. This can be reintroduced via the Stückelberg procedure, but at the expense of the introduction of several new fields. Starting from an action with explicitly broken diffeomorphism symmetry, and involving only a single dynamical field $h_{\mu\nu}$,

$$S[h] = \int d^4x \, \sqrt{-g} \left(\frac{2}{\kappa^2} R - \frac{m_h^2}{2} \left(h_{\mu\nu} h^{\mu\nu} - h^2 \right) \right) , \tag{6.0.1}$$

we then demand that diffeomorphism symmetry is restored by transforming $h_{\mu\nu}$ by a Stückelberg field (scaled by the graviton mass for convenience) that encodes the transformation

$$\delta h_{\mu\nu} = \frac{1}{m_h} \left(\partial_\mu A_\nu + \partial_\nu A_\mu \right) . \tag{6.0.2}$$

The result is the new action

$$S[A, h] = \int d^4x \, \sqrt{-g} \left(\frac{2}{\kappa^2} R - \frac{m_h^2}{2} \left(h_{\mu\nu} h^{\mu\nu} - h^2 \right) - \frac{1}{2} F_{\mu\nu} F^{\mu\nu} - 2 m_h (h_{\mu\nu} \partial^\mu A^\nu - h \partial_\mu A^\mu) \right) . \tag{6.0.3}$$

Subsequently, demanding the gauge invariance of the vector field requires the introduction of another Stückelberg field, this time a scalar, via the transformation

$$\delta A_\mu = \frac{1}{m_h} \partial_\mu \pi \, , \tag{6.0.4}$$

and results in the action

$$S[A, h, \pi] = \int d^4x \, \sqrt{-g} \Big(\quad \tfrac{2}{\kappa^2} R - \tfrac{m_h^2}{2} \left(h_{\mu\nu} h^{\mu\nu} - h^2 \right) - \tfrac{1}{2} F_{\mu\nu} F^{\mu\nu} - 2 m_h (h_{\mu\nu} \partial^\mu A^\nu - h \partial_\mu A^\mu) \\ - 2 (h_{\mu\nu} \partial^\mu \partial^\nu \pi - h \partial^2 \pi) \Big) . \tag{6.0.5}$$

The massive graviton can be coupled to a source $T^{\mu\nu}$ through a source term $\kappa h_{\mu\nu} T^{\mu\nu}$, whose variation (after integration by parts) is

$$\delta \left(h_{\mu\nu} T^{\mu\nu} \right) = \frac{2\pi}{m_h^2} \partial_\mu \partial_\nu T^{\mu\nu} - \frac{2 A_\nu}{m_h} \partial_\mu T^{\mu\nu} . \tag{6.0.6}$$

Assuming stress-energy conservation (i.e. $\partial_\nu T^{\mu\nu} = 0$), this variation is zero, resulting in the diffeomorphism invariant sourced theory with action

$$S[A, h, \pi] = \int d^4x \, \sqrt{-g} \Big(\frac{2}{\kappa^2} R - \frac{m_h^2}{2} \left(h_{\mu\nu} h^{\mu\nu} - h^2 \right) - \frac{1}{2} F_{\mu\nu} F^{\mu\nu} - 2 m_h (h_{\mu\nu} \partial^\mu A^\nu - h \partial_\mu A^\mu) \\ - 2 (h_{\mu\nu} \partial^\mu \partial^\nu \pi - h \partial^2 \pi) + \kappa h_{\mu\nu} T^{\mu\nu} \Big) . \tag{6.0.7}$$

Currently, the $h_{\mu\nu}$ tensor still represents all 5 modes of the graviton, but it can be explicitly decomposed it into the spin-2 and spin-0 modes in an effort to understand

what happens to the kinetically mixed scalar-tensor modes[1]. To this end, let's make a canonical transformation of the form

$$h_{\mu\nu} = \bar{h}_{\mu\nu} + \chi\eta_{\mu\nu}, \tag{6.0.8}$$

where $\bar{h}$ is the tensor mode and χ the scalar. To linear order, the massless spin-2 part transforms as

$$\int d^4x\ \sqrt{-g}\frac{2}{\kappa^2}R \longrightarrow \int d^4x\ \sqrt{-g}\frac{2}{\kappa^2}\bar{R} + 2\left(\partial_\mu\chi\partial^\mu\bar{h} - \partial_\mu\chi\partial_\nu\bar{h}^{\mu\nu} + \frac{3}{2}\partial_\mu\chi\partial^\mu\chi\right), \tag{6.0.9}$$

so that defining $\chi = \pi$ and with a little more manipulation, the action becomes

$$S[A,\bar{h},\chi] = \int d^4x\ \sqrt{-g}\Big(\frac{2}{\kappa^2}\bar{R} - \frac{m_h^2}{2}\left(\bar{h}_{\mu\nu}\bar{h}^{\mu\nu} - \bar{h}^2\right) - \frac{1}{2}F_{\mu\nu}F^{\mu\nu} - 2m_h(\bar{h}_{\mu\nu}\partial^\mu A^\nu - \bar{h}\partial_\mu A^\mu) + \kappa\bar{h}_{\mu\nu}T^{\mu\nu} + 3\chi(\partial^2 + 2m_h^2)\chi + 3(m_h^2\bar{h}\chi + 2m\chi\partial_\mu A^\mu) + \kappa\chi T\Big). \tag{6.0.10}$$

Now that all of the degrees of freedom are accounted for, we can send $m_h \longrightarrow 0$ smoothly. In this limit, we find[2]

$$S[A,\bar{h},\chi] \longrightarrow \int d^4x\ \sqrt{-g}\Big(\frac{2}{\kappa^2}\bar{R} - \frac{1}{2}F_{\mu\nu}F^{\mu\nu} + \kappa\bar{h}_{\mu\nu}T^{\mu\nu} - \frac{1}{2}\partial_\mu\chi\partial^\mu\chi + \sqrt{\frac{1}{6}}\kappa\chi T\Big). \tag{6.0.11}$$

We recognise this as a theory containing an interacting massless scalar field (with a canonical kinetic term), an interacting massless spin-2 graviton and a free spin-1 field. Importantly, the scalar graviton couples to the trace of the stress energy tensor, so that any matter with a traceless stress energy tensor will not feel the effects of the scalar graviton. Of course, the canonical example of such matter is the photon of the electromagnetic interaction and a direct consequence of the above is that, if massive gravity and GR are to agree on their nonrelativistic Newtonian potential, then the bending angle of gravitationally lensed light must be qualitatively different between the two. Viewed as a scattering process, gravitational lensing corresponds to the Feynman diagram,

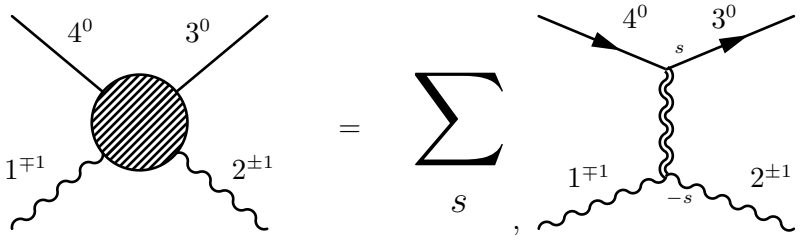

(6.0.12)

[1] We will not consider the spin one mode, since the spin one Stuckelberg field is free

[2] For the terms $\propto \frac{1}{m}\partial_\mu T^{\mu\nu}$, which we have ignored, we have assumed that $\partial_\mu T^{\mu\nu} \longrightarrow 0$ faster than $m \longrightarrow 0$.

where the sum is taken over the two tensor, two vector and one scalar polarization modes of the massive graviton. In this note, we will consider the above scattering process using the BCFW recursion relations, without resorting to the necessity of Lagrangians, polarization vectors or gauges and show that the vDVZ discontinuity exists at the level of the amplitudes, regardless of the underlying off-shell theory.

6.0.1 Calculation of 3-point amplitudes

Let's begin by considering the 3-point function for two massive scalars and a spin-2 massive graviton. Since all the scattering particles are massive, the (chiral) $SL(2)$ space is spanned by the tensors

$$P_{1\alpha\dot{\beta}}(P_2)^{\dot{\beta}}{}_{\beta} \equiv P_{\alpha\beta}, \qquad \varepsilon_{\alpha\beta}\,, \tag{6.0.13}$$

which will form the basis for the amplitude. Moreover, since gravity couples universally with coupling $\sqrt{G} \sim \kappa$, and any 3-point function must have mass-dimension 1, the form of the amplitude can be read off from these building blocks essentially by dimensional analysis. The necessary completely symmetric building blocks with $2S = 4$ indices constructed from these tensors are

$$P_{\{\alpha_1\alpha_2}P_{\alpha_3\alpha_4\}} + P_{\{\alpha_1\alpha_2}\varepsilon_{\alpha_3\alpha_4\}} + \varepsilon_{\{\alpha_1\alpha_2}\varepsilon_{\alpha_3\alpha_4\}} \tag{6.0.14}$$

The associated stripped amplitude is then simply

$$M_{\{\alpha_1\alpha_2\alpha_3\alpha_4\}} = \kappa\left(P_{\{\alpha_1\alpha_2}P_{\alpha_3\alpha_4\}} + P_{\{\alpha_1\alpha_2}\varepsilon_{\alpha_3\alpha_4\}} + \varepsilon_{\{\alpha_1\alpha_2}\varepsilon_{\alpha_3\alpha_4\}}\right)\,. \tag{6.0.15}$$

At this point, we could well express each amplitude with all of the $IJKL$ indices lavishly decorating each piece, but since symmeterisation of the spinor indices translates directly into symmeterisation of the $SL(2)$ indices, this will not be necessary. We will adopt the notation set out in [30], and represent massive spinors in **bold**. We will also suppress the $SL(2)$ indices, in the knowledge that they can always be reinstated in an unambiguous way (they are simply attached to all particles with spin and completely symmetrized). Weighting each term by the graviton mass to give the correct mass dimension, the full amplitude is then given by

$$\begin{aligned} M^{\{IJKL\}} &= M_{\{\alpha_1\alpha_2\alpha_3\alpha_4\}}\lambda_3^{I\alpha_1}\lambda_3^{J\alpha_2}\lambda_3^{K\alpha_3}\lambda_3^{L\alpha_4} \\ &= \kappa\frac{([\mathbf{12}]\,\langle\mathbf{13}\rangle\,\langle\mathbf{23}\rangle)^2}{6m_h^4} + \kappa\frac{[\mathbf{12}]\,\langle\mathbf{13}\rangle\,\langle\mathbf{23}\rangle\,\langle\mathbf{33}\rangle}{4m_h^2} + \frac{\kappa}{2}\,\langle\mathbf{33}\rangle^2\,, \end{aligned} \tag{6.0.16}$$

where the numerical coefficients reflect the number of equivalent ways we can order I, J, K, L in each term.

Unfortunately, this form of the amplitude does not lend itself to a direct application of the BCFW relations since we are unable to find a shift that is valid for all possible choices of helicity. Instead, we will need to extract the individual helicity components (in some limit where the helicity is well defined) and calculate the amplitudes for each helicity individually. This corresponds to making particular choices of I, J, K, L. It should be noted that this is entirely equivalent to contracting the stripped amplitude with an appropriate number of polarization vectors (or tensors). In the language of massive spinor-helicities, these are

$$\epsilon^{-}_{\alpha\beta} = \frac{\lambda_\alpha \lambda_\beta}{m}, \qquad \epsilon^{0}_{\alpha\beta} = \frac{\lambda_\alpha \eta_\beta + \eta_\alpha \lambda_\beta}{2m}, \qquad \epsilon^{+}_{\alpha\beta} = \frac{\eta_\alpha \eta_\beta}{m}\,. \tag{6.0.17}$$

That said, as card-carrying disciples of the "on-shell" philosophy, we would prefer to work without the need for polarization vectors whatsoever. From the amplitude 6.0.16, the $h = -2$ helicity is obtained by setting $I = J = K = L = 1$. Choosing $\lambda_3^1 = |a\rangle$ and $\lambda_3^2 = |b\rangle$ then, this part of the amplitude reads

$$\begin{aligned} M^{1111} &= \kappa \frac{[\mathbf{12}]^2 \langle \mathbf{1}a\rangle^2 \langle \mathbf{2}a\rangle^2}{m_h^4} \\ &= \kappa \frac{\langle a\mathbf{2}\rangle^2 [\mathbf{2}|P_1|a\rangle^2}{m_h^4} \\ &= \kappa \frac{\langle a| P_2 |b]^2}{m_h^2}\,. \end{aligned} \tag{6.0.18}$$

Similarly, the choice of $J = 2$ and $I = K = L = 1$ yields the spin one contribution,

$$\begin{aligned} M^{\{1211\}} &= \frac{\kappa[\mathbf{12}]^2}{3m_h^4}\left(\langle \mathbf{1}a\rangle^2 \langle \mathbf{2}b\rangle \langle \mathbf{2}a\rangle + \langle \mathbf{1}b\rangle \langle \mathbf{2}a\rangle^2 \langle \mathbf{1}a\rangle\right) + \frac{\kappa}{4m_h^2}\langle a| P_1 P_2 |a\rangle \\ &= -\frac{\kappa}{3}\left(\frac{\langle a| P_1|b]}{[ab]^2}\left(\langle b| P_1|b] - \langle a| P_1|a]\right)\right) - \frac{\kappa}{4}\langle a| P_1|b] \\ &= -\frac{\kappa}{12}\langle a| P_1|b]\left(\frac{4\left(\langle b| P_1|b] - \langle a| P_1|a]\right)}{[ab]^2} + 3\right) \\ &= \frac{\kappa}{12}\langle a| P_1|b]\left(\frac{8\left(P_1\cdot(P_a - P_b)\right)}{m_h^2} - 3\right)\,. \end{aligned} \tag{6.0.19}$$

P_b can be eliminated through momentum conservation

$$P_1\cdot(P_a - P_b) = 2P_1\cdot P_a + \frac{1}{2}m_h^2\,. \tag{6.0.20}$$

Consequently,

$$M^{\{1211\}} = \frac{\kappa}{12}\langle a| P_1|b]\left(\frac{16 P_1\cdot P_a + m_h^2}{m_h^2}\right)\,. \tag{6.0.21}$$

Finally, the scalar mode contribution can be extracted by considering the $I = L = 1$ and $J = K = 2$ case

$$\begin{aligned} M^{\{1212\}} &= \kappa\frac{[\mathbf{12}]^2}{3m_h^4}\left(\langle\mathbf{1}a\rangle^2\langle\mathbf{2}b\rangle^2 + \langle\mathbf{1}a\rangle\langle\mathbf{1}b\rangle\langle\mathbf{2}a\rangle\langle\mathbf{2}b\rangle + \langle\mathbf{1}b\rangle^2\langle\mathbf{2}a\rangle^2\right) + \kappa\frac{[\mathbf{12}]\langle ab\rangle\left(\langle\mathbf{1}a\rangle\langle\mathbf{2}b\rangle + \langle\mathbf{1}b\rangle\langle\mathbf{2}a\rangle\right)}{2m_h^2} + \kappa\langle ab\rangle^2 \\ &= \kappa\frac{[\mathbf{12}]^2\left(\langle\mathbf{1}a\rangle\langle\mathbf{2}b\rangle + \langle\mathbf{1}b\rangle\langle\mathbf{2}a\rangle\right)^2 - [\mathbf{12}]^2\langle\mathbf{1}a\rangle\langle\mathbf{1}b\rangle\langle\mathbf{2}a\rangle\langle\mathbf{2}b\rangle}{3m_h^4} + \kappa\frac{[\mathbf{12}]\langle ab\rangle\left(\langle\mathbf{1}a\rangle\langle\mathbf{2}b\rangle + \langle\mathbf{1}b\rangle\langle\mathbf{2}a\rangle\right)}{2m_h^2} + \frac{\kappa}{2}\langle ab\rangle^2 \\ &= \kappa\frac{\left(\langle a|P_1|a] - \langle b|P_1|b]\right)^2}{3m_h^2} - \kappa\frac{\langle a|P_1P_2|a\rangle\langle b|P_1P_2|b\rangle}{3m_h^4} + \kappa\frac{\langle a|P_1|a] - \langle b|P_1|b]}{2} + \frac{\kappa}{2}m_h^2 \\ &= \kappa\frac{\left(\langle a|P_1|a] - \langle b|P_1|b]\right)^2}{3m_h^2} + \kappa\frac{\mathrm{Tr}_+\left(P_1P_bP_1P_a\right)}{3m_h^2} + \kappa\frac{\langle a|P_1|a] - \langle b|P_1|b]}{2} + \frac{\kappa}{2}m_h^2\,. \end{aligned} \tag{6.0.22}$$

The trace term can be evaluated using 6.0.20, the identities

$$\begin{aligned} \mathrm{Tr}_+\left(\sigma^\mu\overline{\sigma}^\nu\sigma^\rho\overline{\sigma}^\lambda\right) &= 2(\eta^{\mu\nu}\eta^{\rho\lambda} - \eta^{\mu\rho}\eta^{\nu\lambda} + \eta^{\mu\lambda}\eta^{\rho\nu} + i\epsilon^{\mu\nu\rho\lambda}) \\ \mathrm{Tr}_-\left(\overline{\sigma}^\mu\sigma^\nu\overline{\sigma}^\rho\sigma^\lambda\right) &= 2(\eta^{\mu\nu}\eta^{\rho\lambda} - \eta^{\mu\rho}\eta^{\nu\lambda} + \eta^{\mu\lambda}\eta^{\rho\nu} - i\epsilon^{\mu\nu\rho\lambda})\,, \end{aligned}$$

and the fact that $\langle a|P_1|a] = 2P_1\cdot P_a$ to get,

$$\begin{aligned} M^{\{1212\}} &= \kappa\frac{\left(\langle a|P_1|a] - \langle b|P_1|b]\right)^2}{3m_h^2} + \kappa\frac{4(P_1\cdot P_b)(P_1\cdot P_a) - 2m_\phi^2m_h^2}{3m_h^2} + \kappa\frac{\langle a|P_1|a] - \langle b|P_1|b]}{2} + \frac{\kappa}{2}m_h^2 \\ &= \kappa\frac{4\left(2P_1\cdot P_a + \frac{1}{2}m_h^2\right)^2}{3m_h^2} + \kappa\frac{4(P_1\cdot P_a)(P_1\cdot P_a + \frac{1}{2}m_h^2) - 2m_\phi^2m_h^2}{3m_h^2} + \kappa\frac{4P_1\cdot P_a + m_h^2}{2} + \frac{\kappa}{2}m_h^2\,. \end{aligned} \tag{6.0.23}$$

As a second example that we will need shortly, we consider two photons interacting with a massive spin-2 graviton. In this case, the entire amplitude is conveniently determined by the helicities of the massless legs, and is given by [30, 54]

$$M^{h_1,h_2}_{\{\alpha_1,\ldots,\alpha_{2S}\}} = \frac{g}{m^{2S+h_1+h_2-1-[g]}}\left(\lambda_1^{S+h_2-h_1}\lambda_2^{S+h_1-h_2}\right)_{\{\alpha_1,\ldots,\alpha_{2S}\}}[12]^{S+h_1+h_2}\,, \tag{6.0.24}$$

where $[g]$ is the dimension of the coupling. This is then used to construct the associated 3-point function as

$$M^{1,-1,\{IJKL\}} = M^{1,-1}_{\{\alpha_1,\ldots,\alpha_{2S}\}}\lambda_3^{I\alpha_1}\lambda_3^{J\alpha_2}\lambda_3^{K\alpha_3}\lambda_3^{L\alpha_4} = \kappa\frac{\langle\mathbf{3}2\rangle^4}{\langle 12\rangle^2}\,. \tag{6.0.25}$$

Note here that the only non-zero components of this amplitude are those that correspond to pure spin-2, i.e. those with $I = J = K = L$. This is because we implicitly demand that the powers of un-contracted spinors in a given amplitude be positive, *i.e.* $S + h_2 - h_1 > 0$ and $S + h_1 - h_2 > 0$. This in turn translates into the condition $|h| > S/2$ for a non-vanishing amplitude[3]. In field theory, this is

[3]Cases where $h_1 \neq -h_2$ results in the final amplitude being zero as a result of Bose symmetry

equivalent to the statement that the spin-1 contribution is automatically zero due to the Landau-Yang theorem[4], and that the photon does not couple to the scalar mode of the graviton in pure gravity since its stress-energy tensor is traceless. This is exactly what we found was the source of the discontinuity in the more familiar Lagrangian formulation with the introduction of Stückleberg fields.

6.1 Four-point functions from BCFW

Having derived the individual helicity components of the 3pt amplitudes, the 4-point amplitudes can now be computed. We could simply stitch these together using what we know about factorisation, however it is enlightening (although technically unnecessary) to again use the BCFW relations [31, 32], using the formula

$$A_n = i \sum_{z_{ib}} \sum_{h} A_L(z_{ib}) \frac{1}{P_{ib}^2 - m_{ib}^2} A_R(z_{ib}), \, . \tag{6.1.1}$$

In order to see the vDVZ discontinuity, we will need to calculate two sets of amplitudes: one that couples to the scalar mode of the graviton and one that does not. We choose to calculate the photon-scalar amplitude in one case, and the scalar-scalar amplitude in the other, with both mediated by a massive graviton.

6.1.1 Photon-Scalar Amplitude

Following [3], we shift momenta $2, 3$ and consider the diagram

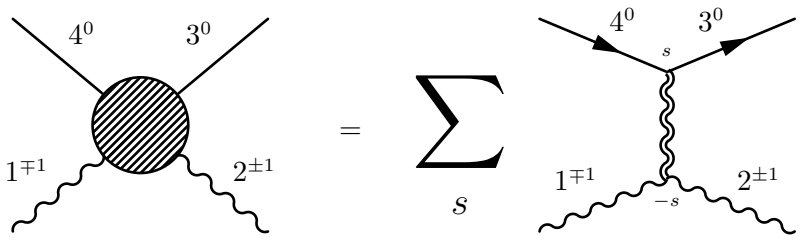

(6.1.2)

[4] By way of self-containedness, we recall here that the Landau-Yang theorem essentially says that, on-shell, a massive spin-1 particle cannot decay into two photons.

Now from eq. 6.1.1, there are five terms that can contribute to the amplitude

$$\begin{aligned}
A_4[1^+,2^-,3,4] = A[1^+,\hat{2}^-,\hat{P}_h^{-2}]\frac{1}{P_h^2-m_h^2}A[-\hat{P}_h^{+2},\hat{3},4] \\
+ A[1^+,\hat{2}^-,\hat{P}_h^{+2}]\frac{1}{P_h^2-m_h^2}A[-\hat{P}_h^{-2},\hat{3},4] \\
+ A[1^+,\hat{2}^-,\hat{P}_h^{-1}]\frac{1}{P_h^2-m_h^2}A[-\hat{P}_h^{+1},\hat{3},4] \\
+ A[1^+,\hat{2}^-,\hat{P}_h^{+1}]\frac{1}{P_h^2-m_h^2}A[-\hat{P}_h^{-1},\hat{3},4] \\
+ A[1^+,\hat{2}^-,\hat{P}_h^{0}]\frac{1}{P_h^2-m_h^2}A[-\hat{P}_h^{0},\hat{3},4] \\
= A[1^+,\hat{2}^-,\hat{P}_h^{-2}]\frac{1}{P_h^2-m_h^2}A[-\hat{P}_h^{+2},\hat{3},4]\,, \qquad (6.1.3)
\end{aligned}$$

with the opposite helicity 3-point function determined by complex conjugation. As a result, the full amplitude is

$$A_4 = \left(\kappa\frac{\langle 2a\rangle^4}{\langle 12\rangle^2}\right)\times\frac{1}{P_h^2-m_h^2}\times\left(\kappa\frac{\langle b|\,P_3|a]^2}{m_h^2}\right). \qquad (6.1.4)$$

In this form[5], we can recover the massless amplitude by taking $m_h \longrightarrow 0$ and $a \longrightarrow P_h$. Using the fact[6] that $[12]\langle 2a\rangle = [1b]\langle ab\rangle = m_h[1b]$, we find

$$\begin{aligned}
A_4 &= \left(\kappa\frac{\langle 2a\rangle^4}{\langle 12\rangle^2}\right)\times\frac{1}{P_h^2-m_h^2}\times\left(\kappa\frac{[1|P_bP_3|a]^2}{[1b]^2\langle ab\rangle^2}\right) \\
&= \left(\kappa\frac{\langle 2a\rangle^4}{\langle 12\rangle^2}\right)\times\frac{1}{P_h^2-m_h^2}\times\left(\kappa\frac{[1|(P_a+P_2)P_3|a]^2}{[1b]^2m_h^2}\right) \\
&= \left(\kappa\frac{\langle 2a\rangle^4}{\langle 12\rangle^2}\right)\times\frac{1}{P_h^2-m_h^2}\times\left(\kappa\frac{[12]^2\langle 2|\,P_3|a]^2}{[1b]^2m_h^2}\right) \\
&\xrightarrow{m_h\longrightarrow 0} \frac{\kappa^2}{P_h^2}\frac{\langle 2P_h\rangle^2\langle 2|\,P_3|P_h]^2}{\langle 12\rangle^2} \\
&= \kappa^2\frac{\langle 2|\,P_3|1]^2}{P_h^2}\,. \qquad (6.1.5)
\end{aligned}$$

In order to have this agree with eq. 5.1.25, we rescale $\kappa \longrightarrow \tilde{\kappa} = \frac{\kappa}{2}$ to find

$$A_4 = \frac{\tilde{\kappa}^2}{4}\frac{\langle 2|\,P_3|1]^2}{P_h^2}\,, \qquad (6.1.6)$$

[5]The positive helicity-2 graviton piece does not contribute. See, for example, eq.4.19 of [3] for a detailed discussion of this point.

[6]Using momentum conservation $-P_h = P_1 + P_2$, we can use the spinor representation to write this as $|1]\langle 1| + |2]\langle 2| = -|a]\langle a| - |b]\langle b|$, then contract with $[1|$ from the left and $|a\rangle$ from the right.

in the $m_h \longrightarrow 0$ limit. This rescaling of the coupling corresponds to the choice of normalisation used in the Einstein-Hilbert action.

6.1.2 Scalar-Scalar Amplitude

Next, we consider the $2 \longrightarrow 2$ scattering of massive scalars in massive gravity. For simplicity, we will take both scalars to have the same mass m_ϕ and the massive graviton to again have mass m_h. Again, we will compute the 4-point amplitude using BCFW with momenta 1 and 3 shifted, as coded in the diagram

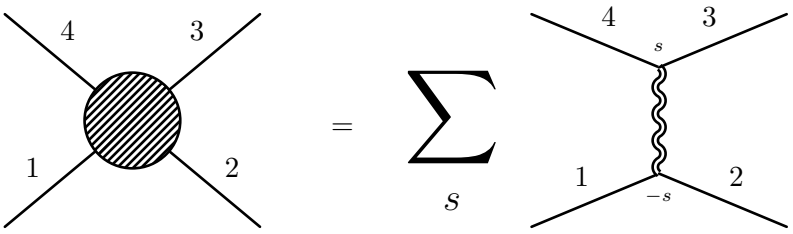

(6.1.7)

To decompose the massive shifted lines into massless ones, we write

$$P_1 = k_1 + xk_3, \qquad P_3 = k_3 + xk_1\,, \tag{6.1.8}$$

where $k_i^2 = 0$ and $x = -\frac{m_\phi^2}{2k_1\cdot k_3}$. With this in mind, it is clear that the on-shell condition $P_i^2 = m_\phi^2$ holds. Subsequently, the vectors are continued to complex values by writing

$$\hat{P}_1(z) = P_1 + z\eta, \qquad \hat{P}_3(z) = P_3 - z\eta\,, \tag{6.1.9}$$

with $\eta \cdot P_1 = \eta \cdot P_3 = 0$ and $\eta^2 = 0$. An obvious choice, given our decomposition, is $\eta = |1\rangle\,[3|$. Again, there are five terms that contribute to the amplitude in (6.1.1),

$$\begin{aligned} A_4[1,2,3,4] \;&= A[1,\hat{2},\hat{P}_h^{-2}]\tfrac{1}{P_h^2-m_h^2}A[-\hat{P}_h^{+2},\hat{3},4] \\ &+A[1,\hat{2},\hat{P}_h^{+2}]\tfrac{1}{P_h^2-m_h^2}A[-\hat{P}_h^{-2},\hat{3},4] \\ &+A[1,\hat{2},\hat{P}_h^{-1}]\tfrac{1}{P_h^2-m_h^2}A[-\hat{P}_h^{+1},\hat{3},4] \\ &+A[1,\hat{2},\hat{P}_h^{+1}]\tfrac{1}{P_h^2-m_h^2}A[-\hat{P}_h^{-1},\hat{3},4] \\ &+A[1,\hat{2},\hat{P}_h^{0}]\tfrac{1}{P_h^2-m_h^2}A[-\hat{P}_h^{0},\hat{3},4]\,, \end{aligned} \tag{6.1.10}$$

and we will evaluate each contribution separately.

Scalar Graviton Contribution

This is the last term in (6.1.10), the piece contributed by the scalar mode of the graviton. This takes the form

$$\kappa^2\left(\frac{2}{3}\right)\left[\frac{4\left(2P_1\cdot P_a+\frac{1}{2}m_h^2\right)^2}{2m_h^2}+\frac{4(P_1\cdot P_a)(P_1\cdot P_a+\frac{1}{2}m_h^2)-2m_\phi^2m_h^2}{2m_h^2}+\frac{3(4P_1\cdot P_a+m_h^2)}{4}+\frac{3}{4}m_h^2\right]$$
$$\times\quad\frac{1}{P_h^2-m_h^2}\left[\frac{4\left(2P_1\cdot P_a+\frac{1}{2}m_h^2\right)^2}{2m_h^2}+\kappa\frac{4(P_1\cdot P_a)(P_1\cdot P_a+\frac{1}{2}m_h^2)-2m_\phi^2m_h^2}{2m_h^2}+\frac{3(4P_1\cdot P_a+m_h^2)}{4}+\frac{3}{4}m_h^2\right].$$

To understand the $m_h\longrightarrow 0$ limit of this amplitude, we first note that

$$\hat{P}_1\cdot P_h=-(\hat{P}_1\cdot\hat{P}_1+\hat{P}_1\cdot\hat{P}_2)=-(m_\phi^2+\hat{P}_1\cdot\hat{P}_2)=-(m_\phi^2+\frac{1}{2}m_h^2-m_\phi^2)=-\frac{m_h^2}{2}\,,\quad(6.1.11)$$

so that $P_1\cdot P_h\longrightarrow 0$ as m_h is taken to zero. Consequently,

$$A_4^0[1,2,3,4]=\frac{4}{3}\kappa^2\frac{m_\phi^4}{t}=\frac{1}{3}\tilde{\kappa}^2\frac{m_\phi^4}{t}\,,\qquad(6.1.12)$$

where, as usual, we have defined $t=(P_1+P_2)^2$. This also has virtue of having the correct mass dimension and vanishes in the $m_\phi=0$ limit, as expected.

Spin-1 Graviton Contribution

The spin-1 contribution to the full amplitude is

$$\begin{aligned}A^{(1)}[1,2,3,4]&=\frac{\kappa^2}{144}\langle a|\,P_1|b]\left(\frac{16P_1\cdot P_a+m_h^2}{m_h^2}\right)\times\frac{1}{P_h^2+m_h^2}\times\langle b|\,P_3|a]\left(\frac{16P_3\cdot P_a+m_h^2}{m_h^2}\right)\\&=\frac{\kappa^2}{144(P_h^2+m_h^2)}\langle a|\,P_1|b]\,\langle b|\,P_3|a]\left(\frac{16P_1\cdot P_a+m_h^2}{m_h^2}\right)\left(\frac{16P_3\cdot P_a+m_h^2}{m_h^2}\right).\end{aligned}\qquad(6.1.13)$$

To find its massless limit, we again take $P_a\longrightarrow P_h$, $|b\rangle\longrightarrow m_h\,|\bar{b}\rangle$, and $|b]\longrightarrow m_h|\bar{b}]$ to find

$$\begin{aligned}A^{(1)}_{m_h\to 0}[1,2,3,4]&=\frac{\kappa^2m_h^2}{144(P_h^2+m_h^2)}\langle P_h|\,P_1|\bar{b}]\,\langle\bar{b}|\,P_3|P_h]\left(\frac{16P_1\cdot P_h+m_h^2}{m_h^2}\right)\left(\frac{16P_3\cdot P_h+m_h^2}{m_h^2}\right)\\&=\frac{49\kappa^2m_h^2}{144(P_h^2+m_h^2)}\langle P_h|\,P_1|\bar{b}]\,\langle\bar{b}|\,P_3|P_h]\ \overset{m_h\longrightarrow 0}{\longrightarrow}\ 0\,,\end{aligned}\qquad(6.1.14)$$

as anticipated.

Spin-2 Graviton Contribution

Finally, we evaluate the spin-2 part of the amplitude, given by

$$\begin{aligned} A^{(2)}[1,2,3,4] &= A^{-+}[1,2,3,4] + A^{+-}[1,2,3,4] \\ &= A[1,\hat{2},\hat{P}_h^{-2}]\frac{1}{P_h^2-m_h^2}A[-\hat{P}_h^{+2},\hat{3},4] + A[1,\hat{2},\hat{P}_h^{+2}]\frac{1}{P_h^2-m_h^2}A[-\hat{P}_h^{-2},\hat{3},4] \\ &= \left(\kappa\frac{\langle b|\,P_1|a]^2}{m_h^2}\right)\times\frac{1}{P_h^2-m_h^2}\times\left(\kappa\frac{\langle a|\,P_3|b]^2}{m_h^2}\right) + a\leftrightarrow b\,, \end{aligned} \tag{6.1.15}$$

where in the last line we have used the 3-point function calculated earlier. Following the same $m_h \longrightarrow 0$ procedure as in the spin zero case we find, with some algebra, that the amplitude ultimately reduces to

$$A^{(2)}[1,2,3,4] = \frac{\kappa^2}{t}\left(\frac{\mathrm{Tr}_+\left(P_1P_aP_3P_b\right)\mathrm{Tr}_-\left(P_1P_aP_3P_b\right)}{m_h^2} + \frac{\mathrm{Tr}_+\left(P_3P_aP_1P_b\right)\mathrm{Tr}_-\left(P_3P_aP_1P_b\right)}{m_h^2}\right), \tag{6.1.16}$$

where, for example, $\mathrm{Tr}_\pm\left(P_1P_aP_3P_b\right) = 2(P_1\cdot P_3)(P_a\cdot P_b) \pm 2i\epsilon_{\mu\nu\rho\sigma}P_1^\mu P_a^\nu P_3^\rho P_b^\sigma$. The antisymmetric piece can be evaluated by noting that $\epsilon_{\mu\nu\rho\sigma}P_1^\mu P_a^\nu P_3^\rho P_b^\sigma = \sqrt{\det(G)}$, where G is the *Gram matrix*, whose determinant

$$\det(G) = \begin{vmatrix} P_1^2 & P_1\cdot P_a & P_1\cdot P_3 & P_1\cdot P_b \\ P_1\cdot P_h & P_a^2 & P_a\cdot P_3 & P_a\cdot P_b \\ P_1\cdot P_3 & P_a\cdot P_3 & P_3^2 & P_3\cdot P_b \\ P_1\cdot P_b & P_a\cdot P_b & P_3\cdot P_b & P_b^2 \end{vmatrix} = \begin{vmatrix} m_\phi^2 & P_1\cdot P_a & P_1\cdot P_3 & 0 \\ P_1\cdot P_a & 0 & P_a\cdot P_3 & \frac{1}{2}m_h^2 \\ P_1\cdot P_3 & P_a\cdot P_3 & m_\phi^2 & 0 \\ 0 & \frac{1}{2}m_h^2 & 0 & 0 \end{vmatrix}$$

$$\begin{aligned} &= m_h^4(-m_\phi^4 + (P_1\cdot P_3)^2) \\ &= \frac{1}{4}m_h^4\left((s-2m_\phi^2)^2 - 4m_\phi^4\right). \end{aligned}$$

Substituting back into the trace gives

$$\mathrm{Tr}_\pm\left(P_1P_aP_3P_b\right) = 2m_h^2\left((P_1\cdot P_3) \pm \frac{i}{2}\sqrt{(s-2m_\phi^2)^2-4m_\phi^4}\right). \tag{6.1.17}$$

The second trace term is evaluated analogously and found to be the same, so that the final expression for the amplitude is

$$A^{(2)}[1,2,3,4] = 2\kappa^2\frac{(s+2m_\phi^2)^2-2m_\phi^4}{t} = \frac{1}{2}\tilde{\kappa}^2\frac{(s+2m_\phi^2)^2-2m_\phi^4}{t}. \tag{6.1.18}$$

Pulling this all together gives the full amplitude

$$A[1,2,3,4] = A^0[1,2,3,4] + A^{(1)}[1,2,3,4] + A^{(2)}[1,2,3,4]\,, \tag{6.1.19}$$

whose massless limit is

$$A_{m_h\to 0}[1,2,3,4] = A^0_{m_h\to 0}[1,2,3,4] + A^{(2)}_{m_h\to 0}[1,2,3,4] = \frac{\tilde{\kappa}^2}{2t}\left[(s+2m_\phi^2)^2 - 2m_\phi^4 - \frac{2}{3}m_\phi^4\right]. \tag{6.1.20}$$

The classical Newtonian potential (in fourier space) is recovered by first going to the center-of-mass frame where,

$$t = -\vec{q}^{\,2}, \qquad s + 2m_\phi^2 = 2m_\phi^2 + 4m_\phi^2\vec{p}^{\,2} + \cdots \tag{6.1.21}$$

If, in addition, we take $\tilde{\kappa}^2 = 32\pi G$, the amplitude becomes

$$A^{COM}_{m_h\to 0}[1,2,3,4] = \frac{16\pi G}{\vec{q}^{\,2}}\left[\frac{4}{3}m_\phi^4 + 16\vec{p}^{\,2}\,m_\phi^4 + \mathcal{O}(\vec{p}^{\,4})\right]. \tag{6.1.22}$$

To find the classical potential, we use the relation [55]

$$T^{COM}_{fi} = \frac{A^{COM}_{fi}}{4E^2}, \tag{6.1.23}$$

where, if we write $E = m_\phi + \frac{\vec{p}^{\,2}}{2m_\phi} + \cdots$ and take $m_\phi \gg \vec{p}^{\,2}$,

$$T^{COM}_{fi} = \frac{16\pi G m_\phi^2}{\vec{q}^{\,2}}\left[\frac{1}{3} + 4\vec{p}^{\,2} + \mathcal{O}(\vec{p}^{\,4}, m_\phi^2)\right]. \tag{6.1.24}$$

To first order, this is exactly $\frac{4}{3}$ the classical Newtonian potential (in momentum space):

$$T^{COM}_{fi}(0) = \frac{4}{3}\left(\frac{4\pi G m_\phi^2}{\vec{q}^{\,2}}\right). \tag{6.1.25}$$

Then, by the standard arguments, these expressions can be reconciled by rescaling the coupling $G \longrightarrow \frac{3}{4}G$. Of course, this comes with the cost that the light bending angle derived from (6.1.6) will now be 3/4 of that predicted by general relativity, manifesting the vDVZ discontinuity.

VII

Conclusion to Part I

In this part of the thesis, we have explored various gravitational phenomena using the modern framework of scattering amplitudes. We have demonstrated that scattering amplitudes provide a valuable tool to extract observable data from (quantum) field theories and, in this thesis, we considered theories of gravity.

Considering gravity as a theory of massless spin-2 particles (gravitons), we showed that, using only the on-shell physical data, it is possible to determine the deflection angle of a light or gravitational wave as it passes a massive object, at least in the small angle approximation. Additionally, using only our knowledge of the Poincaré group, dimensional analysis and Newtonian gravity, we also showed that, should you consider the graviton to have a non-vanishing mass, the Newtonian potential between two scalars is modified in such a way that the massless limit only agrees if one scales the graviton coupling. This results in the deflection angle of a light being noticeably different from the experimentally observed value: the so-called vDVZ discontinuity.

There are many interesting future directions that seem natural to consider as a follow on from this work. Throughout this thesis, we have only worked to linear order in $h_{\mu\nu}$, however it is certainly of importance to understand higher order amplitudes and their role in the Veinshtein mechanism. Since Veinshtein screening is just one in a class of such screening mechanisms, we expect that this could well shed some much needed light on a broad class of interesting problems. Additionally, it would be interesting to consider discontinuities in the supersymmetric counterpart of the massive graviton, the massive gravitino. Such a discontinuity was discovered at the turn of the century by Deser and Waldron [56] and, since higher spin particle scattering is treated in much the same way as for scalars, vectors and gravitons, is likely that this problem may also be treated via a direct construction of the amplitudes.

We have also worked exclusively in flat space, although there is some recent progress to generalising spinor helicity techniques to curved spacetimes [57–60]. Should such techniques reach maturity, an on-shell analysis of vanishing-mass discontinuities may provide valuable insight into the contraversy surrounding whether or not the vDVZ discontinuity persists in Einstein spaces which satisfy $R_{\mu\nu} = \Lambda g_{\mu\nu}$ with non-vanshing cosmological constant Λ and $m_h^2/\Lambda \longrightarrow 0$ (see, for example, [61, 62] and references therin).

Part II

Entanglement Entropy & Complexity

VIII

Introduction to Part II

> *"I want to stand as close to the edge as I can without going over. Out on the edge you see all kinds of things you can't see from the center."*
>
> – Kurt Vonnegut, *Player Piano*

We now switch gears entirely, shifting our focus to the subtleties of entanglement entropy & circuit complexity in quantum field theories. Entanglement is the distinguishing feature of quantum mechanics and, 80 years after its discovery, still probably the most mysterious concept in nature. It was famously dubbed by Einstein as *spukhafte Fernwirkung* ("spooky action at a distance") following the Einstein-Podolsky-Rosen gedanken experiments [63] and, disturbingly, has no classical analogue around which to base our intuition. Despite being a formidable concept to wrestle with, we now know a great deal more about entanglement [64], such that it now is regarded as a fundamental resource in quantum information theory, being the basis of quantum computing and quantum cryptography [65].

Classical systems share information only locally, whereas entanglement between systems means that those systems share information *non-locally* and performing a measurement on one system means extracting information about the other *instantaneously*, even if the other system is spatially separated and causally disconnected. Exactly how much information you will extract is given by the entanglement entropy, a quantity that has uses far beyond what might be expected.

In the realm of quantum field theory, we define subsystems by considering distinct spatial regions and probing the amount of entanglement that exists between them [66–68]. Much of this has been motivated by the surprising result that a black hole's entropy is proportional to its horizon area and not its volume [69], prompting the suggestion that the black hole entropy can be identified with (or is at least deeply related to) the entanglement entropy [70, 71]. This seems reasonable due to the fact that a black hole is a physical system with a natural casually disconnected subsystem and entangling surface.

Recently, a wave of new activity has been initiated by the introduction of holographic entanglement entropy, which, in the context of AdS/CFT, allows one to calculate the entanglement entropy by minimising a surface in the dual

AdS space [72, 73]. This has important implications for the nature of spacetime and quantum gravity, suggesting that spacetime/gravity may emerge from the underlying quantum entanglement structure [74–77].

A black hole is one of the simplest conceptual laboratories we know of in which emergent spacetime is realised, and understanding exactly how this happens in an important step towards understanding how spacetime emerges in general. Motivated by this, in the context of the ER = EPR conjecture [78], it was suggested that entanglement entropy was not enough to capture all aspects of the growth of a black hole interior [79]. This was due to the observation that the entanglement entropy saturates as a black hole thermalizes [80], whereas the wormhole connecting two eternal AdS black holes increases long after thermalization. In the spirit of the AdS/CFT conjecture, it was suggested that the dual quantity to the black hole interior was the *computational complexity* [79, 81, 82], an observable in the quantum field theory that could, according to the conjecture, probe physics behind the black hole horizon.

This lead to two interesting proposals for holographic interpretations of this quantity [81, 83, 84]. The first, dubbed *complexity equals volume* (the CV conjecture), is that the holographic dual to complexity is the volume of a maximal co-dimension-one bulk spacelike surface that emerges from the boundary of AdS. The second, *complexity equals action* (the CA conjecture), posits that the complexity is dual to the bulk action evaluated on the Wheeler-DeWitt (WDW) patch. Both of these bulk quantities probe physics behind the horizon and grow with time after the system has thermalized, and yet the boundary counterpart – the computational complexity in a (conformal) quantum field theory – is not as well defined, with an agreed definition still a work in progress [65, 79, 81–107]. If the idea of complexity and black holes is to be fully grasped, it is essential that we understand complexity in the context of general quantum field theories, which is largely what this part of the thesis aims to explore.

IX

Entanglement Entropy & Complexity Review

"People get a lot of confusion, because they keep trying to think of quantum mechanics as classical mechanics"

– Sidney Coleman, *Quantum Mechanics in Your Face*

In this chapter, we review the basics of entanglement & complexity in quantum field theories. For entanglement entropy in quantum field theory, there are many good reviews available [68, 108–113] and we refer the interested reader there for a more detailed treatment. For complexity in quantum field theories, there are no reviews at the time of writing and to the best of the authors knowledge. For more details, we refer the interested reader to [65, 85–91].

9.1 Entanglement Entropy in Quantum Mechanics

9.1.1 Quantum States & Bi-partite Entanglment

A quantum mechanical system is described by a state vector $|\psi\rangle$ that is an element of a Hilbert space $\mathcal{H}$ [114]. If the system is a composite of smaller systems, then we can imagine considering only a specific subsystem A, whose compliment is then $\bar{A}$.

We can then decompose the systems Hilbert space into a product space, made up of the Hilbert spaces of the subsystems[1]

$$\mathcal{H} = \mathcal{H}_A \otimes \mathcal{H}_{\bar{A}}. \tag{9.1.1}$$

Let's imagine that our *total* system is in some state $|\Psi\rangle \in \mathcal{H}$. Given this specific state, what can we hope to know about the state of the subsystem A?

[1] It is not always the case that we can decompose the Hilbert space in this way in quantum field theories, especially in gauge theories, however we will assume for now that we can.

Product State	Entangled State	Mixed State
$\|\Psi\rangle_{AB} = \|\psi\rangle_A \otimes \|\phi\rangle_B$	$\|\Psi\rangle_{AB} \neq \|\psi\rangle_A \otimes \|\phi\rangle_B$	$\|\Psi\rangle = \sum_i p_i \|\psi_i\rangle$

Before we begin answering this question, it's useful to note a few definitions.

A **pure state** is one in a *definite* quantum state (with probability one), meaning we know *exactly* the state of our system.

A **product state** or **separable state** is one that can be written as a tensor product of pure states, and an **entangled state** is a state that can not.

A **mixed state** is any state that is *not* a pure state, it could be for example a sum of states with associated probabilities.

In general, a system could be in any one of an ensemble of orthogonal states $|\psi_i\rangle$, each one associated with a probability p_i, the probability of measuring that particular state. If we measure the system over and over again using some operator $\mathcal{O}$, we will find that the system is in some average state. We call this the **expectation value** of the operator $\mathcal{O}$, and it is defined as

$$\langle \mathcal{O} \rangle \equiv \sum_i p_i \langle \psi_i | \mathcal{O} | \psi_i \rangle \,. \tag{9.1.2}$$

We can write this expression in a new basis by using the projection operator $\sum_i |i\rangle \langle i| = 1$, to find

$$\begin{aligned}
\langle \mathcal{O} \rangle &= \sum_i p_i \langle \psi_i | \mathcal{O} | \psi_i \rangle && (9.1.3)\\
&= \sum_i p_i \sum_{k,l} \langle \psi_i | k \rangle \langle k | \mathcal{O} | l \rangle \langle l | \psi_i \rangle && (9.1.4)\\
&= \sum_{k,l} \langle k | \mathcal{O} | l \rangle \langle l | \left(\sum_i p_i |\psi_i\rangle \langle \psi_i | \right) | k \rangle && (9.1.5)\\
&= \sum_k \langle k | \mathcal{O} \left(\sum_i p_i |\psi_i\rangle \langle \psi_i | \right) | k \rangle && (9.1.6)\\
&= \mathrm{Tr}\left(\mathcal{O}\rho\right), && (9.1.7)
\end{aligned}$$

where we now define the operator in brackets as the **density matrix operator**

$$\rho = \sum_i p_i |\psi_i\rangle \langle \psi_i | \,. \tag{9.1.8}$$

If you wanted to calculate the probability of finding your system in a specific state $|\phi\rangle$, then you act with the **projection operator** $P_\phi = |\phi\rangle \langle \phi|$. Then, the probability associated to finding the system in this state is simply $p_\phi = \mathrm{Tr}\left(P_\phi \rho\right)$.

The density operator has the following properties:

1. $\mathrm{Tr}\,(\rho) = 1$
2. $\rho^\dagger = \rho$
3. ρ describes *classical* uncertainty
4. ρ is *not* always diagonal, but may be in some basis.
5. If a state is pure, its density matrix is $\rho = |\psi\rangle\langle\psi|$, and $\rho^2 = \rho$. Such a density matrix *defines* a pure state.

The **entropy** of a density matrix $S(\rho)$ tells you exactly how *mixed* your system is, or alternatively, how **disordered**.

Since this ought to be an intrinsic property of the system, we demand that this measure be *basis independent*, i.e. $S(U^\dagger \rho U) = S(\rho)$, and $S(\rho) = 0$ for a pure state. We also require that $S(\rho_{AB}) = S(\rho_A) + S(\rho_B)$, since we can always create a density matrix describing two decoupled systems via a tensor product.

A definition that fits the bill is the **von-Neumann entropy**

$$S(\rho) \equiv -\mathrm{Tr}\,(\rho \log \rho)\,, \tag{9.1.9}$$

which in classical physics is simply $S(\rho) \equiv -\sum_i p_i \log p_i$.

If you have entanglement between two elements of a composite system, you need to be able to talk about the degrees of freedom of the individual subsystems separately: you need a density matrix for each subsystem.

Knowing the full density matrix (or full system state, alternatively), you can simply throw away the degrees of freedom you are not interested in by doing a **partial trace**, defined as taking a trace of your full density matrix, but only over the Hilbert space you wish to ignore. This is usually known as the **reduced density matrix**, and is defined as

$$\rho_A \equiv \sum_i \langle i|_B \left(|\psi_{AB}\rangle\langle\psi_{AB}|\right)|i\rangle_B = \mathrm{Tr}_B\left(\rho_{AB}\right). \tag{9.1.10}$$

For entangled systems, the von-Neumann entropy becomes the **entanglement entropy**, and is a measure of how entangled two subsystems are[2]. Alternatively, we can relate this to the information entangled between two subsystems: Entanglement entropy counts the number of entangled bits between A and B.

[2]Note however that the von Neumann entropy can also capture *classical* correlation and doesn't only measure entanglement. If the two systems are separated causally, i.e. by a Horizon, then it does only measure the entanglement.

Thermal states and Unitarity

Lets consider a system in a generic mixed state

$$\rho = \sum_i p_i \left|\psi_i\right\rangle \left\langle\psi_i\right| . \tag{9.1.11}$$

Given enough time, such a system will always reach thermal equilibrium with it's surroundings, at which point the general mixed state becomes a **thermal state**, meaning the individual probabilities p_i are now proportional to the Boltzmann factor

$$p_i \propto e^{-\beta E_i}. \tag{9.1.12}$$

This happens by mutual particle exchange between the system and the environment, maximising the thermodynamic entropy as it does so.

A pure state $\left|\psi(t)\right\rangle_{pure}$ that only undergoes unitary time evolution $e^{-iHt}\left|\psi(0)\right\rangle_{pure}$ will never reach a thermal state, however. This is because the Hamiltonian maps pure states to pure states and interactions with another external system are required to produce mixed states. This can easily be seen via the cyclic nature of the trace and pure states.

9.1.2 Rényi Entropy

Having defined the entanglement entropy, we can now look at other interesting measures of entropy. The first is a simple generalisation of the entanglement known as **Rényi entropy** [115], defined as

$$S_n(\rho) = \frac{1}{1-n} \ln\left(\sum_{i=1}^{N} p_i^n\right) = \frac{1}{1-n} \ln\left(\mathrm{Tr}\left(\rho^n\right)\right). \tag{9.1.13}$$

Importantly, we can recover the usual definition of entanglement entropy by taking the limit $n \longrightarrow 1$

$$S(\rho) = \lim_{n \longrightarrow 1} S_n(\rho). \tag{9.1.14}$$

This quantity is particularly useful because it doesn't contain a logarithm of a matrix and is often easier to calculate than the entanglement entropy. Indeed, we shall see some explicit cases where computing the Rényi entropy is most convenient. For now though, lets focus on its physical interpretation by considering a thermal system with some notion of Boltzmann entropy.

For a system in a thermal state with initial temperature $T_0 = 1/\beta_0$, we know that the density matrix looks like

$$\rho_0 = \frac{e^{-H\beta_0}}{Z_0}, \tag{9.1.15}$$

with $Z_0 = \mathrm{Tr}\left(e^{-H\beta_0}\right)$. If we now plug this into the Renyí entropy formula, we find that

$$S_n = \frac{1}{1-n} \ln\left(\mathrm{Tr}\left(e^{-nH\beta_0}\right)\right). \tag{9.1.16}$$

Recalling the definition of the free energy $F(T) = -T \ln Z(T)$, we can identify n as the being the amount the system drops in temperature, to a new temp $T = T_0/n$ [116, 117]. We then find

$$S_{T_0/T} = \frac{1}{1-T_0/T} \ln \frac{\mathrm{Tr}\left(e^{-H\beta}\right)}{Z_0^{T_0/T}} \tag{9.1.17}$$

$$= \frac{1}{1-T_0/T} \ln \frac{Z(T)}{Z_0^{T_0/T}} \tag{9.1.18}$$

$$= -\frac{F(T) - F(T_0)}{T - T_0}. \tag{9.1.19}$$

Physically then, we interpret the Rényi entropy at n as being the work done by the system as it goes into thermal equilibrium at a temperature $T = T_0/n$ (from a temperature T_0), divided by the change in temperature. In this way, we can also directly relate the Boltzmann entropy with the Rényi entropy, considering that the Boltzmann entropy is $S_{Boltzmann} = -\frac{\partial F}{\partial T}$. Thus, we find that the Rényi entropy of a thermal system is

$$S_n = \frac{n}{n-1} \frac{1}{T_0} \int_T^{T_0} S_{th}(T')dT'. \tag{9.1.20}$$

9.1.3 2 State Example

Let's imagine the most simple situation we can: a pair of particles A and B with spin created at the same time from some event, i.e. pair creation. Since the pair was created together, and supposing that the total spin of the system before hand was zero, we know that the angular momentum must be preserved and therefore that each particle must have the opposite spin. We will also take the pair to be separated by a vast distance, meaning there can not be any classical communication between them during the time of the experiment. Most importantly, this means we are excluding *classical* correlations between the two particles.

We also know that until we measure them, each particle does not yet have definite spin, and therefore the total system is in a state

$$|\Psi\rangle_{AB} = \frac{1}{\sqrt{2}} \left(|\uparrow\rangle_A |\downarrow\rangle_B + |\downarrow\rangle_A |\uparrow\rangle_B\right) = \frac{1}{\sqrt{2}} \left(|\uparrow\downarrow\rangle + |\downarrow\uparrow\rangle\right). \tag{9.1.21}$$

We observe that there must be some entanglement, since we can *not* write this state as a product state.

The total information available to subsystem A is encapsulated in the density matrix ρ_A, and similarly for B. The total system has density matrix ρ_{AB}, and we define the subsystem density matrix as being the total system matrix with the additional subsystem traced out:

$$\rho_A = \mathrm{Tr}_B\left(\rho_{AB}\right) \tag{9.1.22}$$

$$= \sum_i \langle i|_B \left(|\psi_{AB}\rangle \langle\psi_{AB}|\right) |i\rangle_B \tag{9.1.23}$$

$$= \frac{1}{2}\left[\langle\uparrow|_B \left(|\uparrow\downarrow\rangle + |\downarrow\uparrow\rangle\right)\left(\langle\uparrow\downarrow| + \langle\downarrow\uparrow|\right)|\uparrow\rangle_B + \langle\downarrow|_B \left(|\uparrow\downarrow\rangle + |\downarrow\uparrow\rangle\right)\left(\langle\uparrow\downarrow| + \langle\downarrow\uparrow|\right)|\downarrow\rangle_B\right] \tag{9.1.24}$$

$$= \frac{1}{2}\left[|\downarrow\rangle\langle\downarrow| + |\uparrow\rangle\langle\uparrow|\right] \tag{9.1.25}$$

$$= \frac{1}{2} I_{2\times 2}. \tag{9.1.26}$$

We see then that the density matrix for our subsystem is proportional to the identity, which we say is **maximally mixed** and thus the subsystem is **maximally entangled**[3]. We can also compute the entanglement entropy

$$S(\rho_A) = -\mathrm{Tr}\left(\rho_A \log \rho_A\right) = -\mathrm{Tr}\left(\frac{1}{2}\log\frac{1}{2}\right) = \mathrm{Tr}\left(\frac{1}{2}\log 2\right) = \log 2. \tag{9.1.27}$$

For a system made up of such states (known as qubit states), we see then that *maximal* entanglement would be $S_A = n \log 2$, where n is the number of qubits in each subsystem. To find the number of entangled states, we use the formula

$$N_A = e^{S_A}. \tag{9.1.28}$$

Finally, it is useful to note that when we split a system up into two components, then the entanglement entropy of one component is equal to the entanglement entropy of the other, provided that the full system is in a pure state

$$S(\rho_A) = S(\rho_{\bar{A}}), \qquad \forall \rho = |\psi\rangle\langle\psi|\,. \tag{9.1.29}$$

9.1.4 Properties of Entanglement Entropy

Entanglement entropy enjoys a number of well known properties, which we will simply state without proof for brevity. Consider a system in a generic mixed

[3]Maximally mixed states are *not* in general maximally entangled. However if one finds that the subsystem density matrix of a pure state is maximally mixed, then it is also maximally entangled.

state ρ_{AB}, with entropy $S(\rho_{AB})$. Then, one finds that the Araki-Leib inequality holds [118]

$$|S(\rho_A) - S(\rho_B)| \leq S(\rho_{AB}). \tag{9.1.30}$$

This tells us that mixed state entropy of A differs from that of B. We also find an inequality

$$S(\rho_{AB}) \leq S(\rho_A) + S(\rho_B), \tag{9.1.31}$$

which tells us that entropy is *sub-additive*.

If we consider a system made up of three subsystems A,B,C, then we find a stronger version of this, known as **strong sub-additivity** [65, 119–121]

$$S(\rho_{AB}) + S(\rho_{BC}) \geq S(\rho_B) + S(\rho_{ABC}) \tag{9.1.32}$$
$$S(\rho_{AB}) + S(\rho_{BC}) \geq S(\rho_A) + S(\rho_C), \tag{9.1.33}$$

which in turn allows us to again define the concept of mutual information

$$I(A, B) = S(\rho_A) + S(\rho_B) - S(\rho_{AB}) \geq 0. \tag{9.1.34}$$

Roughly speaking, this quantity tells you how much information system A has about system B and vice versa, since $I(A, B) = I(B, A)$.

9.1.5 Relative & Average Entropy

One additional quantitiy which is often useful is the **relative entropy** [122, 123] of a system ρ with respect to a system σ (σ must describe states in the same Hilbert space), defined as

$$S(\rho|\sigma) \equiv \sum_k \rho_k \log \frac{\rho_k}{\sigma_k} = \mathrm{Tr}\,(\rho \log \rho - \rho \log \sigma) \geq 0. \tag{9.1.35}$$

This quantity is always non-zero for $\rho \neq \sigma$ and is zero *only* when the two systems have the same density matrices. For the relative entropy of a subregion A that is part of the full system C, the following holds

$$S(\rho_A|\sigma_A) \leq S(\rho_C|\sigma_C), \qquad A \subset C. \tag{9.1.36}$$

You should note that the relative entropy is *not* symmetric under $\rho \longleftrightarrow \sigma$. The relative entropy of systems ρ with respect to a *thermal* system σ is also an especially interesting quantity. A system is thermal when its density matrix is

$$\sigma \propto e^{-\beta H}. \tag{9.1.37}$$

Then, the relative entropy is simply

$$S(\rho|\sigma) = \mathrm{Tr}\left(\rho\log\rho - \rho\log\sigma\right) \tag{9.1.38}$$
$$= -S(\rho) + \beta\left\langle H\right\rangle. \tag{9.1.39}$$

This is related to the **first law of entanglement**

$$\delta S = \delta\left\langle H\right\rangle. \tag{9.1.40}$$

We will derive this by considering a variation of ρ at first order, to see what happens to a system upon variation of the entanglement entropy

$$\delta S(\rho) = -\delta Tr(\rho\log\rho) \tag{9.1.41}$$
$$= -Tr(\delta\rho\log\rho) - Tr(\rho\delta\log\rho) \tag{9.1.42}$$
$$= -Tr(\delta\rho\log\rho) - Tr(\delta\rho). \tag{9.1.43}$$

Motivated by the thermal system, we define our *unperturbed* density matrix in terms of a new object: the **entanglement Hamiltonian**[4]

$$H = -\log\rho \qquad \Longleftrightarrow \qquad \rho = \frac{e^{-H}}{\mathrm{Tr}\left(e^{-H}\right)}. \tag{9.1.44}$$

This is *not* the Hamiltonian of our system, but rather an *effective* hamiltonian that is defined as the log of the *unperturbed* density matrix. We can *formally* evolve states via a unitary transformation

$$U(w) \simeq e^{-iHw} \simeq \rho_A^{iw}. \tag{9.1.45}$$

In practice, the entanglement Hamiltonian is not easy to define. For some systems (such as Rindler space, or a free fermion, as we will see later) the entanglement Hamiltonian can be defined explicitly, however often it is highly non-local and difficult to work with.

Having defined the entanglement Hamiltonian, our variation becomes

$$\delta S(\rho) = -Tr(\delta\rho\log\rho) - Tr(\delta\rho) \tag{9.1.46}$$
$$= -Tr(\delta\rho\log\rho) \tag{9.1.47}$$
$$= Tr(\delta\rho H) \tag{9.1.48}$$
$$= \delta\left\langle H\right\rangle. \tag{9.1.49}$$

Taking ρ to be a thermal state, we see that this reduces exactly to the first law of thermodynamics

$$\rho = \frac{1}{Z}e^{-\beta H}. \tag{9.1.50}$$

Thus, $\delta S = \beta\left\langle H\right\rangle$, or in other words, $dE = TdS$.

[4]This is often also called the modular Hamiltonian since it generates modular flow, however we will simply call it the entanglement Hamiltonian.

Average Entropy

Having defined the relative entropy, we now also define the notion of **average entropy**. Lets imagine a system with Hilbert space of dimension mn to be in some pure state. The average entropy of a subsystem of dimension $m \leq n$ is given by [124]

$$S_{m,n} = \sum_{k=n+1}^{mn} \frac{1}{k} - \frac{m-1}{2n}. \tag{9.1.51}$$

In the situation where we have $1 \ll m \leq n$, we find that the average entropy is

$$S_{m,n} \simeq \ln m - \frac{m}{2n}. \tag{9.1.52}$$

Given this, and the fact that the maximum entropy of the subsystem is $S_{m,max} = \ln m$, we can define the **average information**

$$I_{m,n} = S_{m,max} - S_{m,n} \simeq \frac{m}{2n}. \tag{9.1.53}$$

9.1.6 Purifications

Given a mixed state density matrix ρ, we can always find a larger pure state that contains this mixed state, a process called **purification**.

For an ensemble $\{|\psi_i^A\rangle, p_i\}$, part of a Hilbert space $\mathcal{H}_A$, we can generate a pure state by inputting an additional Hilbert space $\mathcal{H}_B$, provided $\dim(\mathcal{H}_A) = \dim(\mathcal{H}_B)$. Assuming this is satisfied, we can perform a **schmidt decomposition**, which essentially allows us to express a vector as the inner product of two other vectors, defined as

$$|\Psi\rangle = \sum_i \lambda_i |\psi_i\rangle \otimes |\phi_i\rangle \in \mathcal{H}_A \otimes \mathcal{H}_B, \tag{9.1.54}$$

where $\lambda_i \in \mathbb{R}^+$ are known as the *Schmidt coefficients* with[5] $\sum_i \lambda_i^2 = 1$. The states $\{|\psi_i\rangle\}$ and $\{|\phi_i\rangle\}$ are both orthonormal states in $\mathcal{H}_A$ and $\mathcal{H}_B$ respectively.

The Schmidt coefficients essentially classify each state, with $\lambda_1 = 1, \lambda_i = 0, \quad \forall \ i > 1$ being a product state and all other states being entangled. The states are maximally entangled if all the coefficients are equal.

If we consider a thermal state (i.e. a system in the canonical ensemble), we assume that the system is in contact with a heat bath. The *full* system including heat bath is described by a pure state, which we could obtain via a purification. However,

[5] To see this, consider that the density matrix in the Schmidt basis means that the probability of a state $|\phi_a\rangle$ being measured is $p_a = \langle\phi_a|\lambda\lambda^\dagger|\phi_a\rangle$, thus $\lambda^2 = probability$.

since we know that the heat bath must have the same entanglement entropy as the system we want to consider, we may as well just make the heat bath a copy of the system, i.e. choose our purification system to be the thermal system. This means that our state will be:

$$|\Psi\rangle = \frac{1}{Z}\sum_i e^{-\beta E_i/2}\,|E_i\rangle \otimes |E_i\rangle\,. \tag{9.1.55}$$

This state is known as the **thermofield double** state, and is important in the study of black holes and conformal field theories, especially in the context of AdS/CFT.

9.2 Entanglement Entropy in Quantum Field Theory

So far, we have discussed entanglement in quantum mechanics, where the Hilbert space of a given system is finite dimensional. In QFT, the Hilbert (or, Fock more precisely) space is necessarily infinite dimensional[6], meaning we can't use the same ideas as easily (we can't localise states/particles in QFT). Our first instinct might be to put this on a lattice, and indeed this will be our starting points, introducing a short distance scale ϵ, such that i.e. 2-point correlators go like $\frac{1}{|\epsilon|^{d-2}}$ for short distances. This allows us to remove any UV states from the Hilbert space (since this would require a shorter distance), meaning we can define a finite-dimensional Hilbert space.

9.2.1 Density Operators as Path Integrals

In order to use the definitions of entanglement entropy, mutual information etc introduced in the last section, we need to recall some connections between quantum mechanics and quantum field theory.

The transition amplitude between two field configurations ϕ_i and ϕ_j is given by the **path integral**

$$\langle\phi_j(t_1)|e^{-iHt}|\phi_i(t_0)\rangle = \mathcal{N}\int_{\phi(t_0)=\phi_i}^{\phi(t_1)=\phi_j}\mathcal{D}\phi\; e^{-iS[\phi]}, \tag{9.2.1}$$

where a time dependent state is given by $|\Psi\rangle = |\phi(t)\rangle = e^{iHt}\,|\phi(0)\rangle$.

[6] An explination for this is that we must demand that $\mathrm{Tr}\,([x,p]) = 0$ for any finite dimensional operators x and p, since in finite dimensions they are trace-class operators and the trace of their commutator must vanish. This is not realisible while respecting $[x,p] = i*\infty$, thus we reason that the Hilbert space must have infinite dimension.

We can write[7] the density matrix as $\rho(\tau) = e^{-H\tau}$, where τ is a parameter with the dimension of (imaginary) time. Elements of the density matrix are given by

$$\rho(\phi_i, \phi_j, \tau) = \langle \phi_i | e^{-H\tau} | \phi_j \rangle \,. \tag{9.2.2}$$

We can split the density matrix up into small Euclidean time-intervals ϵ, meaning we can use it to define a path integral, in complete analogy with the usual procedure in QFT[8], however now in Euclidean time τ. Alternatively, we can recognise that eq. 9.2.2 and eq. 9.2.1 are simply related by a Wick rotation $t \longrightarrow -i\tau$, meaning we can write the density matrix as a Euclidean path integral

$$\rho(|\phi_i\rangle, \langle \phi_j|) = \mathcal{N} \int_{\phi(0)=\phi_i}^{\phi(\beta)=\phi_j} \mathcal{D}\phi \; e^{-S_E[\phi]}. \tag{9.2.3}$$

For a (1+1)-d theory defined on a circle (i.e. on a line with $\phi(a) = \phi(a + 2\pi)$), then we can visualise the *thermal* density matrix path integral as a cylinder, where the end points represent the circular field configurations we are integrating between. If we define the field configurations as being the same (i.e. a vacuum to vacuum amplitude), then this naturally becomes a path integral over a torus.

For completeness, we also note that we can, by the convolution property, always write the density matrix (and hence path integral) as

$$\rho(|\phi_i\rangle, \langle \phi_j|) = \int d\phi_{n_1} \cdots d\phi_{n_N} \rho(|\phi_i\rangle, \langle \phi_{n_1}|) \rho(|\phi_{n_2}\rangle, \langle \phi_{n_3}|) \cdots \rho(|\phi_{n_N}\rangle, \langle \phi_j|). \tag{9.2.4}$$

9.2.2 The Replica Trick

Computing the entanglement entropy can often be a difficult task, and it is often far easier to compute the Renyí entropy instead, which we recall is defined as

$$S_n = -\frac{1}{n-1} \log \mathrm{Tr}\,(\rho^n) \,. \tag{9.2.5}$$

Having defined ρ in terms of path integrals, we might wonder what this quantity is in a field theory. First, we construct $\mathrm{Tr}\,(\rho^n)$, which is given by

$$\mathrm{Tr}\,(\rho^n) = \int [\mathcal{D}\phi_1 \mathcal{D}\phi_2 \cdots \mathcal{D}\phi_n]_{\overline{A}} \;\; \rho[\phi_1, \phi_2] \rho[\phi_2, \phi_3] \cdots \rho[\phi_{n-1}, \phi_n], \tag{9.2.6}$$

[7] This follows from the fact that the density matrix satisfies $\frac{d\rho}{d\tau} = -H\rho(\tau)$ for imaginary time evolution $t \longrightarrow -i\tau$.

[8] For a full derivation, see i.e. [125, 126]

where it is understood that we are tracing out the degrees of freedom in $\overline{A}$ and 'gluing' the degrees of freedom in A by a convolution. Let's make this more precise by considering the ground state of a 2D Euclidean QFT, which means evaluating our path integral for infinite time in one direction[9] $t = -\infty$ to $t = 0$, with boundary condition $\phi(x, 0) = \phi_1$. For a field $\phi(x, t)$, this looks like

$$\Phi_0 = N \int_{\phi(x,-\infty)}^{\phi(x,0)=\phi_1(x)} \mathcal{D}\phi \; e^{-S_E[\phi]}, \qquad \Phi_0^* = N^* \int_{\phi(x,0)}^{\phi(x,\infty)=\phi_2(x)} \mathcal{D}\phi \; e^{-S_E[\phi]}. \tag{9.2.7}$$

The states ϕ_1 and ϕ_2 are states *now*, that is at the time slice $\tau = 0$. Each 'now' state was arrived at differently however: the state ϕ_1 was arrived at from $-\infty$, while the conjugate state ϕ_2 from $+\infty$. Geometrically, we can imagine that the ground state is the lower-half plane, with ϕ_1 existing on the line $\tau = 0$, while the conjugate ground state is the upper half plane, as in figure 9.1.

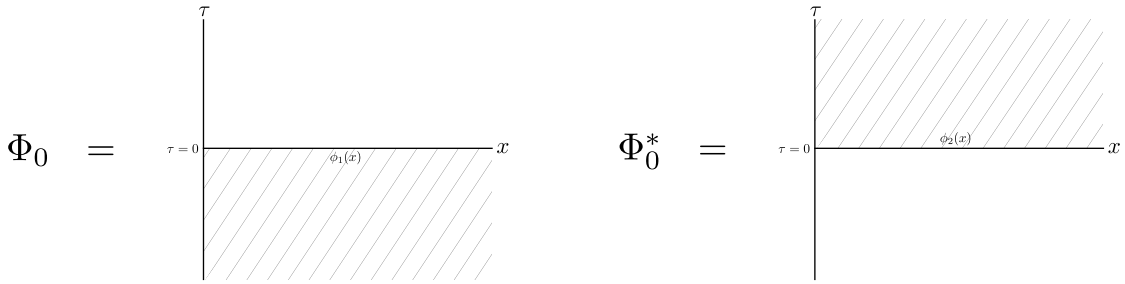

Figure 9.1: The geometric representation of the ground state wave function, and its conjugate.

From our definition of the density matrix, we can sew one of these together with it's complex conjugate to get the *vacuum* density matrix

$$\rho_0 = |0\rangle \langle 0| = \Phi_0^*(\phi_1)\Phi_0(\phi_2). \tag{9.2.8}$$

We have necessarily sewn together one state with it's entire history taken to infinity and its complex conjugate - with its entire future projected.

In order to calculate the entanglement entropy, we need the *reduced* density matrix, which - geometrically - means we need to consider the spatial region $A \in x$ by tracing out the compliment $\bar{A}$, by sewing together all the points $x \in \bar{A}$. This is

[9] To see why, consider a state evolving in time $|\psi\rangle = e^{-H\tau} |0\rangle$ - as $\tau \longrightarrow \infty$, the leading piece in an expansion around τ large is $\sim e^{-\tau E_0}$, therefore selecting the ground state.

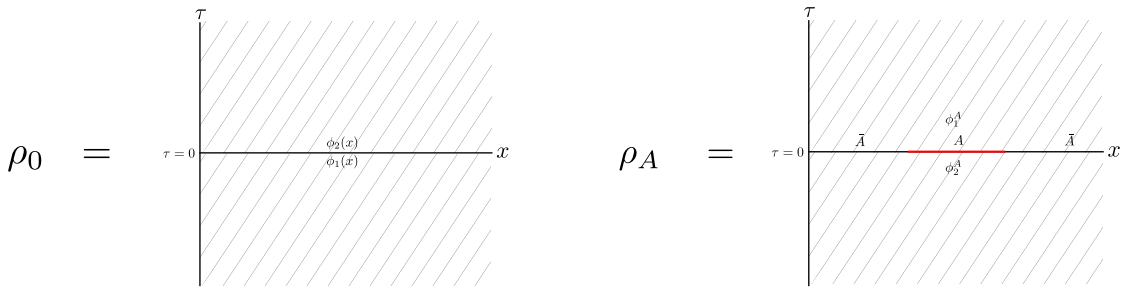

Figure 9.2: The geometric representation of the ground state density matrix: the full plane with a branch cut at $\tau = 0$, and the plane with a section of the $\tau = 0$ line reduced to the a small segment A.

pictured in figure 9.2, and our reduced density matrix now looks like this[10]

$$\rho_A[\phi_1, \phi_2] = \int_{\phi(x,0^-)=\phi_2^A}^{\phi(x,0^+)=\phi_1^A} \mathcal{D}\phi \; e^{-S_E[\phi]}, \tag{9.2.9}$$

where the $0^{\pm}$ are there to remind us that we are approaching zero from $\pm\infty$ (from above or below) respectively.

We see now exactly what eq. 9.2.6 does: it glues together each density matrix along the entanglement cut Σ (by a convolution), dictated by A. For example, taking $n = 2$ gives

$$\rho_A^2 = \int \mathcal{D}\phi \rho_A^{(1)}[\phi_1, \phi'] \rho_A^{(2)}[\phi', \phi_2] \equiv Z_2(A). \tag{9.2.10}$$

This corresponds to identifying the different sides of the cuts along $\tau = 0$ in density matrix (1) with the sides of cuts in (2), geometrically visualised in fig. 9.3.

We can obviously repeat this procedure n times, identifying the bottom of each cut with the top of the cut in the next plane. This method of cloning the system earns it the title of replica trick [68, 108, 127]. Conveniently, this creates the **replicated manifold** $\mathcal{R}_n$, an n-sheeted Riemann surface. Evaluating the free path integral on this manifold is equivalent to computing ρ^n, where it should be pointed out that at the boundaries of the entangling region ∂A is typically singular. For example, the interval we are considering contains two conical singularities at ∂A, meaning any path that 'turns' around these will pick up a phase (winding number). This will be important for what follows.

[10] Another way to think of this reduced path integral is to consider the integrand as being multiplied by a product of delta functions that localise the fields to those configurations which lie within A, i.e. $\prod_{x \in A} \delta(\phi(x) - \phi_2)\delta(\phi(x) - \phi_1)$.

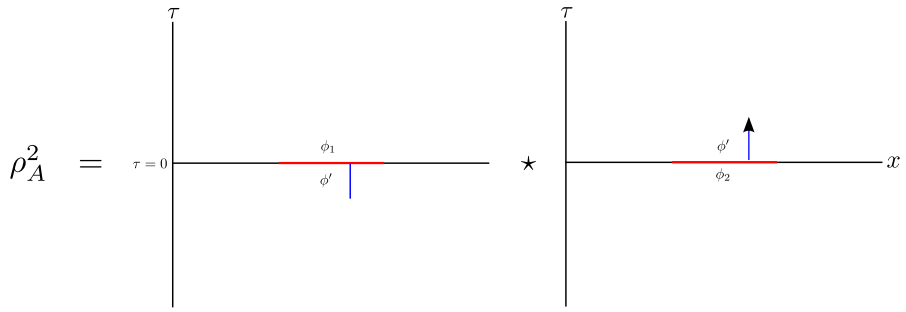

Figure 9.3: The identification of cuts in ρ_A^2

In practice, what you may wish to do is to map the action of the theory to the new manifold, being careful to keep track of how the operators of the action transform under said mapping. You can then evaluate the path integral there (often perturbatively) and from it calculate the log and related Rényi entropy.

Since the entanglement entropy requires you to take a limit in n, in practice we will need to analytically continue the expression S_n to make sure that we can take this limit smoothly, since it is only defined for integer n in it's current form, when to take this limit n should now be real or complex number. This means analytically continuing Z_n to real n.

We label the path integral for this $Z_n(A)$, which is nothing more than the original path integral but now evaluated on the $n-$replica surface - taking $n \longrightarrow 1$ gives back the original path integral on the original surface.

We find then that the trace of the reduced density matrix is

$$\mathrm{Tr}\,(\rho_A^n) = \frac{Z_n(A)}{Z^n}, \tag{9.2.11}$$

where Z_n is the path integral evaluated on the entire replica surface, and the factor $\frac{1}{Z^n}$ is a normalisation to ensure that $\mathrm{Tr}\,(\rho_A) = 1$. If we *can* calculate this trace, we can use equation 9.1.13 to calculate the Rényi entropy

$$S_n = \frac{1}{1-n}\left(\ln Z_n(A) - n \ln Z\right). \tag{9.2.12}$$

Alternatively, we can write $\ln \mathrm{Tr}\,(\rho_A^n) = \ln(\sum_i p_i^n)$ and differentiate to find

$$-\frac{\partial}{\partial n}\mathrm{Tr}\,(\rho_A^n) = -\frac{\sum_i p_i^n \ln(p_i)}{\sum_i p_i^n}. \tag{9.2.13}$$

Which, in the limit of $n \longrightarrow 1$, gives the von Neumann entropy (since $\sum_i p_i = 1$). In other words, we can write the von Neumann entropy as

$$S_A = -\lim_{n\to 1}\frac{\partial}{\partial n}\left(\frac{Z_n(A)}{Z^n}\right), \tag{9.2.14}$$

or alternatively

$$S = \lim_{n\to 1}\left(1 - n\frac{\partial}{\partial n}\right)\ln\left(Z_n(A)\right). \tag{9.2.15}$$

9.2.3 Twist Fields

Twist fields are fields that are associated with some internal symmetry of a given action. They are a way of capturing the behaviour of a symmetry transformation on theory space as a field that lives on the target space. For our purposes, we will consider twist fields as being associated with replica symmetries, specifically we will encode in them the singularity structure of the replica surface [108–110, 127].

One interpretation of the replica trick is that it makes n identical copies of a field theory, including its background geometry. Specifically, the i'th copy of each theory depends only on the field(s) Φ_i, which only exist on one layer of the Riemann surface. The *full* Lagrangian density of the new $n-$replicated model is therefore dependent on all of the fields $\{\Phi_1, \Phi_2, ..., \Phi_n\}$, but in the following way:

$$\mathcal{L}^{(n)}[\Phi_1, \Phi_2, ..., \Phi_n](z) = \mathcal{L}[\Phi_1](z) + \mathcal{L}[\Phi_2](z) + \cdots + \mathcal{L}[\Phi_n](z). \tag{9.2.16}$$

Since the replica trick demands that we identify $n + i = i$, it's obvious that taking $i \to i + 1$ must be a symmetry of the system (a cyclic permutation). If we naively map our full n-CFT from $\mathcal{R}_n$ to $\mathbb{C}$ (the *target space*), then it is exactly this symmetry that will be lost, and so we must introduce a way to recapture it: the twist field.

Lets examine an interval $A = [u, v] \in x$ as pictured in the figure below.

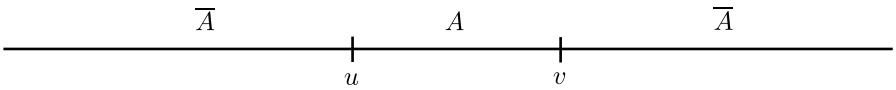

Figure 9.4: U-V Interval

The path integral of a 2D QFT (with Euclidean signature) on a Riemann surface $\mathcal{R}_n$ in general looks like

$$Z_{\mathcal{R}_n} = \int \mathcal{D}\Phi \ \exp\left(-\int_{\mathcal{R}_n} dx d\tau \ \mathcal{L}[\Phi](x,\tau)\right). \tag{9.2.17}$$

For the u, v-interval (the sheets are joined via the segment $x \in [u, v]$, $\tau = 0$), provided we are taking n copies of the original field theory, we can rewrite our

path integral as

$$Z_{\mathcal{R}_{n,u,v}} = \int_{\mathcal{C}(u,v)} \prod_i^n \mathcal{D}\Phi_i \ \exp\left(- \int_{\mathbb{C}} dx d\tau \ \sum_j^n \mathcal{L}[\Phi_j](x,\tau) \right). \tag{9.2.18}$$

Where $\mathcal{C}(u,v)$ are the conditions on the fields that restricts the path integral (similar to eq. 9.2.9) to obey our demands, specifically

$$\mathcal{C}(u,v) \quad : \quad \Phi_i(x,0^+) = \Phi_{i+1}(x,0^-), \qquad x \in [u,v]. \tag{9.2.19}$$

With this condition in mind, let's consider eq. 9.2.16. If we were on the top of the segment $x \in [u,v]$, the sum in this equation would be exactly the same as the as if we were at the bottom, given the cyclic permutation invariance and the path integral condition.

The Riemann surface we are considering is flat everywhere except at the (conically) singular points at each end of the cuts. The curvature inside the cut is still zero, because we can choose the cut however we like, provided we keep the end points the same: the boundaries define the curvature.

Thought of another way, we can think of a general curve that connects points u and v. Crossing this curve from $-\infty$ shifts your field from Φ_i to Φ_{i+1}, while crossing from $+\infty$ shifts your field from Φ_{i+1} to Φ_i. However, since we are free to make any curve we like, we can only be sure that we have crossed a general curve after we have traversed round the point at either edge.

What this means is that the theory with the cut can be thought of as a theory with two insertions at either end of the cut: **branch point twist fields**. The property of these particular twist fields is that they are local operators[11] that mimic the action of the twisted boundary conditions when they operate on the other fields.

They are defined via the cyclic permutations they enact, through the commutation relations

$$\Phi_i(z)\mathcal{T}(w) = \mathcal{T}(w)\Phi_{i+1}(z), \qquad z^i > w^i \tag{9.2.20}$$
$$\Phi_i(z)\mathcal{T}(w) = \mathcal{T}(w)\Phi_i(z), \qquad z^i < w^i \tag{9.2.21}$$
$$\Phi_i(z)\tilde{\mathcal{T}}(w) = \tilde{\mathcal{T}}(w)\Phi_{i-1}(z), \qquad z^i > w^i \tag{9.2.22}$$
$$\Phi_i(z)\tilde{\mathcal{T}}(w) = \tilde{\mathcal{T}}(w)\Phi_i(z), \qquad z^i < w^i \tag{9.2.23}$$
$$\tag{9.2.24}$$

with $\mathcal{T}$ and $\tilde{\mathcal{T}}$ define opposite cyclic permutation transformations and we note that we can identify $\tilde{\mathcal{T}} = \mathcal{T}^\dagger$.

[11] They are local in some sense, but also non-local. Elaborate!

The reason that these fields are interesting is because we can use them to redefine our path integral in eq. 9.2.18, since the insertion of a twist operator is nothing more than insisting on the restriction 9.2.19 and the linear form of the Lagrangian. With that in mind, we can formally define the twist field via

$$\int_{\mathbb{C}} \mathcal{D}\Phi \ \exp\left(-S[\Phi]\right) \mathcal{T}_n(u,0)\tilde{\mathcal{T}}_n(v,0) \ \mathcal{O}_1 \cdots \mathcal{O}_n = \int_{\mathcal{C}(u,v)} \mathcal{D}\Phi \ \exp\left(-S[\Phi]\right) \mathcal{O}_1 \cdots \mathcal{O}_n, \tag{9.2.25}$$

where the subscript n reminds that there is a twist field inserted on each surface, which we will suppress from now on.

Less formally, we can define the path integral of our theory in terms of a correlator of these twist fields

$$Z_{\mathcal{R}_{n,u,v}} \propto \langle \mathcal{T}(u,0)\tilde{\mathcal{T}}(v,0)\rangle_{\mathcal{L}^{(n)},\mathbb{C}}\,. \tag{9.2.26}$$

Up to some irrelevant constant. Normalised correlation functions of operators living on the i^{th} copy of $\mathcal{L}$ on sheet i is given by

$$\langle \mathcal{O}_i(x,y)\cdots\rangle_{\mathcal{R}_{n,u,v}} = \frac{\langle \mathcal{T}(u,0)\tilde{\mathcal{T}}(v,0)\mathcal{O}_i(x,y)\cdots\rangle_{\mathcal{L}^{(n)},\mathbb{C}}}{\langle \mathcal{T}(u,0)\tilde{\mathcal{T}}(v,0)\rangle_{\mathcal{L}^{(n)},\mathbb{C}}}. \tag{9.2.27}$$

In short, twist fields are useful because they allow you to write correlation functions of operators $\mathcal{O}$ on the replicated manifold in terms of correlation functions of $\mathcal{O}$ with twist fields, but now on $\mathbb{C}$.

Twist fields only appear because we map our original field theory on $\mathbb{C}$, with Lagrangian $\mathcal{L}$, to an n-sheeted Riemann surface $\mathcal{R}_n$. We can then evaluate our new theory with Lagrangian $\mathcal{L}^{(n)}$ back on $\mathbb{C}$, provided we insert the twist fields that correspond to the edges of the cuts.

In a conformal field theory, we can work out the scaling dimension of our twist fields by taking the expectation value of the stress energy tensor on $\mathcal{R}_n$ and comparing it with the OPE of the stress energy tensor with the twist fields on $\mathbb{C}$, since these two should now be equivalent.

Suppose our CFT lives on the complex w-plane, with stress tensor $T(w)$. We need to map this to $\mathcal{R}_n$. To do this, we first conformally map our $[u,v]$ interval to $(0,\infty)$ via

$$w \mapsto \zeta = \frac{w-u}{w-v}. \tag{9.2.28}$$

Now we have mapped the interval to the positive domain, we need n copies of it, so we map back n copies of $\mathbb{C}$ via

$$z = \zeta^{1/n} = \left(\frac{w-u}{w-v}\right)^{1/n}. \tag{9.2.29}$$

As is well known for a 2D CFT, $T(w)$ is related to the transformed $T(z)$ via

$$T(w) = \left(\frac{dz}{dw}\right)^2 T(z) + \frac{c}{12}\{z, w\}, \tag{9.2.30}$$

where c is the central charge and $\{z, w\}$ is the Schwartzian derivative $(z'''z' - \frac{3}{2}z''^2)/z'^2$.

Taking the expectation value of this and considering the fact that $\langle T(z)\rangle = 0$, we find

$$\langle T(w)\rangle = \frac{c}{12}\{z, w\} = \frac{c}{24}\left[\frac{(u-v)^2}{(w-u)^2(w-v)^2}\right]\left(\frac{n^2-1}{n^2}\right). \tag{9.2.31}$$

By definition, this must be equal to

$$\langle T(w)\rangle = \frac{\langle \mathcal{T}(u,0)\tilde{\mathcal{T}}(v,0)T(w)\rangle_{\mathcal{L}^{(n)},\mathbb{C}}}{\langle \mathcal{T}(u,0)\tilde{\mathcal{T}}(v,0)\rangle_{\mathcal{L}^{(n)},\mathbb{C}}}. \tag{9.2.32}$$

$\mathcal{T}$ and $\tilde{\mathcal{T}}$ are primary fields, so the right hand side must satisfy the conformal ward identity, meaning

$$\langle \mathcal{T}(u,0)\tilde{\mathcal{T}}(v,0)T(w)\rangle = \left(\frac{\Delta_n}{(w-u)^2} + \frac{\Delta_n}{(w-v)^2} + \frac{1}{w-u}\partial_u + \frac{1}{w-v}\partial_v\right)\langle \mathcal{T}(u,0)\tilde{\mathcal{T}}(v,0)\rangle. \tag{9.2.33}$$

The two point function, since they are primary fields, is

$$\langle \mathcal{T}(u,0)\tilde{\mathcal{T}}(v,0)\rangle = |v-u|^{-2(\Delta+\overline{\Delta})}. \tag{9.2.34}$$

Plugging this in, we find

$$\Delta_n = \overline{\Delta}_n = \frac{nc}{24}\left(1 - \left(\frac{1}{n}\right)^2\right). \tag{9.2.35}$$

Having derived this, we can work out the Rényi entropy of one interval of a 2D conformal field theory. Let's first assume that the length of our interval is $L = |u-v|$ with UV regulator ϵ.

Then, from eq. 9.2.34, we can write

$$Z_{\mathcal{R}_{n,u,v}} = L^{-4\Delta_n}. \tag{9.2.36}$$

And therefore that

$$\mathrm{Tr}\left(\rho^n_{u-v}\right) = g_n \frac{L}{\epsilon}^{\frac{c}{6}(n-1/n)}. \tag{9.2.37}$$

Where g_n is some n dependent constant and $g_1 = 1$ by normalisation. Plugging this into eq. 9.2.14, we find

$$S_{uv} = -\partial_n \left(g_n \frac{L}{\epsilon}^{\frac{c}{6}(n-1/n)} \right)_{n=1} \tag{9.2.38}$$

$$= \left[\frac{c g_n}{6} \left(\frac{L}{\epsilon} \right)^{\frac{c}{6}(n-1/n)} \left(1 + \frac{1}{n^2} \right) \log \frac{L}{\epsilon} \right]_{n=1} + g_n' \frac{L}{\epsilon}^{\frac{c}{6}(n-1/n)} \Big|_{n=1} \tag{9.2.39}$$

$$= \frac{c}{3} \log \frac{L}{\epsilon} + g_1'. \tag{9.2.40}$$

This is the famous *universal* entanglement entropy for a (1+1)-d CFT, originally calculated in [68].

To briefly summarise the last two sections, we saw that we could calculate $\mathrm{Tr}\,(\rho^n)$ via the replica trick, which ultimately means doing one of two things: either computing the Euclidean partition function on the replicated manifold $\mathcal{R}_n$, or computing the partition function for n copies of the original QFT with twist fields inserted into the correlation functions.

9.2.4 Geometric Entanglement Entropy

So far, we have mostly been concerned with finding the reduced density matrix in order to calculate the entanglement entropy. Finding this is tricky, requiring us to trace out all degrees of freedom that the vacuum state cannot access. When we are concerned with a QFT, this amounts to tracing out all the degrees of freedom outside a given region of interest, where the regions are separated by the co-dimension 2 **entangling surface** Σ.

If we look at a particular time slice, say at $t = 0$, then we know what the degrees of freedom accessible to an operator that lives on Σ: they are those degrees of freedom that live inside the **causal diamond** $\mathcal{D}$.

How then do we trace out degrees of freedom *outside* this causal diamond? One way to do this is to bound the space with *horizons* at each edge of the causal diamond [128]. In $D = 2$ Minkowski space, if we choose the semi-infinite half line as our region of interest (seperated by a single point Σ at $x = 0$), then the causal diamond is the right hand wedge, and we recognise that we can easily bound this space by considering **Rindler coordinates**. Now let's think about how this helps us define the reduced density matrix. As we have seen, the density matrix can be written directly in terms of the modular hamiltonian. However, only in rare cases is this modular Hamiltonian *local*: in general, it is a non-local object that

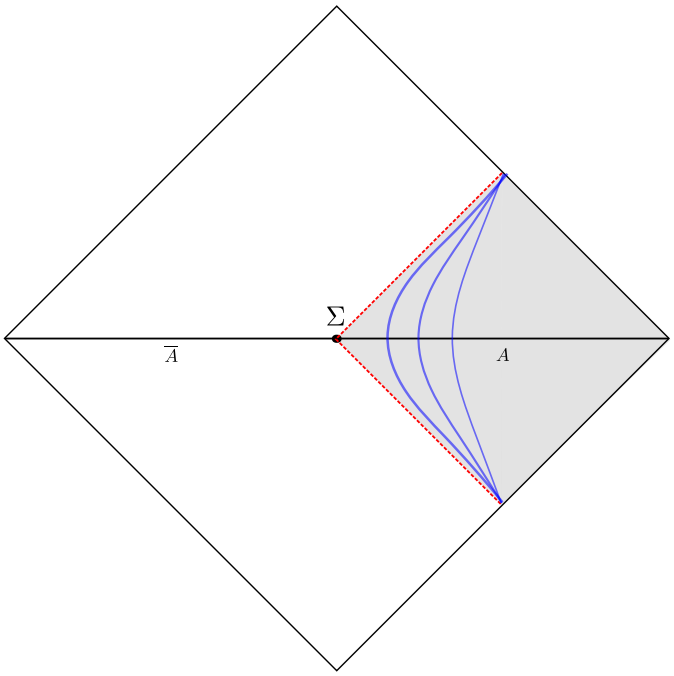

Figure 9.5: The Rindler wedge: the shaded area is the causal region of our chosen sub-region A, the blue paths is the 'modular flow', in this case translations by boosts.

can't be expressed in terms of operators that live on Σ. In the case of Rindler space however, the Hamiltonian *is* local. Due to a theorem of Bisognano and Wichmann [129], we find that the modular Hamiltonian in Rindler space is given by

$$H = \beta K = \beta \int_{x>0,t=0} d^{D-2}x \; xT_{00}, \tag{9.2.41}$$

where T_{00} is the tt component of the stress-energy tensor of the theory and β is the inverse temperature, in this case the **Unruh temperature** $T = 1/2\pi$.

The modular (or entanglement) Hamiltonian generates *modular flow*, which basically just means it generates translations in some time parameter s that preserves modular invariance. These flows take the form

$$U(s) = \rho^{is} = e^{-iHs}. \tag{9.2.42}$$

The benefit of all this is that our theory is now *thermal*, meaning it's no longer defined only at zero temperature and, as we will soon see, the thermal entropy *is* the entanglement entropy. This is due to the fact that the coordinate transformation to Rindler space is equivalent to a unitary transformation of the

density matrix[12], which leaves the entanglement entropy unaffected, since

$$\langle \mathcal{O} \rangle = \mathrm{Tr}\,(\rho \mathcal{O}) = \mathrm{Tr}\,(\rho U(s) \mathcal{O} U(-s))\,. \tag{9.2.43}$$

This invariance is only true for *local* modular Hamiltonians, since this ensures that any operator localised on Σ evolves to some operator again localised in $\mathcal{D}$.

Working in lightcone coordinates defined via $x^{\pm} = x^0 \pm x^1$, we can go to conformally flat Rindler space in any D via the transformation

$$x^{\pm} = z e^{\pm \eta / R}. \tag{9.2.44}$$

This gives the line element

$$ds^2 = dx^+ dx^- + \sum_{i=2}^{D} (dx^i)^2 \tag{9.2.45}$$

$$= -\frac{z^2}{R^2} d\eta^2 + dz^2 + \sum_{i=2}^{D} (dx^i)^2, \tag{9.2.46}$$

and we can now identify the density matrix as being

$$\rho_R = \frac{e^{-\beta H_\eta}}{Z}, \qquad \eta \sim \eta + 2\pi R. \tag{9.2.47}$$

Lets consider the fact that we have selected only a special region, the semi infinite positive half line, and that it would be nice to be able to select arbitrary geometric intervals. We can use the fact that for a CFT, we can use conformal symmetry to map specific regions of interest to the Rindler wedge, once again reducing the problem of calculating the entanglement entropy to calculating the thermal entropy.

9.2.5 Spherical Entangling Surfaces in D dimensions

To illustrate the last point, let's now consider a spherical entangling surface of dimension $D-2$ and radius R, which we label Σ, following [128]. The coordinates x^μ of causal diamond $\mathcal{D}$ of such a region can be mapped to Rindler space via a special conformal transformation and a translation, namely

$$x^\mu = 2R \frac{X^\mu - b^\mu X^2}{1 - 2b \cdot X + b^2 X^2} + R b^\mu, \tag{9.2.48}$$

[12] Recall that for any two spacetimes M and $\overline{M}$ related by a conformal transformation $g(\overline{x}) \longrightarrow \Omega^2 g(x)$, the density matrix is related by $\rho_M = U_\Omega \rho_{\overline{M}} U_\Omega^\dagger$.

Where $b^\mu = (0, -1, 0, ...)$. Working in lightcone coordinates $x^\pm = r \pm t$, where $r = \sqrt{\sum_{i=1}^{D-1}(x^i)^2}$, we note that the causal diamond is given by

$$\{x^+ \leq R\} \cap \{x^- \leq R\}\,. \tag{9.2.49}$$

Focussing on a time slice of $t = 0$, we find that the conformal transformation in these coordinates is

$$x^\pm(s) = r(0) \pm t(s) = R\frac{(R + x^\pm) - e^{\mp 2\pi s}(R - x^\pm)}{(R + x^\pm) + e^{\mp 2\pi s}(R - x^\pm)}. \tag{9.2.50}$$

An infinitesimal modular transformation in s will then tell us what happens in $x^\pm$, i.e. what happens under a small application of H to the system. A short calculation reveals

$$\delta x^\pm = \lim_{t,s\longrightarrow 0} \frac{\pi R(R^2 - r^2)}{R\cosh(\pi s) + r\sinh(\pi s)}\delta s = 2\pi\frac{(R^2 - r^2)}{2R}\delta s. \tag{9.2.51}$$

The modular Hamiltonian is then

$$H_{\mathcal{D}} = 2\pi \int d^{D-1}x\ \frac{(R^2 - r^2)}{2R}T_{00} + c'. \tag{9.2.52}$$

We have now found the modular Hamiltonian inside $\mathcal{D}$, but it isn't thermal. We will now relate *this* modular hamiltonian with a thermal Hamiltonian by transforming it to a new geometry $\mathcal{H} = R \times H^{D-1}$, where H is hyperbolic space, the claim being that on this geometry thermal entropy = entanglement entropy.

The first step is to note that we can easily transform from Rindler space to $R\times H^{D-1}$ at the expense of picking up a conformal factor $\Omega = z/R$

$$ds^2 = \Omega^2\left(-d\tau^2 + \frac{R^2}{z^2}\left[dz^2 + \sum_{i=2}^{D}(dx^i)^2\right]\right). \tag{9.2.53}$$

Now, we need to map $\mathcal{D}$ to $\mathcal{H}$. Starting with D dimensional polar coordinates

$$ds^2 = -dt^2 + dr^2 + r^2 d\Omega^2_{D-2}. \tag{9.2.54}$$

Our entangling surface Σ is again the $r = R$ sphere on a $t = 0$ timeslice. We now need to do a transformation to a set of restricted coordinates that only cover $\mathcal{D}$, which are conveniently given by

$$t = R\frac{\sinh(\tau/R)}{\cosh u + \cosh(\tau/R)}, \qquad r = R\frac{\sinh u}{\cosh u + \cosh(\tau/R)}, \tag{9.2.55}$$

and the metric above now becomes

$$ds^2 = \Omega^2\left(-d\tau^2 + R^2[du^2 + \sinh^2 u\ d\Omega^2_{D-2}]\right), \tag{9.2.56}$$

which is exactly the metric of $R \times H^{D-1}$. We note that the limits are exactly those that cover $\mathcal{D}$

$$\tau \longrightarrow \pm\infty \quad \Longrightarrow \quad (t, r) \longrightarrow (\pm R, 0) \tag{9.2.57}$$
$$u \longrightarrow \infty \quad \Longrightarrow \quad (t, r) \longrightarrow (0, R). \tag{9.2.58}$$

Now that we have successfully mapped the geometries, we know that there is some unitary transformation that must map the density matrix on $\mathcal{D}$ to the thermal state on $\mathcal{H}$, which has temperature $T = \frac{1}{2\pi R}$.

9.2.6 Example: Entanglement Entropy of a (1+1)-d CFT

Consider an interval on the real line of $[-\frac{L}{2}, \frac{L}{2}]$, centered around $x = 0$. In $D = 2$, the entangling surface (sphere) is just a single point.

We need to derive lightcone coordinates that cover the causal diamond of a $t = 0$ timeslice, by using equation 9.2.55 (choosing $R = 1$ for simplicity)

$$x^{\pm} = \frac{\sinh\tau \pm \sinh u}{\cosh u + \cosh\tau} \tag{9.2.59}$$
$$= \frac{\sinh(\frac{\tau \pm u}{2})\cosh(\frac{\tau \mp u}{2})}{\cosh(\frac{\tau \pm u}{2})\cosh(\frac{\tau \mp u}{2})} \tag{9.2.60}$$
$$= \frac{L}{2}\tanh(\frac{y^{\pm}}{2}), \tag{9.2.61}$$

where we have rescaled our coordinates by $L/2$ to bound our specific interval and defined

$$y^{\pm} = \tau \pm u, \qquad \tau \sim \tau + 2\pi i,$$

and we have made use of the trigonometric identities

$$\sinh x \pm \sinh y = 2\sinh\frac{x \pm y}{2}\cosh\frac{x \mp y}{2}, \qquad \cosh x + \cosh y = 2\cosh\frac{x + y}{2}\cosh\frac{x - y}{2}. \tag{9.2.62}$$

$y^{\pm}$ now covers *only* the causal diamond and our partial trace is already done in these coordinates. Furthermore, states in y-space are thermal, given by

$$\rho(y^{\pm}) = e^{-\beta H_{\tau}}, \tag{9.2.63}$$

where $\beta = 2\pi = T^{-1}$. In a 2D CFT, we can use the Cardy formula [130] to calculate the thermal entropy, given by

$$S = \frac{\pi c}{3} RT. \tag{9.2.64}$$

Where R is the length of the interval in y-space at $\tau = 0$ and $R \gg T^{-1}$. R is then given by

$$R = y^+ - y^-\Big|_{\tau=0, x^\pm = L/2} = 2y^+ = 4\,\mathrm{arctanh}\left(\frac{2x^+}{L}\right)\Big|_{x^+ = L/2} = \infty. \tag{9.2.65}$$

This tells us that the entanglement entropy diverges. This is perfectly natural, telling us that close to the boundary of the entangling surface the degrees of freedom are *very* entangled, as we might expect. In order to combat this, we introduce a UV regulator, which amounts to considering the interval $[-\frac{L}{2}+\epsilon, \frac{L}{2}-\epsilon]$. Now,

$$R = 4\,\mathrm{arctanh}\left(\frac{2}{L}\left[\frac{L}{2} - \epsilon\right]\right)\Big|_{\epsilon \longrightarrow 0} = 2\left(\ln[2 - \frac{2\epsilon}{L}] - \ln[\frac{2\epsilon}{L}]\right)\Big|_{\epsilon \longrightarrow 0} = 2\ln(\frac{L}{\epsilon}). \tag{9.2.66}$$

Plugging this in along with $T = \frac{1}{2\pi}$, we find the universal result for a (1+1)-d CFT

$$S = \frac{c}{3}\ln\left(\frac{L}{\epsilon}\right). \tag{9.2.67}$$

Which is exactly what we derived in eq. 9.2.40 using the replica trick and twist fields.

9.2.7 The Entanglement Spectrum & Correlation Matrices

We have seen how to obtain the entanglement entropy geometrically, and via twist fields. We will now consider an alternative approach, namely deriving entanglement entropy from the *correlation matrix* [131, 132], alternatively known as the Nambu-Greens function at equal time, defined as

$$C_{ij} = \langle\psi|c_i^\dagger c_j|\psi\rangle = \mathrm{Tr}\left(\rho c_i^\dagger c_j\right). \tag{9.2.68}$$

Consider a system in a pure state defined by $\rho = |\psi\rangle\langle\psi|$. We can, as we did in eq. 9.1.44, define our reduced density matrix of subsystem A in terms of the entanglement hamiltonian $\mathcal{H}_E$

$$\rho_A = \mathrm{Tr}_A(\rho) = \frac{e^{-\mathcal{H}_E}}{\mathcal{Z}_A}, \tag{9.2.69}$$

where $\mathcal{Z}_A = \mathrm{Tr}\,(e^{-\mathcal{H}_E})$.

The **entanglement spectrum** is defined as the eigenvalues of this Hamiltonian, and often contains deep information about the structure of entanglement for a specific system, usually more than the entanglement entropy alone can provide.

We will consider a generic interacting fermionic system with Hamiltonian

$$H = \sum_{i,j} c_i^\dagger h_{i,j} c_j - \frac{1}{2}\left[c_i^\dagger \Delta_{i,j} c_j^\dagger + c_i \Delta_{i,j}^\dagger c_j\right] \tag{9.2.70}$$

$$= \frac{1}{2}\sum_{i,j} \Psi_i^\dagger h^{BdG} \Psi_j, \tag{9.2.71}$$

where $c_i^\dagger$ (c_i) is a creation (annihilation) operator for site i, and the Nambu spinor Ψ and Bogoliubov-de Gennes (BdG) Hamiltonian h^{BdG} are given by

$$\Psi_i^T = (c_i, c_i^\dagger), \qquad h^{BdG} = \begin{pmatrix} h_{ij} & -\Delta_{ij} \\ -\Delta_{ij}^\dagger & -h_{ij}^* \end{pmatrix}, \tag{9.2.72}$$

and h is hermitian while Δ is skew-symmetric, i.e. $\Delta^T = -\Delta$. We can diagnoloize this Hamiltonian via a Bogoliubov transformation U (see appendix B), such that $a_i = \sum_j U_{ij} c_j$. When $i, j \in A$, the entanglement Hamiltonion must also have this form [131], and we can write

$$\mathcal{H}_E = \frac{1}{2}\sum_{i,j\in A} \Psi_i^\dagger h_A^{BdG} \Psi_j. \tag{9.2.73}$$

With a sufficient choice of U_{ij}, we can completely diagonalize this Hamiltonian, finding

$$\mathcal{H}_E = \frac{1}{2}\sum_{i,j\in A} \Psi_i^\dagger U h_A^{BdG} U^\dagger \Psi_j \tag{9.2.74}$$

$$= \sum_{ij}\sum_k \varepsilon_k (U_{ik} c_i^\dagger)(U_{jk}^\dagger c_i) \tag{9.2.75}$$

$$= \sum_k \varepsilon_k a_k^\dagger a_k, \tag{9.2.76}$$

where ε_k are the Eigenvalues of the (reduced) BdG Hamiltonian in eq. 9.2.72. We can now consider the correlation matrix in terms of these operators

$$C_{ij}^A = \mathrm{Tr}\left(\rho_A c_i^\dagger c_j\right) \tag{9.2.77}$$

$$= \frac{\mathrm{Tr}\left(e^{\sum_k \varepsilon_k a_k^\dagger a_k} \sum_{lm} U_{li}^\dagger U_{jm} a_l^\dagger a_m\right)}{\mathcal{Z}} \tag{9.2.78}$$

$$= \sum_k \frac{U_{ki}^\dagger U_{jk}}{1 + e^{\epsilon_k}}, \tag{9.2.79}$$

where we have used

$$\mathcal{Z} = \mathrm{Tr}\left(e^{\sum_k \varepsilon_k a_k^\dagger a_k}\right) = \sum_{\{n_k\}} \langle n|e^{\sum_k \varepsilon_k a_k^\dagger a_k}|n\rangle = \prod_\alpha (1+e^{-\varepsilon_\alpha}). \tag{9.2.80}$$

We see then that we can write the eigenvalues of the correlation matrix, which we shall label ζ_k, in terms of eigenvalues of the entanglement Hamiltonian, ε_k, via

$$\zeta_k = \frac{1}{1+e^{\varepsilon_k}}. \tag{9.2.81}$$

This means that we can derive the the entanglement spectrum directly from the correlation matrix simply by computing its eigenvalues. We can also write the Rényi entropy in eq. 9.1.13 (and hence the entanglement entropy) in terms of these eigenvalues

$$\begin{aligned} S_n(\rho) &= \frac{1}{1-n}\ln \mathrm{Tr}\,(\rho^n) && (9.2.82)\\ &= \frac{1}{1-n}\ln \mathrm{Tr}\,(\rho^n) && (9.2.83)\\ &= \frac{1}{1-n}\ln\left[\prod_\alpha \frac{1+e^{-n\varepsilon_\alpha}}{(1+e^{-\varepsilon_\alpha})^n}\right] && (9.2.84)\\ &= \frac{1}{1-n}\sum_\alpha \left[\ln(1+e^{-n\varepsilon_\alpha}) - n\ln(1+e^{-\varepsilon_\alpha})\right]. && (9.2.85) \end{aligned}$$

Inverting eq. 9.2.81, we find

$$\varepsilon_k = \ln\left[\frac{1-\zeta_k}{\zeta_k}\right], \tag{9.2.86}$$

meaning we can write the Rényi entropy in terms of eigenvalues of the correlation matrix

$$S_n = \frac{1}{1-n}\sum_\alpha \ln\left[\zeta_\alpha^n + (1-\zeta_\alpha)^n\right]. \tag{9.2.87}$$

9.3 Quantum Circuits and Complexity

Classical circuits are constructed from *paths* and *logic gates*. The paths carry information, while the gates manipulate the information. For a single bit, there is only one possible gate: the NOT gate, which takes $0 \longrightarrow 1$ and $1 \longrightarrow 0$.

Now let's consider a single *qubit*, described by the state

$$|\psi\rangle = c_0|0\rangle + c_1|1\rangle, \qquad |c_0|^2 + |c_1|^2 = 1. \tag{9.3.1}$$

We know what acts on these kinds of states: unitary operators. Therefore, we reasonably conclude that the equivalent of a logic gate in quantum mechanics is a

unitary operation. In fact, a quantum circuit is simply the idea of breaking down some complicated unitary transformation into products of simpler transformations that act on a few qubits at a time.

The equivalent of the NOT gate is given by

$$X \equiv \begin{pmatrix} 0 & 1 \\ 1 & 0 \end{pmatrix}, \tag{9.3.2}$$

which again takes $0 \longrightarrow 1$ and $1 \longrightarrow 0$, but now acting on a quantum state. Unlike for the classical bit, however, there are also other quantum gates that can act on a single qubit, for example the *Hadamard gate*

$$H \equiv \frac{1}{\sqrt{2}} \begin{pmatrix} 1 & 1 \\ 1 & -1 \end{pmatrix}. \tag{9.3.3}$$

This is often thought of as the square root of the NOT gate, since applying it twice is the equivalent of the NOT gate, since

$$H(c_0 |0\rangle + c_1 |1\rangle) = \frac{1}{\sqrt{2}}(c_0 + c_1) |0\rangle + \frac{1}{\sqrt{2}}(c_0 - c_1) |1\rangle . \tag{9.3.4}$$

We might ask the question of how many distinct gates we might need to approximate any reasonable unitary operation, and the answer depends typically on the number of qubits you operate on at a time. A set of gates that can be used to generate almost any complicated unitary is called a *universal gate set*. We are interested in **computational complexity** $C(U)$, which we will define as being the minimum number of one and two qubit gates required to exactly build some complicated target state $U |\psi\rangle$ out of a simple reference state $|\psi\rangle$.

For an n-qubit state, U is a $2^n \times 2^n$ matrix, and it can be argued that for almost all U, $C(U) \geq 4^n$ [82]. We want to know what can be achieved with a finite number of gates taken from some universal gate set (there isn't a unique two-qubit universal set).

For a unitary that acts on two-qubit states, the equivalent of the NOT gate is the CNOT (*controlled* NOT), defined as mapping $|\psi, \varphi\rangle \longrightarrow |\psi, \psi \oplus \varphi\rangle$, where the $\oplus$ represents the operation *XOR*, which acts on a two-qubit, mapping $|10\rangle \longrightarrow |11\rangle$ and $|11\rangle \longrightarrow |10\rangle$. In effect, XOR flips the second qubit iff the first equals 1, or alternatively, can be thought of as $x \oplus y = x + y \mod 2$.

The CNOT gate can be represented as a matrix

$$CNOT = \begin{pmatrix} 1 & 0 & 0 & 0 \\ 0 & 1 & 0 & 0 \\ 0 & 0 & 0 & 1 \\ 0 & 0 & 1 & 0 \end{pmatrix}. \tag{9.3.5}$$

An example of the CNOT gate in action is

$$CNOT\left(c_{00}\left|00\right\rangle + c_{01}\left|01\right\rangle + c_{10}\left|10\right\rangle + c_{11}\left|11\right\rangle\right) = c_{00}\left|00\right\rangle + c_{01}\left|01\right\rangle + c_{10}\left|11\right\rangle + c_{11}\left|10\right\rangle. \tag{9.3.6}$$

Other examples of gates are the *Toffoli gate*, mapping $|\psi, \varphi, \phi\rangle \longrightarrow |\psi, \varphi, \phi \oplus \psi\varphi\rangle$ and the *phase gate*, given by

$$R_\phi = \begin{pmatrix} 1 & 0 \\ 0 & e^{i\phi} \end{pmatrix}, \tag{9.3.7}$$

and the controlled phase gate

$$\Lambda(R_\phi) = \begin{pmatrix} 1 & 0 & 0 & 0 \\ 0 & 1 & 0 & 0 \\ 0 & 0 & 1 & 0 \\ 0 & 0 & 0 & e^{i\phi} \end{pmatrix}. \tag{9.3.8}$$

Using these example gates, we can construct universal sets. For example, {Toffoli, H, R_ϕ} and {CNOT, G} are both universal sets [133] (where G is *almost* any 2×2 unitary matrix, we wouldn't for example include the unit matrix), as is {H, $\Lambda(R_\phi)$}. We note that, should we take G to be *all* one and two qubit gates, then the set is *exactly* universal since, using these, any n-qubit unitary can be built exactly, although we may need an exponentially large circuit to do so. We will then denote any set of gates as universal if it can get us *approximately* close to the target state, to within a tolerance of say ϵ, given by the trace distance from the target state to the state that has been found, i.e. we want $\|\psi - \psi_{target}\| \leq \epsilon$ or, equivalently, $d(U, V) = \|U - V\| \leq \epsilon$.

An important result regarding universal sets is the **Solovay-Kitaev theorem** [134], which states that given a universal set $\mathcal{G}$ and a target unitary U, the number of times N that you need to apply transformations $\in \mathcal{G}$ to reach the target state with tolerance $\epsilon > 0$ is given by $N = \mathcal{O}(\log^c(1/\epsilon))$, where c is a constant of order $1 \leq c \leq 2$ that is determined by properties of the set $\mathcal{G}$. Importantly, this tells us that that there is an upper bound on the complexity, depending on the tolerence we require. If we're only considering single qubits, then $\mathcal{G}$ is some subset of $SU(2)$ (since any phase is irrelevant here). Suppose that our set $\mathcal{G}$ is closed under inverses, meaning that if we include a gate $g \in \mathcal{G}$, then $g^\dagger \in \mathcal{G}$. Under this assumption, then an important implication of the Solovay-Kitaev theorem is that *any* universal one and two qubit gate set is as good as any other provided you only care about a tolerance ϵ [135]. In light of this, we will throughout the remainder of this section not worry about which set of gates we have chosen, implicitly assuming that we only really care about reaching any target state approximately. If we require absolute precision, then we will simply choose $\mathcal{G} = SU(2^n)$ for some n-qubit operation.

Schematically, we think of complexity as the number of elementary gates required to approximate some unitary that takes us from some reference to some target

$$|0000000...0\rangle \xrightarrow{\text{Apply C(U) gates}} |1101001...1\rangle\,. \tag{9.3.9}$$

Or, as a quantum circuit

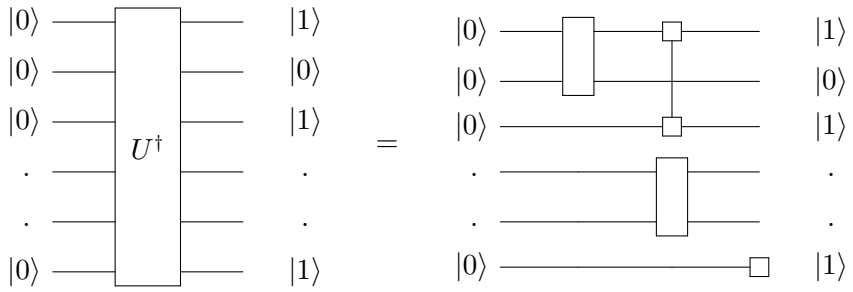

(9.3.10)

Given the upper bound offered by Solovay-Kietaev, it seems like generic states require exponentially large circuits to reach high accuracy. For a classical state, using only basic operations, we can reach any other classical state with maximal complexity of $C(U) \leq n$, something which is of course no longer true with quantum states. However, *defining* the complexity is straightforward: given a fixed number of qubits, we simply pick a tolerance and universal set and count the number of unitaries that approximate our target. We will see that things are not so straightforward for quantum field theories.

9.4 Complexity in Quantum Field Theory

We have seen that defining complexity in quantum mechanics is relatively simple due to the discrete nature of the degrees of freedom. In QFT, we no longer have this luxury and a fully agreed definition of complexity in general QFT's is still, at the time of writing, outstanding. We will review some candidate definitions in what follows, before finally comparing them in a systematic way to highlight their benefits and pitfalls. Before doing so, we will motivate the use of complexity as a way to distinguish states by highlighting the drawbacks of the canonical measure.

9.4.1 Fidelity as a measure of state distinguishability

Consider two states that are described by vectors in an n-dimensional Hilbert space $\mathcal{H}$. Any two vectors describe the same state if there is a non-zero complex number $z \in \mathbb{C}$ that relates them: $|\psi\rangle = z\,|\phi\rangle$. This means that the distinct states in $\mathcal{H}$ form

a complex projective space $\mathbb{CP}^n = S^{2n+1}/U(1)$. Given two pure states $|\psi\rangle$ and $|\phi\rangle$, the distance between them on $\mathbb{CP}^n$ is the Fubini-Study distance $d_{FS} \in [0, \pi/2]$, and is defined in terms of the Fidelity function κ

$$\cos^2 D_{FS} = \kappa = \frac{|\langle\psi|\phi\rangle|^2}{|\langle\psi|\psi\rangle||\langle\phi|\phi\rangle|}. \tag{9.4.1}$$

Assuming that the states are always normalised, we will adopt a simpler form of κ by defining it as being a measure of overlap between a reference state $|\psi\rangle$ and a target state $|\phi\rangle = U|\psi\rangle$

$$\kappa(|\psi\rangle, U) = |\langle\psi|\phi\rangle|^2 = |\langle\psi|U|\psi\rangle|^2. \tag{9.4.2}$$

By considering coordinates x on $\mathbb{CP}^n$, we can derive the line element by considering two infinitesimally close states, choosing $\phi = \psi(x + \delta x)$. The infinitesimal distance is then $\sqrt{ds^2_{FS}}$, such that

$$\cos\sqrt{ds^2_{FS}} = |\langle\psi(x)|\psi(x+\delta x)\rangle|. \tag{9.4.3}$$

Taylor expanding the infinitesimal state $\psi(x+\delta x) = \psi(x) + \partial_\mu\psi(x)dx^\mu + \frac{1}{2}\partial_\mu\partial_\nu\psi(x)dx^\mu dx^\nu + \cdots$ leads to

$$\cos\sqrt{ds^2_{FS}} = 1 + \frac{1}{2}\left(\langle\psi(x)|\partial_\mu\partial_\nu\psi(x)\rangle + \langle\partial_\mu\psi(x)|\psi(x)\rangle\langle\psi(x)|\partial_\nu\psi(x)\rangle\right)dx^\mu dx^\nu + \cdots \tag{9.4.4}$$

$$= 1 - \frac{1}{2}ds^2_{FS} + \cdots \tag{9.4.5}$$

which gives

$$g_{\mu\nu} = \langle\partial_\mu\psi(x)|\partial_\nu\psi(x)\rangle - \langle\partial_\mu\psi(x)|\psi(x)\rangle\langle\psi(x)|\partial_\nu\psi(x)\rangle, \tag{9.4.6}$$

where we have used the definition of the inner product and $\langle\psi(x)|\partial_\mu\partial_\nu\psi(x)\rangle = -\langle\partial_\mu\psi(x)|\partial_\nu\psi(x)\rangle$. In terms of this metric, the distance is of course given by

$$D_{FS} = \int ds = \int dt\sqrt{g_{\mu\nu}\dot{x}^\mu\dot{x}^\nu}. \tag{9.4.7}$$

We would like to compare this distance with the *complexity distance*, defined as the minimum number of gates (given some universal set) needed to construct the target state $|\phi\rangle$ from the refernce state $|\psi\rangle$, represented by $\mathcal{C}(|\psi\rangle, U)$.

Let's consider a target state to be built from unitary operators $A = \prod U$ acting on our reference states, i.e. $|\phi\rangle = A|\psi\rangle$. An important fact about the Fidelity is that

it is insensitive to *which* of the target or reference state gets acted on with A. In other words,

$$\kappa(|\psi_0\rangle, A|\psi_0\rangle) = \kappa(A|\psi_0\rangle, |\psi_0\rangle). \tag{9.4.8}$$

Consider $A = \prod_n^N U_n U_n'$, where U_n and U_n' are different unitary operators. Assuming none of the operators commute, there are $1 + \frac{N}{2}$ distinct configurations we could construct that would all have the same Fubini-Study distance and the same Fidelity. For $N = 1$ for example, we could consider the distance between the states $|\psi\rangle = U_1'|\psi_0\rangle$ and $|\phi\rangle = U_1|\psi_0\rangle$, or equivalently we could consider the distance between $|\psi\rangle = |\psi_0\rangle$ and $|\phi\rangle = U_1 U_1'|\psi_0\rangle$, since the Fidelity is insensitive to the choice. Let's give a ridiculous example of exactly how much the Fubini-Study distance fails to capture. Consider the two identical states

$$|\psi\rangle = |0\rangle \otimes |0\rangle \otimes \cdots \otimes |0\rangle, \qquad |\phi\rangle = |0\rangle \otimes |0\rangle \otimes \cdots \otimes |0\rangle. \tag{9.4.9}$$

The Fubini-Study distance between these states is zero, since the overlap is exactly one. Let's now consider adding just one qubit to the system - a $|0\rangle$ to the $|\psi\rangle$ state and a $|1\rangle$ to the $|\phi\rangle$ state, to give

$$|\psi'\rangle = |0\rangle \otimes |0\rangle \otimes \cdots \otimes |0\rangle \otimes |0\rangle, \qquad |\phi'\rangle = |0\rangle \otimes |0\rangle \otimes \cdots \otimes |0\rangle \otimes |1\rangle. \tag{9.4.10}$$

According to the Fubini-Study distance, these states are now as distinct as possible[13], despite the fact that they differ by only one qubit.

The complexity, however, *is* sensitive to this subtle difference in a much more satisfying way. This is easy to see in the example above: in complexity terms, the states $|\psi'\rangle$ and $|\phi'\rangle$ are very close, differing by only a small number of gates that flips one qubit (for the right choice of universal gates, a single gate will suffice). In fact, complexity fits the bill nicely for being a metric on the space of states (or equivalently unitaries). If we consider the space of unitaries to be $SU(2^n)$ (these are the unitaries that could carry out operations on n-qubit states), then we find that the complexity satisfies the following required properties

- Positivity: $\mathcal{C} \geq 0$
- Distinguishability: $\mathcal{C}(U, V) = 0$ iff $U = V$
- Symmetry: $\mathcal{C}(U, V) = \mathcal{C}(V, U)$
- Triangle Inequality: $\mathcal{C}(U, V) \leq \mathcal{C}(U, W) + \mathcal{C}(W, V)$

The first two items are trivially satisfied by complexity, whereas the third is satisfied by demanding that $\mathcal{G}$ is closed under inverses. To see that the triangle inequality is also satisfied, we can consider composing two circuits. It is feasible

[13] Since their overlap is zero, the FS distance is $\pi/2$, which corresponds to the furthest possible distance in state space.

that two composed circuits may have neighbouring gates that are one another's inverse, meaning the product will simplify to unity and the overall complexity will reduce. There is no obvious way one could *increase* the number of gates simply by composing circuits, therefore the triangle inequality must hold.

The metric that this defines on $SU(2^n)$ is a local *right invariant* Finsler metric [85], which satisfies

$$\mathcal{C}(U,V) = \mathcal{C}(UW,VW), \qquad \mathcal{C}(U,V) \neq \mathcal{C}(WU,WV). \tag{9.4.11}$$

Since the requirements are all satisfied for definition of complexity, it makes sense to utilise the tools of differential geometry to study it and, if possible, extend the definition to QFT.

9.4.2 Circuit Complexity á la Nielsen

We have seen that the circuit complexity captures a lot more than the 'naïve' geometric FS distance does, and that defining a metric based on complexity is possible.

Our goal now is to use the tools of differential geometry to compute the minimum number of elementary unitaries V required to take us from a reference state to a target state, in this section following the construction of [85–87, 136].

Consider a target state ψ_T defined via

$$|\psi_T\rangle = U\,|\psi_R\rangle\,. \tag{9.4.12}$$

Quantum mechanically, we saw that U could be written as a product of simple two-qubit gates, but now that we're dealing with fields we need a continuous description of U, the obvious choice being the path-ordered exponential map

$$U = \overleftarrow{\mathcal{P}} \exp\left[-i\int_0^1 H(s)ds\right]. \tag{9.4.13}$$

Here, the path ordering $\overleftarrow{\mathcal{P}}$ is simply to ensure that we are building the circuit from left to right as the 'time'[14] s increases and $H(s)$ is the time-dependent Hamiltonian that generates the evolution from reference to target. In [85], we are invited to consider a continuous sequence of *parametrised* path-ordered exponentials, such

[14] We will call this parameter time, but really we mean a parameter that tracks 'steps' in a quantum circuit as we move from left to right.

that we are considering an one-parameter family of trajectories in the space of unitary transformations

$$U(\sigma) = \overleftarrow{\mathcal{P}} \exp\left[-i\int_0^\sigma H(s)ds\right], \qquad H(s) = \sum_I Y^I(s)\mathcal{O}_I, \tag{9.4.14}$$

where now we expand $H(s)$ into a basis of Hermitian generators $\mathcal{O}_I$ such that any arbitrary gate can be constructed, i.e. $V_I = \exp[-i\epsilon\mathcal{O}_I]$, where ϵ is some small number that ensures we only produce a small change in the state.

The function $Y(s)^I$ is known as the *control function* which determines which gate is being applied at which time. It is a tangent vector in the space of unitaries in a frame bundle tangent to the trajectory $U(\sigma)$, where the control function needs to satisfy the σ-dependent Schrodinger equation

$$\frac{dU(\sigma)}{d\sigma} = Y(\sigma)^I\mathcal{O}_I U. \tag{9.4.15}$$

We see then that a general strategy is to construct an effective quantum Hamiltonian built only out of unitaries we choose, applied at a time we choose.

Given this set of definitions, our reference & target states are then conveniently expressed as

$$|\psi_T\rangle = U(\sigma = 1)\,|\psi_R\rangle\,. \tag{9.4.16}$$

This gives us boundary conditions for our problem: $U(\sigma = 0) = I, U(\sigma = 1) = U$, taking us from the identity to our chosen unitary. Given boundary conditions, it is natural to treat this as a variational calculus problem, meaning we need to find the shortest path between $U(\sigma = 0) = I$ and $U(\sigma = 1)$. Doing so should correspond to the complexity according to the motivation in the previous section.

To that end, we define a general distance functional associated to some particular unitary

$$\mathcal{D}[U] = \int_0^1 ds\ \mathcal{F}(U(s), Y^I(s)), \tag{9.4.17}$$

and $\mathcal{F}$ is known as the *Finsler function* or *cost function*, and ought to satisfy the same requirements we demanded in section 9.4.1 [85, 87], specifically

- Positivity: $\mathcal{F} \geq 0$, with $\mathcal{F} = 0$ iff $Y^I = 0$
- Continuity & Smoothness: $\mathcal{F} \in C^\infty$
- Homogeneity: $F(U, \lambda Y^I) = \lambda F(U, Y^I)$
- Triangle Inequality: $\mathcal{F}(U, Y^I + Y^{I\prime}) \leq \mathcal{F}(U, Y^I) + \mathcal{F}(U, Y^{I\prime})$,

where homogeneity is required in order to ensure that if we were to, for example, halve the time of application but to double the intensity of $H(s)$, the cost should

remain the same. There is still a lot of freedom in choosing the exact cost function $\mathcal{F}$, and different choices have important implications, especially where the Complexity = Action and Complexity = Volume conjectures are concerned [81, 87, 137].

One choice, corresponding to a Riemannian geometry, is the simple distance function, defined by

$$\mathcal{D}(U) = \int_0^1 d\sigma \sqrt{G_{IJ} Y^I(\sigma) Y^J(\sigma)}, \tag{9.4.18}$$

where G_{IJ} is a metric that can be chosen to favour (or penalise) particular velocities Y^I, however in general we will choose the flat Euclidean metric, meaning every velocity is equally favoured.

When you have made a particular choice of distance function, then a theorem due to Nielsen [85] states that, roughly speaking, the minimum of this curve is equal to the complexity[15]. Whichever choice we make, the complexity is then found by *minimising* the distance function $\mathcal{D}$ with respect to σ, better known as finding a geodesic, or simply solving the Euler-Lagrange equations for the cost function $\mathcal{F}$.

In order to make this problem tractable, we will usually adopt a specific set of (hermitian) operators $\mathcal{O}_I$. Typically, this limits us to a local patch on the state manifold, meaning we can only reach specific target states with our effective Hamiltonian. To simplify problems further, we can choose a set of operators that are closed under some lie algebra $\mathfrak{g}$, allowing us to utilise group-theoretic tools in our calculations. In practice, this just means we choose operators that satisfy $[\mathcal{O}_I, \mathcal{O}_J] = i f_{IJ}{}^K \mathcal{O}_K$. This is particularly useful because circuits can now be thought of as trajectories in the group manifold $\mathcal{G}$, with geodesics in $\mathcal{G}$ obviously being the smallest circuits and corresponding to the complexity. We will return to this point at the end of this section.

Let's take a step back and look at the big picture. We want to build the most efficient quantum circuit that takes us from a reference state to a target state, and we know that circuits built from a typical Hamiltonian are inefficient. We therefore choose a set of simple operations $\mathcal{O}_I$ and build an *effective* Hamiltonian, one that depends on a parameter which we can vary, changing the efficiency of the Hamiltonian. If we choose a simple set of operations that forms a closed algebra, we have a natural group structure on which we can vary our parameter and find the most efficient possible effective Hamiltonian with which to build our circuit.

In [87], they computed the complexity for the coupled harmonic oscillator (a simple Gaussian state), and used the natural operators in the problem, x_i and p_i, to define

[15] There are quite a few technical caveats to this claim, mostly related to ensuring we are in a local coordinate patch on the manifold to ensure the distance function is well defined. The full details can be found in [85], but are largely unimportant for our discussion.

a basis of gates V_I

$$H = e^{i\epsilon x_0 p_0}, \qquad J_a = e^{i\epsilon x_0 p_a}, \qquad K_a = e^{i\epsilon x_a p_0}, \tag{9.4.19}$$

$$Q_{ab} = e^{i\epsilon x_a p_b}, \qquad Q_{aa} = e^{\frac{i\epsilon}{2}(x_a p_a + p_a x_a)} = e^{\epsilon/2} e^{i\epsilon x_a p_a}. \tag{9.4.20}$$

Here, x_0 and p_0 are simply numbers, whereas x_a and p_b are the usual operators whose commutation relations are $[x_a, p_b] = i\delta_{ab}$. The gates act on Gaussian states $\psi(x_1, x_2)$ as follows

- H initiates a global phase change $H\psi(x_1, x_2) = e^{i\epsilon x_0 p_0}\psi(x_1, x_2)$
- J_a a shift of x_a by a number ϵx_0, $J_1\psi(x_1, x_2) = \psi(x_1 + \epsilon x_0, x_2)$
- K_a initiates a *local* phase change $K_1\psi(x_1, x_2) = e^{i\epsilon x_1 p_0}\psi(x_1, x_2)$, or a shift of p_a by a constant
- Q_{ab}, $a \neq b$ *entangles* by shifting x_b by ϵx_a, i.e. $Q_{12}\psi(x_1, x_2) = \psi(x_1, x_2 + \epsilon x_1)$
- Q_{aa} rescales x_a by e^ϵ, $Q_{11}\psi(x_1, x_2) = e^{\epsilon/2}\psi(e^\epsilon x_1, x_2)$.

By keeping ϵ small, we ensure that acting with any of these gates produces nothing but a very small change to the wavefunction. In general, these gates may not be enough to take you from a reference to a target state, but by inspection you can extend this set of gates as required. Knowing the target state, one works with the minimal set of gates that can implement the unitary required.

The generators $\mathcal{O}_I = \mathcal{O}_{ab} = ix_a p_b + \frac{1}{2}\delta_{ab}$ naturally form a closed algebra, in this particular case $\mathfrak{gl}(2, R)$. Therefore, for a Gaussian state the unitary operator can be written

$$U(\sigma) = \overrightarrow{\mathcal{P}} \exp\left[i \int_0^\sigma ds \sum_{a,b} Y^{ab}(s)\mathcal{O}_{ab} \right]. \tag{9.4.21}$$

The complexity is now defined as the length of a geodesic trajectory from the identity to $U(\sigma = 1)$. Choosing the Riemannian distance measure, the complexity for a Gaussian state is then given by

$$\mathcal{C} = \mathcal{D}_{\min} = \min\left\{ \int_0^1 ds \sqrt{\sum_{a,b,c,d} G_{ab,cd} Y^{ab}(s) Y^{cd}(s)} \right\}. \tag{9.4.22}$$

There can be multiple such geodesics (for example in [87] they find a one-parameter family), and in this case the complexity is defined as the shortest geodesic.

In order to actually solve eq. 9.4.22, we need to compute the tangent vectors Y^I, which are given implicitly in terms of the generators $\mathcal{O}$ and the unitary in eq. 9.4.15. Knowing the form of the operators $\mathcal{O}$, we *could* solve this for Y, but one could forsee situations where inverting the operators to solve this might be a

cumbersome undertaking. However, if our operators form a closed algebra then we can simply choose an (invertible) matrix representation of the operators instead, i.e. we can choose $\mathcal{O}_I \to \mathcal{O}_{ab} \in GL(2,R)$ in the case of Gaussian states and we can simply to write out $Y^{ab}(s)$ as

$$Y^{ab}(s) = \mathrm{Tr}\left(\frac{dU(s)}{ds}U^{-1}(s)\mathcal{O}^{ab}\right). \tag{9.4.23}$$

This is an example of where the group theoretic approach is extremely useful, since it means that the physical character of the generators is unimportant: we merely need to identify the Lie algebra $\mathfrak{g}$ that they belong to and the treat circuits as trajectories in the group manifold $\mathcal{G}$, using whichever representation of the group is most convenient. The trick here is to choose the simplest basis of matrices that correspond to the operators $\mathcal{O}$ such that we can construct the unitary circuit. With this defined, we have reduced the problem of computing the complexity to minimizing the action

$$\mathcal{D} = \int_0^1 ds \sqrt{\delta_{IJ}\mathrm{Tr}\left(\frac{dU(s)}{ds}U^{-1}(s)\mathcal{O}^I\right)\mathrm{Tr}\left(\frac{dU(s)}{ds}U^{-1}(s)\mathcal{O}^J\right)} = \int_0^1 ds\sqrt{g_{IJ}\dot{x}^I\dot{x}^J}. \tag{9.4.24}$$

From this, we can read off the line element that defines the right invariant metric

$$ds^2 = \delta_{IJ}\mathrm{Tr}\left(dUU^{-1}\mathcal{O}^I\right)\mathrm{Tr}\left(dUU^{-1}\mathcal{O}^J\right). \tag{9.4.25}$$

If we now choose an explicit parameterisation for U (one that reflects the relevant group structure), then we can identify the underlying geometry and, after identifying the relevant boundary conditions, construct the geodesic that corresponds to the complexity.

Factorizable Gaussian States

Let's now consider a specific type of state, namely a factorizable Gaussian state in normal coordinates. We will consider both the reference state $|\psi_R\rangle$ and the target state $|\psi_T\rangle$ to be of this form

$$|\psi_R\rangle = \mathcal{N}\exp\left[-\frac{\omega_0(x_+^2+x_-^2)}{2}\right], \qquad |\psi_T\rangle = \tilde{\mathcal{N}}\exp\left[-\frac{\omega_+x_+^2+\omega_-x_-^2}{2}\right]. \tag{9.4.26}$$

We will focus on two oscillators, although the generalisation to N oscillators follows automatically from the factorization properties.

We could now pick the gates from eq. 9.4.20 that we need to get from one state to the other, noting that we only require the scaling gates provided $\omega_i \in \mathbb{R}$. However,

as we are going to be using matrix representations, it makes more sense to first rewrite the wavefunctions in terms of matrices

$$|\psi_R\rangle = \mathcal{N}_{s=0} \exp\left[-\frac{v_a \cdot A_{ab}(s=0)\cdot v_b}{2}\right], \qquad |\psi_T\rangle = \mathcal{N}_{s=1} \exp\left[-\frac{v_a \cdot A_{ab}(s=1)\cdot v_b}{2}\right], \tag{9.4.27}$$

where $v = \{x_+, x_-\}$, $A(s=0) = \omega_0 \mathbb{1}$ and $A(s=1) = \text{diag}\{\omega_+, \omega_-\}$. The unitaries will now act, in the form in eq. 9.4.14, as

$$A(s=1) = U(s)A(s=0)U^T(s) \tag{9.4.28}$$

$GL(N,\mathbb{R})$ has N^2 generators $\{\mathcal{O}^I\}$, however the geometry defined by this full set of generators will have too many degrees of freedom (coming from the directions that correspond to, for example, the entangling gates, which we know could only increase the complexity since there is no entanglement of the normal modes[16] in the final state). For a general element of $GL(N,\mathbb{R})$, we can perform an Iwasawa decomposition, writing it in terms of the product of an orthogonal matrix, a diagonal matrix, and an upper triangular matrix ($G = KAN$). We could then simply throw away the non-diagonal matrices K, N, knowing that they can only unnecessarily increase the complexity. For $GL(2,\mathbb{R})$, this is even more trivial since we know that a basis of generators is

$$M_{++} = \begin{pmatrix} 1 & 0 \\ 0 & 0 \end{pmatrix}, \quad M_{+-} = \begin{pmatrix} 0 & 1 \\ 0 & 0 \end{pmatrix}, \quad M_{-+} = \begin{pmatrix} 0 & 0 \\ 1 & 0 \end{pmatrix}, \quad M_{--} = \begin{pmatrix} 0 & 0 \\ 0 & 1 \end{pmatrix}. \tag{9.4.29}$$

We can see that we only require those generators with all off-diagonal components zero, meaning we can discard two of them and write

$$U(s) = \exp\left[\alpha_+(s)M_{++} + \alpha_-(s)M_{--}\right], \tag{9.4.30}$$

with $\alpha_\pm \in \mathbb{R}$. Plugging this into eq. 9.4.25, we find the geometry is simply a flat two-dimensional plane with metric

$$ds^2 = d\alpha_+^2 + d\alpha_-^2. \tag{9.4.31}$$

This picks out a specific subspace in the broader geometry of the $GL(2,\mathbb{R})$ group, as first noted in [87]. Geodesics are trivially obtained in this spacetime, and are of the form

$$\alpha_\pm(s) = \alpha_\pm(s=1)s + \alpha_\pm(s=0). \tag{9.4.32}$$

We need to find boundary conditions now, and we do so by acting with the unitary on the reference wavefunction to find

$$A(s=1) = U(s)A(s=0)U^T(s) = \text{diag}\{e^{2\alpha_+}\omega_0, e^{2\alpha_-}\omega_0,\} = \text{diag}\{\omega_+, \omega_-\}. \tag{9.4.33}$$

[16] This doesn't imply that there is no entanglement in the positions or momenta, just none in the normal modes.

We find then that the boundary conditions are

$$\alpha_{\pm}(s=0)=0, \qquad \alpha_{\pm}(s=1)=\frac{1}{2}\log\frac{\omega_{\pm}}{\omega_0}. \tag{9.4.34}$$

The complexity is given by

$$\mathcal{C}[U]=\int_0^1 ds\sqrt{g_{IJ}\dot{x}^I\dot{x}^J}=\int_0^1 ds\sqrt{g_{IJ}\frac{d\alpha_I}{ds}\frac{d\alpha_J}{ds}} \tag{9.4.35}$$

$$=\frac{1}{2}\sqrt{\left(\log\frac{\omega_+}{\omega_0}\right)^2+\left(\log\frac{\omega_-}{\omega_0}\right)^2}. \tag{9.4.36}$$

9.4.3 Fubini-Study Complexity

Instead of considering complexity as corresponding to a geometric distance on the space of unitaries, we could consider distance on the space of states – using the Fubini-Study metric we derived in eq. 9.4.6. We discussed in section 9.4.1 why the naïve Fubini-Study distance fails to capture the subtle distinctions between states. We call this measure "naïve" since it doesn't take into account exactly how one gets between the reference and target states: generic geodesics on $\mathbb{CP}^n$ can pass through any intermediate states, perhaps those that might require an absurdly vast number of two-qubit operations to reach. However, we could restrict ourselves to curves which only pass through states with low complexity, or rather curves corresponding to a specific set of generators $\mathcal{O}$, a procedure first presented in [88].

In the last subsection, we related reference and target states via unitary transformations, and computed the complexity associated to some particular unitary by tracing out a geodesic in the space of unitaries. However, using the Fubini-Study approach we instead parametrize the state itself, which in practice means casting the target state into coherent state form (an eigenstate of the lowering operator a_-). As in the previous section, it is advantageous to construct the coherent state group-theoretically, which in this case is described eloquently by Perelomov [138, 139] and Gilmore [140].

In this thesis, we will consider bosonic (fermionic) coherent states that are elements of $SU(1,1)$ ($SU(2)$), which transform under the group action as discussed in appendix B. As before, the complexity corresponds to geodesics in the geometry prescribed by $SU(1,1)$ ($SU(2)$), which we find by varying the state parameters and defining our reference and target states via the geometric boundary conditions.

We again consider a path-ordered exponential unitary as in eq. 9.4.14, now

generated by $\mathcal{O}_\mu \in \mathfrak{su}(1,1)$ or $\mathfrak{su}(2)$, meaning a generic state can be defined via

$$|\psi(\sigma)\rangle = \overleftarrow{\mathcal{P}} \exp\left[-i\int_0^\sigma \mathcal{H}(s)ds\right]|\psi_R\rangle\,, \qquad \mathcal{H}(s) = \dot{\lambda}^\mu(s)\mathcal{O}_\mu(\sigma). \tag{9.4.37}$$

The general procedure is to write the reference and target states as generic $SU(1,1)$ or $SU(2)$ coherent states[17] as in eq. B.0.19

$$SU(1,1): \qquad |\psi(\sigma)\rangle = e^{\alpha_+(\sigma)K^+ + \alpha_-(\sigma)K^- + \omega(\sigma)K^0}|\psi_0\rangle = U(\sigma)|\psi_0\rangle\,, \tag{9.4.38}$$

$$SU(2): \qquad |\psi(\sigma)\rangle = e^{\alpha_+(\sigma)S_+ + \alpha_-(\sigma)S_- + \omega(\sigma)S_z}|\psi_0\rangle = U(\sigma)|\psi_0\rangle\,, \tag{9.4.39}$$

where we parameterise the coefficients that determine the state by σ.

In this section we will focus on $SU(1,1)$, however as we will seen in chapter 11, the procedure for $SU(2)$ follows directly.

Using the identity in eq. B.0.20, together with the fact that K^- annihilates ψ_0 (see eq. B.0.16) and that $K^0|\psi_0\rangle = a|\psi_0\rangle$ with a a constant, we can recast a generic $SU(1,1)$ state as

$$|\psi(\sigma)\rangle = \mathcal{N}(\sigma)e^{\gamma^+(\sigma)K^+}|\psi_0\rangle\,, \tag{9.4.40}$$

where $\mathcal{N}(\sigma) = e^{a\ln\gamma^0}$ and choosing the generators in eq. B.0.16 we find that $a = \frac{1}{2}$.

This is a generic state for a single mode, however we wish to consider N modes, and thus we will need to consider an N mode state. For our ground state we have

$$|\psi_0\rangle = \prod_{k=0}^{N-1}|k,-k\rangle\,, \tag{9.4.41}$$

and a generic state is then built out of this

$$|\psi(\sigma)\rangle = \prod_{k=0}^{N-1}\mathcal{N}_k(\sigma)e^{\gamma_k^+(\sigma)K_k^+}|k,-k\rangle\,. \tag{9.4.42}$$

Since these generators only permit specific operations (corresponding to gates from some set, i.e. eq 9.4.20), paths on state space parameterised by σ will only take you to the target via relatively simple states. Ultimately, this requires that we choose the Fubini-Study cost function[18]

$$\mathcal{F} = \langle\partial_\sigma\psi|\partial_\sigma\psi\rangle - \langle\partial_\sigma\psi|\psi\rangle\langle\psi|\partial_\sigma\psi\rangle\,. \tag{9.4.43}$$

[17] There are coherent states associated with other Lie algebras, however for our purposes we won't consider them, even though their construction ought to follow in the same manner.

[18] This is nothing but the Fubini-Study metric where we have demanded that the path depends on our parameter σ

We can derive this if we consider the state above in eq. 9.4.42, however we will supress the k indices until the end of the derivation

$$\partial_\sigma |\psi(\sigma)\rangle = \frac{\left(\gamma^{0'}(\sigma) + 2\gamma^0(\sigma)\gamma^{+'}(\sigma)K^+\right)}{2\sqrt{\gamma^0(\sigma)}} e^{\gamma^+(\sigma)K^+} |\psi_0\rangle \tag{9.4.44}$$

$$= \left[\frac{1}{2}\frac{\gamma^{0'}(\sigma)}{\gamma^0(\sigma)} + \gamma^{+'}(\sigma)K^+\right] |\psi(\sigma)\rangle\,, \tag{9.4.45}$$

which leads to

$$\langle\psi(\sigma)|\partial_\sigma|\psi(\sigma)\rangle = \frac{\gamma^{0'}(\sigma)}{2\gamma^0(\sigma)} + \gamma^{+'}(\sigma)\langle K^+\rangle\,. \tag{9.4.46}$$

In order to compute the expectation value $\langle K^+\rangle = \langle\psi(\sigma)|K^+|\psi(\sigma)\rangle$, we need to consider the effect of unitary transformations on the generators K_i. We could consider the conjugation of a single generator gK_ig^{-1}, however it is simpler to consider a matrix operation of the form

$$U(\sigma)^\dagger K^i U(\sigma) = M_{ij}K^j \tag{9.4.47}$$

Meaning we can write

$$\langle\psi(\sigma)|K^+|\psi(\sigma)\rangle = M_{+j}\langle\psi_0|K^j|\psi_0\rangle \tag{9.4.48}$$

$$= \frac{1}{2}M_{+0}, \tag{9.4.49}$$

where we have used $\langle\psi_0|K^+|\psi_0\rangle = \langle\psi_0|K^-|\psi_0\rangle = 0$. This leads to

$$\langle\psi(\sigma)|\partial_\sigma|\psi(\sigma)\rangle = \frac{1}{2}\left[\frac{\gamma^{0'}(\sigma)}{\gamma^0(\sigma)} + \gamma^{+'}(\sigma)M_{+0}\right], \tag{9.4.50}$$

where we still need to work out M_{+0}. Squaring this, we find

$$|\langle\psi(\sigma)|\partial_\sigma|\psi(\sigma)\rangle|^2 = \frac{1}{4}\left[\frac{\gamma^{0'}(\sigma)^*}{\gamma^0(\sigma)^*} + \gamma^{+'}(\sigma)^*M_{-0}\right]\left[\frac{\gamma^{0'}(\sigma)}{\gamma^0(\sigma)} + \gamma^{+'}(\sigma)M_{+0}\right], \tag{9.4.51}$$

The first piece of eq. 9.4.43 is calculated analogously, with

$$\langle\partial_\sigma\psi|\partial_\sigma\psi\rangle = \langle\psi|\left[\frac{1}{2}\frac{\gamma^{0'}(\sigma)^*}{\gamma^0(\sigma)^*} + \gamma^{+'}(\sigma)^*K^{+*}\right]\left[\frac{1}{2}\frac{\gamma^{0'}(\sigma)}{\gamma^0(\sigma)} + \gamma^{+'}(\sigma)K^+\right]|\psi\rangle \tag{9.4.52}$$

$$= \frac{1}{4}\left[\frac{\gamma^{0'}(\sigma)^*}{\gamma^0(\sigma)^*} + \gamma^{+'}(\sigma)^*M_{-0}\right]\left[\frac{\gamma^{0'}(\sigma)}{\gamma^0(\sigma)} + \gamma^{+'}(\sigma)M_{+0}\right] + |\gamma^{+'}|^2\langle\psi(\sigma)|K^{+*}K^+|\psi(\sigma)\rangle \tag{9.4.53}$$

Plugging this into eq. 9.4.43, we find

$$\mathcal{F} = |\gamma^{+'}|^2 \langle\psi(\sigma)|K^- K^+|\psi(\sigma)\rangle \tag{9.4.54}$$

$$= |\gamma^{+'}|^2 N_{-i} N_{+j} \langle\psi_0|K^i K^j|\psi_0\rangle \tag{9.4.55}$$

$$= |\gamma^{+'}|^2 N_{--} N_{++}, \tag{9.4.56}$$

where we have used $\langle\psi_0|K^- K^-|\psi_0\rangle = \langle\psi_0|K^+ K^+|\psi_0\rangle = 0$. One can show that we can write $N_{--}N_{++}$ as [98]

$$N_{--}N_{++} = \frac{1}{|\gamma^0|^2}, \tag{9.4.57}$$

and using eq. B.0.25, restoring the index k, we can write the final result – the Fubini-Study line element

$$ds = \sum_k^{N-1} ds_k^2 = \sum_k^{N-1} \frac{|d\gamma_k^+|^2}{(1-|\gamma_k^+|^2)^2}. \tag{9.4.58}$$

We can use this to define the distance on $\mathbb{CP}^n$

$$D_{FS} = \sqrt{\sum_k^{N-1} s_k^2}, \tag{9.4.59}$$

and the distance for a given k is

$$s_k = \int_0^1 d\sigma \frac{1}{1-|\gamma_k^+(\sigma)|^2} \left|\frac{d\gamma_k^+(\sigma)}{d\sigma}\right|. \tag{9.4.60}$$

With this distance in mind, we define the complexity as the minimal length of this curve as determined by the $\gamma^+(\sigma)$, i.e.

$$\mathcal{C} = \min_{\gamma^+(\sigma)} \{D_{FS}\} \tag{9.4.61}$$

We need to introduce a σ-dependent paramaterisation of γ^+ in order to compute the geometry on which to derive the complexity geodesic. Knowing that $|\gamma_{k,\sigma}| \leq 1$ by unitarity, we choose

$$\gamma_k^+(\sigma) = |\gamma_k| \exp(i\,\phi_k(\sigma)) \quad , \quad |\gamma_k| = \tanh\left(\frac{\theta_k(\sigma)}{2}\right). \tag{9.4.62}$$

Plugging this in to eq. 9.4.60 then gives a simple hyperbolic geometry $\mathbb{H}^2$

$$ds^2 = \frac{1}{4}\sum_{k=0}^{N-1}(d\theta_k^2 + \sinh(\theta_k)^2 d\phi_k^2). \tag{9.4.63}$$

Our goal having derived this metric is to simply compute the geodesic having identified suitible boundary conditions. We will see this is action repeatedly over the next two chapters.

9.4.4 Covariance Matrix Complexity

The physical content of a generic Gaussian state can be completely characterized not only its wavefunction, but also by its *covariance matrix*. This alternative representation of an N-dimensional system comes from describing it directly on $2N$-dimensional phase space $\mathbb{R}^{2N}$ [141–145], with canonical coordinates $\xi = [x_1, p_1, x_2, p_2 ..., x_N, p_N] \in \mathbb{R}^{2N}$.

The two point function of any generic quantum state may be written as

$$\langle\psi|\xi^a\xi^b|\psi\rangle = \frac{1}{2}\langle\psi|\{\xi^a,\xi^b\} + [\xi^a,\xi^b]|\psi\rangle = G^{a,b} + i\Omega^{a,b}, \tag{9.4.64}$$

where ξ^a is a (dimensionless) operator on phase-space and $\Omega^{a,b}$ is the symplectic form. For bosonic states, $\Omega^{a,b}$ is completely fixed by the canonical commutation relations to be

$$\Omega^{a,b} = \begin{pmatrix} 0 & \mathbb{1} \\ -\mathbb{1} & 0 \end{pmatrix}, \tag{9.4.65}$$

and is in some sense trivial, simply encoding the commutation relations. For a fermionic system, the opposite is true, and $G^{a,b} = \delta_{a,b}$ is trivial, whereas Ω characterizes the fermionic Gaussian states.

In this formalism, the Robertson–Schrödinger uncertainty principle demands that $G^{a,b} + i\Omega^{a,b} \geq 0$, where $G^{a,b}$ is a real, positive definite symmetric matrix known as the covariance matrix.

For a pure bosonic (fermionic) Gaussian state with mean(s) $\langle\psi|\xi^a|\psi\rangle = 0$, the state is entirely characterized by $G_{a,b}$ ($\Omega_{a,b}$), where

$$G^{a,b} = \frac{1}{2}\langle\psi|\{\xi^a,\xi^b\}|\psi\rangle, \qquad i\Omega_{a,b} = \frac{1}{2}\langle\psi|[\xi^a,\xi^b]|\psi\rangle. \tag{9.4.66}$$

Under these circumstances, the objects $G_{a,b}$ and $\Omega_{a,b}$ are simply the *correlation matrices* discussed in section 9.2.7, meaning we can use the correlation matrix and covariance matrix interchangeably when the situation allows.

For a mixed bosonic (fermionic) Gaussian state with $\mathrm{Tr}\,(\rho\xi^a) = 0$, we have

$$G^{a,b} = \mathrm{Tr}\,(\rho\{\xi^a,\xi^b\}), \qquad i\Omega_{a,b} = \mathrm{Tr}\,(\rho[\xi^a,\xi^b]). \tag{9.4.67}$$

Since this is simply the two-point function, Wicks theorem tells us that we can use it to construct any higher point functions we need. In order to compute the complexity, we consider the transformation from a reference covariance matrix to a target, taking the unitary doing the transformations to be the same as in the previous sections

$$G_T = U^\dagger(\sigma)G_T U(\sigma), \qquad U(\sigma) = \overleftarrow{\mathcal{P}}\exp\left[-i\int_0^\sigma K(s)ds\right], \qquad K(s) = \sum_I Y^I(s)K_I \tag{9.4.68}$$

The complexity is then given as before

$$C(U) = \int ds \sqrt{\sum_I |Y^I(s)|^2} \tag{9.4.69}$$

Where we have again assumed the same penalty factor for each gate, i.e. $G_{IJ} = \delta_{IJ}$.

Given a particular parameterisation of $U(\sigma)$, one can derive the (right invariant) line element from eq. 9.4.68, determine the boundary conditions and use the methods of differential geometry to determine the complexity, as in the previous two sections.

Let's consider the state

$$\psi(x) = \left(\frac{a}{\pi}\right)^{1/4} \exp\left(-\frac{1}{2}(a+ib)x^2\right). \tag{9.4.70}$$

We can easily compute the two point functions of this state, for example

$$\begin{aligned}\langle\psi|\{\xi^1,\xi^1\}|\psi\rangle &= 2\langle\psi|x^2|\psi\rangle = 2\sqrt{\frac{a}{\pi}}\int dx x^2 e^{-ax^2} \\ &= 2\sqrt{\frac{a}{\pi}}\frac{\partial}{\partial a}\int dx e^{-ax^2} = \frac{1}{a},\end{aligned} \tag{9.4.71}$$

$$\begin{aligned}\langle\psi|\{\xi^1,\xi^2\}|\psi\rangle &= \langle\psi|x\partial_x + \partial_x x|\psi\rangle = -i + \sqrt{\frac{a}{\pi}}\int dx e^{-\frac{1}{2}(a-ib)x^2} x\partial_x e^{-\frac{1}{2}(a+ib)x^2} \\ &= -i - 2i\sqrt{\frac{a}{\pi}}(a+ib)\int dx x^2 e^{-2ax^2} = -i(1-\frac{a+ib}{a}) = -\frac{b}{a}.\end{aligned} \tag{9.4.72}$$

This results in the covariance matrix

$$G = \begin{pmatrix} \frac{1}{a} & -\frac{b}{a} \\ -\frac{b}{a} & \frac{a^2+b^2}{a^2}. \end{pmatrix} \tag{9.4.73}$$

In order to compute the transformation that takes you between reference and target states, we will consider a general symplectic transformation of $SP(2N,\mathbb{R})$, which acts on the covariance matrices as discussed in appendix B. Specifically,

$$G^{a,b}(\sigma) = \frac{1}{2}\langle\psi(\sigma)|\{\xi^a,\xi^b\}|\psi(\sigma)\rangle \tag{9.4.74}$$

$$= \frac{1}{2}\langle\psi(0)|e^{i\sigma K}\{\xi^a,\xi^b\}e^{-i\sigma K}|\psi(0)\rangle \tag{9.4.75}$$

$$= \frac{1}{2}U(\sigma)^a{}_c U(\sigma)^b{}_d \langle\psi(0)|\{\xi^c,\xi^d\}|\psi(0)\rangle \tag{9.4.76}$$

$$= U(\sigma)^a{}_c U(\sigma)^b{}_d G^{cd}(0). \tag{9.4.77}$$

Given this, we find then that the general evolution of the covariance matrix

$$G_T = U G_R U^T. \tag{9.4.78}$$

Suppose we wanted to compute the complexity for the reference and target states given by eq. 9.4.26. The covariance matrix representations of these states would be given by

$$G_R = \begin{pmatrix} \frac{1}{\omega_0} & 0 & 0 & 0 \\ 0 & \omega_0 & 0 & 0 \\ 0 & 0 & \frac{1}{\omega_0} & 0 \\ 0 & 0 & 0 & \omega_0 \end{pmatrix}, \qquad G_T = \begin{pmatrix} \frac{1}{\omega_+} & 0 & 0 & 0 \\ 0 & \omega_+ & 0 & 0 \\ 0 & 0 & \frac{1}{\omega_-} & 0 \\ 0 & 0 & 0 & \omega_- \end{pmatrix}. \tag{9.4.79}$$

As in the case of the state representation, we see that the covariance matrices trivially factorize in this (normal mode) basis

$$G_R = G_R^0 \oplus G_R^0, \qquad G_T = G_T^+ \oplus G_T^-. \tag{9.4.80}$$

This allows us to work with a single 2×2 matrix (since both reference and target are diagonal), noting that any geometry or complexity that we derive will now have to be a sum over both $\pm$ modes, or more generally over k blocks each corresponding to a pair $\{x_k, p_k\}$, i.e.

$$ds^2 = \sum_k ds_k^2, \qquad \mathcal{C} = \sum_k \mathcal{C}_k. \tag{9.4.81}$$

We see then that we only need to consider a single mode at a time, meaning we can consider the reference and target covariance matrices

$$G_R^0 = \begin{pmatrix} \frac{1}{\omega_0} & 0 \\ 0 & \omega_0 \end{pmatrix}, \qquad G_T^\pm = \begin{pmatrix} \frac{1}{\omega_\pm} & 0 \\ 0 & \omega_\pm \end{pmatrix}. \tag{9.4.82}$$

To make computations easier, it is advantageous to change basis using a squeezing operator, i.e.

$$\tilde{G}_R^0 = S G_R^0 S^T, \qquad \tilde{G}_T^\pm = S G_T^\pm S^T, \qquad S = \begin{pmatrix} \sqrt{\omega_0} & 0 \\ 0 & \frac{1}{\sqrt{\omega_0}} \end{pmatrix}. \tag{9.4.83}$$

This results in

$$\tilde{G}_R^0 = \mathbb{1}, \qquad \tilde{G}_T^\pm = \begin{pmatrix} \frac{\omega_0}{\omega_\pm} & 0 \\ 0 & \frac{\omega_\pm}{\omega_0} \end{pmatrix}. \tag{9.4.84}$$

In order to actually compute the complexity, we need to find the geodesic that takes us from

$$\tilde{G}_T^\pm(\sigma) = U(\sigma)^T \tilde{G}_R^0 U(\sigma). \tag{9.4.85}$$

As before, we could decide to consider only the submanifold generated by the scaling gate, since adding any off-diagonal terms during intermediate steps will always increase the complexity, because both reference and target are diagonal. However, it is instructive to derive the full geometry and see how this subspace emerges, and so we will consider the full general parameterisation of $U \in SP(2,\mathbb{R})$

$$U_\pm(\phi,\rho,\theta) = \begin{pmatrix} \cos\phi_\pm \cosh\rho_\pm - \sin\theta_\pm \sinh\rho_\pm & -\sin\phi_\pm \cosh\rho_\pm + \cos\theta_\pm \sinh\rho_\pm \\ \sin\phi_\pm \cosh\rho_\pm + \cos\theta_\pm \sinh\rho_\pm & \cos\phi_\pm \cosh\rho_\pm + \sin\theta_\pm \sinh\rho_\pm \end{pmatrix}. \tag{9.4.86}$$

Plugging this into eq. 9.4.85 and defining $\beta_\pm \equiv \phi_\pm + \theta_\pm$, we find that we need to solve the system

$$\begin{pmatrix} \cosh(2\rho_\pm) - \sin(\beta_\pm)\sinh(2\rho_\pm) & \cos(\beta_\pm)\sinh(2\rho_\pm) \\ \cos(\beta_\pm)\sinh(2\rho_\pm) & \cosh(2\rho) + \sin(\beta_\pm)\sinh(2\rho_\pm) \end{pmatrix} = \begin{pmatrix} \frac{\omega_0}{\omega_\pm} & 0 \\ 0 & \frac{\omega_\pm}{\omega_0} \end{pmatrix}. \tag{9.4.87}$$

A particular solutions is

$$\rho_\pm(\sigma=1) = \frac{1}{2}\log\left(\frac{\omega_\pm}{\omega_0}\right), \qquad \rho(\sigma=1)_\pm = 0, \qquad \beta_\pm = \phi_\pm + \theta_\pm = \frac{\pi}{2}. \tag{9.4.88}$$

We can of course use eq. 9.4.86 along with eq. 9.4.68 to derive the full geometry (assuming now that ρ, θ, ϕ all depend on s), i.e. we take

$$ds_k^2 = \delta_{IJ}\mathrm{Tr}\left(\frac{dU_k}{ds}U_k^{-1}K^I\right)\mathrm{Tr}\left(\frac{dU_k}{ds}U_k^{-1}K^J\right) \tag{9.4.89}$$

$$= d\rho_k^2 + \cosh(2\rho_k)\sinh^2\rho_k d\theta_k^2 - \sinh^2(2\rho) d\theta_k d\phi_k + \cosh^2\rho_k \cosh(2\rho_k) d\phi_k^2 \tag{9.4.90}$$

Where $k = \pm$ and

$$K^I = \left[\begin{pmatrix} 1 & 0 \\ 0 & -1 \end{pmatrix}, \begin{pmatrix} 0 & 0 \\ -\sqrt{2} & 0 \end{pmatrix}, \begin{pmatrix} 0 & \sqrt{2} \\ 0 & 0 \end{pmatrix}\right]^T \tag{9.4.91}$$

The *full* geometry is then given by

$$ds^2 = \sum_k ds_k^2 \tag{9.4.92}$$

In the case of the particular solution derived, we see that θ_k and ϕ_k are constant, and as such the full geometry is reduced simply to flat space, as before

$$ds^2 = d\rho_+^2 + d\rho_-^2 \tag{9.4.93}$$

Geodesics are again trivial

$$\rho_k(\sigma) = \rho_k(\sigma=1)\sigma + \rho_k(\sigma=0) = \frac{1}{2}\log\left(\frac{\omega_k}{\omega_0}\right)\sigma \tag{9.4.94}$$

The complexity is then given by

$$C(U) = \int_0^1 d\sigma \sqrt{g_{ij} \frac{d\rho_i}{d\sigma} \frac{d\rho_j}{d\sigma}} = \frac{1}{2} \sqrt{\log\left(\frac{\omega_+}{\omega_0}\right)^2 + \log\left(\frac{\omega_-}{\omega_0}\right)^2} \tag{9.4.95}$$

We will see more general examples, with less trivial geometries, in the next two chapters.

X

Time Evolution of Complexity: A Critique of Three Methods

> *"One of the symptoms of an approaching nervous breakdown is the belief that one's work is terribly important."*
>
> – Bertrand Russell, *The Conquest of Happiness*

In the previous chapter we discussed three different proposals for computing the complexity in a generic quantum field theory. A natural place to begin investigations into the *growth* of complexity in quantum field theories is to look at the simplest possible examples of dynamical theories. In [92, 94], the growth of complexity was studied for a quenched free scalar field, a simple example of a field theory with controlled evolution. This was then compared with the growth of entanglement entropy, and it was shown in [94] that the complexity does indeed probe features that the entanglement entropy cannot. In this chapter, we will compare the three proposals we discussed by considering a simple model of a free scalar field. We will compare two different information theoretic measures with which to explore each method: the fidelity introduced in section 9.4.1, and the *Loschmidt echo*, a closely related quantity. Strictly speaking, the Loschmidt echo is a special case of the fidelity, defined as the fidelity between a reference state $\langle\psi|$ and a target state that has been forward and then backward evolved in time. One begins with a reference state $|\psi_0\rangle$, forward evolves with a Hamiltonian H_1, backwards evolves with a *different* Hamiltonian H_1' (typically a slightly perturbed Hamiltonian H_1, although in the case of complexity we can consider an arbitrary different Hamiltonian) to find the reference and target states

$$|\psi_0\rangle\,, \qquad |\psi_2\rangle = e^{iH_1't}e^{-iH_1t}\,|\psi_0\rangle\,. \tag{10.0.1}$$

The Loschmidt echo is defined as

$$\mathcal{F}_{\text{LE}} = |\langle\psi_0|\psi_2\rangle|\ . \tag{10.0.2}$$

This overlap can be thought of as the $\mathbb{CP}^1$ distance between two states, defined by a reference state and a product of simple unitaries. The overlap distance does

not, however, uniquely correspond to any one particular set of evolutions, but to at least[1] $(\frac{n}{2}+1)$ possible ways of acting with n (for n even) unitaries. For example, one of the states is obtained from forward evolving a reference state $|\psi_0\rangle$ in time $(|\psi_1\rangle = \exp(-iH_1 t)|\psi_0\rangle)$, with the other again a state that we get by forward evolving the same reference state with slightly different Hamiltonian $(|\tilde{\psi}_1\rangle = \exp(-iH_1')|\psi_0\rangle)$. Abusing the nomenclature slightly, we will call this specific form of overlap between these two wave functions simply the fidelity

$$\tilde{\mathcal{F}} = |\langle\tilde{\psi}_1|\psi_1\rangle|. \tag{10.0.3}$$

As we know from section 9.4.1, these two quantities have the same value, making it insensitive to the specific details of the evolution, which only depends on the the Hamiltonians H_1 and H_1' and the reference state $|\psi_0\rangle$ [146]. However, the different overlaps contain important physical information about the underlying system, and as such the central question addressed in this chapter is, "*Is there any difference between* $\mathcal{F}_{\text{LE}}$ *and* $\tilde{\mathcal{F}}$*?*"

Our central result is that the *complexity* can distinguish the difference between $\mathcal{F}_{\text{LE}}$ and $\tilde{\mathcal{F}}$, but as we will see, not all measures of complexity are equal.

10.1 The Model and Quench Protocol

In order to investigate the differences between the two, we will compute the complexity – using all three methods – for a simple free bosonic field theory defined on a lattice and described by the Hamiltonian

$$H(q,\hat{q},q') = \frac{1}{2}\sum_l \left[p_l^2 + q^2\, x_l^2 + \hat{q}\, q'\; x_{l+1}x_l\right] \ . \tag{10.1.1}$$

Where we have set the lattice spacing to unity. The Hamiltonian is parameterized by $\{q,\hat{q},q'\}$, making the theory very general and allowing one to explore various interesting phenomena and a natural testing ground for our procedure.

We can diagonalise this Hamiltonian in the normal way, by expanding it in fourier modes

$$x_l = \frac{1}{\sqrt{N}}\sum_k e^{-i\frac{2\pi k\, l}{N}}\tilde{x}_k \quad , \quad p_l = \frac{1}{\sqrt{N}}\sum_k e^{-i\frac{2\pi k\, l}{N}}\tilde{p}_k \ , \tag{10.1.2}$$

where $0 \le k \le (N-1)$ with N being the total number of (lattice) sites. Plugging

[1] We assume that none of the unitaries commute.

this in, we find

$$H(q,\hat{q},q') = \frac{1}{2N}\sum_{l=0}^{N-1}\sum_{k,k'} e^{-i\frac{2\pi l}{N}(k+k')}\left[\tilde{p}_k\tilde{p}_{k'} + q^2\tilde{x}_k\tilde{x}_{k'} + \hat{q}q' e^{\frac{-i2\pi k}{N}}\tilde{x}_k\tilde{x}_{k'}\right] \tag{10.1.3}$$

$$= \frac{1}{2N}\sum_{k,-k'}\sum_{l=0}^{N-1} e^{-i\frac{2\pi l}{N}(k-k')}\left[\tilde{p}_k\tilde{p}_{-k'} + (q^2 + \hat{q}q' e^{\frac{-i2\pi k}{N}})\tilde{x}_k\tilde{x}_{-k'}\right] \tag{10.1.4}$$

$$= \frac{1}{2}\sum_k \left[\tilde{p}_k\tilde{p}_{-k} + \omega_k^2\tilde{x}_k\tilde{x}_{-k}\right]. \tag{10.1.5}$$

Where we have used the orthogonality condition $\sum_{l=0}^{N-1} e^{-i\frac{2\pi l}{N}(k-k')} = N\delta_{k,k'}$ and defined $\omega^2 = q^2 + \hat{q}q'\cos\left(\frac{2\pi k}{N}\right)$. Introducing the creation and annihilation operators

$$\tilde{x}_k = \frac{1}{\sqrt{2\omega_k}}\left(a_k + a^\dagger_{-k}\right) \quad , \quad \tilde{p}_k = \frac{1}{i}\sqrt{\frac{\omega_k}{2}}\left(a_k - a^\dagger_{-k}\right). \tag{10.1.6}$$

We rewrite the Hamiltonian in its standard diagonal form

$$H(q,\hat{q},q') = \sum_k \omega_k\left(a_k^\dagger a_k + 1/2\right) \ , \tag{10.1.7}$$

We are interested in studying quenches in the above model, employing the protocol

$$H = H(q,\hat{q},q') \qquad \text{for } t \le 0 \tag{10.1.8a}$$

$$H = H_1(q_1,\hat{q}_1,q_1') \quad \text{for } t > 0 \ , \tag{10.1.8b}$$

where $(q,\hat{q},q')$ and $(q_1,\hat{q}_1,q_1')$ are different. For $t \le 0$, we prepare the system in the ground state of $H(q,\hat{q},q')$; then we evolve the state by $U_1(t) = \exp[-i\,H_1(q_1,\hat{q}_1,q_1')\,t]$. In what follows, we will consider the evolution of the complexity following the quench, treating the $t \le 0$ state as the reference and $t > 0$ as the target. To do so, we first need to compute the reference and (time-evolved) target wavefunctions.

To compute the ground state of 10.1.8a, we consider

$$\psi_0(\tilde{x}_k) = \prod_{k=0}^{N-1}\mathcal{N}_k(t=0)\exp\Big(-\frac{1}{2}\,\omega_k\,\tilde{x}_k^2\Big), \tag{10.1.9}$$

where $\mathcal{N}_k(t=0) = \left(\frac{\omega_k}{\pi}\right)^{1/4}$.

We are interested in finding the position representation of the target time evolved state

$$|\psi(t)\rangle = e^{-iH_1(q,\hat{q},q')t}\,|\psi_0\rangle\,, \tag{10.1.10}$$

for $t > 0$. This is easily computed via

$$\begin{aligned}\psi(\tilde{x}_k, t) &= \langle x_k|\psi(t)\rangle \\ &= \langle \tilde{x}_k|\, e^{-iH_1 t}\, |\psi_0\rangle \\ &= \int d\tilde{x}'_k\ \ \langle \tilde{x}_k|\, e^{-iH_1 t}\, |\tilde{x}'_k\rangle\, \langle \tilde{x}'_k|\psi_0\rangle \\ &= \prod_{k=0}^{N-1} \mathcal{N}_k(t=0) \int d\tilde{x}'_k\ K(\tilde{x}_k, t|\tilde{x}'_k, 0) \exp\Big(-\frac{1}{2}\,\omega_k\,\tilde{x}'^2_k\Big)\end{aligned} \tag{10.1.11}$$

where

$$K(\tilde{x}_k, t|\tilde{x}'_k, 0) = \sqrt{\frac{\omega_{1,k}}{2\pi i \sin(\omega_{1,k}\, t)}} \exp\Big(\frac{i\,\omega_{1,k}}{2\sin(\omega_{1,k}\, t)}\Big[((\tilde{x}_k)^2 + (\tilde{x}'_k)^2)\cos(\omega_{1,k}\, t)\Big] - 2\,\tilde{x}_k\,\tilde{x}'_k\Big)\ . \tag{10.1.12}$$

Using the identity

$$\int dx e^{-ax^2+bx} = \sqrt{\frac{\pi}{a}}\, e^{\frac{b^2}{4a}}, \tag{10.1.13}$$

we can compute the Gaussian integral(s) to obtain

$$\psi(\tilde{x}_k, t) = \prod_{k=0}^{N-1} \mathcal{N}_k(t) \exp\Big(-\frac{1}{2}\Omega_k \tilde{x}_k^2\Big)\ , \tag{10.1.14}$$

where

$$\Omega_k = \omega_{1,k}\Big[\frac{\omega_{1,k} - i\,\omega_k \cot(\omega_{1,k}\, t)}{\omega_k - i\,\omega_{1,k}\cot(\omega_{1,k}\, t)}\Big], \tag{10.1.15}$$

$$\mathcal{N}_k = \Big(\frac{\omega_k}{\pi}\Big)^{1/4} \sqrt{\frac{1}{\omega_k - i\,\omega_{1,k}\cot(\omega_{1,k}\, t)}} \sqrt{\frac{\omega_{1,k}}{i\,\sin(\omega_{1,k}\, t)}}. \tag{10.1.16}$$

10.2 Quench Complexity á la Nielsen

With the reference and target states in hand, let's begin by computing the complexity for this model using the first method introduced in section 9.4. For this method, it's useful to write the state in matrix form

$$\psi^{\tau=1}(\tilde{x}, t) = \mathcal{N}^{\tau=1}(t)\ \exp\Big[-\frac{1}{2}\Big(v_a . A^{\tau=1}_{ab} . v_b\Big)\Big]\ , \tag{10.2.1}$$

where $v = \{\tilde{x}_0, \cdots \tilde{x}_{N-1}\}$ and $A^{\tau=1}$ is an $N \times N$ diagonal matrix

$$A^{\tau=1} = \mathrm{diag}\{\Omega_0, \cdots, \Omega_k\}. \tag{10.2.2}$$

Also we take the reference as (in the same basis v)

$$A^{\tau=0} = \text{diag}\{\omega_r, \cdots, \omega_r\}. \tag{10.2.3}$$

As these are both diagonal, we have a similar situation to the one in section 9.4.2, except now ω_r can in general be complex. Hence, similarly as before, $\tilde{U}(\tau)$ will take the form

$$\tilde{U}(\tau) = \exp\left(\sum_{k=0}^{N-1} \alpha^k(\tau) M_k^{diag}\right) , \tag{10.2.4}$$

where the $\{\alpha_k(\tau)\}$ are complex, and the $\{M_k^{diag}\}$ are the N diagonal generators of GL(N, R), analogous to M_{++} and M_{--} in eq. 9.4.29 in the $N = 2$ case. As before, we obtain a flat metric

$$ds^2 = \sum_{k=0}^{N=1} ((d\alpha^{k,1})^2 + (d\alpha^{k,2})^2) , \tag{10.2.5}$$

where the superscripts 1 and 2 denote the real and imaginary part of α^k, respectively. It follows the geodesic is simply a straight line of the form

$$\alpha_k^j(\tau) = \alpha_k^j(\tau = 1)\,\tau + \alpha_k^j(\tau = 0) \tag{10.2.6}$$

for each value of k ($j = 1, 2$); using the boundary conditions, one obtains

$$\begin{aligned} &\alpha_k^1(\tau = 0) = \alpha_k^2(\tau = 0) = 0, \\ &\alpha_k^1(\tau = 1) = \frac{1}{2}\log\frac{|\Omega_k|}{|\omega_r|} \quad , \quad \alpha_k^2(\tau = 1) = \frac{1}{2}\arctan\frac{\Re(\omega_r)\Im(\Omega_k) - \Re(\Omega_k)\Im(\omega_r)}{\Re(\omega_r)\Re(\Omega_k) + \Im(\Omega_k)\Im(\omega_r)} \end{aligned} \tag{10.2.7}$$

for each k, where the real and imaginary parts of Ω_k are

$$\begin{aligned} \Re(\Omega_k) &= \frac{\omega_{1,k}^2 \omega_k}{\sin(\omega_{1,k}\,t)^2(\omega_k^2 + \omega_{1,k}^2\cot(\omega_{1,k}\,t)^2)}, \\ \Im(\Omega_k) &= \frac{\omega_{1,k}(\omega_{1,k}^2 - \omega_k^2)\sin(2\,\omega_{1,k}\,t)}{2\sin(\omega_{1,k}\,t)^2(\omega_k^2 + \omega_{1,k}^2\cot(\omega_{1,k}\,t)^2)}. \end{aligned} \tag{10.2.8}$$

Then the complexity is given by

$$\mathcal{C}(\tilde{U}) = \int_0^1 ds\sqrt{g_{ij}\dot{x}^i\dot{x}^j} , \tag{10.2.9}$$

where g_{ij} denote the components of the metric eq. 10.2.5, and the x^i's are coordinates associated with this metric. Finally, one obtains

$$\mathcal{C}(\tilde{U}) = \frac{1}{2}\sqrt{\sum_{k=0}^{N-1}\left[\left(\log\frac{|\Omega_k|}{|\omega_r|}\right)^2 + \left(\arctan\frac{\Re(\omega_r)\Im(\Omega_k) - \Re(\Omega_k)\Im(\omega_r)}{\Re(\omega_r)\Re(\Omega_k) + \Im(\Omega_k)\Im(\omega_r)}\right)^2\right]}. \tag{10.2.10}$$

Choosing the reference as the ground state of $H(q,q')$ at $t=0$, we see that ω_r will be ω_k, as defined in eq. 10.1.7, giving

$$\mathcal{C}(\tilde{U}) = \frac{1}{2}\sqrt{\sum_{k=0}^{N-1}\left[\left(\log\frac{|\Omega_k|}{\omega_k}\right)^2 + \left(\arctan\frac{\Im(\Omega_k)}{\Re(\Omega_k)}\right)^2\right]}\,. \tag{10.2.11}$$

This expression is similar to the one derived in the two-oscillator case, and in fact we see that we can recover this complexity by simply taking $N=2$ and $\Omega_k \in \mathbb{R}$.

10.3 Quench Complexity from Fubini-Study

In this section, we will calculate the complexity using the Fubini-Study approach. This follows section 9.4.3, where we write the eigenoperators of H_1 (the Hamiltonian for $t>0$) in terms of the eigenoperators of H (the Hamiltonian for $t\leq 0$), as discussed in detail in appendix B. As per eq. 10.1.6, we have[2]

$$\begin{aligned}
&\text{for } H(q,\hat{q},q'): \quad \begin{pmatrix}\tilde{x}_k\\ \tilde{p}_k\end{pmatrix} = \frac{1}{\sqrt{2\omega_k}}\begin{pmatrix}1 & 1\\ -i\,\omega_k & i\,\omega_k\end{pmatrix}\begin{pmatrix}a_k\\ a^\dagger_{-k}\end{pmatrix},\\
&\text{for } H_1(q_1,\hat{q}_1,q_1'): \quad \begin{pmatrix}\tilde{x}_k\\ \tilde{p}_k\end{pmatrix} = \frac{1}{\sqrt{2\omega_{1,k}}}\begin{pmatrix}1 & 1\\ -i\,\omega_{1,k} & i\,\omega_{1,k}\end{pmatrix}\begin{pmatrix}a_{1,k}\\ a^\dagger_{1,-k}\end{pmatrix};
\end{aligned} \tag{10.3.1}$$

from which we can obtain the Bogoliubov transformation relating $(a_{1,k}, a^\dagger_{1,-k})$ to $(a_k, a^\dagger_{-k})$

$$\begin{pmatrix}a_{1,k}\\ a^\dagger_{1,-k}\end{pmatrix} = \begin{pmatrix}\mathcal{U}_k & \mathcal{V}_k\\ \mathcal{V}_k & \mathcal{U}_k\end{pmatrix}\begin{pmatrix}a_k\\ a^\dagger_{-k}\end{pmatrix}, \tag{10.3.2}$$

where

$$\mathcal{U}_k = \frac{\omega_{1,k}+\omega_k}{2\sqrt{\omega_{1,k}\omega_k}} \quad , \quad \mathcal{V}_k = \frac{\omega_{1,k}-\omega_k}{2\sqrt{\omega_{1,k}\omega_k}}\,,$$

and $|\mathcal{U}_k|^2 - |\mathcal{V}_k|^2 = 1$.

This allows us to write the Hamiltonian in terms of $SU(1,1)$ generators and Bogoliubov coefficients

$$H_1(q_1,\hat{q},q_1') = \sum_{k=0}^{N-1}\omega_{1,k}[(\mathcal{U}_k^2+\mathcal{V}_k^2)K_k^0 + \mathcal{U}_k\mathcal{V}_k K_k^+ + \mathcal{U}_k\mathcal{V}_k K_k^-], \tag{10.3.3}$$

where the generators K^i satisfy the $SU(1,1)$ algebra eq. B.0.15 and are defined in eq. B.0.16.

[2]Note that $\omega_{1,k}$ and ω_k are functions of $(q_1,\hat{q}_1,q_1')$ and $(q,\hat{q},q')$, respectively.

We again take the ground state of $H(q, \hat{q}, q')$ as our reference state, given by

$$|\psi_0\rangle = \prod_{k=0}^{N-1} |k, -k\rangle \ , \tag{10.3.4}$$

where $|k, -k\rangle$ denotes the Fock vacuum for modes k and $(-k)$. We are interested in the complexity of the time-evolved state

$$|\psi_1(t)\rangle = U_1(t)|\psi_0(t=0)\rangle. \tag{10.3.5}$$

To evaluate this, we choose the generic $SU(1,1)$ coherent state as in eq. 9.4.42, i.e. we choose the state

$$|\psi_1(t)\rangle = \prod_{k=0}^{N-1} \mathcal{N}_k(t) \exp(\gamma^+_{1,k}(t)\, a^\dagger_k a^\dagger_{-k})|k, -k> \ , \tag{10.3.6}$$

where the $\gamma' s$ are defined in eq. B.0.21 and are in this case

$$\gamma^+_{1,k} = \Big(\frac{\alpha^+_{1,k}}{\mu_{1,k}}\Big)\Big(\frac{\sinh(\mu_{1,k})}{\cosh(\mu_{1,k}) - \frac{\beta_{1,k}}{2\,\mu_{1,k}}\sinh(\mu_{1,k})}\Big) \quad , \quad \mu^2_{1,k} = \frac{\beta^2_{1,k}}{4} - \alpha^+_{1,k}\alpha^-_{1,k} \ , \tag{10.3.7}$$

with

$$\beta_{1,k} = -i\,t\,\omega_{1,k}\,(\mathcal{U}_k^2 + \mathcal{V}_k^2) \quad , \quad \alpha^+_{1,k} = \alpha^-_{1,k} = -i\,t\,\omega_{1,k}\,\mathcal{U}_k\mathcal{V}_k \ .$$

In this (Fubini-Study) approach, the complexity geodesic distance between the reference and target states follows from eq. 9.4.59, and the complexity is

$$\mathcal{C}_{FS} = \sqrt{\sum_{k=0}^{N-1} \mathcal{C}_k^2} \ , \tag{10.3.8}$$

where $\mathcal{C}_k$ is the geodesic distance for a particular k.

Choosing again the parameterisation

$$\gamma_{k,\sigma} = |\gamma_k| \exp(i\,\phi_k) \quad , \quad |\gamma_k| = \tanh\Big(\frac{\theta_k}{2}\Big) \ ; \tag{10.3.9}$$

we again find $\mathbb{H}^2$

$$ds^2 = \frac{1}{4}\sum_{k=0}^{N-1}(d\theta_k^2 + \sinh(\theta_k)^2 d\phi_k^2). \tag{10.3.10}$$

Considering two points $(\theta_{1,k}, \phi_{1,k})$ and $(\theta_{2,k}, \phi_{2,k})$, the complexity (eq. 10.3.8) takes the form

$$\mathcal{C}_{FS} = \frac{1}{2}\sqrt{\sum_{k=0}^{N-1}\Big(\operatorname{arccosh}\Big[\cosh(\theta_{1,k})\cosh(\theta_{2,k}) - \sinh(\theta_{1,k})\sinh(\theta_{2,k})\cos(\phi_{1,k}-\phi_{2,k})\Big]\Big)^2} \ . \tag{10.3.11}$$

For reference and target states given by eqs. 10.3.4 and 10.3.6, respectively, $\theta_{1,k} = 0$ and $\theta_{2,k} = 2\,\mathrm{arctanh}\,|\gamma_{1,k}|$ with $\gamma_{1,k}$ defined in eq. 10.3.7, the complexity takes the form

$$\mathcal{C}_{FS} = \sqrt{\sum_{k=0}^{N-1} (\mathrm{arctanh}\,|\gamma_{1,k}|)^2}. \tag{10.3.12}$$

10.4 Quench Complexity from the Covariance Matrix

We will now compute the complexity again, this time using the covariance matrix approach. The derivation essentially follows section 9.4.4, however we must now consider N modes and the possibility of complex frequencies. The reference and target covariance matrix G, in this case, takes the form

$$G = \begin{pmatrix} (G^{k=0})_{2\times 2} & \cdots & 0 \\ \vdots & \ddots & \ddots \\ 0 & \cdots & (G^{k=N-1})_{2\times 2} \end{pmatrix}, \tag{10.4.1}$$

For each value of k, the matrix G factorizes further into 2×2 symmetric blocks, each one enjoying a one-to-one corresponds with the canonical pair $\{\tilde{x}_k, \tilde{p}_k\}$. There will therefore be $2N$ of the 2×2 blocks, and the matrix G is of rank $(2N\times 2N)$ and symmetric. For our target state in eq. 10.1.14, each of the (2×2) matrices takes the form

$$G^{\tau=1\,,k}_{2\times 2} = \begin{pmatrix} \frac{1}{\Re(\Omega_k)} & -\frac{\Im(\Omega_k)}{\Re(\Omega_k)} \\ -\frac{\Im(\Omega_k)}{\Re(\Omega_k)} & \frac{|\Omega_k|^2}{\Re(\Omega_k)} \end{pmatrix}, \tag{10.4.2}$$

also for the reference state in eq. 10.2.3 we have

$$G^{\tau=0\,,k}_{2\times 2} = \begin{pmatrix} \frac{1}{\Re(\omega_r)} & -\frac{\Im(\omega_r)}{\Re(\omega_r)} \\ -\frac{\Im(\omega_r)}{\Re(\omega_r)} & \frac{|\omega_r|^2}{\Re(\omega_r)} \end{pmatrix}. \tag{10.4.3}$$

We can again change basis via a squeezing operator

$$\tilde{G}^{\tau=1\,,k} = S\cdot G^{\tau=1\,,k}\cdot S^T, \qquad \tilde{G}^{\tau=0\,,k} = S\cdot G^{\tau=0\,,k}\cdot S^T, \tag{10.4.4}$$

with

$$S = \frac{1}{\sqrt{\Re(\omega_r)(\Im(\omega_r)^2 + (\Re(\omega_r)-1)^2)}} \begin{pmatrix} |\omega_r|^2 - \Re(\omega_r) & \Im(\omega_r) \\ \Im(\omega_r) & 1-\Re(\omega_r) \end{pmatrix}, \tag{10.4.5}$$

such that $\tilde{G}^{\tau=0\,,k} = I$ as before, and the target state becomes

$$\begin{pmatrix} \frac{|\Omega|^2\Im(\omega)^2+\left(|\omega|^2-\Re(\omega)\right)\left(|\omega|^2-2\Im(\omega)\Im(\Omega)-\Re(\omega)\right)}{\left(|\omega|^2-2\Re(\omega)+1\right)\Re(\omega)\Re(\Omega)} & \frac{\Im\left(\omega\left(|\omega|^2+\Omega\left(\Omega^*-2\omega^*\right)\right)\right)+\Im\left(\Omega\left(\omega^*-\Omega^*\right)\omega-\omega+\Omega\right)\Re(\omega)}{\left(|\omega|^2-2\Re(\omega)+1\right)\Re(\omega)\Re(\Omega)} \\ \frac{\Im\left(\omega\left(|\omega|^2+\Omega\left(\Omega^*-2\omega^*\right)\right)\right)+\Im\left(\Omega\left(\omega^*-\Omega^*\right)\omega-\omega+\Omega\right)\Re(\omega)}{\left(|\omega|^2-2\Re(\omega)+1\right)\Re(\omega)\Re(\Omega)} & \frac{|\Omega|^2(\Re(\omega)-1)^2+\Im(\omega)\Im(\omega+2\Omega(\Re(\omega)-1))}{\left(|\omega|^2-2\Re(\omega)+1\right)\Re(\omega)\Re(\Omega)} \end{pmatrix} \tag{10.4.6}$$

Proceeding as before, we identify $U(\tau)$ as an element of $SP(2N,\mathbb{R}) = SP(2,\mathbb{R}) \otimes SP(2,\mathbb{R}) \otimes \cdots \otimes SP(2,\mathbb{R})$ (since the covariance matrices are block diagonal), and we can again use the parameterisation in eq. 9.4.86, now for modes k. Since everything is block diagonal, we can simply compute things for one block and generalise.

For each block we have,

$$\tilde{U}^k(\tau) = \begin{pmatrix} \cos\phi_k(\tau)\cosh\rho_k(\tau) - \sin\theta_k(\tau)\sinh\rho_k(\tau) & -\sin\phi_k(\tau)\cosh\rho_k(\tau) + \cos\theta_k(\tau)\sinh\rho_k(\tau) \\ \sin\phi_k(\tau)\cosh\rho_k(\tau) + \cos\theta_k(\tau)\sinh\rho_k(\tau) & \cos\phi_k(\tau)\cosh\rho_k(\tau) + \sin\theta_k(\tau)\sinh\rho_k(\tau) \end{pmatrix}. \tag{10.4.7}$$

Next, we set the boundary conditions

$$\tilde{G}^{\tau=1\,,k} = \tilde{U}^k(\tau=1)\cdot\tilde{G}^{\tau=0\,,k}\cdot(\tilde{U}^k(\tau=1))^T. \tag{10.4.8}$$

Plugging in $U(\tau)$ and defining $\beta_k \equiv \phi_k + \theta_k$, we can take the trace of both sides here to isolate ρ, meaning we need to solve

$$\frac{|\omega_k|^2 + |\Omega_k|^2 + 2i\Im(\Omega_k)(\omega_k - \Re(\omega_k))}{2\Re(\omega_k)\Re(\Omega_k)} = \cosh(2\rho_k(\tau=1)). \tag{10.4.9}$$

To isolate β, we divide the difference between the diagonal components of eq. 10.4.7 with the sum of the off-diagonal components to find

$$\tan\beta_k(\tau=1) = \frac{\tilde{G}_{11}^{\tau=1,\,k} - \tilde{G}_{22}^{\tau=1,\,k}}{2\,\tilde{G}_{12}^{\tau=1,\,k}} \tag{10.4.10}$$

$$\{\cosh 2\rho_k(\tau=1), \tan(\beta_k(\tau=1)\} = \{\frac{\Re(\omega_r)^2 + \Re(\Omega_k)^2 + (\Im(\omega_r) - \Im(\Omega_k))^2}{2\,\Re(\omega_r)\,\Re(\Omega_k)}, \frac{\tilde{G}_{11}^{\tau=1,\,k} - \tilde{G}_{22}^{\tau=1,\,k}}{2\,\tilde{G}_{12}^{\tau=1,\,k}}\}, \tag{10.4.11}$$

where $\tilde{G}_{ij}^{\tau=1,\,k}$ denote various components of the matrix $\tilde{G}^{\tau=1,\,k}$.

Considering the boundary conditions for the reference state, in this case described by a unit matrix, we find

$$\{\rho_k(\tau=0), \theta_k(\tau=0) + \phi_k(\tau=0)\} = \{0, c_k\}. \tag{10.4.12}$$

where c_k is an arbitrary constant. For simplicity we will choose

$$\phi_k(\tau=1) = \phi_k(\tau=0) = 0 \quad \text{and} \quad \theta_k(\tau=1) = \theta_k(\tau=0) = c_k = \arctan\left(\frac{\tilde{G}_{11}^{\tau=1,\,k} - \tilde{G}_{22}^{\tau=1,\,k}}{2\,\tilde{G}_{12}^{\tau=1,\,k}}\right).$$

Given this form of $\tilde{U}^k(\tau)$ we can write down the metric as before, but now for k modes, i.e.

$$ds_k^2 = d\rho_k^2 + \cosh(2\rho_k)\cosh^2\rho_k\,d\phi_k^2 + \cosh(2\rho_k)\sinh^2\rho_k\,d\theta_k^2 - \sinh(2\rho_k)^2\,d\phi_k d\theta_k. \tag{10.4.13}$$

The total complexity is defined as,

$$\mathcal{C}(\tilde{U}) = \int_0^1 ds \sqrt{\sum_{k=0}^{N-1} g_{ij}^k \dot{x}_k^i \dot{x}_k^j}, \tag{10.4.14}$$

where g_{ij}^k denote the components of the metric for each k and x^i's are coordinates associated with this metric for each value of k. The simplest solution for the geodesic is again a straight line on this geometry [87].

$$\rho_k(\tau) = \rho_k(\tau = 1)\ \tau, \theta_k(\tau) = \theta_k(\tau = 0), \phi_k(\tau) = 0. \tag{10.4.15}$$

So finally we get ,

$$\mathcal{C}(\tilde{U}) = \sqrt{\sum_{k=0}^{N-1} \rho_k(\tau = 1)^2} = \frac{1}{2}\sqrt{\sum_{k=0}^{N-1} \left(\text{arccosh}\left(\frac{\Re(\omega_r)^2 + \Re(\Omega_k)^2 + (\Im(\omega_r) - \Im(\Omega_k))^2}{2\,\Re(\omega_r)\Re(\Omega_k)} \right)^2 \right)}. \tag{10.4.16}$$

Choosing the reference state as the ground state of eq. 10.1.8a, this gives simply

$$\mathcal{C}(\tilde{U}) = \frac{1}{2}\sqrt{\sum_{k=0}^{N-1} \left(\text{arccosh}\left(\frac{\omega_k^2 + |\Omega_k|^2}{2\,\omega_k\,\Re(\Omega_k)} \right)^2 \right)}. \tag{10.4.17}$$

10.5 A Complexity Comparison: The Loschmidt Echo vs the Fidelity

Having derived the complexity for our quench model, we now turn to their comparison. As discussed at the begining of this chapter, we will compare the advantages and disadvantages of each method by comparing the Loschmidt Echo with the Fidelity.

The Loschmidt echo (LE) is considered as a measure of the sensitivity of a system in some quantum mechanical state to perturbations by some operator. As mentioned earlier, the LE is defined as [147, 148][3]

$$\mathcal{F}_{\text{LE}}(t) = |\langle\psi_0| \exp(iH_1' t) \exp(-iH_1 t)|\psi_0\rangle|. \tag{10.5.1}$$

One essentially forward evolves the state by some Hamiltonian, and backward evolves by some different Hamiltonian, taking the overlap with the initial state: the Loschmidt echo quantifies the 'irreversibility' in a quantum system.

[3]For a more comprehensive review of the application of the Loschmidt echo, interested readers are referred to the thesis [149].

In our case, we will take $|\psi_0\rangle$ as the ground state of the Hamiltonian at $t = 0$ (eq. 10.1.8a), which is defined in eq. 10.3.4. The Hamiltonian H_1 (defined in eq. 10.1.8b) is a function of $(q_1, \hat{q}, q_1')$., and we will take H_1' to be of the form eq. 10.1.7, but with *different* values of $(q, \hat{q}, q')$, say $(q_2, \hat{q}_2, q_2')$. We define

$$|\psi_2\rangle = \exp(iH_1' t)\exp(-iH_1 t)|\psi_0\rangle. \tag{10.5.2}$$

Then rewrite eq. 10.5.1 as,

$$\mathcal{F}_{\text{LE}}(t) = |\langle\psi_0|\psi_2\rangle|. \tag{10.5.3}$$

We can view eq. 10.5.1 is a different way. We define the following,

$$|\psi_1\rangle = \exp(-iH_1 t)|\psi_0\rangle, |\tilde{\psi}_1\rangle = \exp(-iH_1' t)|\psi_0\rangle \tag{10.5.4}$$

In terms of these we can rewrite eq. 10.5.1 in the following way,

$$\tilde{\mathcal{F}}(t) = |\langle\tilde{\psi}_1|\psi_1\rangle|. \tag{10.5.5}$$

We termed this as *Fidelity*. Basically here we have defined the overlap of two wave functions evolved from the same initial state but with different Hamiltonian. Quantum mechanically, defined as distances on $\mathbb{CP}^1$ determined by the usual Fubini-Study metric, eqs. 10.5.1 and 10.5.5 are equivalent.

In order to compare complexities, we will consider the complexity associated with both of these. In terms of the overlap, we will use the 'bra' as the reference state and 'ket' as the target state. Explicitly, for the Loschmidt echo we will compute the complexity of ψ_2 with respect to ψ_0, whereas for fidelity we will compute the complexity of ψ_1 with respect to $\tilde{\psi}_1$. Although the overlap of states – eqs. 10.5.1 and 10.5.5 – are the same, we find that the circuit complexity (using the wave function, as done in section 10.2) differs. On the other hand, complexities coming from either Fubini-Study method (section 10.3) and the covariance matrix method (section 10.4) are the same. For each method, we will now compute the complexity of the Loschmidt echo, $\mathcal{C}_{LE}$, and the complexity of Fidelity, $\mathcal{C}_F$. For comparison, we will plot the complexity for a specific set of parameters

$$\{q^2 = 5, q_1^2 = 20, q_2^2 = 29, \hat{q} = \hat{q}_1 = \hat{q}_2 = 2, q' = 2, q_1' = 8, q_2' = -10\}. \tag{10.5.6}$$

10.5.1 LE vs F: Nielsen Complexity

To compute the complexity for the Fidelity from the wavefunction, we will need to use eq. 10.2.10, and define the state $\tilde{\psi}_1$ following eq. 10.1.14

$$\tilde{\psi}_1(\tilde{x}_k, t) = \mathcal{N}(t)\ \exp\left[-\frac{\sum_{k=0}^{N-1}\Omega_{1,k}\,\tilde{x}_k^2}{2}\right], \tag{10.5.7}$$

where $\mathcal{N}(t)$ is the normalization and

$$\Omega_{1,k} = \omega_{2,k}\Big[\frac{\omega_{2,k} - i\,\omega_k \cot(\omega_{2,k}\,t)}{\omega_k - i\,\omega_{2,k}\cot(\omega_{2,k}\,t)}\Big]. \tag{10.5.8}$$

Here, $\omega_{2,k}$ is associated with H_2 and $\omega_{2,k}^2 = q_2^2 + \hat{q}_2 q_2' \cos(\frac{2\pi\,k}{N})$. Now in eq. 10.1.14, we simply need to replace ω_r by $\Omega_{1,k}$.

To compute the Loschmidt echo, we will need the state

$$\psi_2(\tilde{x}_k, t) \;=\; \prod_{k=0}^{N-1} \hat{\mathcal{N}}_k(t) \exp\Big[-\frac{1}{2}\hat{\Omega}_k \tilde{x}_k^2\Big], \tag{10.5.9}$$

where

$$\hat{\Omega}_k = \Big[i\;\omega_{2,k}\cot\omega_{2,k}t + \frac{\omega_{2,k}^2}{\sin^2\omega_{2,k}t(\Omega_k + i\omega_{2,k}\cot\omega_{2,k}t)}\Big] \tag{10.5.10}$$

and $\hat{\mathcal{N}}_k(t)$ is the normalization factor so that the inner-product of the wave function with itself remains one.

Plugging these in, we find

$$\mathcal{C}_{\rm LE}(\tilde{U}) = \frac{1}{2}\sqrt{\Big[\sum_{k=0}^{N-1}\Big(\log\frac{|\hat{\Omega}_k|}{\omega_k}\Big)^2 + \Big(\arctan\frac{\Im(\hat{\Omega}_k)}{\Re(\hat{\Omega}_k)}\Big)^2\Big]}, \tag{10.5.11}$$

$$\mathcal{C}_{\rm F}(\tilde{U}) = \frac{1}{2}\sqrt{\sum_{k=0}^{N-1}\Big[\Big(\log\frac{|\Omega_k|}{|\Omega_{1,k}|}\Big)^2 + \Big(\arctan\frac{\Re(\Omega_{1,k})\Im(\Omega_k) - \Re(\Omega_k)\Im(\Omega_{1,k})}{\Re(\Omega_{1,k})\Re(\Omega_k) + \Im(\Omega_k)\Im(\Omega_{1,k})}\Big)^2\Big]}, \tag{10.5.12}$$

where, Ω_k and $\Omega_{1,k}$ are defined in eqs. 10.1.15 and 10.5.8 respectively. To compare the two, we can plot them for the parameters in eq. 10.5.6. From fig. 10.1 it is evident that the two complexities are quite different, at least when derived using the circuit complexity method. Moreover, the complexity related to the Loschmidt Echo is larger than the complexity for the Fidelity.

$$|\langle\psi_0|\psi_2\rangle| = |\langle\tilde{\psi}_1|\psi_1\rangle| \tag{10.5.13}$$

$$\mathcal{C}(\psi_2, \psi_0) > \mathcal{C}(\psi_1, \tilde{\psi}_1) \tag{10.5.14}$$

Therefore, although the closeness of states between (ψ_0 and ψ_2) is same as the closeness between ($\tilde{\psi}_1$ and ψ_1), the complexity of ψ_2 with respect to ψ_0 is larger than the complexity of ψ_1 with respect to $\tilde{\psi}_1$, implying that it is a much better measure of state distinguishability.

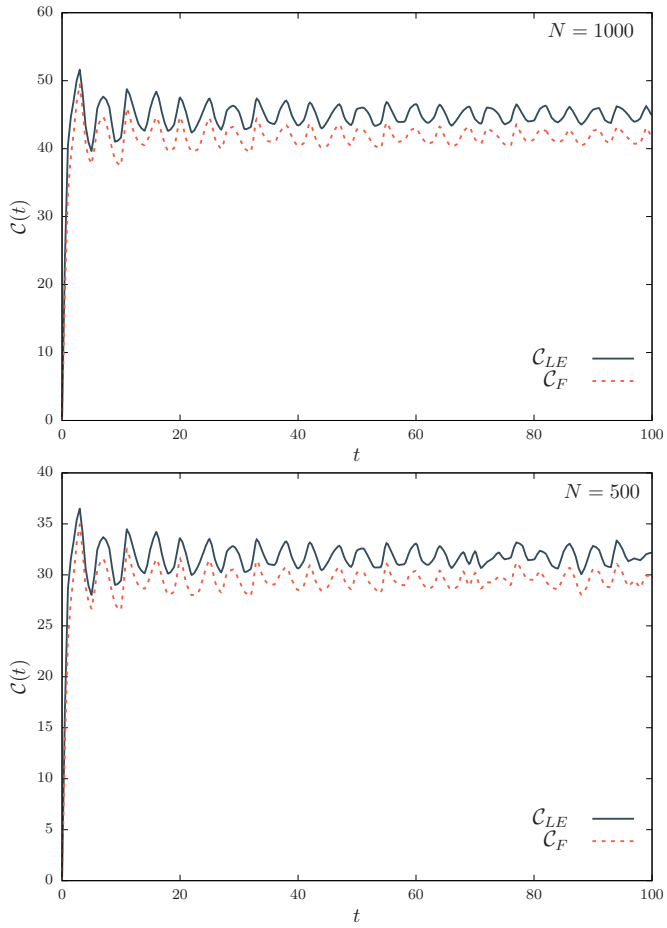

Figure 10.1: LE vs F Test for Circuit Complexity

10.5.2 LE vs F: Fubini-Study Complexity

We will now repeat this test, but using the Fubini-Study complexity. We again start with the state defined in eq. 10.3.6, this time acting with $\exp(i\, H_1'\, t)$, and we

can again use the $SU(1,1)$ decomposition, explicitly

$$\begin{aligned}
&\exp(i\,H_1'\,t) = \exp(\gamma_{2,k}^{+}\tau_k^{+})\exp((\ln\gamma_{2,k}^{0})\tau_k^{z})\exp(\gamma_{2,k}^{-}\tau_k^{-}),\\
&\gamma_{2,k}^{0} = \Big(\cosh(\mu_{2,k}) - \frac{\beta_{2,k}}{2\mu_{2,k}}\sinh(\mu_{2,k})\Big)^{-2}, \gamma_{2,k}^{\pm} = \Big(\frac{\alpha_{2,k}^{\pm}}{\mu_{2,k}}\Big)\Big(\frac{\sinh(\mu_{2,k})}{\cosh(\mu_{2,k}) - \frac{\beta_{2,k}}{2\,\Omega_{2,k}}\sinh(\mu_{2,k})}\Big),\\
&\Omega_{2,k}^{2} = \frac{\beta_{2,k}^{2}}{4} - \alpha_{2,k}^{+}\alpha_{2,k}^{-}, \beta_{2,k} = i\,t\,\omega_{2,k}\,(\tilde{\mathcal{U}}_k^{2} + \tilde{\mathcal{V}}_k^{2}), \alpha_{2,k}^{+} = \alpha_{2,k}^{-} = i\,t\,\omega_{1,k}\tilde{\mathcal{U}}_k\tilde{\mathcal{V}}_k,\\
&\tilde{\mathcal{U}}_k = \frac{\omega_{2,k}+\omega_k}{2\sqrt{\omega_{2,k}\omega_k}}, \tilde{\mathcal{V}}_k = \frac{\omega_{2,k}-\omega_k}{2\sqrt{\omega_{2,k}\omega_k}}.
\end{aligned} \tag{10.5.15}$$

Given this we need to evaluate

$$|\psi_2\rangle = \prod_{k=0}\mathcal{N}_k(t)\,\exp(\gamma_{2,k}^{+}K_k^{+})\exp((\ln\gamma_{2,k}^{0})K_k^{0})\exp(\gamma_{2,k}^{-}K_k^{-})\exp(\gamma_{1,k}^{+}(t)\,a_k^{\dagger}a_{-k}^{\dagger})|k,-k>. \tag{10.5.16}$$

Repeating the procedure from section 10.3, we can write this as

$$|\psi_2\rangle = \prod_{k=0}\tilde{\mathcal{N}}_k(t)\exp(\hat{\gamma}_k\,\tau_k^{+})|k,-k\rangle \tag{10.5.17}$$

where

$$\hat{\gamma}_k = \gamma_{2,k}^{+} + \frac{\gamma_{1,k}^{+}\gamma_{2,k}^{0}}{1-\gamma_{1,k}^{+}\gamma_{2,k}^{-}}. \tag{10.5.18}$$

To compute the complexity for this case, we can simply use the formula in eq. 10.3.12 and replace $\gamma_{1,k}$ by $\hat{\gamma}_k$ as mentioned in eq. 10.5.18.

This gives

$$\mathcal{C}_{LE}(\tilde{U}) = \sqrt{\sum_{k=0}^{N-1}(\operatorname{arctanh}|\hat{\gamma}_k|)^2}, \tag{10.5.19}$$

$$\mathcal{C}_F(\tilde{U}) = \frac{1}{2}\sqrt{\sum_{k=0}^{N-1}\Big(\operatorname{arccosh}\Big[\cosh(\theta_{1,k})\cosh(\theta_{2,k}) - \sinh(\theta_{1,k})\sinh(\theta_{2,k})\Re\Big(\frac{\gamma_{1,k}}{\gamma_{2,k}}\frac{|\gamma_{2,k}|}{|\gamma_{1,k}|}\Big)\Big]\Big)^2}, \tag{10.5.20}$$

where $\theta_{1,k} = 2\operatorname{arctanh}|\gamma_{1,k}|$, $\theta_{2,k} = 2\operatorname{arctanh}|\gamma_{2,k}|$ and $\gamma_{1,k}$ and $\hat{\gamma}_k$ are defined in eqs. 10.3.7 and 10.5.18 respectively.

From fig. 10.2, we immediately see that the Fubini-Study approach cannot distinguish between the two complexities, unlike the complexity derived from Nielsen's method.

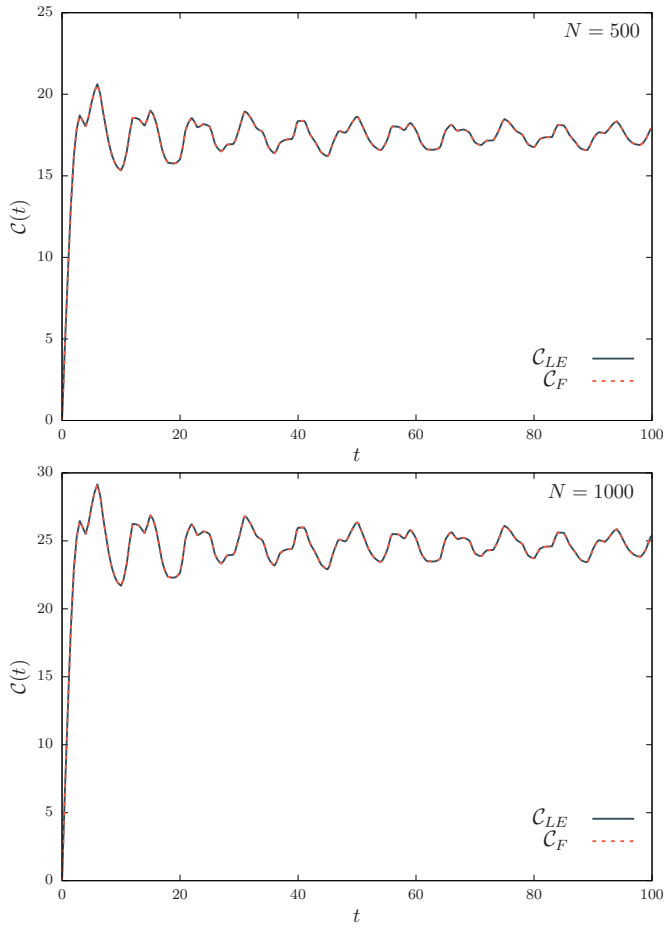

Figure 10.2: LE vs F Test for for Fubini-Study

10.5.3 LE vs F: Covariance Matrix Complexity

This is the simplest to modify, since we can simply use the general formula for the complexity given in eq. 10.4.16, where we just replace $\omega_r = \Omega_{1,k}$. We immediately find that

$$\mathcal{C}_{\mathrm{LE}}(\tilde{U}) = \frac{1}{2}\sqrt{\sum_{k=0}^{N-1}\left(\operatorname{arccosh}\left(\frac{\omega_k^2 + |\hat{\Omega}_k|^2}{2\ \omega_k \Re(\hat{\Omega}_k)}\right)\right)^2}, \tag{10.5.21}$$

$$\mathcal{C}_{\mathrm{F}}(\tilde{U}) = \frac{1}{2}\sqrt{\sum_{k=0}^{N-1}\left(\operatorname{arccosh}\left(\frac{\Re(\Omega_{1,k})^2 + \Re(\Omega_k)^2 + (\Im(\Omega_{1,k}) - \Im(\Omega_k))^2}{2\,\Re(\Omega_{1,k}), \Re(\Omega_k)}\right)^2\right)}, \tag{10.5.22}$$

where, Ω_k and $\Omega_{1,k}$ are defined in eq. 10.1.15 and 10.5.8 respectively.

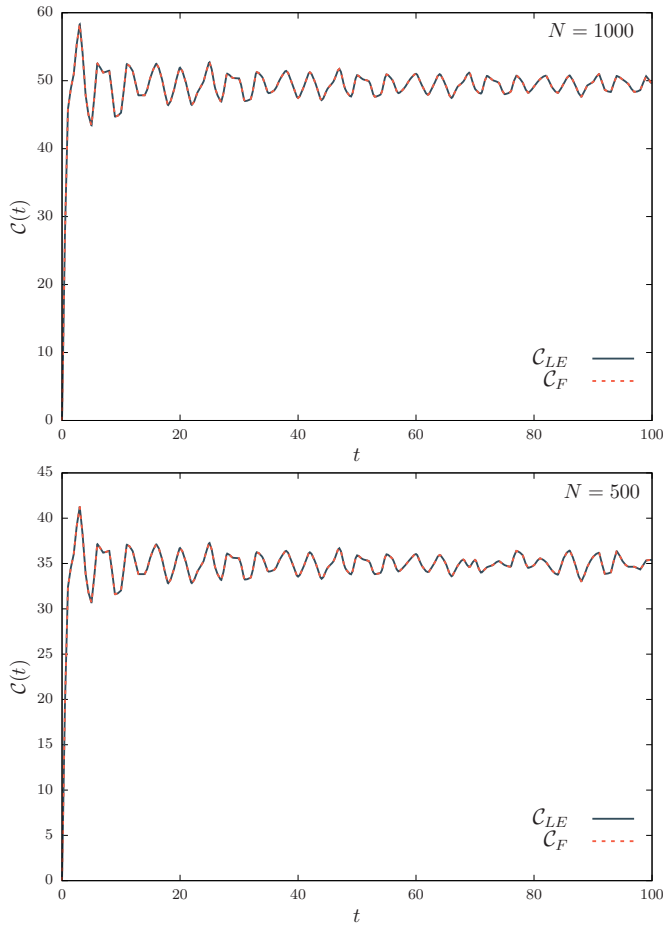

Figure 10.3: LE vs F Test for Covariance Matrix Method (Section (3.3))

Just like the Fubini-Study approach, we observe in fig. 10.3 that the covariance matrix method also cannot distinguish between the two complexities. They overlap with each other completely and again this behaviour is independent of the values of the parameters and N.

10.6 A general statement on complexity

We have seen then that only circuit complexity derived á la Nielsen can distinguish between the Loschmidt echo and the Fidelity, and therefore one could argue that it is a better measure of complexity. However, we only looked at a single forward-backward evolution, and we might wonder if there is a more generic statement to be made. We can imagine doing n forward-backward evolutions (n even), meaning there would be $\frac{n}{2}+1$ ways to write the overlap, for example for

$n = 2$ the state would be

$$|\psi_4(\tilde{x}_k, t)\rangle = e^{iH_2' t} e^{-iH_2 t} e^{iH_1' t} e^{-iH_1 t} |\psi_0\rangle \tag{10.6.1}$$

with corresponding overlaps

$$\langle\psi_4|\psi_0\rangle = \langle\psi_1|\psi_3\rangle = \langle\tilde{\psi}_2|\psi_2\rangle, \tag{10.6.2}$$

and the analogue of Loschmidt echo as

$$\mathcal{F}_{\rm LE} = \langle\psi_4|\psi_0\rangle \tag{10.6.3}$$

where

$$\begin{aligned} |\psi_3(\tilde{x}_k, t)\rangle = \quad & e^{-iH_2 t} e^{iH_1' t} e^{-iH_1 t} |\psi_0\rangle, |\psi_1(\tilde{x}_k, t)\rangle = e^{-iH_2' t} |\psi_0\rangle \\ |\psi_2(\tilde{x}_k, t)\rangle = \quad & e^{iH_1' t} e^{-iH_1 t} |\psi_0\rangle, |\tilde{\psi}_2(\tilde{x}_k, t)\rangle = e^{iH_2 t} e^{-iH_2' t} |\psi_0\rangle \end{aligned} \tag{10.6.4}$$

We will label $\langle\psi_1|\psi_3\rangle$ as Fidelity $\mathcal{F}_1$ and $\langle\tilde{\psi}_2|\psi_2\rangle$ as Fidelity $\mathcal{F}_2$.

After performing the appropriate number of evolutions, we compute the corresponding complexities. The result is that the complexity for the LE is always larger than complexity computed for any combinations of intermediate states corresponding to Fidelity. This result can be written as

$$\mathcal{C}_{\rm LE}^{(\psi_4,\psi_0)}(\tilde{U}) > \mathcal{C}_{\rm F_1}^{(\psi_3,\psi_1)}(\tilde{U}) > \mathcal{C}_{\rm F_2}^{(\psi_2,\tilde{\psi}_2)}(\tilde{U}) \tag{10.6.5}$$

The superscripts denote the pair of wave functions for which we compute the complexity. Now we can perform the same operations for arbitrary number of Hamiltonians, leading to arbitrary number of evolutions for the state. Interestingly, we find that the complexity corresponding to Loschmidt echo is always larger than any possible fidelity. Moreover, for different fidelities, the number of evolutions performed on reference state dictates the magnitude of their complexities. While we do not offer a proof (although we have numerically checked up to $n = 4$) we make the following conjecture

Acting on a fixed reference state, the overlap with the largest number of evolutions always corresponds to the highest complexity.

$$\mathcal{C}_{\rm LE}^{(\psi_n,\psi_0)}(\tilde{U}) > \mathcal{C}_{\rm F_1}^{(\psi_{n-1},\psi_1)}(\tilde{U}) > \mathcal{C}_{\rm F_2}^{(\psi_{n-2},\psi_2)}(\tilde{U}) > ..... > \mathcal{C}_{\rm F_n}^{(\psi_{n/2},\tilde{\psi}_{n/2})}(\tilde{U}). \tag{10.6.6}$$

This result tells us which pair of states will have the smallest complexity for a given set of Hamiltonians. Moreover, it gives us an upper bound on the complexity for a given overlap evolved with a fixed number of Hamiltonians.

XI

Complexity in a Topological System

"The loveliest melodies are not too sublime to be expressed by notes."

– W. Somerset Maugham, *A Writers Notebook 1902*

In this chapter, we consider the complexity and entanglement following a quench in a one-dimensional topological system, namely the Su-Schrieffer-Heeger (SSH) model. As in the last chapter, we will compare the evolution of the complexity using both Nielsen's approach and the Fubini-Study approach. Unlike before, however, we will now also compare these with both the fidelity with measures of entanglement. This is interesting since, in the holographic setting, it has been suggested that the complexity saturates a bound[1] later than the entanglement entropy, especially where considering black hole interiors and the volume of wormholes. It is this feature of complexity/entanglement that we would like to explore in this chapter.

Our medium of investigation will be the one dimensional topological insulator, described by the SSH model, which has a number of interesting features that we will probe using both complexity and entanglement. The system has a non-trivial phase diagram, exhibiting a $c = 1$ CFT at a critical point, along with topological and trivial phases. It is natural, then, for us to explore the sensitivity of the complexity to such phase transitions and to compare with the sensitivity of the entanglement entropy. Additionally, we will also investigate *revivals* in the evolution of complexity, a phenomena which is routinely observed in the entanglement and conjectured to occur in the complexity [79, 82] on long enough timescales. In addition to this, we will explore whether or not the complexity is sensitive to the topological order.

11.1 The Su-Schrieffer-Heeger Model

The Su-Schrieffer-Heeger (SSH) model was first introduced in 1979 to understand the electronic properties of poly-acetylene [151], and has recently been realized

[1] It has been suggested [137] that complexity ought to saturate the Lloyd bound [150], however this has been shown to be violated in many contexts [96]

experimentally in cold atom systems [152–155]. The SSH model is a chirally symmetric topological model given by Hamiltonian

$$\hat{H} = \sum_l \left[t \left(a_l^\dagger b_l + b_l^\dagger a_l \right) + t' \left(a_{l+1}^\dagger b_l + b_l^\dagger a_{l+1} \right) \right] \ , \tag{11.1.1}$$

where a_l (b_l) destroys a fermion on site-l of sublattice-A (sublattice-B), and t (t') is the intracell (intercell) tunneling matrix element (see fig. 11.1). The topological properties are determined by (t, t'). For $|t| < |t'|$ ($|t| > |t'|$), the system is a topological (topologically trivial) insulator; $|t| = |t'|$ is a quantum critical point (QCP), described by a $c = 1$ CFT.

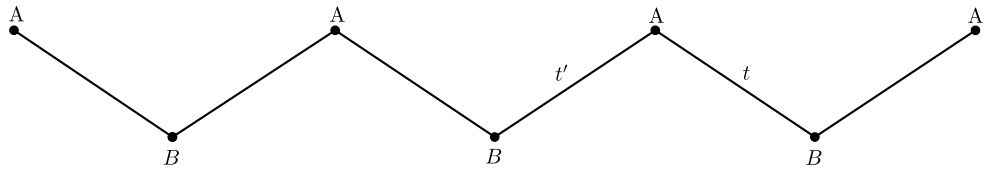

Figure 11.1: The Su-Schreiffer-Heeger model – a one-dimensional system with A and B sublattices; electrons can tunnel between nearest-neighbor sites with intracell (intercell) tunneling amplitude t (t').

In what follows, we work in the Neveu-Schwarz sector. The system is readily analyzed in momentum space. By expanding the fermion operators in Fourier modes [$k = (2\pi/N)(m + 1/2)$ with $1 \leq m \leq N$]

$$a_l = \frac{1}{\sqrt{N}} \sum_k e^{ikl} \tilde{a}_k \text{ and } b_l = \frac{1}{\sqrt{N}} \sum_k e^{ikl} \tilde{b}_k \ , \tag{11.1.2}$$

we get

$$\hat{H} = \sum_k (\tilde{a}_k^\dagger, \tilde{b}_k^\dagger) \begin{pmatrix} 0 & t + t' e^{-ik} \\ t + t' e^{ik} & 0 \end{pmatrix} \begin{pmatrix} \tilde{a}_k \\ \tilde{b}_k \end{pmatrix} \ . \tag{11.1.3}$$

In this form, eq. 11.1.3 is diagonalized by a Bogoliubov transformation, as discussed in appendix B, and the diagonal Hamiltonian is

$$\hat{H}_F = \sum_k E_k \left(\alpha_k^\dagger \alpha_k - \beta_k^\dagger \beta_k \right) \ , \tag{11.1.4}$$

where $E_k = \sqrt{|\Delta_k|^2}$, where $\Delta = t + t' e^{ik}$ and $\{\alpha_k, \beta_k\}$ are related to the $\{\tilde{a}_k, \tilde{b}_k\}$ by the Bogoliubov transformation

$$\begin{pmatrix} \tilde{a}_k \\ \tilde{b}_k \end{pmatrix} = \begin{pmatrix} u_k & -v_k^* \\ v_k & u_k^* \end{pmatrix} \begin{pmatrix} \alpha_k \\ \beta_k \end{pmatrix} \ . \tag{11.1.5}$$

In eq. 11.1.5,

$$u_k = \sqrt{\frac{1}{2}} \quad , \quad v_k = \exp(-i\theta_k)\sqrt{\frac{1}{2}} \tag{11.1.6}$$

with the phase defined via $\Delta_k = |\Delta_k| \exp(i\theta_k)$. Physically, α_k (β_k) destroys a fermion of momentum-k in the conduction (valence) band.

In the last chapter, we considered a quantum quench of a bosonic theory in order to study the evolution of complexity. We considered $SU(1,1)$ coherent states and described pre- and post-quench states in terms of eigenoperators of the different Hamiltonians. In this case, we are considering a fermionic model, and as such we will now need to consider $SU(2)$ coherent states.

We consider the following quench

$$\underline{t<0} : \hat{H} = \hat{H}_<(t_<, t'_<) \quad , \quad \underline{t>0} : \hat{H} = \hat{H}_>(t_>, t'_>) \ . \tag{11.1.7}$$

More generally, we consider

$$\underline{t<0} : \hat{H}_< = \sum_k \Psi_k^\dagger \begin{pmatrix} \xi_k^< & \Delta_k^< \\ (\Delta_k^<)^* & -\xi_k^< \end{pmatrix} \Psi_k \quad ; \quad \underline{t>0} : \hat{H}_> = \sum_k \Psi_k^\dagger \begin{pmatrix} \xi_k^> & \Delta_k^> \\ (\Delta_k^>)^* & -\xi_k^> \end{pmatrix} \Psi_k \ . \tag{11.1.8}$$

Let $\{\alpha_{<k}, \beta_{<k}\}$ ($\{\alpha_{>k}, \beta_{>k}\}$) be eigenoperators of $\hat{H}_<$ ($\hat{H}_>$):

$$\begin{pmatrix} \tilde{a}_k \\ \tilde{b}_k \end{pmatrix} = \begin{pmatrix} u_{<k} & -v^*_{<k} \\ v_{<k} & u^*_{<k} \end{pmatrix} \begin{pmatrix} \alpha_{<k} \\ \beta_{<k} \end{pmatrix} \longrightarrow \hat{H}_< = \sum_k E_k^< \left(\alpha^\dagger_{<k} \alpha_{<k} - \beta^\dagger_{<k} \beta_{<k} \right) , \tag{11.1.9}$$

$$\begin{pmatrix} \tilde{a}_k \\ \tilde{b}_k \end{pmatrix} = \begin{pmatrix} u_{>k} & -v^*_{>k} \\ v_{>k} & u^*_{>k} \end{pmatrix} \begin{pmatrix} \alpha_{>k} \\ \beta_{>k} \end{pmatrix} \longrightarrow \hat{H}_> = \sum_k E_k^> \left(\alpha^\dagger_{>k} \alpha_{>k} - \beta^\dagger_{>k} \beta_{>k} \right) . \tag{11.1.10}$$

The $\{\alpha_{>k}, \beta_{>k}\}$ are related to the $\{\alpha_{<k}, \beta_{<k}\}$ by the unitary transformation

$$\begin{pmatrix} \alpha_{>k} \\ \beta_{>k} \end{pmatrix} = \begin{pmatrix} \mathcal{U}_k & -\mathcal{V}^*_k \\ \mathcal{V}_k & \mathcal{U}^*_k \end{pmatrix} \begin{pmatrix} \alpha_{<k} \\ \beta_{<k} \end{pmatrix} \tag{11.1.11}$$

where

$$\mathcal{U}_k = u^*_{>k} u_{<k} + v^*_{>k} v_{<k} \quad , \quad \mathcal{V}_k = u^*_{>k} v_{<k} - v^*_{>k} u_{<k} \ . \tag{11.1.12}$$

Then, $\hat{H}_>$ can be written in terms of the eigenoperators of $\hat{H}_<$ as

$$\hat{H}_> = \sum_k 2E_k^> \left[(|\, \mathcal{U}_k \,|^2 - |\, \mathcal{V}_k \,|^2)\, \tau_k^z - \mathcal{U}_k^* \mathcal{V}_k^* \tau_k^+ - \mathcal{U}_k \mathcal{V}_k \tau_k^- \right] \ , \tag{11.1.13}$$

where

$$\tau_k^- = \beta_{<k}^\dagger \alpha_{<k} \ , \ \tau_k^+ = \alpha_{<k}^\dagger \beta_{<k} \ , \ \tau_k^z = (\alpha_{<k}^\dagger \alpha_{<k} - \beta_{<k}^\dagger \beta_{<k})/2 \tag{11.1.14}$$

obey an $SU(2)$ algebra.

We can then construct an $SU(2)$ state as our reference state $|\psi_R\rangle$, which we wish to be the ground state of $\hat{H}_<$. We then define the target state $|\psi_T\rangle$ as the state obtained by evolution with $\hat{H}_>$, $|\psi_T\rangle = \exp(-it\hat{H}_>)|\psi_R\rangle$. More explicitly, let $\{\alpha_{<k}, \beta_{<k}\}$ denote the destruction operators of $\hat{H}_<$. The initial state is given by

$$|\psi_R\rangle = \prod_k \beta_{<k}^\dagger |0\rangle \ , \tag{11.1.15}$$

where $|0\rangle$ is the Fock vacuum as before. In order to construct the target state, we need to employ the $SU(2)$ decomposition, which is thankfully identical to eq. B.0.20, but with the generators K_i replaced with those of $SU(2)$. First, we write the time-evolution operator as a general $SU(2)$ state

$$\hat{U}(t) = \prod_k \exp\left(\omega_k \tau_k^z + \alpha_k^+ \tau_k^+ + \alpha_k^- \tau_k^-\right) \ , \tag{11.1.16}$$

where

$$\{\omega_k = -it2E_k^> \left(|\ \mathcal{U}_k\ |^2 - |\ \mathcal{V}_k\ |^2\right) \ , \ \alpha_k^+ = it2E_k^> \ \mathcal{U}_k^* \mathcal{V}_k^* \ , \ \alpha_k^- = it2E_k^> \ \mathcal{U}_k \mathcal{V}_k\} \ . \tag{11.1.17}$$

Then, utilizing the decomposition in eq. B.0.20 and proceeding as in the last chapter, we write final state as

$$|\psi_T\rangle = \prod_k \frac{1}{\sqrt{1 + |\bar{\gamma}_k^+(t)|^2}} \left(\beta_{<k}^\dagger + \bar{\gamma}_k^+(t) \ \alpha_{<k}^\dagger\right) |0\rangle \ . \tag{11.1.18}$$

11.2 Complexity in the SSH model

We will now compute the complexity associated with reaching the target state (eq. 11.1.18) from the reference state (eq. 11.1.15). We will begin by computing the complexity from the correlation matrix as discussed in section 9.4.4, meaning we use

$$\hat{C}_k(t) = \langle\psi(t)|\Psi_k \Psi_k^\dagger|\psi(t)\rangle \ , \tag{11.2.1}$$

where $\Psi_k^T = (\tilde{a}_k, \tilde{b}_k)$.

Explicitly, one obtains

$$C_k(t) = \begin{pmatrix} |u_k(t)|^2 & u_k(t)v_k^*(t) \\ v_k(t)u_k^*(t) & |v_k(t)|^2 \end{pmatrix} \ , \tag{11.2.2}$$

where

$$\begin{pmatrix} u_k(t) \\ v_k(t) \end{pmatrix} = \exp(-itH_>) \begin{pmatrix} u_{<k} \\ v_{<k} \end{pmatrix} \quad \text{with} \quad H_> = \begin{pmatrix} \xi_k^> & \Delta_k^> \\ (\Delta_k^>)^* & -\xi_k^> \end{pmatrix} . \tag{11.2.3}$$

Using eq. 11.2.3 and eq. 11.2.2, we can define the reference and target correlation matrices

$$C_k(s=0) = \begin{pmatrix} |u_{k,<}|^2 & u_{k,<}v_{k,<}^* \\ v_{k,<}u_{k,<}^* & |v_{k,<}|^2 \end{pmatrix} , \tag{11.2.4}$$

We proceed as before, and consider evolving the initial covariance matrix $\hat{C}_k$ by the unitary operator $\tilde{U}_k$,

$$\tilde{C}_k(s) \equiv \tilde{U}_k(s)\hat{C}_k(t=0)\tilde{U}_k^\dagger(s) , \tag{11.2.5}$$

with the boundary condition $\tilde{C}_k(s=1) = \hat{C}_k(t)$ i.e. at $s=1$ we recover the final correlation matrix. We parameterize $\tilde{U}_k$ in the usual way

$$\tilde{U}_k(s) = \mathcal{P}\exp\left[-\sum_I \int_0^1 ds\ Y_k^I(s)M_I\right] , \tag{11.2.6}$$

where the $\{M_I\}$ are $SU(2)$ generators in this case.

This means that we can parameterise $\tilde{U}_k$ as

$$\tilde{U}_k(s) = \begin{pmatrix} \cos\rho_k(s)\exp[i\phi_k(s)] & -i\sin\rho_k(s)\exp[-i\chi_k(s)] \\ -i\sin\rho_k(s)\exp[i\chi_k(s)] & \cos\rho_k(s)\exp[-i\phi_k(s)] \end{pmatrix} . \tag{11.2.7}$$

Repeating the procedure in section 9.4.4, one obtains the (right-invariant) metric

$$ds^2 = \sum_k \left[d\rho_k^2 + \cos^2(\rho_k)d\phi_k^2 + \sin^2(\rho_k)d\chi_k^2\right] . \tag{11.2.8}$$

To derive the boundary conditions, we again apply the squeezing operator

$$S = \begin{pmatrix} 1 & -\frac{u_<}{v_<} \\ 1 & \frac{v_<^*}{u_<^*} \end{pmatrix} , \tag{11.2.9}$$

to find that

$$\tilde{C}(s=0) = S\cdot C(s=0)\cdot S^{-1} = \begin{pmatrix} 0 & 0 \\ 0 & |u_<|^2+|v_<|^2 \end{pmatrix} = \begin{pmatrix} 0 & 0 \\ 0 & 1 \end{pmatrix} , \tag{11.2.10}$$

The target state is defined via

$$\tilde{C}^T = S\cdot C^T(s=1)\cdot S^{-1}, \tag{11.2.11}$$

and we can derive the boundary conditions via

$$\bar{C}_{i,j} = \tilde{U}_k(s) \cdot C_k(s=0) \cdot \tilde{U}_k^\dagger(s) = \begin{pmatrix} \sin^2(\rho_k) & -ie^{i(\beta_k)}\cos(\rho_k)\sin(\rho_k) \\ ie^{-i(\beta_k)}\cos(\rho_k)\sin(\rho_k) & \cos^2(\rho_k) \end{pmatrix}, \tag{11.2.12}$$

where $\beta_k = \phi_k - \chi_k$.

Setting this equal to eq. 11.2.11 gives the final boundary conditions and setting it equal to eq. 11.2.10 the initial. We can isolate the ρ coordinate by taking $\bar{C}_{22} - \bar{C}_{11} = \cos(2\rho_k)$, and the β coordinate by taking $\frac{\Re(\bar{C}_{12})}{\Im(\bar{C}_{12})} = -\tan(\beta_k)$.

For the SSH model, using eqs. 11.1.6, 11.2.3, 11.2.2 and 11.2.11, we find the following boundary conditions

$$\rho_k(s=0) = 0, \qquad \rho_k(s=1) = \frac{1}{2}\arccos\left[\sin^2(E_k^> t)\cos(2\theta_k^> - 2\theta_k^<) + \cos^2(E_k^> t)\right] \tag{11.2.13}$$

$$\beta_k(s=0) = c_k, \qquad \beta_k(s=1) = \arctan\left[\cot(E_k^> t)\sec(\theta_k^> - \theta_k^<)\right] \tag{11.2.14}$$

The simplest solution for the geodesic is, as before,

$$\rho_k(s) = \rho_k(s=1)s, \quad \chi_k(s) = \chi_k^0 \quad , \quad \phi_k(s) = 0. \tag{11.2.15}$$

Then the complexity is given by

$$\mathcal{C}[\{\tilde{U}_k\}] = \frac{1}{2}\sqrt{\sum_k \left(\arccos\left[\sin^2(E_k^> t)\cos(2\theta_k^> - 2\theta_k^<) + \cos^2(E_k^> t)\right]\right)^2}\,. \tag{11.2.16}$$

As in the last chapter, we will be interested in comparing the results for the circuit complexity obtained with the covariance matrix method with that obtained from the Fubini-Study method. In section 9.4.3, we derived the Fubini-Study line element for $SU(1,1)$ coherent states (eq. 9.4.52). We are now dealing with $SU(2)$ coherent states, and the derivation essentially follows in exactly the same way, with the $SU(1,1)$ generators replaced with the $SU(2)$ generators. As should be expected (by analytic continuation), the two line elements differ only by a minus sign, giving the $SU(2)$ Fubini-Study line element

$$ds^2 = \sum_k \frac{|d\bar{\gamma}_k^+|^2}{\left(1 + |\bar{\gamma}_k^+|^2\right)^2}\,. \tag{11.2.17}$$

We recognize each individual term in eq. 11.2.17 a the line element of a two-sphere S^2 (in the CP^1 representation), which again we should expect by analytic continuation, given the that we found H^2 in the previous case.

The full state manifold is then $S^2 \times S^2 \times \cdots \times S^2$. Writing $\bar{\gamma}_k^+ = |\bar{\gamma}_k^+| \exp(i\phi_k)$ with $|\bar{\gamma}_k^+| = \tan\theta_k/2$, one obtains the line element in the spherical coordinates

$$ds^2 = \sum_k \frac{1}{4}\left(d\theta_k^2 + \sin^2\theta_k \; d\phi_k^2\right) \; . \tag{11.2.18}$$

We define a metric on the state manifold as [156]

$$s = \sqrt{\sum_k s_k^2} \; , \tag{11.2.19}$$

where

$$s_k = \int_0^t dt' \; \frac{1}{1+|\bar{\gamma}_k^+|^2} \left| \frac{d\bar{\gamma}_k^+}{dt'} \right| \tag{11.2.20}$$

is a (natural) metric on S^2.

The geodesics are, analagously with the last chapter, given by

$$\mathcal{C}_k = \frac{1}{2} \arccos\left[\cos\theta_{1,k}\cos\theta_{2,k} + \sin\theta_{1,k}\sin\theta_{2,k}\cos(\phi_{1,k}-\phi_{2,k})\right] \; , \tag{11.2.21}$$

where $(\theta_{1,k}, \phi_{1,k})$ $((\theta_{2,k}, \phi_{2,k}))$ are the spherical coordinates of the initial (final) point. The reference and target states are given by eqs. 11.1.15 and 11.1.18 respectively. Recalling that we parameterise $|z_k| = \tan\theta_k/2$, we have the boundary conditions that $\theta_{1,k} = 0, \theta_{2,k} = 2\arctan|\bar{\gamma}_k^+|$. Plugging this into eq. 11.2.21 then gives

$$\mathcal{C}_k = \arctan|\bar{\gamma}_k^+| \; . \tag{11.2.22}$$

For the full state manifold, $S^2 \times S^2 \times \cdots \times S^2$, we again define the metric

$$s = \sqrt{\sum_k s_k^2} \; . \tag{11.2.23}$$

The complexity is then given by

$$\mathcal{C} = \sqrt{\sum_k \mathcal{C}_k^2} = \sqrt{\sum_k \arctan|\bar{\gamma}_k^+|} \; . \tag{11.2.24}$$

11.3 Entanglement Entropy, Spectrum and Complexity

We will now, for concreteness, consider specific quenches of the model, namely:
(1) topological $\leftrightarrow$ non-topological
(2) non-topological $\leftrightarrow$ critical
(3) topological $\leftrightarrow$ critical.

Where each phase is given by the following parameters:
(1) topological – (t=0.2, t'=1)
(2) non-topological – (t=1, t'=0.2)
(3) critical – (t=1, t'=1).

We will compute the entanglement entropy and entanglement spectrum using the correlation matrix method described in section 9.2.7, specifically we will write the entanglement entropy as a function of the eigenvalues of the correlation matrix in eq. 11.2.2.

We partition the system into two subsystems A and B and consider the correlation matrix restricted to subsystem-A, $\hat{C}^A(t)$, whose elements are $(m, n \in A)$

$$\hat{C}^A_{mn}(t) = \frac{1}{N} \sum_k \exp[ik(m-n)]\ \hat{C}_k(t)\ . \tag{11.3.1}$$

We denote the eigenvalues of $\hat{C}^A(t)$ by $\{\lambda_n\}$, the set of which constitutes the entanglement spectrum. By taking the $\alpha \longrightarrow 1$ limit of the Renyi entropy defined in eq. 9.2.87, we find the entanglement entropy as a function of the eigenvalues

$$S = -\sum \left[\lambda_n \ln \lambda_n + (1-\lambda_n)\ln(1-\lambda_n)\right]\ . \tag{11.3.2}$$

We can plot the entanglement entropy for the various quenches under consideration.

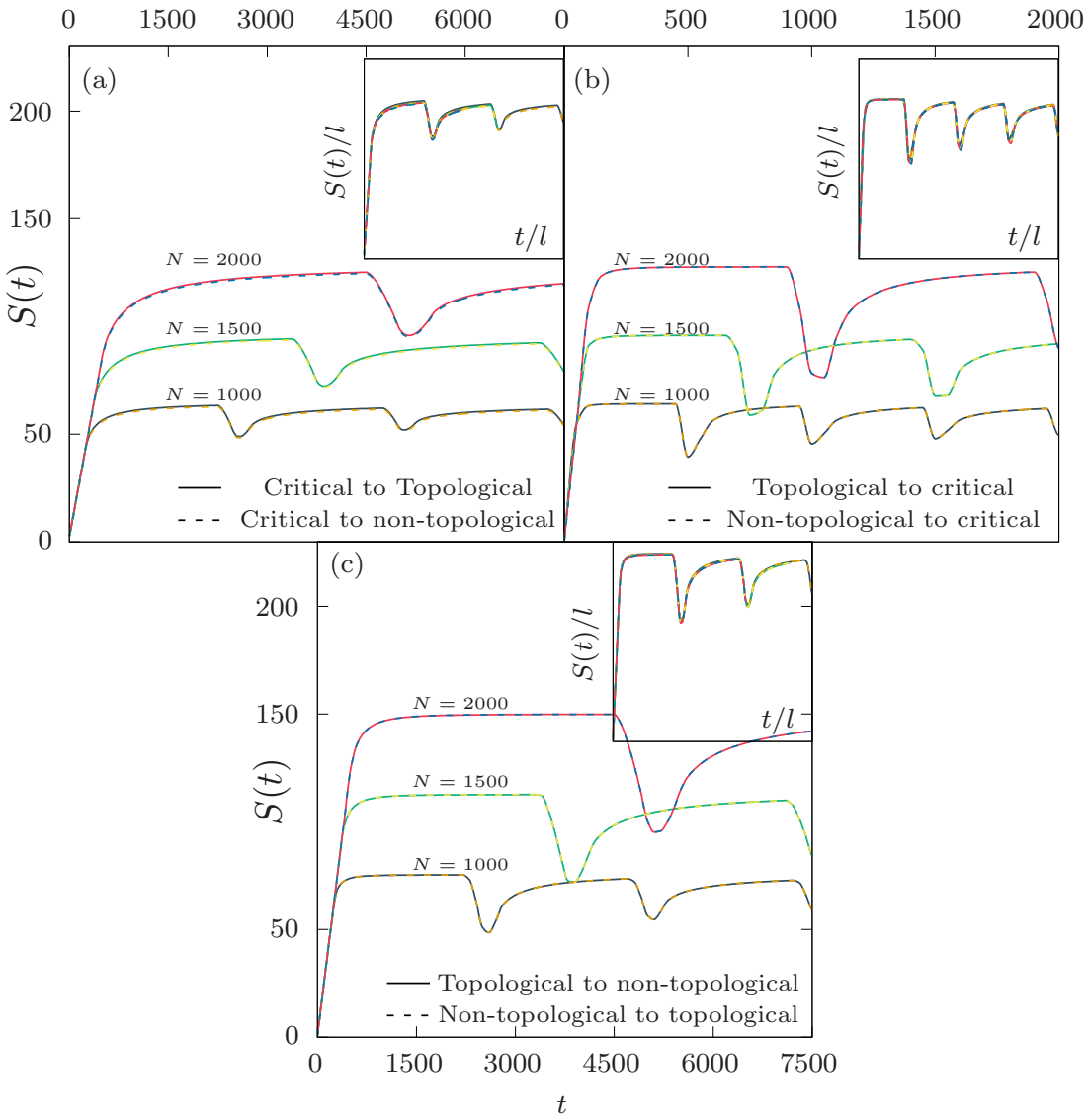

Figure 11.2: Entanglement entropy as a function of time – results are shown for system sizes of N=1000, N=1500, N=2000 and entanglement partitions of length l=100, l=150, l=200, respectively. Quenching from (a) the critical point to a massive phase (b) a massive phase to the critical point (c) between massive phases. Insets: Entanglement entropy vs time scaled by the partition size, $S(t)/l$ vs t/l.

Fig. 11.2 shows the results for the time-dependent entanglement entropy, shown for quenches from
(a) the critical point to a massive phase
(b) a massive phase to the critical point

(c) between massive phases.

In all of the quenches, the entanglement entropy first grows linearly before saturating. At later times, we observe revivals due to the finite system size. Furthermore, we see that the amplitude is larger when quenching between massive phases when compared with quenching to/from the critical point. The (pseudo-) period of the revivals is larger when quenching to a massive phase when compared with quenching to the critical point.

As shown in the insets, by working with scaled variables, namely S/l vs. t/l, the results collapse onto universal curves.

While the results for the quenches have similar features, there are quantitative differences. In particular, when the initial phase is the topological phase, the entropy is a small fraction larger, since the topological phase has greater entanglement.

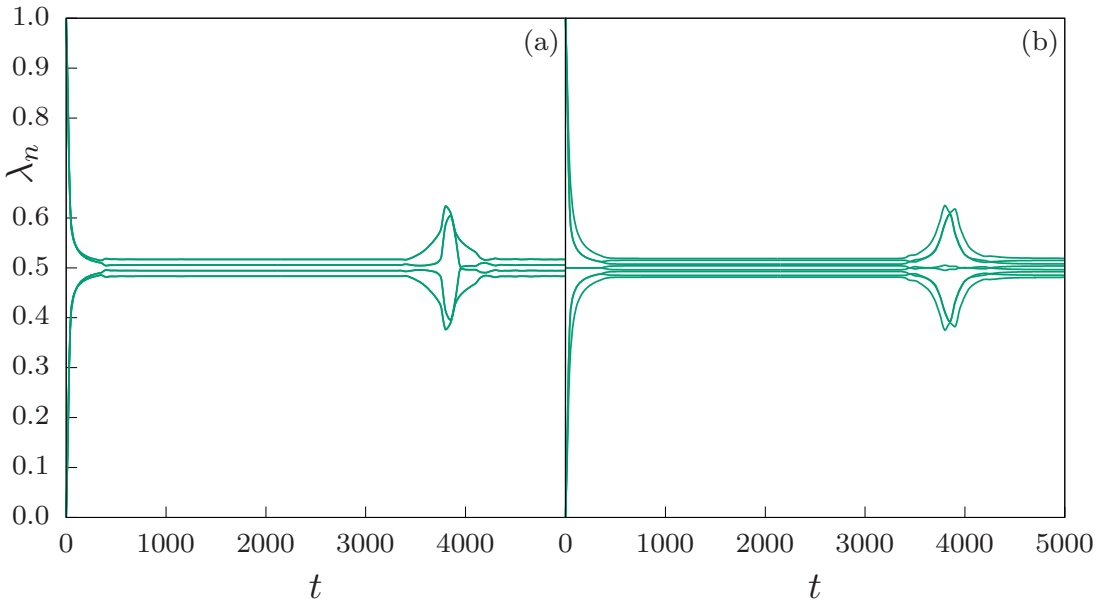

Figure 11.3: Entanglement spectrum as a function of time – results are shown for a system size of N=1500 and an entanglement partition of l=150. Quenching from (a) the non-topological to the topological phase (b) the topological to the non-topological phase.

To further characterize the properties of this system, the entanglement spectrum is shown in fig. 11.3. Fig. 11.3a (fig. 11.3b) shows the entanglement spectrum for a quench from the non-topological (topological) to the topological (non-topological) phase. This shows very distinctly the differences in the quenches. In particular,

the topological phase has "zero-modes" in the entanglement spectrum, namely states where $\lambda_n \simeq 1/2$, and when one starts initially in the topological phase, the zero-mode stays pinned [157]. These modes are due to the edge states that are present in the topological phase (and absent otherwise) [132, 158].

We now compare these findings with those from complexity. To get some intuition for how the complexity arises, we will plot the evolution of the target state upon quenching from the non-topological phase to the critical point for several values of k (see fig. 11.4 below).

As discussed above, eq. 11.1.18 describes a trajectory on S^2 for each k.

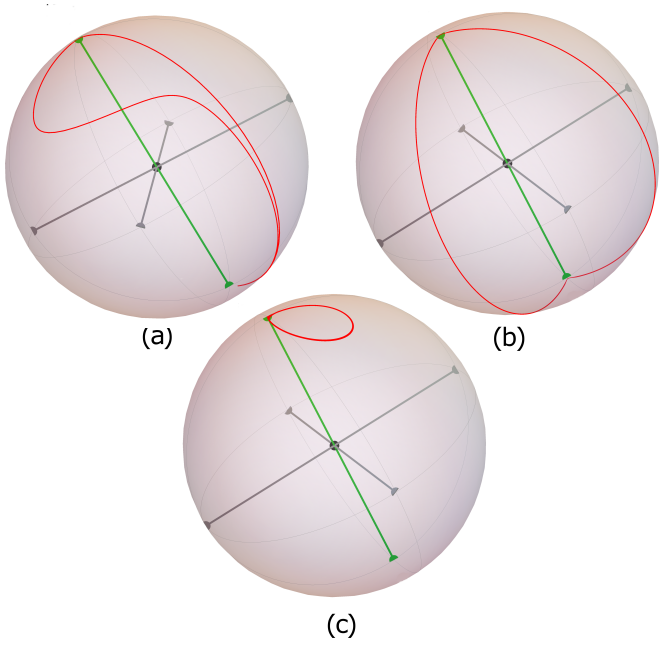

Figure 11.4: Motion on the Bloch sphere upon quenching from the non-topological phase to the critical point: (a) $m = 470$ (b) $m = 505$ (c) $m = 870$. The system size is N=1000.

We see that Hamiltonian evolution gives rise to a variety of behaviors. Depending on the values of k, the evolution can be close to the geodesic for some values of k (figs. 11.4a and b), while it can be rather distant for other values of k (fig. 11.4c). Hence, for some values of k the path from Hamiltonian evolution gives the complexity, while for other values of k the contribution to the complexity comes from a very different path. We only considered one particular phase here, but all other phases give rise to similar behaviour.

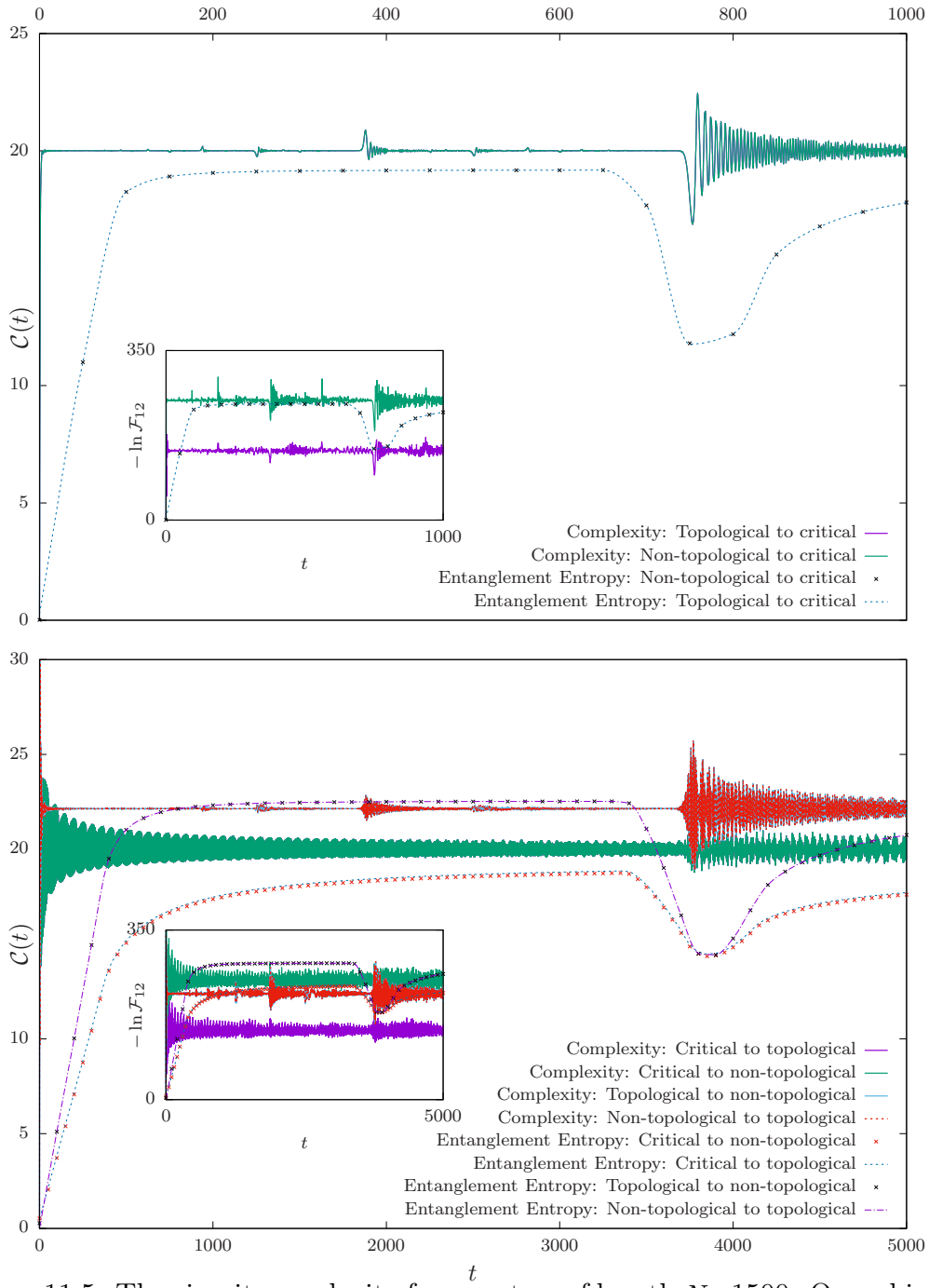

Figure 11.5: The circuit complexity for a system of length N=1500. Quenching (a) from a massive phase to the critical point (b) to a massive phase. Insets: Negative logarithm of the fidelity: $-\ln \mathcal{F}_{12}$.

The evolution of the complexity is shown in Figs. 11.5 and 11.6. Figs. 11.5 shows

results for the covariance matrix complexity, while Figs. 11.6 shows results from the Fubini-Study line element. In both, figure (a) shows quenches from the massive phases to the critical point, while figure (b) shows quenches to a massive phase. For all quenches, the complexity grows extremely rapidly and then saturates, with some oscillations about the saturation value.

When quenching to the critical point, distinct revivals appear in the complexity, similar to what occurs in the entanglement entropy; when quenching to a massive phase, revivals also occur, but they are more pronounced when quenching between massive phases.

To better understand these results, the insets of fig. 11.5 show results for the negative logarithm of the fidelity: $-\ln \mathcal{F}_{12}$.

This quantity behaves similarly to the complexity, and gives insight into the behavior of the complexity and, in particular, its rapid growth and saturation. This arises because the target state becomes orthogonal to the reference state rapidly.

Note also that revivals appear in the fidelity when quenching to the critical point [159, 160]. However, we see that the signature in the complexity is more pronounced.

Fig. 11.6 shows the complexity obtained from the Fubini-Study method. This measure of complexity (like the fidelity) can clearly identify the different types of quenches. On the other hand, it appears the circuit complexity, just like entanglement entropy, can only distinguish quenches between the critical point and a massive phase from the quenches between the massive phases.

It is not surprising that the circuit complexity and the entanglement entropy behave similarly, while the Fubini-Study complexity and fidelity behave similarly. Both the circuit complexity and entanglement entropy are derived from the correlation matrix, while the Fubini-Study complexity essentially follows from the fidelity. However, it is not immediately clear why the Fubini-Study approach provides a more sensitive measure of complexity than the covariance matrix approach.

For the SSH model, we saw that the complexity saturated much more rapidly than the entanglement entropy. This is contrary to expectation of what happens in the black hole scenario, where the complexity is expected to saturate exponentially slower than the entanglement entropy [79, 82].

Furthermore, there are additional sources of entanglement introduced after the system becomes topologically non-trivial, coming from the entanglement at the boundary. The complexity, however, appears to be much less (or not at all, depending the measure used) sensitive to this topological phase transition.

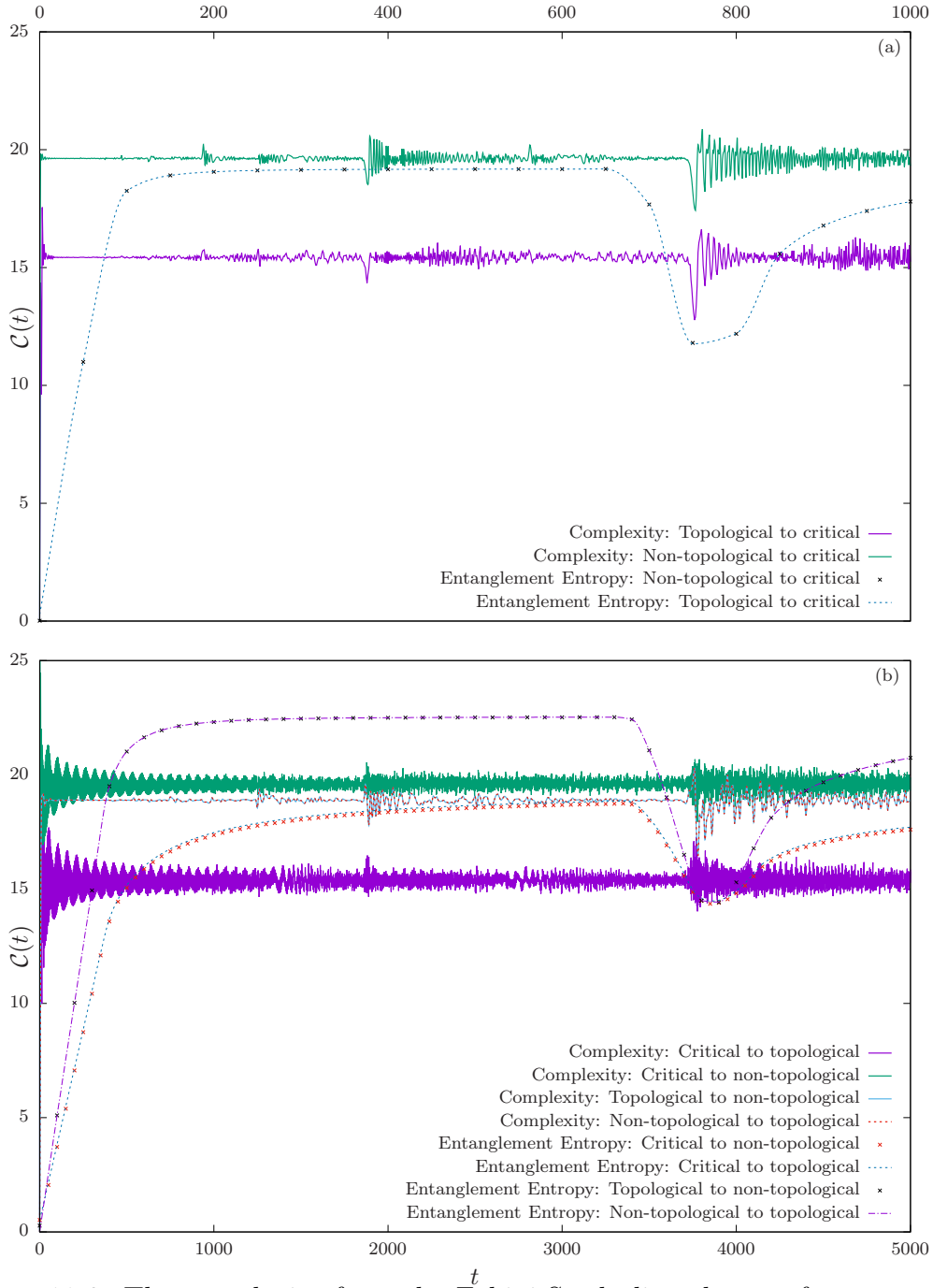

Figure 11.6: The complexity from the Fubini-Study line element for a system of length N=1500. Quenching (a) from a massive phase to the critical point (b) to a massive phase.

However, as we saw, the evolution of entanglement entropy is only fractionally different when compared to the system with no boundary entanglement, so this does not explain why the entanglement entropy saturates much later than complexity. In fact, the rapid saturation of the complexity is tied to the rapid decay of the fidelity, namely because the final state becomes orthogonal to the initial state very rapidly, apparently much quicker than the entanglement in the system can build, which scales with area. In the context of AdS/CFT this may seem surprising, since the reason complexity is of interest there is due to the fact that complexity saturates *later* than the entanglement entropy (in fact, exponentially slower), in order to explain e.g. the growth of extremal surfaces of eternal black holes. On the QFT side, however, the complexity need only continue to evolve after the saturation of entanglement entropy in systems which thermalize: one might guess that in systems that exhibit many-body localization, for example, the complexity could saturate faster.

Another interesting observation is the signature of revivals in the complexity. This is specifically interesting, since the complexity is much less demanding to compute than the entanglement entropy, yet the complexity captures similar information such as revivals and information about different topological transitions. This makes the complexity an appealing quantitiy with which to probe quantum phase transitions.

Finally, we highlight potential drawback of complexity in systems with topological order. The topological order of a system can be characterized using the entanglement entropy [161] or the entanglement spectrum [162]. For the SSH model, the topological order is attained from the nontrivial topology of its Hilbert space [163,164], and in general, topological orders are readily probed on a manifold with a boundary. The complexity is a property of the system's entire wave function [94], and yet it does not give information about the topological order: the complexity appears to be a less sensitive probe than the entanglement under some circumstances.

XII

Conclusion to Part II

In this part of the thesis, we explored various aspects of compuational complexity in quantum field theories and entanglement. Utilising group theoretic methods, we contrasted multiple different measures of complexity in quantum field theories, comparing them using the evolution of states, specifically various incarnations of the Loschmidt echo. We found that the complexity constructed directly from the wave function (following Nielsen's approach [85, 87]) was the most sensitive to certain physical effects, at least when compared with the complexity as derived from the Fubini-Study line element or the covariance matrix.

We also showed that, contrary to the expectation from AdS/CFT (and the bahaviour of black hole interiors) [79,82], there are situations where the complexity saturates *before* the entanglement entropy. Additionally, we showed that the complexity is sensitive to *revivals*, and in fact can detect the same revivals as the entanglement entropy. However, we also showed that there are situations where the entanglement entropy/spectrum is able to capture physical effects that the complexity is blind to; in our example, the topological order.

There are many natural follow ups to this work. Given our observation that the complexity saturates very quickly in the SSH model, it is important to understand the issue of time scales, namely the relation between the equilibration time and the time for the complexity to saturate. Additionally, it was observed in [97,165] that locality has an important role in the saturation rates of complexity, and it would be interesting to understand this relationship in a controllable manner, perhaps learning something about gravity in the process. In order to better understand the relationship between complexity in quantum field theories and holography, it is important to extend the definitions of complexity to *interacting* field theories, with some recent work in this direction being [93].

The Loschmidt echo is closely related to the out of time order correlation function (the OTOC) and as such it might be interesting to evaluate $\mathcal{C}_{\text{LE}}(t)$ for chaotic theories, in the hope that we can understand its relation to chaos and perhaps even find an expression for the Lyapunov exponent in terms of the complexity.

Part III

Appendix

I

Passarino-Veltman Integral Reduction

Due to a result by Passarino and Veltman [166], any one-loop integral with arbitrary tensorial structure in the numerator can be written in terms of scalar one-loop integrals I_j [37, 167, 168]

$$\mathcal{I}_n = \sum_{j_4} c_4 I_4^{(j4)} + \sum_{j_3} c_3 I_3^{(j3)} + \sum_{j_2} c_2 I_2^{(j2)} + \sum_{j_1} c_1 I_1^{(j1)} + \mathcal{R} + \mathcal{O}(\epsilon) \tag{A.0.1}$$

Where $I_n^{(j} = \int d\eta\, I(n, \Delta)$, j refers to the various distributions of the different n legs and $\mathcal{R}$ is a rational function of mandelstam variables left over from dimensional regularisation. The coefficients c_j are also rational functions of mandelstam variables. Diagrammatically, for four external particles, this looks like

$I_n = c_2$ 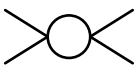 $+ \quad c_3$ 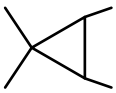 $+ \quad c_4$ 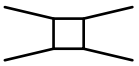

We note that the one-loop scalar integrals are given by

$$I_j = \int \frac{d^D k}{(2\pi)^D} \frac{1}{\prod_j D_j}, \qquad D_j = (k + q_j)^2 - \Delta_j^2 + i\epsilon \tag{A.0.2}$$

Where q_i is the *region momentum*, the sum of the external momentum flowing into the propagator from a connected vertex, $q_i = \sum_j^i p_j$, i.e. $q_1 = p_1, \quad q_2 = p_1 + p_2 \ldots$. It is useful to note that we can write any external momentum in terms of region momentum, since $p_i = q_i - q_{i-1}$.

The reduction of tensor numerators to scalars is known as Passarino-Veltman reduction [166], and it essentially follows directly from Lorentz invariance and momentum conservation. This is because we known that the result of any tensor integration must be proportional to some known tensorial object in the problem, objects we can use as a basis for doing loop computations.

Any one-loop tensor integral has the form

$$C^{\mu\nu\cdots\rho} = \int \frac{d^D k}{(2\pi)^D} \frac{k^\mu k^\nu \cdots k^\rho}{\prod_j D_j(p^2, k^2, m^2)} = A_n^{(1)}[k^\mu k^\nu \cdots k^\rho] \tag{A.0.3}$$

Where the j, the number of propagators D in the denominator, can be at most equal to the number of external legs n. We want to motivate the idea that, in agreement with eq. A.0.1, we can represent such an integral as

$$\int \frac{d^D k}{(2\pi)^D} \frac{k^\mu k^\nu \cdots k^\rho}{\prod_j D_j(p^2, k^2, m^2)} = \sum_{j \leq D} \int \frac{d^D k}{(2\pi)^D} \frac{1}{\prod_j D_j(p^2, k^2, m^2)} \tag{A.0.4}$$

Let's consider a general rank one integral

$$C^\mu = \int \frac{d^D k}{(2\pi)^D} \frac{k^\mu}{[k^2 - \Delta][(k+q_i)^2 - \Delta_j] \cdots [(k+q_n)^2 - \Delta_n]} \tag{A.0.5}$$

The only rank one tensor that this can be proportional to is the momentum p_i^μ

$$C^\mu = \sum_i^{n-1} C_{n;i}(p) p_i^\mu \tag{A.0.6}$$

Contracting this with p_j, we find

$$C \cdot p_j = \int \frac{d^D k}{(2\pi)^D} \frac{k \cdot p_j}{[k^2 - \Delta][(k+q_i)^2 - \Delta_j] \cdots [(k+q_n)^2 - \Delta_n]} = \sum_i^{n-1} C_{n;i}(p) G^{ij} \tag{A.0.7}$$

Where $G^{ij} = p_i \cdot p_j$ is known as the Gram matrix. Rewriting everything in terms of region momentum using $p_j = q_j - q_{j-1}$, we can rewrite the numerator as

$$\begin{aligned} 2k \cdot p_j &= \Big([(k+q_j)^2 - \Delta_j] - [(k+q_{j-1})^2 - \Delta_{j-1}] + \Delta_j - \Delta_{j-1} - q_j^2 - q_{j-1}^2 \Big) \\ &= D_j - D_{j-1} + \Delta_j - \Delta_{j-1} - q_j^2 - q_{j-1}^2 \end{aligned} \tag{A.0.8}$$

The D_j & D_{j-1} factors cancel a propagator each, meaning we can write

$$\sum_i^{n-1} C_{n;i}(p) G^{ij} = \frac{1}{2} \left[A^{(1)}_{n-1,j} - A^{(1)}_{n-1,j-1} + (\Delta_j - \Delta_{j-1} - q_j^2 + q_{j-1}^2) A^{(1)}_n \right] = R^j_n \tag{A.0.9}$$

This is a linear system involving an $(n-1, j)$ degree matrix, simply solved by inverting the matrix and reading off the coefficients $C_{n;i}$. Doing so means we have successfully reduced our tensor integral to scalars. However, we see that the coefficients necessarily depend on the inverse of the Gram matrix: we require that $\det G \neq 0$. This means that care must be taken when $n > D$, due to the fact that in D dimensions there can be at most D linearly independent vectors. Therefore, when expanding into a basis we only need ever consider at most D vectors, even for $n > D$. This is the reason we only consider a basis of D scalar integrals.

For simplicity, lets consider a rank-one three-point one-loop function, i.e.

$$C^\mu = \int \frac{d^D k}{(2\pi)^D} \frac{k^\mu}{D_1 D_2 D_3} = C_{3;1} p_1^\mu + C_{3;2} p_2^\mu \tag{A.0.10}$$

Contracting both with p_1 and p_2, we find

$$G\begin{pmatrix}C_{3;1}\\C_{3;2}\end{pmatrix} = \begin{pmatrix}R_{3;1}\\R_{3;2}\end{pmatrix} \qquad \Longrightarrow \qquad \begin{pmatrix}C_{3;1}\\C_{3;2}\end{pmatrix} = G^{-1}\begin{pmatrix}R_{3;1}\\R_{3;2}\end{pmatrix} \tag{A.0.11}$$

Where the Gram matrix in this case is given by

$$G = \begin{pmatrix}m_1^2 & p_1\cdot p_2\\ p_1\cdot p_2 & m_2^2\end{pmatrix}, \qquad G^{-1} = \frac{1}{m_1^2m_2^2-(p_1\cdot p_2)^2}\begin{pmatrix}m_2^2 & -p_1\cdot p_2\\ -p_1\cdot p_2 & m_1^2\end{pmatrix} \tag{A.0.12}$$

We can now simply read off the coefficients $C_{n;i}$.

We can of course use this procedure for higher-rank one-loop integrals. Lets consider the three-point one-loop function again

$$C^{\mu\nu} = \int \frac{d^Dk}{(2\pi)^D}\frac{k^\mu k^\nu}{D_1D_2D_3} \tag{A.0.13}$$

This must be equal to a rank two tensor, the only choices being $g^{\mu\nu}$ and $p_i^\mu p_j^\nu$, meaning

$$C^{\mu\nu} = C_{2;00}g^{\mu\nu} + \sum_{ij} C_{2;ij}p_i^\mu p_j^\nu \tag{A.0.14}$$

We can solve for $C_{2;ij}$ by contracting these objects with our known tensors. We could, for example, contract this object with $g_{\mu\nu}$ or $p_{i,\mu}p_{j,\nu}$ but it should be obvious that this unnecessary if we have already worked out the vector integral case. For a tensor integral of any order, one may simply contract with a single momentum or single metric tensor in order to reduce the rank of the integral to that of a known integral.

Contracting with p_μ, for example, we find

$$\begin{aligned}
C^{\mu\nu}p_\mu &= [C_{2;0}+C_{2;1}m^2]p^\nu && \text{(A.0.15)}\\
&= \int \frac{d^Dk}{(2\pi)^D}\frac{(k\cdot p)k^\nu}{k^2(k+p)^2} && \text{(A.0.16)}\\
&= \frac{1}{2}\int \frac{d^Dk}{(2\pi)^D}\frac{k^\nu[(k+p)^2-k^2-m^2]}{k^2(k+p)^2} && \text{(A.0.17)}\\
&= \frac{1}{2}\int \frac{d^Dk}{(2\pi)^D}\frac{k^\nu}{k^2} - \frac{1}{2}\int \frac{d^Dk}{(2\pi)^D}\frac{k^\nu}{(k+p)^2} - \frac{m^2}{2}\int \frac{d^Dk}{(2\pi)^D}\frac{k^\nu}{k^2(k+p)^2} && \text{(A.0.18)}
\end{aligned}$$

We now have everything in terms of vector integrals, which we already solved above. For a generic rank r tensor integral, this procedure can simply be iterated as many times as is required until the integral is in a known form.

II

Bogoliubov Transformations, SU(1,1) and SP(2N, ℝ)

In this appendix, we give a short overview of the Bogoliubov transformations and the groups $SU(1,1)$ and $SP(2N,\mathbb{R})$, mainly following [139, 169, 170]. Consider a scalar field theory with Lagrangian and equations of motion

$$\mathcal{L}(x) = \frac{1}{2}\left(\partial_\mu\phi\partial^\mu\phi + m^2\phi^2\right), \qquad (\partial^2 - m^2)\phi = 0. \tag{B.0.1}$$

This has a canonical solution

$$\phi(x,t) = \int \frac{d^{d-1}p}{\sqrt{2\omega_p}}\left[a_p e^{ip\cdot x - i\omega t} + a_p^\dagger e^{-(ip\cdot x - i\omega t)}\right], \tag{B.0.2}$$

where $\omega = \sqrt{p^2+m^2}$.

In general, however, we are free to choose any basis of positive frequency modes $\{f, f^\star\}$, where in this case we have chosen specifically a plane wave

$$f_p = \frac{1}{\sqrt{2\omega_p}} e^{ip\cdot x - i\omega t}. \tag{B.0.3}$$

Generically, we want to choose modes that are orthonormal with respect to the Klien-Gordon inner product

$$(f, f') = -i\int d^{d-1}x\left(f\dot{f}'^\star - \dot{f}f'^\star\right), \qquad (f_p, f_{p'}) = \delta(p-p'). \tag{B.0.4}$$

We can expand our scalar field in this basis

$$\phi = \sum_p \left(a_p f_p + a_p^\dagger f_p^\star\right). \tag{B.0.5}$$

The commutation relations for the creation and annihilation operators is

$$[a_p, a_{p'}^\dagger] = \delta(p-p'), \qquad [a_p, a_{p'}] = [a_p^\dagger, a_{p'}^\dagger] = 0, \tag{B.0.6}$$

and the vacuum state is defined as the state annihilated by the annihilation operator

$$a_p \left|0\right\rangle = 0. \tag{B.0.7}$$

However, it is important to note that we could have expanded our field in a different basis, and the operators obtained in that case will not, in general, annihilate the same vacuum: the vacuum is not unique.

Let's imagine a state which, at time $t \leq 0$, is in the ground state of some Hamiltonian H_1. At time $t > 0$, the parameters of the system change and the state's time evolution is now described by a different Hamiltonian H_2, meaning it is no longer in the ground state of H_1. Our system to be described by operators $\hat{x}$ and $\hat{p}$, which can be written in terms of the creation and annihilation operators in the usual way. However, each Hamiltonian H_1 and H_2 have different creation and annihilation operators, and $\hat{x}$ and $\hat{p}$ can be written in terms of both, meaning

$$\hat{x} = \frac{1}{\sqrt{2\omega_1}}(a + a^\dagger) = \frac{1}{\sqrt{2\omega_2}}(b + b^\dagger), \qquad \hat{p} = \sqrt{\frac{\omega_1}{2}}(a - a^\dagger) = \sqrt{\frac{\omega_2}{2}}(b - b^\dagger). \tag{B.0.8}$$

Essentially this reflects the basis change in eq. B.0.5, and from this we can derive the famous Bogoliubov transformations.

The Bogoliubov transformations are linear relations among operators, given by

$$\begin{pmatrix} b_p \\ b_p^\dagger \end{pmatrix} = \begin{pmatrix} \mathcal{U}_p & \mathcal{V}_p \\ \mathcal{V}_p^* & \mathcal{U}_p^* \end{pmatrix} \begin{pmatrix} a_p \\ a_p^\dagger \end{pmatrix}. \tag{B.0.9}$$

We require that $b, b^\dagger$ satisfy the same commutation relations as $a, a^\dagger$, i.e.

$$[b_p, b_{p'}^\dagger] = \delta(p - p'), \qquad [b_p, b_{p'}] = [b_p^\dagger, b_{p'}^\dagger] = 0. \tag{B.0.10}$$

This places the requirement that the determinant of the Bogoliubov matrix is unity, i.e. that

$$|\mathcal{U}_p|^2 - |\mathcal{V}_p|^2 = 1$$

In the case of the system above, we find that

$$\mathcal{U}_p = \frac{\omega_1 + \omega_2}{2\sqrt{\omega_1\omega_2}}, \qquad \mathcal{V}_p = \frac{\omega_1 - \omega_2}{2\sqrt{\omega_1\omega_2}}$$

Packaged in the form of eq. B.0.9, we see that Bogoliubov transformations are nothing more than transformations under the group $SU(1,1)$, whose elements are complex matrices of the form

$$g = \begin{pmatrix} \alpha & \beta \\ \beta^* & \alpha^* \end{pmatrix} \in SU(1,1), \qquad |\alpha|^2 - |\beta|^2 = 1. \tag{B.0.11}$$

Elements of $SU(1,1)$ have three real parameters, which we can choose to be, for example,

$$g(\omega,\phi,\theta) = \begin{pmatrix} e^{i\phi}\cosh(\theta) & e^{i\omega}\sinh(\theta) \\ e^{-i\omega}\sinh(\theta) & e^{-i\phi}\cosh(\theta) \end{pmatrix}. \tag{B.0.12}$$

The associated Lie algebra that generates the group is $\mathfrak{su}(1,1)$, which has three generators K_1, K_2, K_0, and commutation relations

$$[K_1,K_2] = -iK_0, \qquad [K_2,K_0] = iK_1, \qquad [K_1,K0] = -iK_2. \tag{B.0.13}$$

There is a simpler basis which is more useful

$$K_\pm = \pm i(K_1 \pm iK_2), \qquad K_0, \tag{B.0.14}$$

$$[K_0,K_\pm] = \pm K_\pm, \qquad [K_-,K_+] = 2K_0. \tag{B.0.15}$$

In terms of creation and annihilation operators for modes $\{k,-k\}$, we can write the generators as

$$K_+ = a_k^\dagger a_{-k}^\dagger \qquad K_- = a_{-k}a_k \qquad K_0 = \frac{a_k^\dagger a_k + a_{-k}a_{-k}^\dagger}{2}. \tag{B.0.16}$$

Note that $SU(1,1)$ is related to $SL(2,\mathbb{R})$ by way of a *Caley transformation* C [169]

$$C\cdot SL(2,\mathbb{R})\cdot C^{-1} = SU(1,1), \qquad C\cdot \mathfrak{sl}(2,\mathbb{R})\cdot C^{-1} = \mathfrak{su}(1,1), \qquad C = \frac{1}{\sqrt{2i}}\begin{pmatrix} 1 & -i \\ 1 & i \end{pmatrix}. \tag{B.0.17}$$

Representations $T(g)$ of $SU(1,1)$ can be used to define coherent states

$$|\psi_{Coherent}\rangle = T(g)\,|\psi_0\rangle\,, \tag{B.0.18}$$

with a generic $SU(1,1)$ coherent state parameterised by

$$|\psi\rangle = e^{\alpha_+K_+ + \alpha_-K_- + \omega K_0}\,|\psi_0\rangle\,. \tag{B.0.19}$$

We can decompose this state with the useful identity

$$\exp\left[\alpha_+K_+ + \alpha_-K_- + \omega K_0\right] = \exp\left(\gamma_+K_+\right)\exp\left(\ln\gamma_0 K_0\right)\exp\left(\gamma_-K_-\right), \tag{B.0.20}$$

where[1]

$$\gamma_0 = \frac{1}{\left(\cosh\mu - \frac{\beta}{2\mu}\sinh\mu\right)^2}, \qquad \gamma_\pm = \frac{2\alpha_\pm\sinh\mu}{2\mu\cosh\mu - \beta\sinh\mu}, \qquad \mu^2 = \frac{\beta^2}{4} - \alpha_+\alpha_-\,. \tag{B.0.21}$$

[1]For $SU(2)$, the decomposition is identical bar the definition

$$\mu^2 = \frac{\beta^2}{4} + \alpha_+\alpha_-$$

We can also derive a useful identity by considering the fact that unitarity demands that $\alpha_+^\star = -\alpha_-$ and $\beta^* = -\beta$ with $\mu \in \mathbb{R}$. Then, we find that

$$|\gamma_0| = \sqrt{\frac{1}{\left(\cosh\mu - \frac{\beta}{2\mu}\sinh\mu\right)^2}\frac{1}{\left(\cosh\mu + \frac{\beta}{2\mu}\sinh\mu\right)^2}} = \frac{1}{\cosh^2\mu - \frac{\beta^2}{4\mu^2}\sinh^2\mu}, \quad \text{(B.0.22)}$$

and

$$|\gamma_+^2| = \frac{2\alpha_+\sinh\mu}{2\mu\cosh\mu - \beta\sinh\mu}\frac{-2\alpha_-\sinh\mu}{2\mu\cosh\mu + \beta\sinh\mu} \quad \text{(B.0.23)}$$

$$= \frac{-\alpha_+\alpha_-\sinh^2\mu}{\mu^2(\cosh^2\mu - \frac{\beta^2}{4\mu^2}\sinh^2\mu)}. \quad \text{(B.0.24)}$$

Adding these together and simplifying via $\alpha_+\alpha_- = \frac{\beta^2}{4} - \mu^2$, we discover a useful identity

$$|\gamma_0| + |\gamma_+|^2 = 1. \quad \text{(B.0.25)}$$

A closely related group is the symplectic group $SP(2,\mathbb{R})$, which is locally isomorphic to $SU(1,1)$, although we will more consider the more general $SP(2N,\mathbb{R})$ for now. The action of $SP(2N,\mathbb{R})$ preserves the canonical commutation relations between phase-space coordinates, given by

$$\xi = [x_1, p_1, x_2, p_2 ..., x_N, p_N] \in \mathbb{R}^{2N}, \qquad [\xi^a, \xi^b] = i\Omega^{a,b}, \qquad \Omega = \begin{pmatrix} 0 & \mathbb{1}_{N\times N} \\ -\mathbb{1}_{N\times N} & 0 \end{pmatrix}. \quad \text{(B.0.26)}$$

Formally, $SP(2N,\mathbb{R})$ is defined as the group of $2N \times 2N$ matrices S that obey $S\Omega S^T = \Omega$. We can build S via the generators of the algebra $J \in \mathfrak{sp}(2N,\mathbb{R})$,

$$S(\sigma) = \exp(-i\sigma J) \simeq 1 - i\sigma J, \qquad |\sigma| \ll 1, \qquad J^* = -J. \quad \text{(B.0.27)}$$

The genrator J is a pure imaginary matrix, meaning $S(\sigma) = e^{\sigma\bar{J}} \in SP(2N,\mathbb{R})$, where $\bar{J} = iJ$ is a real matrix. Alternatively, we can define this in terms of a quadratic operator

$$K = \frac{1}{2}\xi^a k_{ab}\xi^b, \quad \text{(B.0.28)}$$

where k_{ab} is a real symmetric form. We consider such objects in order to define σ-dependent states as

$$|\psi(\sigma)\rangle = e^{-i\sigma K}|\psi\rangle = U(\sigma)|\psi(0)\rangle. \quad \text{(B.0.29)}$$

The matrix associated with this operator is given by

$$K^a{}_b = iJ^a{}_b = \Omega^{ac}k_{cb} \in SP(2,\mathbb{R}). \quad \text{(B.0.30)}$$

Importantly, the action on the canonical coordinate vector is

$$U(\sigma)^\dagger \xi^a U(\sigma) = U^a{}_b \xi^b. \tag{B.0.31}$$

For the purposes of this thesis, a useful representation of $SP(2N,\mathbb{R})$ is the metaplectic representation [170], given in terms of the hermitian phase space operators as

$$W_{ij} = \frac{1}{2}\{x_i, p_j\}, \qquad V_{ij} = \frac{x_i x_j}{\sqrt{2}}, \qquad Z_{ij} = \frac{p_i p_j}{\sqrt{2}}. \tag{B.0.32}$$

For $N = 1$, this simplifies, since $i = j$, and we find a simple closed Lie algebra $\mathfrak{sp}(2,\mathbb{R})$ (which, as you may notice, is isomorphic to $\mathfrak{su}(1,1)$ as given in eq. B.0.13)

$$[V, W] = -2iV, \qquad [V, Z] = 2iW, \qquad [W, Z] = 2iZ. \tag{B.0.33}$$

Matrix generators can be constructed from eq. B.0.28 by writing, for example,

$$\frac{1}{2}\xi^a k_{ab}(W)\xi^b = \frac{1}{2}(xp + px). \tag{B.0.34}$$

We determine that $k_{12}(W) = k_{21}(W) = 1$ and $k_{11} = k_{22} = 0$, and similarly for others, finding

$$k(W) = \begin{pmatrix} 0 & 1 \\ 1 & 0 \end{pmatrix}, \qquad k(V) = \begin{pmatrix} \sqrt{2} & 0 \\ 0 & 0 \end{pmatrix}, \qquad k(Z) = \begin{pmatrix} 0 & 0 \\ 0 & \sqrt{2} \end{pmatrix}. \tag{B.0.35}$$

We can then use eq. B.0.30 to construct matrix representations

$$W = \begin{pmatrix} 1 & 0 \\ 0 & -1 \end{pmatrix}, \qquad V = \begin{pmatrix} 0 & 0 \\ -\sqrt{2} & 0 \end{pmatrix}, \qquad Z = \begin{pmatrix} 0 & \sqrt{2} \\ 0 & 0 \end{pmatrix}, \tag{B.0.36}$$

which obey the Lie algebra

$$[V, W] = 2V, \qquad [W, Z] = 2Z, \qquad [V, Z] = 2W. \tag{B.0.37}$$

We can then exponentiate these generators to find matrix elements of $SP(2,\mathbb{R})$

$$U_W(\epsilon) = e^{\epsilon W} = \begin{pmatrix} e^{\epsilon} & 0 \\ 0 & e^{-\epsilon} \end{pmatrix}, \quad U_V(\epsilon) = e^{\epsilon V} = \begin{pmatrix} 1 & 0 \\ -\sqrt{2}\epsilon & 1 \end{pmatrix}, \quad U_Z(\epsilon) = e^{\epsilon Z} = \begin{pmatrix} 1 & \sqrt{2}\epsilon \\ 0 & 1 \end{pmatrix}. \tag{B.0.38}$$

Elements of $SP(2,\mathbb{R})$ can be parameterised as

$$g(\omega,\phi,\theta) = \begin{pmatrix} \cos\phi\cosh\theta - \sin\omega\sinh\theta & -\sin\phi\cosh\theta + \cos\omega\sinh\theta \\ \sin\phi\cosh\theta + \cos\omega\sinh\theta & \cos\phi\cosh\theta + \sin\omega\sinh\theta \end{pmatrix} \in SP(2,\mathbb{R}). \tag{B.0.39}$$

Index

(BdG Hamiltonian, 94

Araki-Leib inequality, 77
asymptotic states, 8
average entropy, 79
average information, 79

bcfw recursion, 31, 35
bcfw with massive particles, 35
Bogoliubov transformations, VI
Bogoliubov-de Gennes Hamiltonian, 94

causal diamond, 89
classical scattering, 5
colour ordering, 15
complex projective space, 99
computational complexity, 96
correlation matrix, 94
covariance matrix, 111
covariance matrix complexity, 112
cross section, 6

deflection angle, 50
density matrix, 72
domain of dependence, 89

entanglement cut, 83
entanglement hamiltonian, 78
entanglement spectrum, 94
entanglement surface, 83, 89
entropy, 73

fidelity, 99
Finsler geometry, 101
first law of entanglement, 78
first law of thermodynamics, 78
Fubini-Study complexity, 107
Fubini-Study distance, 99
Fubini-Study metric, 99

gates, 96
Gaussian state complexity, 106
geometric entanglement entropy, 89

Hilbert space, 71

impact parameter, 5

light bending, 42
little group, 22

mixed state, 72
modular hamiltonian, 78, 89

Nielsen complexity, 101

optical theorem, 11

partial amplitudes, 15
path integral, 80
polarization vectors, 21
product state, 72
projection operator, 72
pure state, 72
purification, 79

recursion (infinite), XI
recursion relations, 28
relative entropy, 77

Renyí entropy, 74
residue theorem, 31
Rindler coordinates, 89
Rindler wedge, 89

S Matrix, 9
schmidt decomposition, 79
separable state, 72
Solovay-Kitaev theorem, 98
spinor-helicty, 18
spinors, 17
Stückelberg procedure, 56
stabiliser group, 22
strong sub-additivity, 77
sub-additivity, 77

The SSH model, 133
The Su-Schrieffer-Heeger model, 133
thermal states, 74
thermofield double, 80
transition matrix, 9

uncomplexity, 131
unitarity, 10, 74
Unruh temperature, 89

vDVZ discontinuity, 57, 66
von-Neumann entropy, 73

Weyl equation, 19
Weyl spinor, 18

Bibliography

[1] D. J. Burger, N. Moynihan, S. Das, S. Shajidul Haque and B. Underwood, *Towards the Raychaudhuri Equation Beyond General Relativity*, *Phys. Rev.* **D98** (2018) 024006, [arXiv:1802.09499].

[2] R. Carballo-Rubio, F. Di Filippo and N. Moynihan, *Taming higher-derivative interactions and bootstrapping gravity with soft theorems*, arXiv:1811.08192.

[3] D. J. Burger, R. Carballo-Rubio, N. Moynihan, J. Murugan and A. Weltman, *Amplitudes for Astrophysicists: Known Knowns*, *Gen. Rel. Grav.* (2017) , [arXiv:1704.05067].

[4] N. Moynihan and J. Murugan, *Comments on scattering in massive gravity, vDVZ and BCFW*, *Class. Quant. Grav.* **35** (2017) 155005, [arXiv:1711.03956].

[5] T. Ali, A. Bhattacharyya, S. Shajidul Haque, E. H. Kim and N. Moynihan, *Time Evolution of Complexity: A Critique of Three Methods*, arXiv:1810.02734.

[6] T. Ali, A. Bhattacharyya, S. Shajidul Haque, E. H. Kim and N. Moynihan, *Post-Quench Evolution of Distance and Uncertainty in a Topological System: Complexity, Entanglement and Revivals*, arXiv:1811.05985.

[7] S. Weinberg, *The Quantum Theory of Fields*, vol. 1. Cambridge University Press, 1995, 10.1017/CBO9781139644167.

[8] E. P. Wigner, *On Unitary Representations of the Inhomogeneous Lorentz Group*, *Annals Math.* **40** (1939) 149–204.

[9] V. Bargmann and E. P. Wigner, *Group Theoretical Discussion of Relativistic Wave Equations*, *Proc. Nat. Acad. Sci.* **34** (1948) 211.

[10] S. J. Parke and T. R. Taylor, *Amplitude for n-gluon scattering*, *Phys. Rev. Lett.* **56** (Jun, 1986) 2459–2460.

[11] F. Cachazo, P. Svrcek and E. Witten, *Gauge theory amplitudes in twistor space and holomorphic anomaly*, *JHEP* **10** (2004) 077, [arXiv:hep-th/0409245].

[12] F. Cachazo, P. Svrcek and E. Witten, *MHV vertices and tree amplitudes in gauge theory*, *JHEP* **09** (2004) 6, [arXiv:hep-th/0403047].

[13] E. Witten, *Perturbative gauge theory as a string theory in twistor space*, *Commun. Math. Phys.* **252** (2004) 189–258, [arXiv:hep-th/0312171].

[14] C. Cheung and G. N. Remmen, *Twofold symmetries of the pure gravity action*, *Journal of High Energy Physics* **1** (Jan., 2017) 104, [arXiv:1612.03927].

[15] F. Loebbert, M. Mojaza and J. Plefka, *Hidden Conformal Symmetry in Tree-Level Graviton Scattering*, *JHEP* **05** (2018) 208, [arXiv:1802.05999].

[16] J. M. Drummond, J. Henn, G. P. Korchemsky and E. Sokatchev, *Dual superconformal symmetry of scattering amplitudes in N=4 super-Yang-Mills theory*, *Nuclear Physics B* **828** (Mar., 2010) 317–374, [arXiv:0807.1095].

[17] N. Arkani-Hamed and J. Trnka, *The Amplituhedron*, *Journal of High Energy Physics* **10** (Oct., 2014) 30, [arXiv:1312.2007].

[18] G. 't Hooft and M. J. G. Veltman, *DIAGRAMMAR*, *NATO Sci. Ser. B* **4** (1974) 177–322.

[19] L. Landau, *On analytic properties of vertex parts in quantum field theory*, *Nuclear Physics* **13** (1959) 181 – 192.

[20] S. Abreu, R. Britto, C. Duhr and E. Gardi, *From multiple unitarity cuts to the coproduct of Feynman integrals*, *JHEP* **10** (2014) 125, [arXiv:1401.3546].

[21] Z. Bern, *Perturbative quantum gravity and its relation to gauge theory*, *Living Reviews in Relativity* **5** (2002) 1–57, [arXiv:0206071].

[22] F. A. Berends and W. Giele, *The Six Gluon Process as an Example of Weyl-Van Der Waerden Spinor Calculus*, *Nucl. Phys.* **B294** (1987) 700–732.

[23] M. L. Mangano, S. J. Parke and Z. Xu, *Duality and Multi - Gluon Scattering*, *Nucl. Phys.* **B298** (1988) 653–672.

[24] S. Parke and M. Mangano, *The structure of gluon radiation in qcd*, .

[25] H. Elvang and Y.-t. Huang, *Scattering Amplitudes*, arXiv:1308.1697.

[26] J. J. M. Carrasco, *Gauge and Gravity Amplitude Relations*, arXiv:1506.00974.

[27] L. J. Dixon, *A brief introduction to modern amplitude methods*, in

Proceedings, 2012 European School of High-Energy Physics (ESHEP 2012), pp. 31–67, 2014. arXiv:1310.5353. DOI.

[28] P. Benincasa and F. Cachazo, *Consistency Conditions on the S-Matrix of Massless Particles*, *ArXiv e-prints* (May, 2007) , [arXiv:0705.4305].

[29] R. Boels, *Covariant representation theory of the Poincare algebra and some of its extensions*, *JHEP* **01** (2010) 10, [arXiv:0908.0738].

[30] N. Arkani-Hamed, T.-C. Huang and Y.-t. Huang, *Scattering Amplitudes For All Masses and Spins*, arXiv:1709.04891.

[31] R. Britto, F. Cachazo and B. Feng, *New recursion relations for tree amplitudes of gluons*, *Nucl. Phys.* **B715** (2005) 499–522, [arXiv:hep-th/0412308].

[32] R. Britto, F. Cachazo, B. Feng and E. Witten, *Direct proof of tree-level recursion relation in Yang-Mills theory*, *Phys. Rev. Lett.* **94** (2005) 181602, [arXiv:hep-th/0501052].

[33] B. Feng and M. Luo, *An Introduction to On-shell Recursion Relations*, *Front. Phys.(Beijing)* **7** (2012) 533–575, [arXiv:1111.5759].

[34] T. Cohen, H. Elvang and M. Kiermaier, *On-shell constructibility of tree amplitudes in general field theories*, *JHEP* **04** (2011) 53, [arXiv:1010.0257].

[35] S. D. Badger, E. W. N. Glover, V. V. Khoze and P. Svrcek, *Recursion Relations for Gauge Theory Amplitudes with Massive Particles*, *JHEP* **07** (2005) 025, [arXiv:hep-th/0504159].

[36] S. D. Badger, E. W. N. Glover and V. V. Khoze, *Recursion relations for gauge theory amplitudes with massive vector bosons and fermions*, *JHEP* **01** (2006) 66, [arXiv:hep-th/0507161].

[37] Z. Bern, L. Dixon and D. A. Kosower, *Dimensionally regulated one-loop integrals*, *Physics Letters B* **302** (Mar., 1993) 299–308, [arXiv:hep-ph/9212308].

[38] Z. Bern, L. J. Dixon, D. C. Dunbar and D. A. Kosower, *Fusing gauge theory tree amplitudes into loop amplitudes*, *Nucl. Phys.* **B435** (1995) 59–101, [arXiv:hep-ph/9409265].

[39] Z. Bern and A. G. Morgan, *Massive loop amplitudes from unitarity*, *Nucl. Phys.* **B467** (1996) 479–509, [arXiv:hep-ph/9511336].

[40] R. Britto, F. Cachazo and B. Feng, *Generalized unitarity and one-loop amplitudes in N=4 super-Yang-Mills*, *Nucl. Phys.* **B725** (2005) 275–305, [arXiv:hep-th/0412103].

[41] Z. Bern and Y.-t. Huang, *Basics of generalized unitarity*, *Journal of Physics*

A Mathematical General **44** (Nov., 2011) 454003, [arXiv:1103.1869].

[42] G. 't Hooft and M. J. G. Veltman, *Regularization and Renormalization of Gauge Fields*, *Nucl. Phys.* **B44** (1972) 189–213.

[43] F. Cachazo and P. Svrcek, *Lectures on twistor strings and perturbative Yang-Mills theory*, *PoS* **RTN2005** (2005) 004, [arXiv:hep-th/0504194].

[44] R. Britto, *Loop Amplitudes in Gauge Theories: Modern Analytic Approaches*, *J. Phys.* **A44** (2011) 454006, [arXiv:1012.4493].

[45] J. J. M. Carrasco and H. Johansson, *Generic multiloop methods and application to N=4 super-Yang-Mills*, *J. Phys.* **A44** (2011) 454004, [arXiv:1103.3298].

[46] R. K. Ellis, Z. Kunszt, K. Melnikov and G. Zanderighi, *One-loop calculations in quantum field theory: from Feynman diagrams to unitarity cuts*, *Phys. Rept.* **518** (2012) 141–250, [arXiv:1105.4319].

[47] Z. Bern, L. J. Dixon and D. A. Kosower, *On-Shell Methods in Perturbative QCD*, *Annals Phys.* **322** (2007) 1587–1634, [arXiv:0704.2798].

[48] L. J. Dixon, *Calculating scattering amplitudes efficiently*, in *QCD and beyond. Proceedings, Theoretical Advanced Study Institute in Elementary Particle Physics, TASI-95, Boulder, USA, June 4-30, 1995*, pp. 539–584, 1996. arXiv:hep-ph/9601359.

[49] A. Hall, *On-shell recursion relations for gravity*, *Phys. Rev.* **D77** (2008) 124004, [arXiv:0803.0215].

[50] M. E. Peskin and D. V. Schroeder, *An Introduction to quantum field theory*. 1995.

[51] A. Zee, *Quantum field theory in a nutshell*. 2003.

[52] V. I. Zakharov, *Linearized Gravitation Theory and the Graviton Mass*, *Soviet Journal of Experimental and Theoretical Physics Letters* **12** (1970) 312.

[53] H. van Dam and M. J. G. Veltman, *Massive and massless Yang-Mills and gravitational fields*, *Nucl. Phys.* **B22** (1970) 397–411.

[54] E. Conde and A. Marzolla, *Lorentz Constraints on Massive Three-Point Amplitudes*, *JHEP* **09** (2016) 41, [arXiv:1601.08113].

[55] G. Feinberg, S. Barbara and I. Introduction, *Two-photon-exchange force between charged systems: Spinless particles*, .

[56] S. Deser and A. Waldron, *(Dis)continuities of massless limits in spin 3/2 mediated interactions and cosmological supergravity*, *Phys. Lett.* **B501**

(2001) 134–139, [arXiv:hep-th/0012014].

[57] J. M. Maldacena and G. L. Pimentel, *On graviton non-Gaussianities during inflation*, *JHEP* **09** (2011) 45, [arXiv:1104.2846].

[58] S. Raju, *New Recursion Relations and a Flat Space Limit for AdS/CFT Correlators*, *Phys. Rev.* **D85** (2012) 126009, [arXiv:1201.6449].

[59] S. Raju, *Four Point Functions of the Stress Tensor and Conserved Currents in AdS_4/CFT_3*, *Phys. Rev.* **D85** (2012) 126008, [arXiv:1201.6452].

[60] Y. Neiman, *Antipodally symmetric gauge fields and higher-spin gravity in de Sitter space*, *Journal of High Energy Physics* **10** (Oct., 2014) 153, [arXiv:1406.3291].

[61] I. Kogan, S. Mouslopoulos and A. Papazoglou, *The $m \longrightarrow 0$ limit for massive graviton in dS_4 and AdS_4*, *Physics Letters B* **503** (Mar., 2001) 173–180, [arXiv:hep-th/0011138].

[62] F. A. Dilkes, M. J. Duff, J. T. Liu and H. Sati, *Quantum discontinuity between zero and infinitesimal graviton mass with a Lambda term*, *Phys. Rev. Lett.* **87** (2001) 41301, [arXiv:hep-th/0102093].

[63] A. Einstein, B. Podolsky and N. Rosen, *Can quantum-mechanical description of physical reality be considered complete?*, *Phys. Rev.* **47** (May, 1935) 777–780.

[64] J. S. BELL, *On the problem of hidden variables in quantum mechanics*, *Rev. Mod. Phys.* **38** (Jul, 1966) 447–452.

[65] M. A. Nielsen and I. L. Chuang, *Quantum Computation and Quantum Information: 10th Anniversary Edition*. Cambridge University Press, New York, NY, USA, 10th ed., 2011.

[66] L. Bombelli, R. K. Koul, J. Lee and R. D. Sorkin, *Quantum source of entropy for black holes*, *Phys. Rev. D* **34** (Jul, 1986) 373–383.

[67] M. Srednicki, *Entropy and area*, *Phys. Rev. Lett.* **71** (1993) 666–669, [arXiv:hep-th/9303048].

[68] C. Holzhey, F. Larsen and F. Wilczek, *Geometric and renormalized entropy in conformal field theory*, *Nucl. Phys.* **B424** (1994) 443–467, [arXiv:hep-th/9403108].

[69] J. D. Bekenstein, *Black holes and entropy*, *Phys. Rev. D* **7** (Apr, 1973) 2333–2346.

[70] T. Jacobson, *Black hole entropy and induced gravity*, arXiv:gr-qc/9404039.

[71] S. N. Solodukhin, *Entanglement entropy of black holes*, *Living Rev. Rel.* **14**

(2011) 8, [arXiv:1104.3712].

[72] S. Ryu and T. Takayanagi, *Holographic derivation of entanglement entropy from AdS/CFT*, *Phys. Rev. Lett.* **96** (2006) 181602, [arXiv:hep-th/0603001].

[73] V. E. Hubeny, M. Rangamani and T. Takayanagi, *A Covariant holographic entanglement entropy proposal*, *JHEP* **07** (2007) 062, [arXiv:0705.0016].

[74] M. Van Raamsdonk, *Comments on quantum gravity and entanglement*, arXiv:0907.2939.

[75] M. Van Raamsdonk, *Building up spacetime with quantum entanglement*, *Gen. Rel. Grav.* **42** (2010) 2323–2329, [arXiv:1005.3035].

[76] T. Faulkner, M. Guica, T. Hartman, R. C. Myers and M. Van Raamsdonk, *Gravitation from Entanglement in Holographic CFTs*, *JHEP* **03** (2014) 051, [arXiv:1312.7856].

[77] B. Swingle and M. Van Raamsdonk, *Universality of Gravity from Entanglement*, arXiv:1405.2933.

[78] J. Maldacena and L. Susskind, *Cool horizons for entangled black holes*, *Fortsch. Phys.* **61** (2013) 781–811, [arXiv:1306.0533].

[79] L. Susskind, *Entanglement is not enough*, *Fortsch. Phys.* **64** (2016) 49–71, [arXiv:1411.0690].

[80] T. Hartman and J. Maldacena, *Time Evolution of Entanglement Entropy from Black Hole Interiors*, *JHEP* **05** (2013) 014, [arXiv:1303.1080].

[81] D. Stanford and L. Susskind, *Complexity and shock wave geometries*, *Phys. Rev.* **D90** (2014) 126007, [arXiv:1406.2678].

[82] L. Susskind, *Computational Complexity and Black Hole Horizons*, *Fortsch. Phys.* **64** (2016) 44–48, [arXiv:1403.5695].

[83] A. R. Brown, D. A. Roberts, L. Susskind, B. Swingle and Y. Zhao, *Complexity Equals Action*, *ArXiv e-prints* (Sept., 2015) , [arXiv:1509.07876].

[84] A. R. Brown, D. A. Roberts, L. Susskind, B. Swingle and Y. Zhao, *Complexity, action, and black holes*, *Phys. Rev.* **D93** (2016) 086006, [arXiv:1512.04993].

[85] M. A. Nielsen, *A geometric approach to quantum circuit lower bounds*, *eprint arXiv:quant-ph/0502070* (Feb., 2005) , [arXiv:quant-ph/0502070].

[86] M. A. Nielsen, M. R. Dowling, M. Gu and A. C. Doherty, *Quantum Computation as Geometry*, *Science* **311** (Feb., 2006) 1133–1135,

[arXiv:quant-ph/0603161].

[87] R. A. Jefferson and R. C. Myers, *Circuit complexity in quantum field theory*, *Journal of High Energy Physics* **10** (Oct., 2017) 107, [arXiv:1707.08570].

[88] S. Chapman, M. P. Heller, H. Marrochio and F. Pastawski, *Toward a Definition of Complexity for Quantum Field Theory States*, *Phys. Rev. Lett.* **120** (2018) 121602, [arXiv:1707.08582].

[89] L. Hackl and R. C. Myers, *Circuit complexity for free fermions*, *JHEP* **1807** (2018) , [arXiv:1803.10638].

[90] S. Chapman, J. Eisert, L. Hackl, M. P. Heller, R. Jefferson, H. Marrochio et al., *Complexity and entanglement for thermofield double states*, arXiv:1810.05151.

[91] M. Guo, J. Hernandez, R. C. Myers and S.-M. Ruan, *Circuit complexity for coherent states*, *Journal of High Energy Physics* **2018** (Oct, 2018) .

[92] D. W. F. Alves and G. Camilo, *Evolution of complexity following a quantum quench in free field theory*, *JHEP* **06** (2018) 029, [arXiv:1804.00107].

[93] A. Bhattacharyya, A. Shekar and A. Sinha, *Circuit complexity in interacting QFTs and RG flows*, *JHEP* **10** (2018) 140, [arXiv:1808.03105].

[94] H. A. Camargo, P. Caputa, D. Das, M. P. Heller and R. Jefferson, *Complexity as a novel probe of quantum quenches: universal scalings and purifications*, arXiv:1807.07075.

[95] P. Caputa, N. Kundu, M. Miyaji, T. Takayanagi and K. Watanabe, *Liouville action as path-integral complexity: From continuous tensor networks to ads/cft*, *JHEP* **1711** (2018) , [arXiv:1706.07056].

[96] W. Cottrell and M. Montero, *Complexity is simple!*, *JHEP* **02** (2018) 039, [arXiv:1710.01175].

[97] K. Hashimoto, N. Iizuka and S. Sugishita, *Time evolution of complexity in Abelian gauge theories*, *Phys. Rev.* **D96** (2017) 126001, [arXiv:1707.03840].

[98] R. Khan, C. Krishnan and S. Sharma, *Circuit Complexity in Fermionic Field Theory*, *Phys. Rev.* **D98** (2018) 126001, [arXiv:1801.07620].

[99] K. Hashimoto, N. Iizuka and S. Sugishita, *Thoughts on holographic complexity and its basis-dependence*, *arXiv preprint arXiv:1805.04226* (2018) .

[100] J. Jiang and X. Liu, *Circuit complexity for fermionic thermofield double states*, *arXiv preprint arXiv:1812.00193* (2018) .

[101] R.-Q. Yang and K.-Y. Kim, *Complexity of operators generated by quantum*

mechanical hamiltonians, *arXiv preprint arXiv:1810.09405* (2018) .

[102] V. Balasubramanian, M. DeCross, A. Kar and O. Parrikar, *Binding complexity and multiparty entanglement*, *arXiv preprint arXiv:1811.04085* (2018) .

[103] A. Bhattacharyya, P. Caputa, S. R. Das, N. Kundu, M. Miyaji and T. Takayanagi, *Path-integral complexity for perturbed cfts*, *arXiv preprint arXiv:1804.01999* (2018) .

[104] M. Ghodrati, *Complexity growth rate during phase transitions*, *Physical Review D* **98** (2018) 106011.

[105] A. Belin, A. Lewkowycz and G. Sarosi, *Complexity and the bulk volume, a new york time story*, *arXiv preprint arXiv:1811.03097* (2018) .

[106] D. W. Alves and G. Camilo, *Evolution of complexity following a quantum quench in free field theory*, *Journal of High Energy Physics* **2018** (2018) 29.

[107] X.-H. Ge and B. Wang, *Quantum computational complexity, einstein's equations and accelerated expansion of the universe*, *Journal of Cosmology and Astroparticle Physics* **2018** (2018) 047.

[108] P. Calabrese and J. L. Cardy, *Entanglement entropy and quantum field theory*, *J. Stat. Mech.* **0406** (2004) P06002, [arXiv:hep-th/0405152].

[109] J. L. Cardy, O. A. Castro-Alvaredo and B. Doyon, *Form Factors of Branch-Point Twist Fields in Quantum Integrable Models and Entanglement Entropy*, *Journal of Statistical Physics* **130** (Jan., 2008) 129–168, [arXiv:0706.3384].

[110] P. Calabrese and J. Cardy, *Entanglement entropy and conformal field theory*, arXiv:0905.4013.

[111] H. Casini and M. Huerta, *Entanglement entropy in free quantum field theory*, *J. Phys.* **A42** (2009) 504007, [arXiv:0905.2562].

[112] M. Rangamani and T. Takayanagi, *Holographic Entanglement Entropy*, *Lect. Notes Phys.* **931** (2017) pp.1–246, [arXiv:1609.01287].

[113] T. Nishioka, *Entanglement entropy: Holography and renormalization group*, *Reviews of Modern Physics* **90** (July, 2018) 035007, [arXiv:1801.10352].

[114] J. von Neumann, *Mathematical Foundations of Quantum Mechanics*. Goldstine Printed Materials. Princeton University Press, 1932.

[115] A. RÃl'nyi, *On measures of entropy and information*, in *Proceedings of the Fourth Berkeley Symposium on Mathematical Statistics and Probability, Volume 1: Contributions to the Theory of Statistics*, (Berkeley, Calif.), pp. 547–561, University of California Press, 1961.

[116] J. C. Baez, *Renyi Entropy and Free Energy*, *arXiv e-prints* (Feb., 2011) , [arXiv:1102.2098].

[117] L.-Y. Hung, R. C. Myers, M. Smolkin and A. Yale, *Holographic calculations of Rényi entropy*, *Journal of High Energy Physics* **12** (Dec., 2011) 47, [arXiv:1110.1084].

[118] H. Araki and E. H. Lieb, *Entropy inequalities*, *Comm. Math. Phys.* **18** (1970) 160–170.

[119] E. H. Lieb and M. B. Ruskai, *Proof of the strong subadditivity of quantumâĂŘmechanical entropy*, *Journal of Mathematical Physics* **14** (1973) 1938–1941, [arXiv:https://doi.org/10.1063/1.1666274].

[120] M. A. Nielsen and D. Petz, *A simple proof of the strong subadditivity inequality*, arXiv:quant-ph/0408130.

[121] M. Headrick and T. Takayanagi, *A Holographic proof of the strong subadditivity of entanglement entropy*, *Phys. Rev.* **D76** (2007) 106013, [arXiv:0704.3719].

[122] C. Davis, *Operator-valued entropy of a quantum mechanical measurement*, *Proc. Japan Acad.* **37** (1961) 533–538.

[123] H. Umegaki, *Conditional expectation in an operator algebra. iv. entropy and information*, *Kodai Math. Sem. Rep.* **14** (1962) 59–85.

[124] D. N. Page, *Average entropy of a subsystem*, *Phys. Rev. Lett.* **71** (1993) 1291–1294, [arXiv:gr-qc/9305007].

[125] M. Srednicki, *Quantum field theory*. Cambridge University Press, 2007.

[126] R. Feynman, *Statistical mechanics, a set of lectures*, 1972.

[127] P. Calabrese, J. Cardy and E. Tonni, *Entanglement entropy of two disjoint intervals in conformal field theory*, *J. Stat. Mech.* **0911** (2009) P11001, [arXiv:0905.2069].

[128] H. Casini, M. Huerta and R. C. Myers, *Towards a derivation of holographic entanglement entropy*, *JHEP* **05** (2011) 036, [arXiv:1102.0440].

[129] J. J. Bisognano and E. H. Wichmann, *On the duality condition for quantum fields*, *Journal of Mathematical Physics* **17** (1976) 303–321.

[130] J. Cardy, *Conformal Field Theory and Statistical Mechanics*, *arXiv e-prints* (July, 2008) , [arXiv:0807.3472].

[131] I. Peschel, *Calculation of reduced density matrices from correlation functions*, *J. Phys* **36** (2003) .

[132] E. H. Kim, *Characterizing topological order in superconductors via*

entanglement, *J. Phys* **26** (2014) .

[133] A. Barenco, C. H. Bennett, R. Cleve, D. P. Divincenzo, N. Margolus, P. Shor et al., *Elementary gates for quantum computation*, *Phys. Rev. A* **52** (1995) 3457–3467, [arXiv:quant-ph/9503016].

[134] A. Y. Kitaev, *Quantum computations: algorithms and error correction*, *Russian Mathematical Surveys* **52** (1997) 1191.

[135] C. M. Dawson and M. A. Nielsen, *The Solovay-Kitaev algorithm*, *eprint arXiv:quant-ph/0505030* (May, 2005) , [arXiv:quant-ph/0505030].

[136] M. R. Dowling and M. A. Nielsen, *The geometry of quantum computation*, *eprint arXiv:quant-ph/0701004* (Dec., 2007) , [arXiv:quant-ph/0701004].

[137] A. R. Brown, D. A. Roberts, L. Susskind, B. Swingle and Y. Zhao, *Holographic Complexity Equals Bulk Action?*, *Phys. Rev. Lett.* **116** (2016) 191301, [arXiv:1509.07876].

[138] A. M. Perelomov, *Coherent states for arbitrary Lie group.*, *Commun. Math. Phys.* **26** (1972) 222–236, [arXiv:math-ph/0203002].

[139] A. Perelomov and A. Perelomov, *Generalized Coherent States and Their Applications*. Modern Methods of Plant Analysis. Springer-Verlag, 1986.

[140] R. Gilmore, *Geometry of symmetrized states*, *Annals of Physics* **74** (1972) 391 – 463.

[141] A. S. Holevo and R. F. Werner, *Evaluating capacities of bosonic gaussian channels*, *Phys. Rev. A* **63** (Feb, 2001) 032312.

[142] X.-B. Wang, T. Hiroshima, A. Tomita and M. Hayashi, *Quantum information with Gaussian states*, *Phys.Rept.* **448** (Aug., 2007) , [arXiv:0801.4604].

[143] S. Olivares, *Quantum optics in the phase space. A tutorial on Gaussian states*, *European Physical Journal Special Topics* **203** (Apr., 2012) , [arXiv:1111.0786].

[144] C. Weedbrook, S. Pirandola, R. García-Patrón, N. J. Cerf, T. C. Ralph, J. H. Shapiro et al., *Gaussian quantum information*, *Reviews of Modern Physics* **84** (Apr., 2012) 621–669, [arXiv:1110.3234].

[145] G. Adesso, S. Ragy and A. R. Lee, *Continuous variable quantum information: Gaussian states and beyond*, *Open Systems & Information Dynamics* **21** (Jun, 2014) 1440001.

[146] A. R. Brown and L. Susskind, *Second law of quantum complexity*, *Phys. Rev.* **D97** (2018) 086015, [arXiv:1701.01107].

[147] A. Goussev, R. A. Jalabert, H. M. Pastawski and D. Wisniacki, *Loschmidt Echo*, *arXiv e-prints* (June, 2012) , [arXiv:1206.6348].

[148] T. Gorin, T. Prosen, T. H. Seligman and M. Žnidarič, *Dynamics of Loschmidt echoes and fidelity decay*, Phys. Rep. **435** (Nov., 2006) 33–156, [arXiv:quant-ph/0607050].

[149] F. M. Cucchietti, *The Loschmidt echo in classically chaotic systems: Quantum chaos, irreversibility and decoherence*. PhD thesis, PhD Thesis, 2004, 2004.

[150] S. Lloyd, *Computational capacity of the universe*, *Phys. Rev. Lett.* **88** (2002) 237901, [arXiv:quant-ph/0110141].

[151] W. P. Su, J. R. Schrieffer and A. J. Heeger, *Solitons in polyacetylene*, *Phys. Rev* **42** (1979) .

[152] M. Atala, M. Aidelsburger, J. T. Barreiro, D. Abanin, T. Kitagawa, E. Demler et al., *Direct measurement of the zak phase in topological bloch bands*, *Nat* **9** (2013) .

[153] M. Lohse, C. Schweizer, O. Zilberberg, M. Aidels-burger and I. A. Bloch, *Thouless quantum pump with ultracold bosonic atoms in an optical superlattice*, *Nat* **12** (2016) .

[154] T. T. S. Nakajima, S. Taie, T. Ichinose, H. Ozawa, L. Wang, M. Troyer et al., *Topological thouless pumping of ultracold fermions*, *Nat* **12** (2016) .

[155] E. J. Meier, F. A. An and B. Gadway, *Observation of the topological soliton state in the su-schrieffer-heeger model*, *Nat* **7** (2016) .

[156] M. OâĂŹSearcoid, *Metric Spaces*. Springer Undergraduate Mathematics Series. Springer London, 2006.

[157] M. c. Chung, Y. h. Jhu, P. Chen, C. y. Mou and X. Wan, *A memory of majorana modes through quantum quench*, *Sci. Rep* **6** (2016) 29172.

[158] X. G. Wen, *Quantum Field Theory of Many-body Systems*. Oxford University Press, New York, 2004.

[159] R. Jafari and H. Johannesson, *Loschmidt echo revivals: Critical and noncritical*, *Phys. Rev. Lett.* **118** (Jan, 2017) 015701.

[160] H. T. Quan, Z. Song, X. F. Liu, P. Zanardi and C. P. Sun, *Decay of loschmidt echo enhanced by quantum criticality*, *Phys. Rev. Lett.* **96** (Apr, 2006) 140604.

[161] A. Kitaev and J. Preskill, *Topological Entanglement Entropy*, *Physical Review Letters* **96** (Mar., 2006) 110404, [arXiv:hep-th/0510092].

[162] H. Li and F. D. M. Haldane, *Entanglement Spectrum as a Generalization of Entanglement Entropy: Identification of Topological Order in Non-Abelian Fractional Quantum Hall Effect States*, *Physical Review Letters* **101** (July, 2008) 010504, [arXiv:0805.0332].

[163] M. Z. Hasan and C. L. Kane, *Colloquium: Topological insulators*, *Rev. Mod. Phys.* **82** (Nov, 2010) 3045–3067.

[164] X.-L. Qi and S.-C. Zhang, *Topological insulators and superconductors*, *Rev. Mod. Phys.* **83** (Oct, 2011) 1057–1110.

[165] Z. Fu, A. Maloney, D. Marolf, H. Maxfield and Z. Wang, *Holographic complexity is nonlocal*, *JHEP* **02** (2018) 072, [arXiv:1801.01137].

[166] G. Passarino and M. J. G. Veltman, *One Loop Corrections for e+ e- Annihilation Into mu+ mu- in the Weinberg Model*, *Nucl. Phys.* **B160** (1979) 151–207.

[167] D. B. Melrose, *Reduction of feynman diagrams*, *Il Nuovo Cimento A (1965-1970)* **40** (Nov, 1965) 181–213.

[168] W. van Neerven and J. Vermaseren, *Large loop integrals*, *Physics Letters B* **137** (1984) 241 – 244.

[169] D. Bump, *Lie Groups*. Graduate Texts in Mathematics. Springer, 2004.

[170] Arvind, B. Dutta, N. Mukunda and R. Simon, *The real symplectic groups in quantum mechanics and optics*, *Pramana* **45** (Dec, 1995) 471âĂŞ497.